Attention-related modulation of neuronal synchrony in the auditory cortex of rats during a two-tone discrimination task

By

Paulo Vianney Vilela Rodrigues

A dissertation submitted in partial fulfillment of the requirements for the degree of Doctor of Philosophy
Department of Physiology and Pharmacology
Oregon Health Science University
May 2009

_____

John P. Welsh, Ph.D.
Thesis Advisor
Professor, Department of Pharmacology and Physiology
Drexel University College of Medicine

_____

Curtis Bell, Ph.D.
Emeritus Professor, Department of Physiology and Pharmacology
Oregon Health Science University

_____

Claudio V. Mello, MD/Ph.D.
Associate Professor, Behavioral Neuroscience Department
Oregon Health Science University

_____

Robert Duvoisin, Ph.D.
Associate Professor, Department of Physiology and Pharmacology
Oregon Health Science University

_____

Christine Portfors, Ph.D.
Assistant Professor, Department of Biology
Washington State University Vancouver

_____

Beth A. Habecker, PhD
Associate Professor of Physiology & Pharmacology,
Oregon Health Science University

This dissertation is dedicated
to
Jose and Ana
for their unconditional love...

Acknowledgements

I would like to thank my wife, Stephanie Severs, for her love, caring and understanding of the weekends without my companionship. Also for her wiliness to leave our lovely life in Portland and join me in Philadelphia, and to painfully help me proofread this dissertation. I am also in debt to my dearest friend Dr. Dan Lancu for teaching me MATLAB and for helping me to develop the analysis used in this thesis. Without him, this thesis would not be the same. I also like to express my appreciation to Dr. Claudio Mello, who gave me the opportunity to join his lab and learn about the fascinating field of auditory processing and vocal learning of the birdsong. I would like to thank my advisor Dr. John Welsh who kindly opened the doors of his lab for me to develop my research project. I would like to thank Dr. Paul Cordo and Sandra Oster for offering me the course of scientific writing. Finally, I would like to thank the Conselho Nacional de Desenvolvimento e Pesquisa (CNPq) and Autism Speaks Foundation for financial support and funding.

Abstract

The purpose of this dissertation is to study the role of neuronal synchrony and high frequency oscillations in perceptual processing in the auditory cortex of awake behaving rats. In order to do so, I first characterized these oscillations in the primary auditory cortex of rats passively listening to tones. After finding that high frequency oscillations are induced by auditory stimulus in the passively listening rats, I then proceeded to correlate these oscillations with meaningful simple tone patterns. I trained rats in a two-tone discrimination paradigm in which they had to perceive that two successive acoustic events signaled a reward. Moreover, because these two-tones were played in a fast temporal succession, which is commonly seen in a variety of animal vocalizations, the data produced can, in principle, indicate time processing properties of the auditory cortex.

The experimental data gathered in this thesis strongly suggest that high frequency oscillations at gamma and high gamma ranges are modulated by auditory perception. I will show in Chapter 1 that tones induce high frequency oscillations. Then, in subsequent chapters (chapters 3 and 5), I will demonstrate that these oscillations are modulated by attention-related processes involved in auditory processing.

Table of Contents

List of Figures

List of Tables

List of Abbreviations

A1 – primary auditory cortex
A2 – secondary auditory cortex
AAF – anterior auditory field
ACH – auto-correlogram
AM – amplitude modulated tones
ASA – auditory scene analysis
AUC – area under the curve
AVCN – anterior ventral cochlear nucleus
BM – basilar membrane
BMF – best modulation frequency
CCH – cross-correlogram
CF – characteristic frequency
CN – cochlear nucleus
CM- caudo-medial border of A1
CMR – co-modulation masking release
DCN- dorsal cochlear nucleus
DLPFC – dorsolateral pre-frontal cortex
EEG – electroencephalogram
FM – frequency modulation
FS – fast spiking neuron
FRB – fast rhythmic bursting neurons
FMR – forward masking ratio
IB – intrinsically bursting neurons
IC – inferior colliculus
ICC – central nucleus of inferior colliculus
ICP – pericentral nucleus of inferior colliculus
ICX – external nucleus of inferior colliculus
ISI – interspike interval
LDT – laterodorsal tegmental nucleus
LFP local field potential
LGN – lateral geniculate nucleus
LGNp – lateral geniculate nucleus part parvocellular
LGNm – lateral geniculate nucleus part magnocellular
LL – lateral lemniscus nucleus
MAEP- middle latency auditory evoked response
MEG – magnetoencephalogram
MGB- medial geniculate bogy
vMGB – ventral part of medial geniculate body
dMGB – dorsal part of medial geniculate body
mMGB- medial part of medial geniculate body
MMN – mismatch negativity
MT – temporal visual area
MUA – multi-unit activity recordings
NB – nucleus basalis of the anterior forebrain
NEX – neuroexplorer software
NFR – normalized firing rate
PAF – posterior auditory fields
PFC – pre-frontal cortex
vPFC – ventrolateral pre-frontal cortex
PIL – posterior intrathalamic nucleus
PO – posterior nucleus of the thalamus
PPT – pedunculopontine tegmentum nucleus
PSD – power spectrum density
PSTH - peri- event histogram
PVCN – postero-ventral cochlear nucleus
RF – receptive field
ROC – receiver operator analysis
RT – rostral border of the primary auditory field
RMS – root mean square
SG – suprageniculate nucleus
SNR – signal noise ratio
SOC – superior olivary complex
SPL – sound pressure level
SRAF – supra-rhinal auditory fields
SV – scale vestibule
SM - scale media
ST – scale tympani

STRF – spectro-temporal receptive field
TRN – thalamic reticular nucleus
V4 – visual area IV
VPAF – ventro-posterior auditory fields

Chapter 1

The auditory system and the role of high frequency oscillations in processing neuronal information

1.1 Introduction

In this chapter, I will be discussing the general organization of the auditory system, general principles of auditory scene analysis, temporal processing, and finally I'll give an overview of the proposed role of synchronization and high frequency oscillations in sensory processing and attention.

It is first necessary to provide a structure-function framework of the auditory system in which the role of synchronization and high frequency oscillations in the representation of neuronal information can be explored. Thus, the focus of this introduction is the organization of the auditory system; however, I will be comparing it to some key concepts of the organization of the visual system where the importance of the functional-anatomical organization in constraining neuronal processing is well documented and understood. Because both systems (auditory and visual) parcel the sensory information in parallel and serial channels, synchronization and high frequency oscillations have great appeal in explaining how these sensory systems might extract relevant sensory information from a noisy background and bind them in a coherent percept.

1.2 Key concepts in Acoustic Scene Analysis

Because our acoustic environment consists typically of a mixture of sounds, an evolutionary selective pressure must have played a significant role in shaping the auditory system to optimize a set of algorithms to disentangle meaningful acoustic information from background noise. Bregman has coined the term Acoustic Scene Analysis (ASA) to describe how the auditory system can group and follow acoustic events along time by forming acoustic perceptual objects (also called auditory streaming) (Bregman, 1990).

Spectral features, time onsets, and the time interval between auditory stimuli are the main acoustic attributes used by the auditory system to accomplish auditory streaming (Dannenbring & Bregman, 1976; Bregman, 1990; Bregman et al., 2000). Temporal cues are essential for intelligibility of speech (Rose, 1992), and it is well documented that subjective rhythm is a fundamental component for auditory grouping, music perception, and language (Handel 1998). For instance, a trained person can easily extract meaningful information from Morse code. This code only uses temporal cues, such as click duration and inter-click silence intervals in order to convey information. Other studies posit that auditory attention itself has evolved to predict time regularities of acoustic objects, and as such, temporal regularities of acoustic events greatly capture auditory attention (Larger & Jones, 1999).

1.3 Brief review of the auditory system

The disentanglement of the sound mixtures in our environment starts to take place at the cochlea, which essentially performs a decomposition of the sounds in its spectral components. The small variations in air pressure constituting sound waves travel through

the auditory canal and vibrate the tympanic membrane (eardrums) which then vibrates the small middle ear ossicles (malleus, incus and stapes), that are connected to the oval window of the cochlea. The cochlea is a fluid-filled three chamber compartment composed of the scala vestibule (SV), scala media (SM), and scala tympani (ST) (reviewed in Raphael & Altschuler, 2003). The scale media compartment is bounded by the vestibular membrane (separating the SV and SM) and the basilar membrane (separating the SM and ST) (reviewed in Raphael & Altschuler, 2003; Fettiplace & Hackney, 2006). The oval window is located at the base of the SV and it is sealed by the footplate of the stapes. Thus, vibration of the stapes will set the cochlear fluids in motion, which will cause movement of the basilar membrane (BM). These small vibrations of the BM are transmitted to hair cells which are the sensory receptors of the cochlea (Raphael & Altschuler, 2003)

The mechanical properties of the BM cause the cochlea to perform a spectral Fourier transform that decomposes complex sounds into its sinusoidal components (Moore, 2004). This is because at the base of the cochlea, and close to the stapes, the BM is thin and stiff, whereas towards the apical side of the cochlea, it is thick and loose. Thus, the low frequency components of the sound will vibrate the apical endof the BM whereas the high frequency components will vibrate the basal end of the BM. A particular hair cell is innervated by 10 to 20 apical peripheral processes (sometimes called dendrites of the primary auditory neurons) of bipolar neurons in whose axons constitute the VIII cranial nerve (Roullier, 1996). Track-tracing and intra-axonal recordings show that the axon of the bipolar neurons are highly tuned to a particular frequency, thus, reflecting the anatomical connection to a particular inner hair cell (Roullier, 1996).

The spectral decomposition performed by the cochlea is maintained in a point-to-point map in the brainstem. This is because the activity of hair cells located at the base of the BM is transmitted to the rostral cochlear nucleus whereas the activity of hair cells located at the apex of the BM is transmitted to the caudal cochlear nucleus. Thus, the spectral components of the sound have a tonotopic representation at the cochlear nucleus (CN*) (Altschuler et al., 1991; Roullier, 1996; Frisina, 2001).* This tonotopic organization is also present in the nuclei that receive projections from the cochlear nucleus (CN). Neurons of the CN send ipsilateral and contralateral projections to the superior olivary complex (SOC: lateral olivary nucleus, medial olivary nucleus, and medial nucleus of the trapazoid body). Therefore, the pattern of ipsi and contralateral afferent projections from the CN converge to the SOC complex. This structure integrates and processes binaural cues (interaural level difference and interaural spectral difference between the ears) and therefore, it is the main brainstem structure processing sound localization (Tsuchitani & Johnson, 1991). The CN also sends a direct contralateral projection to the lateral lemniscus (LL) and inferior colliculus (IC)(Altschuler et al., 1991; Roullier, 1996;)

The IC is the auditory structure of the mesencephalum(check) that integrates ascending brainstem auditory pathways on route to the thalamus, since it receives direct and indirect projections from neurons of the SOC and LL (reviewed in Roullier, 1997; Ehret, 1997). The IC is subdivided in three main regions: 1) central nucleus (ICC), 2) pericentral nucleus (ICP), and 3) external nucleus (ICX). The ICC is a laminar structure, in which its neurons have V shape type tuning curve. The ICC shows an increasing characteristic frequency (CF) representation at its dorsoventral axis (Merzenich & Reid, 1974). Thus, the ICC has a tonotopic organization and it is the main relay of auditory

information to the auditory thalamus. Moreover, the ICC neurons have a synchronized phase-locked response to amplitude modulated tones, thus, they synchronize their action potential discharges to the phase of the amplitude modulated tones (Schreiner & Langer, 1988; Langner & Schreiner, 1988; Langner, 1992). The maximum precision by which ICC neurons synchronize their firing rate varies between 10 to 1000 Hz of the modulated tone amplitude (the best modulation frequency, BMF), and in addition, their neurons have a topographic representation of the BMF (Schreiner & Langner., 1988).

The auditory thalamus is a very complex structure comprising several distinct nuclei. It consists of the following structures: 1) the medial geniculate body (MGB; which is further subdivided into ventral MGB, medial MGB, and dorsal MGB); 2) the lateral part of the posterior nucleus of the thalamus (PO); 3) the auditory sector of the thalamic reticular nucleus (TRN); 4) posterior intrathalamic nucleus (PIL); 5) suprageniculate nucleus (SG) (Winer, 1991, 1992; Roullier, 1996; Brett & Barth, 1997; Hu, 2003). These thalamic structures, combined with the projection from IC, give rise to two distinct functional pathways: 1) A lemniscal pathway that displays tonotopic organization, 2) a non-lemniscal pathway that displays some tonotopic characteristics, but mostly have diffuse non-tonotopic and polysensory characteristics (Weinberger & Diamond, 1985; Winer, 1991, 1992; Roullier, 1996; Brett & Barth, 1997; Hu, 2003).

The lemniscal pathway is defined as a specific pathway that is topographically organized and maintains high fidelity modality specific sensory information from the periphery (Weinberger & Diamond, 1987). The primary auditory, visual and somato-sensory cortices are traditionally viewed as modality specific pathways (Weinberger & Diamond, 1987). In the case of the auditory system, the lemniscal pathway originates

from the tonotopic projections from the ICC to the vMGB and PO which are also tonotopically organized (cats: Winer, 1992; Roullier, 1996; DeRibaupierre, 1997; Huang & Winer, 2000; Lee & Winer, 2005, 2008; rats: Winer et al. 1999; Hu, 2003; monkeys: reviewed in Rauschecker & Tian, 2000). These thalamic structures send topographic projections to the auditory cortex of mammals, thus preserving some of the basic spectral decompositions of the sound carried out by the cochlea (Winer, 1992; Roullier, 1997; DeRibaupierre, 1997; Huang & Winer, 2000; Lee & Winer, 2005, 2008; Winer et al. 1999). There are four areas receiving projections from vMGB/PO in the auditory cortex of cats (reviewed in Roullier, 1997; Lee & Winner, 2008) and rats (Rutkowski et al., 2003; Kalatski et al., 2005; Polley et al., 2007) that are tonotopically organized: primary auditory cortex (A1), anterior auditory field (AAF), posterior auditory field (PAF), and ventro-posterior auditory field (VPAF, or suprarhinal auditory field (SRAF)). In monkeys there are three structures having clear tonotopic organization: A1, the rostral border of A1 (RT), and the caudomedial border of A1 (CM). A1 and RT receive projections from vMGB and CM receives projections from dMGB (reviewed in Rauschecker & Tian, 2000). Therefore, while there are some minor specie-specific differences, the general organization appears to be similar between mammals. Moreover, the precise cochleotopic organization of these structures argues that they transmit precise acoustic information.

The non-lemniscal pathway consists of the afferent and efferent projection patterns of the medial MGB, the dorsal MGB, PIL, TRN and SG. The dorsal MGB receives its projection from the ICP and sends widespread divergent projections to the non-tonotopic secondary auditory cortex, insular cortex, temporal cortex (Te, auditory region ventro-rostral to A1 and A2), piriform cortex as well as the tonotopic PAF and

VPAF cortices (cats: Roullier, 1996; Huang & Winer, 2000), and to the lateral nucleus of the amygdala (Shinanoga et al., 1994; Doran & Ledoux, 2000; Hu, 2003). The medial MGB receives projections from neurons of the ICX and ICC and it has a partial tonotopic organization (reviewed in Roullier, 1996). The medial MGB has a widespread projection to the whole extension of the tonotopic (A1, AAF, PAF,VPAF) and the non-tonotopic auditory cortex (AII, insula, Te, and unidentified posterior auditory field), as well as the lateral nucleus of amygdala and to the basal ganglia (Huang & Winer, 2000). The PIL is also part of the non-lemniscal pathway because it sends a diffuse projection to layer I of A1 and AII (Linke, 1999). Although the TRN does not project directly to the auditory cortex, it has reciprocal connections with the ventral, medial and dorsal MGB, as revealed by retrograde track-tracers injected in the MGB (Crabtree, 1998). The TRN also receives cortico-thalamic feedback projection from layer V of A1 (Roger & Arnault., 1989), and from regions of the pre-frontal cortex (PFC) (Zikopoulos and Barbas, 2006) that receive projections from secondary auditory cortex (Romansky., et al 1999; 2009). It is interesting to note that the Te cortex and insular cortex, as well as the PIL and SG also project to the lateral nucleus of amygdala (Doran & Ledoux, 2000; Ledoux, 2000).

The non-lemniscal pathway might convey relevant acoustic and/or multimodal sensory information to the auditory cortex in order to implement goal-directed behaviors. For instance, extracellular recordings in the dorsal MGB and medial MGB show that they have a broad tuning curve, long latencies, and rapid habituation to consecutive tones (Bordi & Ledoux, 1994). Second, the medial MGB has neurons that respond to tactile stimulation (somestesic), auditory stimuli(Bordi & Ledoux, 1994a, 1994b), and to the electrical stimulation of the vestibular nerve (Blum & Gilman, 1979; reviewed in

Roullier, 1996). Additionally, recent extracellular recordings in the medial, dorsal MGB, and PIL of rats identifying tones that indicate a specific reward (water, sucrose or electrical stimulation in the medial forebrain bundle), showed that these structures have an early phasic response to auditory stimuli and a late tonic and sustained discharge (climbing response) to the time and value of reward (Komura et al., 2001). Moreover, the magnitude of the phasic response to tone onset as well as the late response co-varied with the experience of the rats. For instance, in trials in which tones no longer predicted reward ("extinction trials") the phasic and the climbing response to tones diminished Komura et al., 2001). The same type of activity was not identified in the ventral MGB (Komura et al., 2001). This finding shows that the non-leminiscal pathway is related to attention/anticipation because it is time-locked to the timing of reward (Komura et al., 2001; Hu, 2003). Moreover, the diffuse projection pattern of the medial MGB to the cortex strongly suggests a sparseness of connectivity. It is expected that the number of synaptic contacts between the thalamo-cortical non-lemniscal pathways should be relatively low. As a consequence, the efficacy of synaptic transmission would be enhanced if the cortical auditory neurons receiving inputs from the non-lemniscal pathway display a synchronous activity.

1.4 Representation of time-varying sounds

The majority of studies in auditory neurophysiology have focused on how the auditory system represents time-varying acoustic signals by measuring neuron responses to relatively simple acoustic elements with varying temporal and frequency modulation in anesthetized or awake passively listening animals (reviewed in Langner, 1992; Frisina, 2001; Wang et al., 2008). Time-varying signals are fundamental components of speech

and animal vocalizations (Rose, 1992). The axons of the spiral ganglion cells (VIII cranial nerve), some neurons of the cochlear nuclei, olivary nucleus complex, and nucleus of the lateral lemniscus can faithfully phase-lock to the carrier frequency at an astonishing 4000 kHz (reviewed in Altschler et al., 1991; Langner, 1992; Frisina, 2001). However, at the midbrain level (IC), there is a reduction of synchronization of spike discharges to time-varying sounds (Langner & Schreiner, 1988; Langer, 1992). At the thalamus (MGB) and auditory cortex there is an even higher reduction of synchronization to time-varying signals (DeRibeaupierre et al., 1972; Creutzfeldt et al., 1980; Schreiner & Urbas, 1988; Bartlett & Wang, 2007). Therefore, results of periodicity coding have shown that the precision of a temporal based representation is greatly reduced in the auditory cortex because neurons do not synchronize their action potentials to time-varying signals to higher frequencies than 30 Hz in some studies (Creutzfeldt et al., 1980; Schreiner & Urbas, 1988; Liang & Wang, 1992., Eggermont, 1992; 1994; Eggermont & Smith, 1995, Lu & Wang, 2000) or 100-165 Hz in other studies (DeRibaupierre et al., 1972; Andersen et al., 2007).

The earlier studies of neuronal synchronization to time varying sounds have suggested that periodicity coding is reduced in the auditory cortex. However, more recent studies in awake marmosets have shown that a subclass of neurons in A1 can follow very short inter-tone intervals (2 to 10 ms) with a non-synchronized firing rate-based code (Lu & Wang, 2002; Lu & Wang, 2004; Lu et al., 2001a, 2001b). Moreover, by using damped and ramped sinusoids at various inter-stimulus intervals, Wang and collaborators showed that neurons in A1 can concurrently represent a coarse time-varying slow temporal pattern with a firing rate representation of fine temporal features (Lu et al., 2001a;

2001b). Thus, based on these results, it is proposed that the auditory cortex transforms a temporal based code into a rate-based code to represent time-varying signals (Wang et al., 2008). However, it is unclear if these neurons form functional maps representing short time intervals. Additionally, other studies found that A1 neurons synchronize their firing rate to fast transitions in frequency and amplitude within ripple noise and vocalizations (Elhilali et al., 2005; Schnupp et al., 2006; Walker et al., 2008). Therefore, these results show that neurons in A1 can synchronize to acoustic features within complex vocalizations. However, these studies do not clarify how these acoustic events can form an auditory stream that can be followed as a separate entity amid other sounds over time.

Besides the extrinsic neuronal synchronization to time-varying acoustic features, there is also an intrinsic synchronization among neurons to process sensory information. Several earlier studies (Dickson & Gerstein, 1974; Frostig et al., 1983; Espinosa & Gerstein, 1988; DeCharms & Merzenich, 1996; Brosch & Schreiner, 1999), have used cross-correlogram (CCH) techniques to explore how neuronal synchrony in the auditory cortex to process acoustic events. These studies demonstrate that most of the neurons in A1 display a symmetrical positive peak centered at the CCH origin (Dickson & Gerstein, 1974; Frostig et al., 1983; Espinosa & Gerstein, 1988). There is some evidence that auditory neuronal synchrony depends on receptive field characteristics (DeCharms & Merzenich, 1996; Brosch & Schreiner, 1999). For instance, neurons with similar characteristic frequency tend to have higher CCH strength and lower temporal dispersion of their spike trains (DeCharms & Merzenich, 1996; Brosch & Schreiner, 1999; Eggermont, 1992, 1994, 2006). Recent studies used clustering analysis based on CCH

and spectrotemporal receptive field (STRF) properties of simultaneous single-unit recordings in A1 and posterior auditory fields (PAF) of anesthetized cats (Eggermont, 2006a, 2006b). These studies have claimed that the formation of functional neuronal clusters rarely extend beyond the boundaries of A1 (they are mostly within a 1.0 mm diameter), and functional clusters are rarely seen between A1 and PAF (Eggermont, 2006a, 2006b). Eggermont suggested that there are other unidentified factors that are relevant for neuronal synchrony in the auditory cortex besides the divergent anatomical projections from the MGB to A1, or the divergent projections from A1 to PAF. For instance, less than 15% of the overlapping STRF neurons between A1 and PAF form functional clusters (Eggermont, 2006a). Therefore, the author argues that cortico-cortical connections are not determinant in forming functional clusters (Eggermont, 2006a). Other studies have shown that the CCH among neurons to time-varying acoustic signals show a secondary peak around 60 ms and 100 ms from the origin (Eggermont, 1991; 1994; Eggermont & Smith, 1995). This suggests that neuronal synchrony in A1 has low pass band characteristics around 25 Hz (Eggermont, 1992; 1994; Eggermont & Smith, 1995).

In summary, prior studies suggest that neuronal synchrony in A1 does not represent fast acoustic transitions present in complex vocalizations. However, these studies were performed in anesthetized animals, and it is known that anesthesia modifies the strength and timing of neuronal responses to clicks (Zurita et al., 1994; Syka et al., 2005), and slows the frequency and disrupts the amplitude of oscillations (Faulkner et al., 1998). Moreover, it is possible that neuronal under-sampling, and/or a bias to record from particular big pyramidal neurons with high spontaneous firing rates, might underestimate the role of synchrony in processing acoustic information. Further studies recording from

LFP and MUA in awake animals could provide new information in the role of neuronal synchrony in auditory processing.

1.5 Synchronization, perception and attention

It is well established that neurons in the visual cortex are anatomically wired to form maps that represent simple physical features of sensory objects (Hubel, 1995). For instance, the primary visual cortex forms maps of micro-columns containing neurons with a similar selective orientation (Hubel & Wiesel., 1962, 1963; Horton & Adams, 2005). Similar to the visual system, the somatosensory cortex forms micro-columns of organization representing the mechanical receptors of a given place of the body (Mountcastle, 1957; Mountcastle, 1997). Moreover, in the visual system, the sensory input is further fragmented in parallel streams of processing (Livingstone & Hubel, 1988; Hubel, 1995; Van Essen & Gallant, 1994).There are two parallel streams of visual processing: dorsal (where) and ventral (what) streams. The dorsal parietal stream processes visual spatial relations and the ventral infero-temporal stream processes pattern recognition (Van Essen & Gallant, 1994; Livingstone & Hubel, 1988).

The auditory cortex appears to have a similar functional modular pattern of organization as the one displayed by the visual cortex (Ehret, 1997; Schreiner et al., 2000; Read et al., 2002; Linden & Schreiner, 2003). Several areas of the auditory cortex show a cochleotopic organization (A1, AAF, PAF, VPAF; Polley et al., 2007; Rutkowski et al., 2003; Kalatski et al., 2005). For example, radial micro-columns of characteristic frequency bands (CF) with low frequency tuning are located at the caudal A1 whereas high frequency tuning is located at rostral A1. Moreover, A1 is organized in precise dorso-lateral iso-frequency bands (Merzenich et al., 1974; Sally & Kelly, 1988;

Polley et al., 2007; Rutkowski et al., 2003; Kalatski et al., 2005; Read et al., 2001). Additionally, there is a directional selectivity map in which neurons located in low iso-frequency bands respond better to up frequency modulation (FM) sweeps and neurons located at high iso-frequency bands responds better to down FM sweeps (Zhang et al., 2003). Orthogonally to these iso-frequency maps, there are broad and narrow frequency integration maps, low and high intensity-threshold maps, long and short latency maps, and binaural integration maps corresponding to the EE (excitatory/excitatory) and EI (excitatory/inhibitory) response patterns to contralateral/ipsilateral ears (reviewed in Ehret, 1997; Schreiner et al., 2000; Read et al., 2002; Linden & Schreiner, 2003). Additionally, there is anatomical and physiological evidence supporting the sub-division of the auditory system in dorsal and ventral processing streams (Rauschecker & Tian, 2000; Romanski et al., 1999; Tian et al., 2001). These patterns of modular organization impose a daunting problem to the integration of elementary acoustic features implemented by sensory systems. How these neurons can be coordinated to represent coherent perceptual objects is a fundamental problem in systems neuroscience.

It has been shown that striate and extra-striate neurons of the visual cortex synchronize their firing rate at precise intervals in response to simple visual features, thus, creating oscillations at specific frequency ranges (Gray & Singer, 1989a; Gray et al., 1989b; Engel et al., 1991a, 1991b, 1991c). In the visual cortex, there is a strong correlation between induced gamma oscillations (30-90 Hz) at the cellular level with coherent perception formation. For instance, Fries and collaborators induced strabismus in cats to create the binocular rivalry phenomenon, in which, because the image into the two eyes are incongruent, only signals from one dominant eye are selected to form a

coherent percept. The image from the non-dominant eye is not perceived. Neurons that responded to the stimulus that continued to be perceived, displayed a high degree of neuronal synchronization at a gamma frequency range during binocular stimulation (Fries et al., 1997, 2002). Other experiments demonstrate that simultaneous multi-unit activity (MUA) recordings with receptive fields having a similar preferred orientation tuning in V1 (Grey & Singer, 1989a, 1989b; Engel et al., 1991b), between V1 hemispheres (Engel et al., 1991a) and between V1 and extrastriate areas (Engel et al., 1991c) shows high degree of synchrony at a gamma frequency range (reviewed in Singer & Gray, 1995). Furthermore, these oscillations were dependent on the configuration of the visual stimulus being presented. For instance, two visual bars moving in opposite directions did not evoke oscillatory synchronization between two neurons with non-overlapping receptive fields, while two or one visual bar moving in the same direction elicited great synchronization in these neurons (Gray & Singer, 1989a; Engel et al., 1991c). These findings suggest that neuronal network synchronization is stronger when single contours move coherently, and therefore appear to be part of a single figure. This type of neuronal response is reminiscent of the Gestalt criteria in which features in images tend to be grouped together if they are spatially continuous or show a common direction of movement (common fate) (reviewed in Singer, 1999; Gray & Singer, 1995).

There are relatively few studies exploring the relationship between high frequency oscillations and neuronal processing in non-visual areas compared to the work done in the visual system. However, it appears that induced gamma oscillations are an ubiquitous phenomenon occurring in other sensory and motor areas of the cortex. For instance, odorant stimuli induce high frequency oscillation in the olfactory bulb and piriform

cortex (Adrian, 1950; Freeman 1978, Bressler, 1980; 1984; Bressler et al., 1987). Moreover, the emergence of these oscillations correspond to specific odors, past experiences with the odors, and behavioral significance (review in Sannita, 2000; Wehr & Laurent, 1996; Stopfer et al., 1997). These oscillations also occur in the primary and frontal motor cortex during motor preparation (Donoghue et al., 1998) and in the somatosensory cortex they are enhanced when animals are paying attention to performing complex movements (Murphy & Fetz, 1992; 1996), but they are suppressed during the movement itself (Murphy & Fetz, 1992, 1996, 1996b; Sanes & Donoghue, 1993). Gamma and very high frequency oscillations (200 Hz) are also found in the hippocampus (Buzsaki et al., 1989; 1992; Ylinen et al., 1995).

Attention is a complex phenomenon without a clear and precise definition. However, it is a cognitive process that allows animals to focus on a sub-set of incoming sensory information. Several researchers propose that attention-related processes can be subdivided into several different sub-mechanisms: 1) cross-modality versus within modality switches mechanisms; 2) spatial attention versus object-selective mechanisms; 3) voluntary versus automatic selection mechanisms (reviewed in Hermann & Knight, 2001). In the case of the visual and auditory systems, attention can be driven by bottom-up salient sensory that capture attention or a top-down cognitive regulator process that regulates the salience of sensory stimuli (reviewed in Allport, 2003; Frizt et al., 2007b; 2007c). The essential idea behind the theories of attention is that the brain has a limited capacity to handle information. Classical theories proposed that attention is a filter mechanism in which some sensory features are selected for further processing while others are filtered out (reviewed in Allport, 2003). Whether this filter occurs at early

stages or later stages of sensory processing is still a matter of debate (Allport, 2003; Näätänen & Alho, 2004; Woldorff et al., 1993; Poghosyn & Ioannides, 2008). Other theories propose that there is a flexible mechanism for selecting only the sensory parameters that are important to a coherent control of a goal-directed action (Allport, 2003). Recent theories of attention propose that it would be implemented in the visual system by reducing the threshold of neurons tuned to particular visual features, thereby, increasing their firing rate in relation to baseline levels (Reynolds et al., 2000). This mechanism could provide a competitive bias whereby the contrast gain of competing visual features would be enhanced, and therefore, the stimulus that will be selected would have a advantage in activating post-synaptic neurons along the visual serial processing pathway (Desimone & Duncan, 1995; Reynolds & Chelazzi, 2004; Maunshell & Treue, 2006). Other theories propose that selective attention would be mechanistically implemented by synchronizing neuronal networks (Hermann & Knight, 2001; Fell et al., 2003; Womesdorf & Fries, 2007). Particularly relevant would be the synchronization of neuronal networks at the gamma frequency range (Fries, 2005). This is because coincident spikes from a presynaptic neuron are more likely to drive a postsynaptic neuron above the spike threshold (Mainen & Sejnowski, 1995; Azouz et al., 2000; Azouz et al., 2003; Salinas & Sejnowski, 2000; 2001; Wespatat et al., 2004; Fries, 2005). Indeed, besides the results suggesting that synchronization at high frequency ranges underlies feature binding and stimulus selection in the primary visual cortex (Grey & Singer, 1989a, 1989b; Engel et al., 1991b; Fries et al., 1997, 2001a, 2002), experimental data in the visual area IV (V4) demonstrates that synchrony at this frequency range is modulated by selective spatial attention (Fries et al., 2001b; Fries et al., 2008;

Wolmesdorf et al., 2006, 2008) and feature-based attention as well (Bichot et al., 2005, 2006). For instance, there are higher evoked gamma oscillations of the multi-unit (MUA) and local field potentials (LFP) in V4 when monkeys are paying attention to the visual space corresponding to the receptive field (RF) of the MUA being recorded as opposed to the trial in which they move their attention away from this RF (Fries et al., 2001, 2008). Moreover, there is a correlation between fast reaction times and high frequency oscillations in monkeys performing this spatial visual attention task (Wolmesdorf et al., 2006).

It is apparent that brain oscillations represent the synchrony of large neuronal populations. Moreover, the apparent ubiquity of oscillations at specific frequency ranges during perception provides a mechanism by which neurons could keep track of elapsed time. Oscillations, by definition, have a peak and trough that determine the amplitude and phase of the oscillation. Moreover, any sub-threshold oscillation has a peak closer to the spike threshold and a trough that will prevent the neurons from firing an action potential. Thus, when a pre-synaptic input is appropriately coincident with oscillatory peaks, it will likely drive the neuron to fire an action potential. If the oscillation has a consistent frequency, then a population of neurons would be able to track the time as a function of the period of the oscillation. If the hypothesis that attention has evolved to predict time regularities, which is obviously characteristic of our perceptual world, is correct (Larger & Jones, 1999; Jones, 2004), then oscillations could be an essential neuronal mechanism to keep track of acoustic streams over time.

Although several experiments suggest that neuronal synchronization at the gamma frequency range is the neuronal substrate by which a coherent perception of

visual objects might emerge (reviewed in Singer, 1999) very little is known about the role of neuronal synchronization at this frequency range in the auditory system. For instance, despite a wealth of data supporting the role of gamma oscillations in the processing of sensory information in the visual system (Engel et al., 1991; Grey & Singer, 1989a, 1989b; Fries et al., 1997; Gray & Singer, 1995; Singer, 1999), there are only a handful of studies exploring the role of high frequency oscillations in the auditory cortex (Barth & MacDonald, 1996; Brosch et al., 2002; Steinschneider et al., 2008; Medvedev & Kanwall, 2008). Moreover, the experimental evidence regarding the occurrence and role of gamma oscillations in the auditory system of experimental animals is conflicting. Some evidence suggests that gamma oscillations might not be related to auditory processing. For example, epipial recordings in anesthetized rats have shown that induced gamma oscillations to a sequence of clicks played at a 40 Hz frequency occur at long latencies (300 ms) after the stimulus onset. Moreover, stimulation of the main thalamic sources of projections to the auditory cortex (i.e. the ventral and dorsal Medial Geniculate Body - MGBv and MGBd) inhibits these oscillations (Franowicz & Barth, 1995; Barth & MacDonald, 1996). In fact, it was reported that auditory stimulation with clicks did not induce gamma oscillations in awake rats (Cotillon-Williams & Edeline, 2003) or awake mustached bats (*Pteronolus parnelli parnelli*) (Horikawa et al., 1994). These studies challenge the hypothesis that oscillations at the gamma range are necessarily involved in auditory processing. However, recent studies have shown that tones induce gamma oscillations in the auditory cortex of awake monkeys (Steinschneider et al., 2008) and complex auditory stimuli induces these oscillations in the awake mustached bats (Medvedev & Kanwall, 2008) at considerably shorter latencies. Additionally, time

reversed complex vocalization suggests that the temporal, but not the spectral structure of these vocalizations, strongly modulates high frequency oscillations (Medvedev & Kenwal, 2008). Moreover, the stimulation of the nucleus basalis in the anterior forebrain, the stimulation of the thalamic reticular, and the stimulation of the posterior intralaminar nuclei induces the occurrence of gamma oscillations in the auditory cortex at considerably short latencies (Metherate et al., 1992; Sukov & Barth, 1998, 2000; MacDonald et al., 1998; Barth & MacDonald, 1996).Thus, suggesting that the activity of these nuclei in awake animals could shape the oscillatory behavior of auditory neurons during the processing of relevant auditory information. Because earlier studies were performed mainly in anesthetized rats, it is possible that the effects of anesthesia changed the occurrence, frequency and latency of oscillations (Faulkner et al., 1998; Zurita et al., 1994). Still another possibility is that the lack of gamma oscillations in response to an auditory stimuliin awake rats could be due to species-specific differences. Overall, however, the occurrence of high frequency oscillations in the auditory cortex in response to sensory stimuli in experimental animals remains largely unexplored.

Despite of the paucity of high frequency oscillations in the auditory cortex of experimental animals, gamma oscillations have been documented in the temporal lobe of humans passively listening to sequences of clicks played at 40 Hz (Galambos et al., 1981). These high frequency oscillations are also induced in humans listening to transient tones and phonemes (Edwards et al., 2005), discriminating pure tones and phonemes (Crones et al., 2001), in the contexts of focused attention (Tiitinen et al., 1993), temporal binding of successive sensory events (Joliot et al., 1994), phantom perception of tinnitus (Weisz et al., 2007), and word processing (Canolty et al., 2007). Some models of

auditory attention have proposed that attention is a mechanism to predict and anticipate time regularities of acoustic objects (Larger & Jones, 1999; Jones, 2004). Moreover, this anticipatory attention model assumes that the phase and amplitude of intrinsic neural oscillators would be the substrate by which attention is brought about. These neural oscillators would precisely regulate the phase and amplitude of its oscillation to coincide to expected sensory auditory events (Larger & Jones, 1999; Jones, 2004). Indeed there is some data showing that gamma oscillations are evoked by omitted sensory events in a previously learned sequence of tones (Snyder & Large, 2005; Zanto et al., 2007). Therefore, in the auditory cortex, synchronization at high frequency oscillations could be a mechanism by which top-down auditory attention generates a time framework in which each acoustic event is bound in an acoustic stream over time.

Moreover, clinical observations in patients with schizophrenia, early psychosis, and autism have led to the hypothesis that normal gamma oscillations in the auditory cortex might be compromised under pathological states (Uhlhaas & Singer, 2006; Welsh et al., 2005). However, experiments in humans using subdural electrodes have a coarse spatial resolution ($\approx 1.0\ cm^2$ in diameter, Lachaux et al., 2003). Therefore, this technique record the activity of a relatively large neuronal population spread over the temporal lobe. Thus, it is hard to rule out that higher-order cortical areas might be sources of gamma oscillations in those experiments. Moreover, it is important to consider the possible contamination of muscle activity at the gamma frequency range in the interpretation of experiments carried out using EEG (Yuval-Greenberd et al., 2008). Given the importance of gamma oscillations in normal human behavior and under pathophysiological

conditions, it is important to establish animal models in which the functions of neuronal synchrony can be explored.

1.6 Specific aims and hypothesis testing

The specific aim of this dissertation is the study of neuronal synchrony and high frequency oscillations in the auditory cortex of awake rats actively perceiving simple auditory stimuli. I first hypothesized that auditory stimuli induce high frequency oscillations, which reflect neuronal synchrony, in the auditory cortex of awake rat. This hypothesis was tested in Chapter 2, by recording LFP and MUA in the auditory cortex of awake rats passively listening to a tone.

If synchrony at high frequency ranges is a neuronal mechanism of perceptual processing, then we should expect that these oscillations are modulated by animals perceiving acoustic elements. Thus, in Chapter 3, I aim to investigate if these high frequency oscillations are modulated, not only by passive sensory processing of simple attributes of sounds, but by actively perceiving these simple sounds. I compared rats passively listening to tones with rats that reported that they perceive a tone (cross-comparison experiment). These comparisons could indicate whether these high frequency oscillations are possible neuronal mechanism by which sounds are grouped in meaningful acoustic objects.

There are several experimental data showing that attention modulates the activity of some neurons in A1 (Hubel et al., 1959; Miller et al., 1972; Hocherman et al., 1976; Fritz et al., 2003, 2005, 2007). However, is possible that the activity of this auditory area does not predict performance. Therefore, in Chapter 4, I tested the hypothesis that the activity of the auditory cortex, as measured by its firing rate, not only is modulated by

attention-related processes, but it can be a reliable indicator of goal-directed behavior. In order to test this hypothesis, I trained rats in a two-tone discrimination task and correlated neuronal activity with incorrect and correct performance. Because of the importance of temporal processing for the auditory system, this behavioral paradigm might also reveal whether the activity of A1 is modulated by abstract temporal cues processing.

Finally, in Chapter 5 I tested the hypothesis that the synchronization of neuronal networks in A1 can also be reliably used to predict future goal-directed behavior. Moreover, the experiments of this Chapter aimed to rule out the possibility that high frequency oscillations could be explained by structural anatomical changes induced by plasticity in the experiment of Chapter 3.

Chapter 2

High frequency oscillations are induced by simple auditory stimuli in the auditory cortex of awake rats.

2.1 Introduction

Gamma oscillations are induced in the temporal lobe of humans passively listening to sequences of clicks played at 40 Hz (Galambos, 1981). These high frequency oscillations are also induced in humans listening to transient tones and phonemes (Edwards et al., 2005), discriminating pure tones and phonemes (Crones et al., 2001), in the contexts of focused attention (Tiitinen et al., 1993), temporal binding of successive sensory events (Joliot et al., 1994), and phantom perception of tinnitus (Weisz et al., 2007). Moreover, clinical observations in patients with schizophrenia, early psychosis, and autism have led to the hypothesis that normal gamma oscillations in the auditory cortex might be compromised under pathological states (Uhlhaas & Singer, 2006; Welsh et al., 2005).

Despite the large number of reports describing the occurrence of high frequency oscillations in the auditory cortex of humans perceiving simple and complex auditory stimuli, there are only limited studies exploring the occurrence and role of such oscillations in the auditory cortex of experimental animals. Some evidence suggests that these oscillations might not be related to auditory processing. For instance, epipial recordings in anesthetized rats have shown that induced gamma oscillations to a sequence of clicks played at a 40 Hz frequency occur at long latencies (300 ms) after the stimulus onset. Moreover, stimulation of the main thalamic source of projections to the auditory cortex (i.e. the ventral and medial geniculate body - vMGB and mMGB) inhibits these

oscillations (Franowicz & Barth, 1995; Barth & MacDonald, 1996). Other studies have proposed auditory stimulation does not induce gamma oscillations in awake rats (Cotillon-Williams & Edeline, 2003) or awake mustached bats (*Pteronolus parnelli parnelli*) (Horikawa et al., 1994). These studies challenge the hypothesis that oscillations at the gamma range are necessarily involved in auditory processing. However, recent studies have shown that simple and complex auditory stimuli induce gamma oscillations in the auditory cortex of awake monkeys (Steinschneider et al., 2008) and awake mustached bats (Medvedev & Kenwall, 2008). Therefore the occurrence of these oscillations is largely unexplored in the auditory cortex and still a matter of debate.

In this chapter, I aimed to determine whether there were high frequency oscillations in the auditory cortex of awake rats passively listening to an auditory stimulus. I used spectral techniques to describe the occurrence of high frequency oscillations in the auditory cortex of awake rats hearing a simple auditory stimulus. I describe neuronal synchronization at the population level by measuring the power spectrum of Local Field Potentials (LFP) and by measuring coherence among LFP sites.

The results showed that a simple auditory stimuli evoke time-locked and non time-locked oscillations in the auditory cortex. Additionally, there is a high degree of coherence among LFP sites around an area of 1.0 mm^2. Moreover, the spike train coherence analysis results suggest that the high frequency oscillations found in the LFP do not necessarily imply that neurons separated by distances larger than 300 μm coherently fire action potentials at these high frequencies. However, the coherence analysis of spike trains with their respective LFP sites suggests that small clusters of neurons are synchronized at the gamma frequency range. The results indicate that

auditory stimuli induce neuronal synchronization in the auditory cortex of awake rats and that this synchronization is likely a consequence of small synchronized networks.

2.2 Methods

Animal preparation

The experiments were carried out in a total of 7 Sprague-Dawley albino rats (Taconic Farms, Germantown, NY). All surgical procedures and experimental protocols were in accordance to NIH guidelines and were approved by OHSU Institutional Animal Care and Use Committee (IACUC). Rats were anesthetized (ketamine (66 mg/kg) and Xylazine(13 mg/kg)) prior to the recording session, and a small craniotomy was performed in the temporal bone above the stereotaxic coordinates of A1 (A/P:-4.75 mm; M/L:7.5 mm; D/V:3.0-4.0 mm from Bregma). It is important to point it out that this small craniotomy in these steriotaxic coordinates were consistently performed in all rats analyzed in this dissertation. Because the primary auditory cortex has a 3.2 mm antero-posterior by 3.0 mm medio-lateral extension I am confident that I am recording from A1.

After the craniotomy, a stainless steel electrode was inserted into the frontal cortex to serve as a reference. Four screws were inserted into the cranium in order to fabricate a cement head cap to firmly restrain the rat's head in an atraumatic stereotaxic apparatus (David Kopf Instruments, Model 880 semi-chronic head holder). This cement was used to build a cistern having a small aperture (approximately 1.5mm in diameter) above the craniotomy performed in the temporal bone. A very thin silicone layer was then placed on top of the exposed cortex in order to seal it, to prevent it from drying, and to allow access to the exposed auditory cortex after recovery from surgery. Two days post surgery rats were placed daily (2 to 3 hours) in the atraumatic head holder for 2 to 4

days before the recording sessions in order to adapt them to the recording conditions. A small plastic body restrainer was built to prevent movement during the recording session

Data set

The auditory stimulus protocol used in the process of searching and isolation of the multi-unit clusters (MUA) consisted of 50 ms tones ranging from 1 to 30 kHz presented every 500 ms at 1 kHz random steps (50 ms tone pip protocol). Once a MUA was isolated, I used auditory stimuli consisting of a 20 ms tone at 10 kHz presented every 30 seconds (± 5 s) as the experimental protocol utilized to further analysis. After the experimental session and in a few neurons, a 50 ms tone pip protocol similar to the protocol utilized to isolate MUA was used in an attempted to physiologically define A1 by its neurons' characteristic V-shape tuning curve. This protocol consisted of ten iterations of 1 to 30 kHz, 50 ms tones, ranging from 75 dB to 20 dB SPL. MUA that displayed an onset response to tones ranging from 5 kHz to 20 kHz at 30 dB SPL were included in this study.

In order to test the hypothesis that auditory stimuli evoke synchronized neuronal activity throughout the primary auditory cortex, up to 10 simultaneous MUA and LFP sites from A1 of awake rats passively hearing single tones were recorded. The analysis was restricted to 63 LFP sites that show the classic middle auditory evoked potential (MAEP) and MUA that had short response latencies (<20 ms) to the 10 kHz tones used as auditory stimuli in this study. Thus, the criterion to collect the LFP was that they showed a MAEP consistent with the evoked response of A1 (Talwar et al., 2001; Barth & Di, 1990, 1991; Franowicz & Barth, 1995), and the MUA collected in parallel to the LFP had to show a short latency with frequencies ranging between 5 kHz to 20 kHz.

Stimulus generation and Multielectrode Neurophysiology

The auditory stimuli were generated by a programmable function generator (32120A, Hewlett Packard, Denver, CO, USA) attached to a manually controlled attenuator (HP, model 350D). The function generator was controlled by a personal computer and coupled to a tweeter speaker (P. Audio, model PHT 409, Bangkratuk, Thailand). The sound intensity was calibrated to 70dB SPL by condenser microphone (Bruel & Kjaer, model 4135) placed 25 cm in front of the speaker and coupled to a sound level calibrator.

Recordings were conducted in a sound attenuated chamber manufactured inside of an electrically shielded Faraday cage. This acoustic attenuated chamber was manufactured from Plexiglas (0.63 cm) placed underneath the faraday cage wires. Thick sound insulated foam (Sonex 12.6 cm) was attached to the Plexiglas in order to allow 30dB SPL attenuation from environmental noise.

Simultaneous recordings of multiple neural signals were performed with an array of 16 insulated microelectrodes arranged in a 4x4 matrix. The microelectrodes were fabricated from 100 μm diameter tungsten rod (No. 7190, AM Systems, Inc. Carlsborg. WA, USA.), insulated with Epoxylite, and they have an 2-8 MΩ impedance measured at 1 kHz (FHC Inc., Bowdoinham, ME, USA) as previously described elsewhere (Johnson & Welsh, 2003; Schwarz & Welsh, 2001). Figure 2.1 shows the set up and the general methodology utilized to record multiple single-units and LFPs. The microelectrodes were carefully loaded into a honeycomb array fabricated with polyimide tubes (HV technologies, Trenton, GA) and soldered at their end to 16 microplug pins of a microdrive terminal of sixteen flexible shafts connected to a micromanipulator (Alpha-

Omega Inc., Nazareth, Illit, Israel) that were used to push each one of the microelectrodes independently. This array arrangement had inter-electrode distances of approximately 250-300 μm and allowed us to record up to 16 MUA from a 1.0 mm^2 small cortical area. The microelectrodes were lowered into A1 by the micromanipulator controlled by a personal computer in the remote workstation. Prior to lowering the microelectrodes into the brain, the silicone seal covering the auditory cortex was carefully cleaned with saline solution. After assuring that the polyimide tubes contacted the silicone seal the electrodes were simultaneously moved in 100 μm steps until they touched the brain. Thereafter, the microelectrodes were independently moved in 10 um steps until a neuron could be isolated.

Recording of the electrophysiological signal from the microelectrode array was performed by a MultiNeuron Acquisition Processor (MNAP) system developed by Plexon Inc. (Dallas, TX, USA). Action potentials were amplified 5,000 to 15,000 times and filtered between 0.4 and 8 kHz at 40 kHz sampling rate. The LFP signals were filtered between 1 to 170 Hz, fed into an analog-digital card (PCI-6071E, National Instruments) in a host personal computer that sampled each analog channel at 1 kHz at 12 bit resolution.

The discrimination of spike waveforms was performed using a real-time hardware-implemented time-voltage window discriminator (boxes template sorting), which is part of the RASPUTIN-software package that controls the MNAP. Raw and discriminated signals were also displayed on an oscilloscope (Hameg Instruments Inc. model HM 407) and concomitantly played through a small speaker for further inspection. After all spike signals were collected, off-line spike sorting software (Off-Line Sorter,

Plexon Inc.) was used to further separate spikes from background and to isolate single-units. The template-matching cluster algorithm provide by the offline sorter software was used to isolate clusters of the multiple single-unit recordings performed in the auditory cortex. Spikes were accepted as coming from the same cell only if they were clustered in a principal component analysis (PCA) with statistically significant (0.05) separation as determined by a multivariate analysis of variance (MANOVA) (see Figure 2.1). Each channel yields 2 to 4 well isolated neurons. Since there are several reports suggesting that single-unit are less suitable to detect synchrony among neurons and between neurons and LFP signals (Fries et al., 2001; DeChams & Merzenich, 1996; Womesdorf et al., 2006), I decided to restrict the analysis to multi-unit clusters of 2 to 4 neurons.

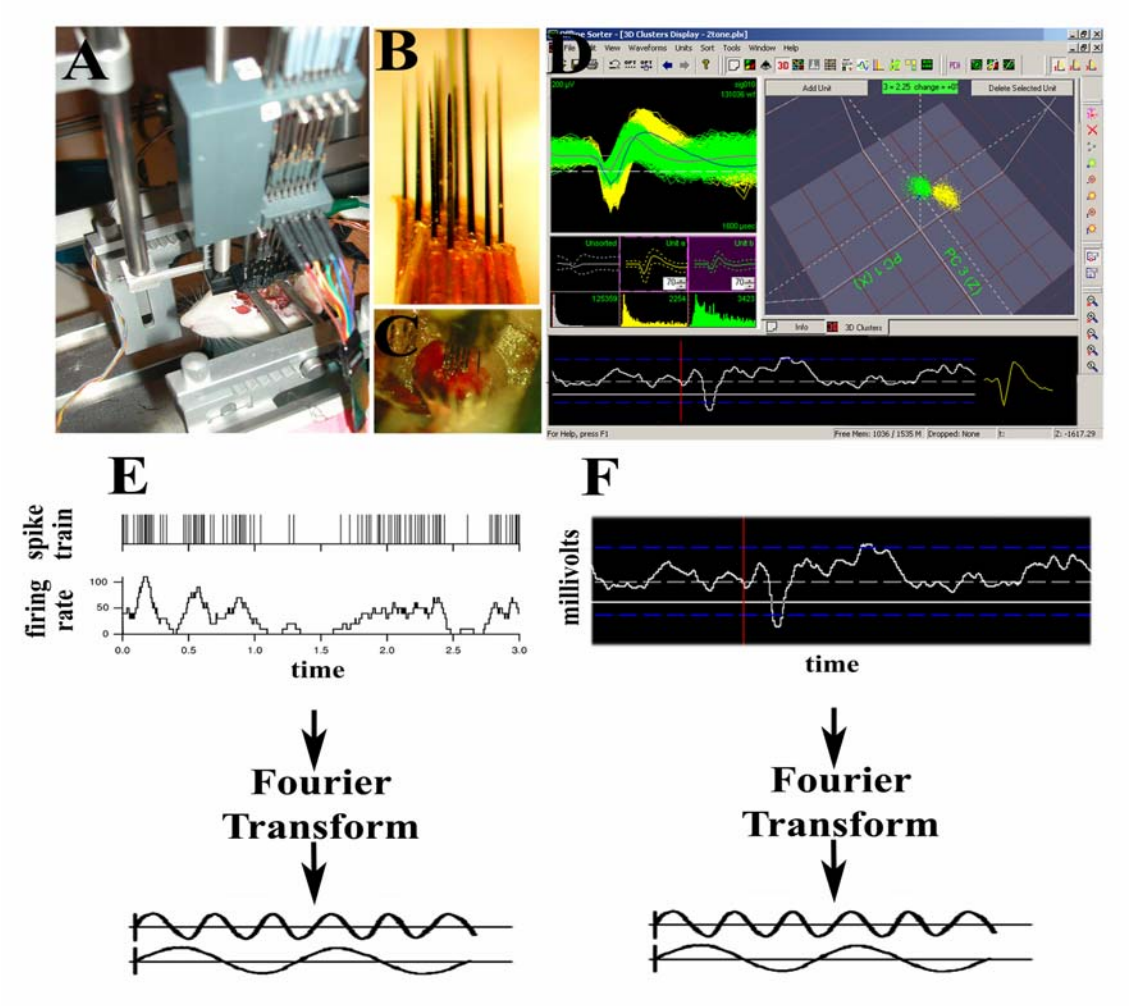

Figure 2.1. Experimental set up. A) Photograph of an awake rat in the recording apparatus. It is possible to see the atraumautic head holder, the micro-manipulator and the electrode array. B and C) Details of the electrode array, and multiple electrodes being lowered into the cortex (C) . D) Figure showing the cluster analysis provided by the offline sorter software. In the top left corner are shown two isolated units and in the top right is displayed their clusters. These clusters are based on a template matching algorithm and were statistically validated by a principal component analysis. Below the clusters is display an example of a LFP signal and the waveform of a single isolated spike (far right bottom corner). The blue dash lines of this figure show three standard deviations of the mean (white dash line) and the solid vertical red line indicates tone onset. E and F) Graphs showing the general concept of the spectral analysis performed in this chapter. The instantaneous firing rate of the spike train (E) was determined with a 1 ms bin and smoothed with a 5 ms gaussian window. Thereafter the spike train is treated as an analogous signal and it is Fourier transformed exactly in the same way as in the LFP signal (F).

Data Analysis

The data set was pre-processed to select segments without contamination with noise caused by movements and powerline currents. Once the channels containing spikes and LFP traces activated by tones were selected, I used custom-written Neuroexplorer software (NEX) programming language code to select 1600 ms data segments. Each data segment consisted of 500 ms of baseline (period before tone onset) and 1100 ms of data after tone onset. The data segments of the LFP traces were further inspected to detect and discard movement noise artifacts. In addition, I performed a power spectrum density analysis of the LFP traces in order to discard channels that had 60 Hz power line artifact noise. The data selection and off-line data analyses were performed with NEX and MATLAB (The MathWorks, Inc., Natick MA, USA).

Spectral analysis

Synchronization was studied by analyzing the power spectrum of the LFP, by analyzing the coherence spectrum of the LFP sites, by analyzing coherence spectrum of simultaneous multi-unit recordings, and by analyzing the coherence spectrum of simultaneous LFP and spike recordings.

Prior to performing the spectral analysis of the LFP signals that were considered to be from A1 (see data set session), I filtered each single LFP trace at 40-70 Hz and at 90 -150 Hz using a 5 pole Butterworth filter (≈ roll-off of 30 db/octave) in order to detect any oscillatory pattern. This analysis is shown in Figure 2.2A and Figure 2.4A. After this preliminary analysis of the LFP traces I then quantified any oscillatory behavior by computing the spectrogram and power spectrum of the LFP. The spectral analyses were

performed with the Chronux data analysis toolbox for Matlab (www.chronux.org) which uses multitaper methods to estimate the power spectrum of the LFP (continuous process), of the spike train (point process), and of the mixed spike train and LFP. This methodology has the advantage of providing a unified framework to study the temporal structure of the LFP, spikes and spike-LFP.

The multitaper method and spectral analysis of LFP and spike trains has been extensively used in the visual cortex, the parietal cortex, and several other systems (Prechtl et al., 1997; Mitra & Pesaran., 1999; Halliday & Rosenberg., 1999; Jarvis & Mitra., 2001; Pesaran et al., 2002, Mitra & Bokil., 2008) and will be briefly discussed here. An estimative of the power spectrum by a Fourier transform has "bias" (or spectral leakage, in which the power of nearby frequencies contributes to the power of any given frequency which then distorts the estimation) and variance (the estimation of the spectrum does not converge for the true value, even by increasing the time length analyzed). It is possible to minimize "bias" by applying tapers (or windowing) to the signal in which the power will be estimated. Variance can be reduced by segmenting the data in overlap windows and averaging them. The multitaper method utilizes an optimal set of orthogonal tapers known as prolate spheroidal functions (Slepian functions), that have optimal variance and bias properties, before applying the Fast Fourier Transform (FFT) algorithm. The Slepian functions are concentrated in a specific time duration (T) and frequency bandwidth (W). For each choice of T and W, a maximum of K=2TW-1 tapers can be used for spectrum estimation. Each data epoch is multiplied for each of these orthogonal tapers and then Fourier Transformed, which gives the windowed Fourier Transform:

$$\tilde{X}_k(f) = \sum_{t}^{N} W_k(t) X_t e^{-2\pi i f t}$$

in which X_t is the time series of the signal being considered (LFP or spike trains) and $W_k(t)$ are taper functions. The spike can be treated as a point process in which each sequence of spike trains is binned in 1 ms width, smoothed with a window that generates a spike density function and then Fourier transformed as in the LFP signal. The power spectrum density is formally defined as the magnitude-square of the Fourier transform and it is expressed with units of volts^2 / Hz. (for spikes: (spk/s)^2 / Hz). Therefore the power spectrum of the LFP (or spike trains) is the squared Fourier Transform of the tapered signal.

The coherence is the magnitude squared of the correlation between two Fourier Transform signals (the cross-spectrum of two signals) normalized by the spectrum of each signal. The cross-spectrum is the sum of the product of the two signal spectrum correlation. The spectrum and cross-spectrum are averaged over trials/channels in order to compute the coherence. The multitaper estimates for the spectrum ($S_x(f)$), the cross-spectrum ($S_{xy}(f)$, and the coherence ($C_{yx}(f)$) of point process and continuous process, are given by the following equations:

$$S_x(f) = \frac{1}{K}\sum_{k=1}^{K}\left|\tilde{X}_k(f)\right|^2 \quad ; \quad S_{yx}(f) = \frac{1}{K}\sum_{k=1}^{K}\tilde{y}_k(f)\tilde{x}_k(f) \quad ; \quad C_{yx}(f) = \frac{S_{yx}(f)}{\sqrt{S_x(f)\,S_y(f)}}$$

(Pesaran et al., 2002; Womelsdorf et al., 2006; Fries et al., 2008; Halliday & Rosenberg., 1999; Mitra & Bokil., 2008).

The coherence measures the strength of correlation between two signals as a function of frequency. The coherence value provides a normalized linear association of

phase and amplitude between two signals ranging from 0 to 1. A value of 1 indicates that two signals have a constant phase and amplitude co-variation while a value of 0 indicates that two signals are independent, not having any phase or amplitude relationship (reviewed in Halliday & Rosenberg., 1999; Mitra & Bokil., 2008). I will only describe the averaged coherence among electrode pairs within a 1.0 mm^2 area. Although the analysis of the correlation between the coherence of each pair and distance can give us some insight in how the auditory cortex might process sensorial information, this analysis was not performed. This is because in order to perform recordings in awake rats we used a silicone that covered the exposed cortex in combination with independently movable electrodes. Thus, it was not possible to visualize the electrodes being lowed in the cortical surface or guarantee that they entered the cortical tissue in a 90° angle in relation to the cortical surface. Hence, it was not possible to assure that the electrodes were in the same cortical plane. Moreover, although the electrode array always had a 1.0 mm^2 dimension, during the process of finding the best recording conditions we constantly adapted the electrode array which prevented us from being certain about the exact relative position of each electrode within the array. These technical limitations prevented us from having a more detailed description of the coherence by distance.

In order to compute the power spectrum, spectrogram, coherence spectrograms, and coherence of the LFP signal we used a time bandwidth product of 3 and 5 Slepian taper functions in 125 to 150 ms data epoch windows, which effectively concentrates the spectral estimative in approximately 20 Hz. The spectrogram was computed using 125 ms overlapping windows in 10 ms steps. For the spike-LFP and spike-spike coherence I used a bandwidth product of 5 and 9 slepian tapers functions (in order to reduce the

variance of the signals). Therefore, given the small windows used throughout this dissertation, it was not possible to study modulations of low frequency ranges by auditory stimulation. Thus, I group the low frequencies in alpha/beta frequencies.

The chronux software provides measurements of 95% confidence interval of the spectral and coherence estimate which was used to test significant differences of the power spectrum and coherence values between time intervals after stimulus onset and baseline levels. The spectrum estimates were assumed to have $\chi 2$ distributions, because the number of trials is equal to 20 for each channel which yield large samples (Jarvis & Mitra, 2001). For the estimate of coherence values the significance levels were calculated by estimating the variance using the jackknife error bars methodology over tapers and trials. The jackknife method is a resample statistical methodology that leaves one taper estimation out for each coherence estimate across tapers. This creates a set of coherence estimations in which a variance can be computed and tested for difference in means by using a non-parametric t-test (Thomson & Chave, 1991; Efron & Tibshirani, 1993; Pesaran et al., 2002). To compare the power spectrum density depicted in Figure 2.2 and the coherence spectrum I used a non-parametric Arvesen's Jackknife U statistical test implemented in MATLAB by the two_group_test_spectrum (or two_group_test_coherence) test functions available at chronux.org.

The increase in power across different frequencies observed in the spectrogram was further quantified by computing the LFP power spectrum in 150 ms time epochs after the tone and statistically comparing it to 150 ms time window during baseline using a paired student t test. Increases in power evoked by the tone were normalized to baseline according to the formula Pi-Pb/Pi+Pb, in which the power of the period of interest (Pi) is

subtracted from the power of the baseline (Pb) and divided by the sum of both powers. This calculation creates an index in which a normalized power towards +1 indicates increase in power in relation to baseline and the normalized power equal to -1 indicates decrease in power in relation to baseline. These normalized power values were then used to compute significant differences among power at the alpha/beta range (1-30 Hz), gamma range (40-70 Hz), and high gamma range (90-150 Hz). We used a t student test, paired t student test or ANOVA followed by a Scheffe post hoc test at 0.05 significance level provided by MATLAB in order to detect significant differences among different frequency ranges.

Auto-correlogram analysis

In order to quantify whether neurons in A1 display oscillatory spiking in response to tones, the auto-correlogram of each neuron was computed followed by a estimation of its power spectrum (PSD). The temporal pattern of the spike trains was examined by computing the auto-correlogram of 200 ms after tone onset. Auto-correlogram histogram (ACH) functions were calculated from the spike trains generated by 60 tone presentations that were binned at a 1.0 ms resolution and normalized by the number of spikes in the spike train. To test for the hypothesis that the neuron displays oscillatory spiking, I also generated a poisson spike train that matched the mean firing rate for each individual neuron. After calculating the auto-correlogram for each neuron and its poissonian neuron counterpart, I then proceeded to calculate the spectrum of the auto-correlogram. The multitaper power spectrum with bandwidth/time product to 5 and 9 slepian taper was used to compute the PSD of the ACH. The non-parametric Arvesen's Jackknife U statistical t test provided by the chronux software package (the two_group_test_spectrum

function) was used to test significant differences between the PSD of each neuron and the PSD of the poisson spike train.

The synchronization of spike trains was also estimated by calculating the cross-correlogram functions (CCH) of simultaneous recorded MUA during 200 ms intervals of the baseline and during 200 ms after the tone onset (T1 interval). The CCH were calculated using the NEX software built in CCH function, which counts the number of spike coincidences for various time shifts (-200 ms to +200 ms) of each MUA train pair in a 1 ms bin size. The CCH was normalized by dividing the spike coincidences by the total number of bins, which gives a probability of coincidences during each interval analyzed (CCH coefficients). In order to remove spurious correlations due to sensory stimulation, we subtracted the shift-predictor from the CCH (Perkel et al., 1967a; 1967b). We then averaged the CCH pairs from each experiment during 200 ms of tone onset and baseline in which one example is displayed in Figure 2.9a. In order to have a measurement of correlation strength of the CCH across experiments we compared the CCH coefficients at half height peak during the T1 interval and the baseline for 190 averaged CCH pairs. In order to have a measurement of the temporal dispersion between the correlated spikes train pairs, we also computed the width at half height peak for each CCH pair and averaged them during baseline and the T1 interval. We used a student t test to detect significant differences between baseline and T1 interval.

In order to detect LFP oscillations induced by tones, I also computed the auto-correlogram for each LFP site. The auto-correlograms of ten randomly selected trials of each LFP site was computed by using the MATLAB xcorr function (MATLAB, MathWorks, Natick, MA, USA) during 0 ms to 200 ms followed tone onset. I used a bin

window of 1.0 ms with time delays of -200 ms to +200 ms to compute each LFP auto-correlogram. Each time bin correlation is expressed as correlation coefficients. The correlation coefficient at zero lag have by definition the highest value which is assign a value equal 1,0 and the correlation coefficients of the other various time lag shifts (± 200 ms) are normalized accordingly to the auto-correlation at this zero lag. Figure 2.3 B shows an example of the auto-correlogram of the LFP trace displayed in Figure 2.3A.

2.3 Results

Spike train analysis

Whenever possible, tuning curves of the MUA clusters were generated in an attempt to confirm that I was recording from the primary auditory cortex. Figure 2.2A shows an example of a MUA that has a V-shape tuning curve. The color-coded z-axes shows the baseline normalized firing rate (50 ms post-tone onset divided by mean 100 ms baseline) for each tone frequency across tone intensity. Figure 2.2B shows the raster plot (top) and the PSTH for this MUA cluster. Note that it shows short latency and also it had characteristic MAEP responses (not shown). This result combined with the typical shape and latency of MAEP across the recordings performed in awake (this chapter) and behaving rats (following chapters) indicates that the recordings were performed in the primary auditory cortex.

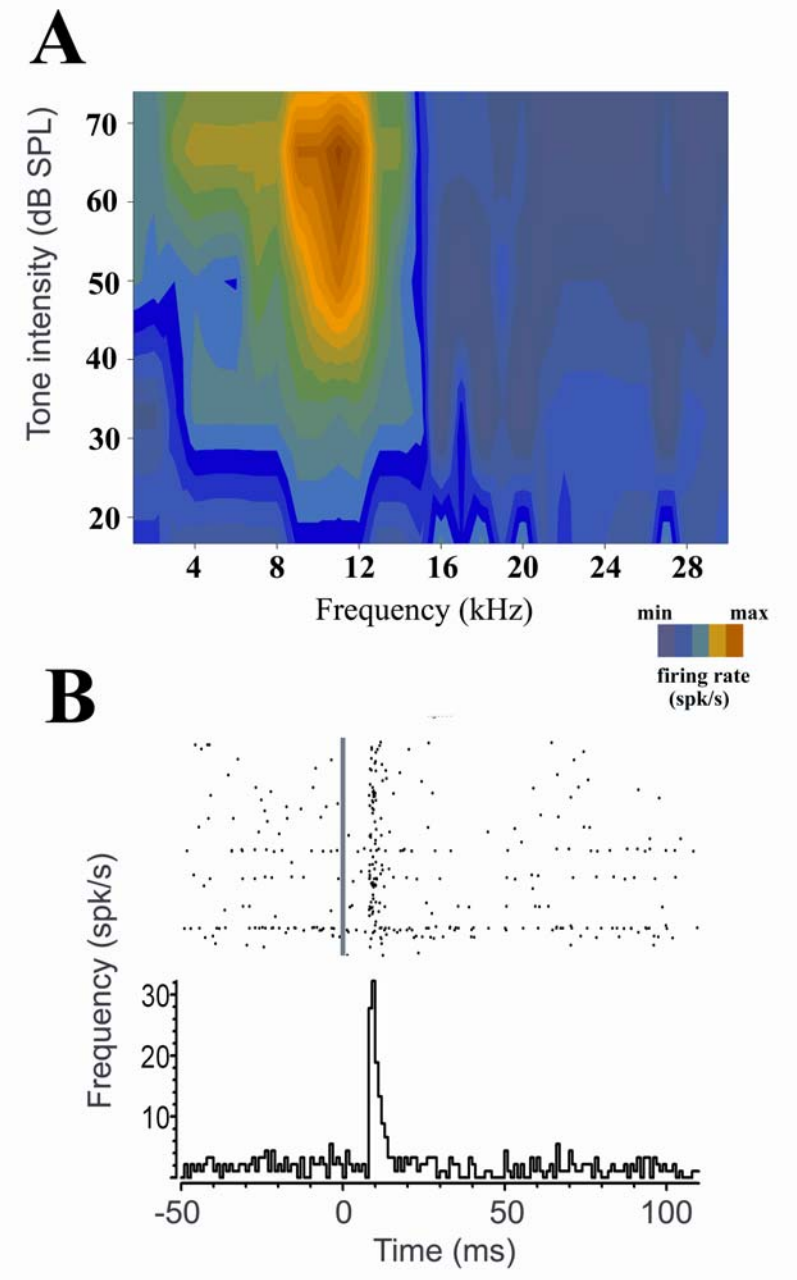

Figure 2.2. The MUA recordings were performed in A1. A) Figure 2A shows a V-shape tuning curve of MUA that is characteristic of the A1. Ordinate is tone intensity (dB SPL) and abscissa is frequency of the tones (kHz), the z-axes is color-coded baseline normalized firing rate. Figure 2B) shows the raster plot (top) and the PSTH (1 ms bins) of this MUA. Each dot corresponds to a spike, the vertical gray bar is tone onset. Ordinate is frequency (spk/s) and abscissa is time (ms).

Figure 2.3 shows several analyses performed in the spike train that demonstrates spike oscillations to the auditory stimulus. Figure 2.3A shows the averaged and smoothed PSTH with a 5 ms gaussian window of the 63 MUA demonstrating short latency response to the tone onset. These neurons maintain a high firing rate for up to 80 ms post stimulus onset (Figure 2.3A). I computed the inter-spike histograms (ISI) in order to verify whether these neurons have a high concentration of short ISI which could indicate a oscillatory spike train in response to tone. Figure 2.3B shows an example of a typical neuron in A1 that shows peaks of inter-spike intervals at short intervals (5 ms-10 ms, 15 ms, 25 ms, and 50 ms). Moreover, I also generated 63 poisson spike trains with same firing rate as the 63 MUA and computed the ISI for both data sets. I found a high concentration of ISI at < 20 ms during the T1 interval of the MUA spike train. Figure 2.3C shows the averaged ISI interval of the T1 interval of the neurons recorded in the auditory cortex (black) compared to a mean poisson ISI distribution (gray).

The MUA oscillatory spiking was further investigated by computing auto-correlograms (ACH) during the T1 interval. Figure 2.3D shows a typical auto-correlogram of a neuron in A1 that shows oscillatory spiking at high frequency range. The ACH of the MUA was further compared to an ACH generated from the poisson spike train. The power spectrum estimate (PSD) of the ACH between T1 and poisson intervals was statistically compared using a non-parametric Arvesen's Jackknife U statistical test implemented in MATLAB by the two_group_test_spectrum test function available at chronux.org. I detected significant differences between the PSD of at low frequency range (1-30 Hz) in 48% and high frequency range (40-150 Hz) in 37% of the neurons analyzed (Arvesen's Jackknife U statistical t test, $p<0.01$). Figure 2.3E shows an

example of the 200 ms interval mean ACH during T1 interval (black) and the poisson spike train (gray). The peak at origin was omitted in order to highlight secondary peaks in the ACH. The ACH shows secondary peaks at intervals below 60 ms. Figure 2.3F shows the PSD analysis from 6 simultaneous recorded neurons of a particular recording session. This figure shows the comparison of the T1 interval and the PSD of a poisson interval. We observed that there is an increase in amplitude at alpha/beta and gamma frequency ranges as compared to a poisson spike train distribution.

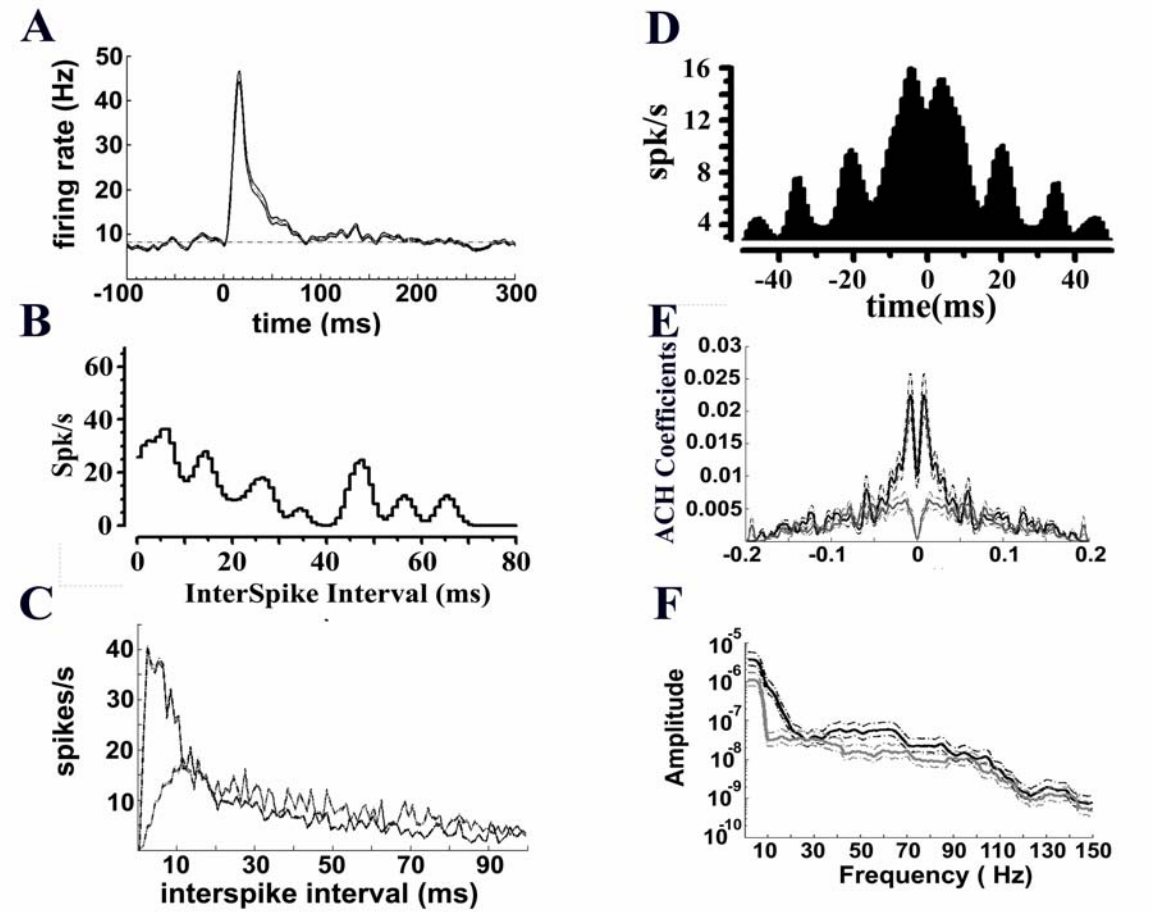

Figure 2.3. Neurons in the auditory cortex show oscillatory behavior in response to auditory stimuli in the awake rat. A) Figure 1a shows the averaged PSTH (mean: dash lines; SEM: solid lines; background firing rate: gray dash line). B) The middle left graph shows an example of the interspike interval (ISI) of a typical neuron in A1. C) The bottom left graph shows the ISI for the population of neurons in the time period (T1) of 200ms after tone onset (black line) and for a population of neurons with a poisson spike train distribution (grey line) with equal firing rate of the neurons in A1 during the T1 time period. D) The right top graph shows an example of the neuron auto-correlogram of A1. E) The middle right graph shows the averaged auto-correlogram for an experiment with 6 simultaneous recorded MUA in A1 during the T1 interval (black line) compared to the correspondent poisson spike train matching the firing rate for each of the 6 MUA sites(grey traces). F) The bottom right graph shows the PSD along with its 95% confidence interval (dash trace) of the cross-correlogram showed in Figure 1D (black traces= A1 neurons; gray traces= poisson neurons).

LFP analysis

The auto-correlogram of the LFP trace was measured to further explore if the high frequency oscillations observed at MUA levels is also seen at the population level. Figure 4A shows an example of a single LFP trace in which we see the MAEP to the tone onset followed by an oscillatory pattern. Figure 2.4B shows the normalized auto-correlogram (ACH) by the highest correlation coefficient at ± 100ms time lags. This analysis clearly demonstrates that the LFP traces have an oscillatory pattern after tone onset. The frequency of oscillations appears to be around 100 Hz, which is in the high gamma frequency band (90-150 Hz). The ACH analysis for the LFP traces was performed in 10 single trials per LFP site revealing that 60% of the sites show this oscillatory pattern. However, there is great variability across trials and sites.

The filtered LFP demonstrates that the auditory cortex show time-locked oscillations at gamma frequency range (40-70 Hz) and high gamma range (90-150 Hz) in response to auditory stimuli (Figure 2.5). Moreover, the filtered single LFP traces show a second induced high frequency oscillatory burst which is not time-locked to the. Figure 2.5Ai shows a single unfiltered LFP trace in which we can see the MAEP response followed by a fast oscillation at approximately 50 ms and a second burst at 100-150 ms after the tone onset. Figures 2.5Aii and 2.5Aiii show the LFP trace filtered at 40-70 Hz and 90-150 Hz respectively. The high gamma frequency range oscillation pattern started immediately after the MAEP and lasted approximately 80-100 ms after the tone onset. The low gamma frequency range is more restricted in time, lasting a few milliseconds after the tone onset (see Figure 2.5). The time-locked high frequency oscillations were observed in all the channels analyzed (n = 63).

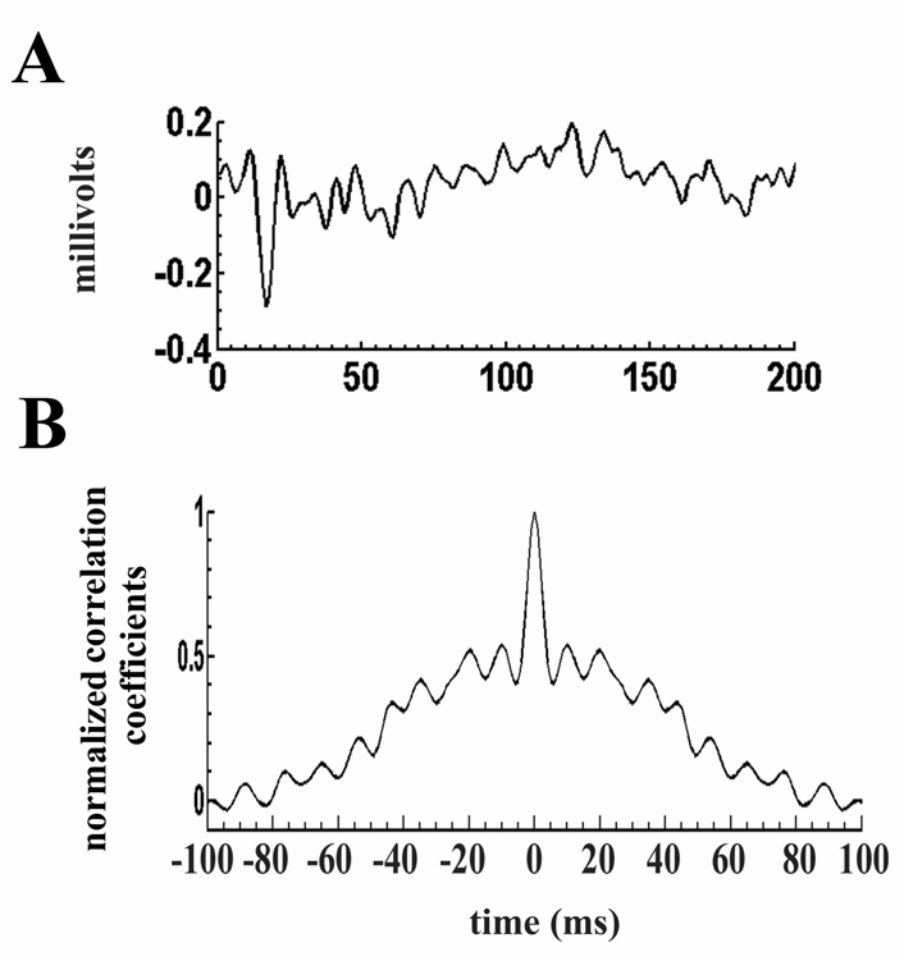

Figure 2.4. LFP site in the auditory cortex show oscillatory behavior in response to auditory stimuli in the awake rat. Figure 3A shows a single LFP trace (abscissa= time (ms); ordinate = millivolts) . Figure 3B shows the auto-correlogram of this trace in 1ms bins at ±100ms time lags. The highest coincidence value was set to 1 and the other values were normalized in relation to it. (abscissa= time (ms); ordinate=normalized ACH coefficients).

I also observed induced bursts of gamma and high oscillations of up to 300 ms after the tone onset. Figure 2.5Aii and 2.5Aiii exemplifies these findings. The high frequency range has an oscillatory burst at 100-150 ms and at 250-300 ms while the gamma frequency range has an oscillatory burst at 250-300 ms. We saw these induced oscillation patterns in 60% of the channels analyzed. However, these induced oscillations are quite variable across rats and electrodes. Moreover, they had a latency that was quite variable across trials and did not show any obvious time-locked pattern to the auditory stimuli used in this study. Figure 2.5Bi, 2.5Bii, and 2.5Biii shows the average and standard error of the mean (SEM) of 20 trials from a single channel. These averaged traces show the time-locked oscillations to the tones, but not the induced oscillatory pattern.

The LFP spectrograms using the multitaper methods are shown in Figure 2.5C. Figure 2.5Ci shows the spectrogram between 1 to 150 Hz and Figure 2.5Cii shows frequencies filtered between 50 to 150 Hz. Figure 2.5Ciii shows specific frequency bands for frequencies at 20 Hz, 40 Hz, 80 Hz and 120 Hz. Moreover, Figure 2.5Ciii suggests that the power of < 20 Hz frequencies is maintained above baseline levels up to 250 ms after the tone onset, the same does not occur for the power of high frequency. The spectrogram suggests that the auditory stimulation increases power of low frequencies and high frequencies during a time period of approximately 250 ms for low frequencies and 150 ms for high frequencies.

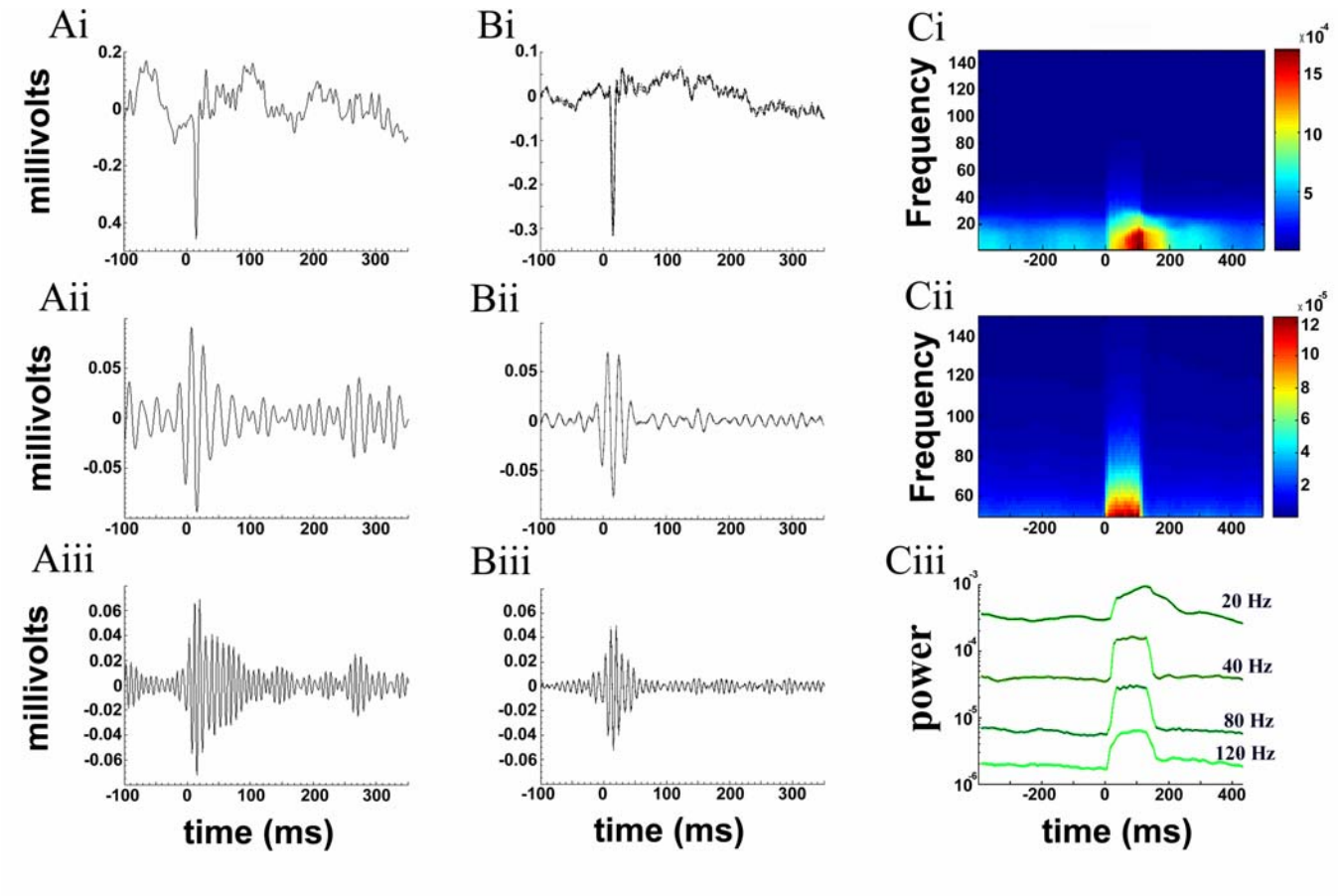

Figure 2.5. Auditory stimuli evoke high frequency oscillations in the auditory cortex.5A) Figure A shows example of three trials from one LFP site in which 0 ms is tone onset. Figure 2.5Ai shows the raw LFP trace (1-170 Hz). Figure 2.5Aii shows the same trace filtered between 40 Hz and 70 Hz. Figure 2.5Aiii shows the trace filtered between 90 Hz and 150 Hz. Figures 2.5Bi, 2.5Bii, and 2.5Biii show the average of 20 trials. Figure 5Ci shows the spectrogram of all sites for 1-150 Hz and Figure 5Cii for 50-150 Hz only. Figure 5Ciii shows the mean power estimative and 95% confidence interval for 20 Hz, 40 Hz 80 Hz and 120 Hz of the spectrogram depicted in Figure 2.5 Ci.

The spectrogram provides us a view of the change of power in the components of the LFP over time. I further quantified it by calculating the PSD of 150 ms intervals at specific time periods and normalized it by baseline. I selected a time window T1 that encompassed 50 ms to 200 ms after the tone onset and a time window T2, which encompassed 200 ms to 350 ms after the tone onset. The first 50 ms after tone onset were excluded from the PSD measurements, because the fast and sharp P1 and N1 components of the MAEP have a big increase in power that might distort the PSD estimate. During the T1 period there was a significant increase (paired t-student test, $p<0.01$) in total power in all frequencies studied (1-150 Hz) in relation to the baseline. There were also significant differences in power between T1 and T2 (paired t test, $p<0.001$). During the interval T2, which ranges from 200 ms to 350 ms after the tone onset, the increase in the total power was not statistically significant from baseline levels (paired t test, $p = 0.7737$). However, by observing the power spectrum it was apparent that there were specific power modulations restricted to some frequency ranges but not others. Thus, I tested the null hypothesis that there are no differences in power between T1 or T2 and baseline at specific frequency ranges. There were significant differences for the low frequency range, gamma frequency range, and high gamma range for T1 and T2 periods in relation to baseline levels (paired t test, $p<0.001$). I took the mean of the PSD for each frequency across trials/channels, normalized it by the baseline and tested the hypothesis that different frequency ranges in periods T1 and T2 have a different power distribution.

Figure 2.6 shows that the increase in the normalized power during T1 was different among alpha/beta frequency, gamma, and high gamma frequency range (ANOVA, $F_{(2,84)}=280.05, p<0.01$), and these differences were significantly different

among all the frequencies tested, where the highest increase in normalized power was at alpha/beta range, followed by high gamma, and gamma range (Scheffe post hoc test, $p<0.05$). The normalized power from different frequency ranges of the T2 time period were significantly different (ANOVA, $F_{(2,42)}=87$, $p<0.01$), where the increase in normalized power during T2 was greater at very high frequencies (Scheffe's post hoc test, $p<0.05$), but showed a decrease in power in relation to the baseline for alpha/beta and gamma frequencies. These results showed that tone increases the occurrence of oscillations during 150-200 ms after stimuli onset, that relative increases in power were higher for alpha/beta and high gamma frequencies during the first 150 ms after the tone and for high gamma ranges afterwards.

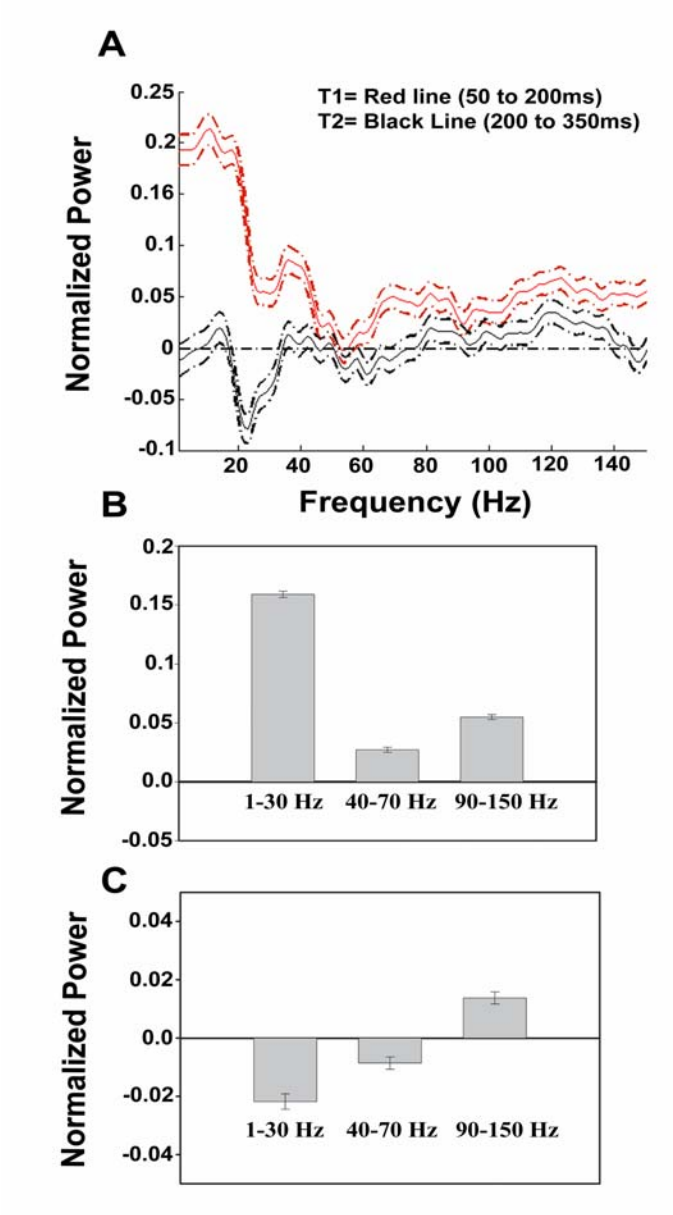

Figure 2.6. Normalized power spectrum density of time T1 (50 ms to 200 ms) and T2 (200 ms to 350 ms) by baseline (-100 ms to -250 ms). A) Top graph shows the mean (± SEM) normalized power of T1 (red) and T2 (black). B) Middle graph shows a bar plot (mean and SEM) of different frequency bands normalized by baseline during the T1 and C) T2 time interval. These figures show the power comparison of frequencies at alpha/beta band (1-30 Hz), gamma band (40-70 Hz), and the high frequency range (90-150 Hz). The solid black line in the top graph shows the normalized power in which there is no difference between baseline and T1 or T2 period.

LFP coherence analysis

After characterizing increases in power I turned to study the synchrony among the simultaneously recorded LFP sites. The coherence analysis could reveal if the observed increase in power of the high frequency bands are widespread within A1 or if it is a local phenomenon in which local neuronal populations that are ≈300 μm apart synchronize their activity locally but not globally. Figure 2.7 displays four simultaneous recorded sites from -100 ms to 330 ms after tone onset at different frequency bands. I filtered the LFP raw signal (1-170 Hz, top four traces in Figure 2.7A) from four LFP sites at 40-70 Hz (middle four LFP traces) and 90-150 Hz (bottom four LFP traces). It was very difficult to detect any significant differences among the LFP sites by visually inspecting the wide band LFP (four top traces) and the filtered LFP at gamma range (middle four traces). However, I detected subtle differences in the LFP filtered at high frequency range (90-150 Hz, bottom four traces) both in amplitude and latency of short time periods in some sites. I observed that some bursts of oscillatory behavior have different amplitudes at the baseline and after the tone onset.

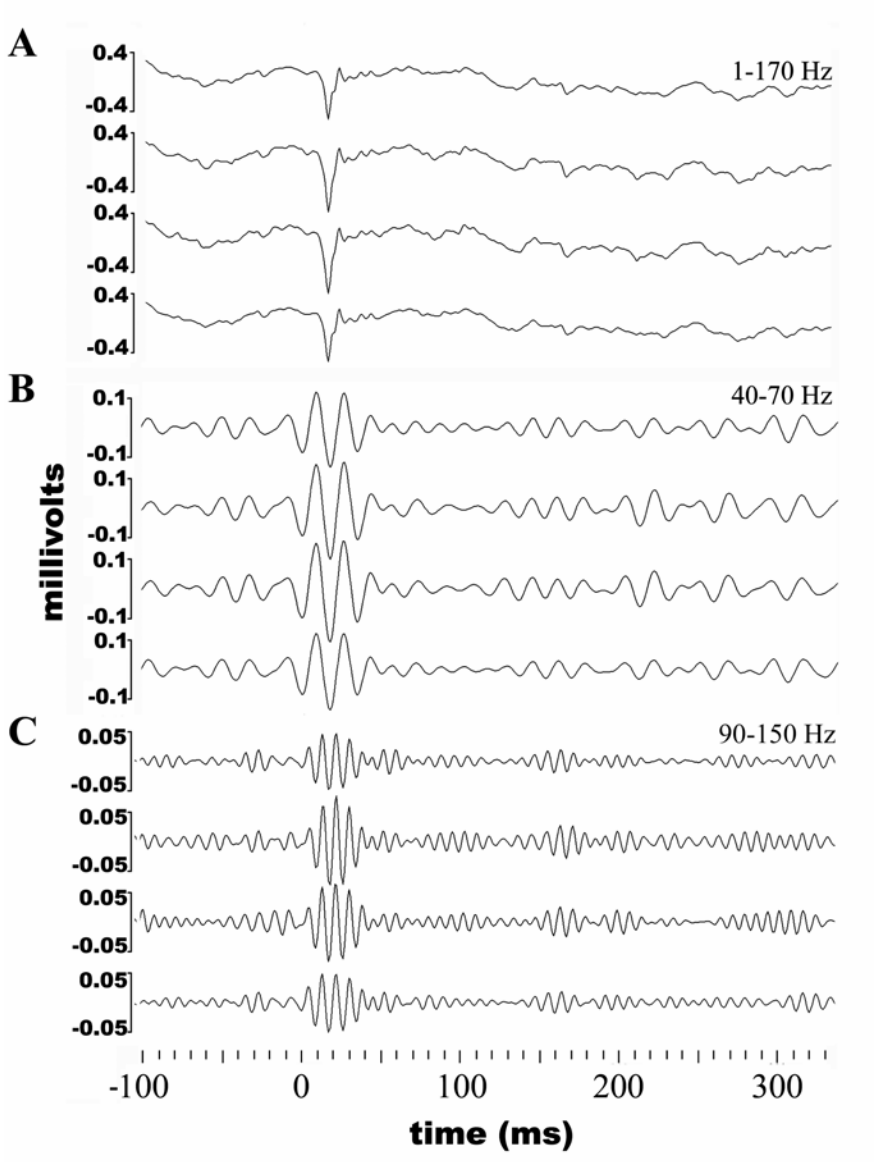

Figure 2.7. Tones synchronize the LFP in the auditory cortex of the rat. A) Top four raw LFP traces (1-170 Hz) show simultaneous recordings during a 430 ms time period.. B) Middle four traces show same recordings filtered in the gamma frequency range (40-70 Hz). C) Bottom four traces show recordings filtered in the high gamma frequency range (90-150 Hz). Ordinate is millivolts and abscissa is milliseconds. Time 0 ms is tone onset

I further analyzed the coherency of the LFP traces by computing the coherence spectrogram (coherogram). Figure 2.8A shows the coherogram among 150 possible combinations of 63 electrode pairs unfolding in time in the various frequency ranges. This analysis shows that the MAEP increases the coherence among LFP sites which extends to a wide frequency range. Moreover, this increase in coherence last for 100 ms and sharply decreases to baseline level afterwards. This analysis shows that the coherence at low frequency range (< 35 Hz) is high at baseline levels and drops at higher frequencies. I also noted that while the coherence at low frequency range is high and basically constant at baseline levels, the coherence at high frequency (40-100 Hz) has very complex dynamics (Figure 2.8A). There are peaks of high coherence that last for approximately 100-300 ms and suddenly stop, reappearing moments later. This baseline activity pattern is disrupted by tone stimulation, which evokes a very high degree of coherence across a wide frequency range, and reappears again after 100 ms after tone onset. The coherogram depicted in Figure 2.8A provides us with a measure of the coherence varying over time. Figure 2.8B and 2.8C display coherence during time T1 (50 ms to 200 ms), and time T2 (200 ms to 350 ms) compared to baseline levels (-100 ms to -300 ms) with their respective 95% confidence interval. Moreover, I used a non-parametric Arvesen's Jackknife U statistical t test to test the null hypothesis that the spectral coherence at T1 is not different from baseline levels. I found significant differences for frequencies below 25 Hz during T1 ($p<0.01$). However, I did not find statistical differences during time T2 and baseline. The results demonstrates that coherence is high across at low frequency range (<20 Hz) in the first 200 ms after the tone onset and decreases during 200 ms to 350 ms post tone onset.

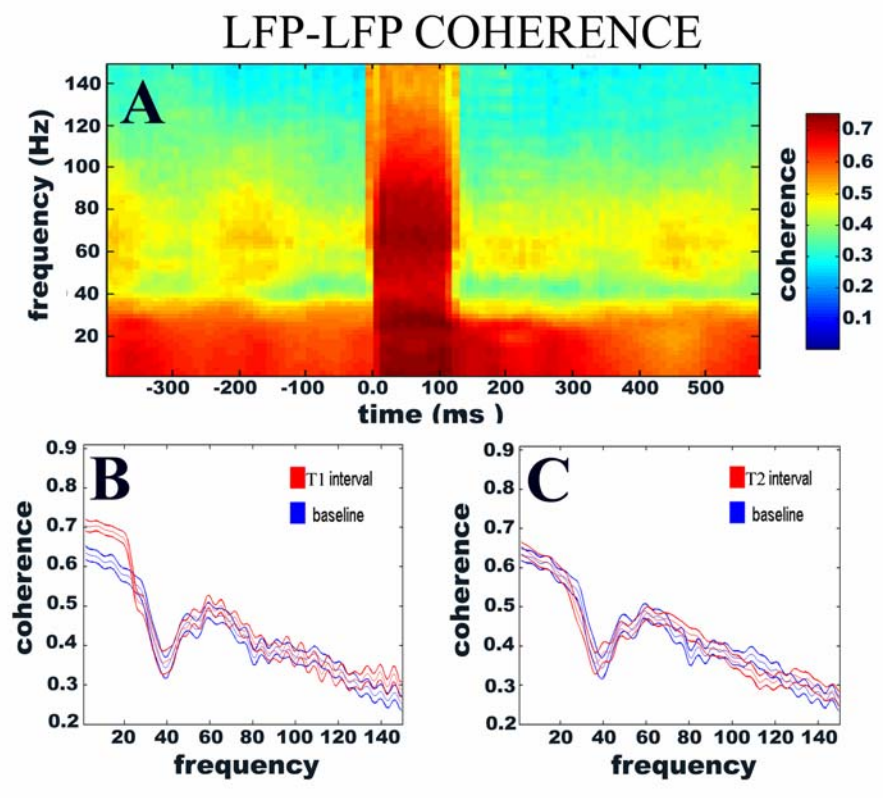

Figure 2.8. Auditory stimulation increases the coherence at low frequency band. A) Top figure shows the average coherence spectrogram (coherogram) for 150 LFP pairs. Ordinate: frequency (Hz); abscissa: time (ms); z axes: coherence (0-1 range). B) Bottom left figure shows the comparison between coherence during baseline (-100 ms to -300 ms, blue traces) and T1 interval (50 ms to 200 ms, red traces). C) Bottom right figure shows the comparison between coherence during interval T2 (200 ms to 350 ms, red trace) and baseline. Thick traces show 95% confidence intervals using a Jackknife methodology.

I further quantified the coherence results by normalizing the coherence values of T1 and T2 by the baseline and statistically comparing them. There is a higher coherence in time T1 than time T2 (t test, $p<0.001$). These results demonstrate that coherence increases 150 ms after the tone onset and decreases to baseline levels afterwards. Moreover, there is a high coherence at the low frequency range frequency during T1 (<20 Hz). I then compared the averaged coherence at alpha/beta (1-30 Hz), gamma (40-70 Hz) and high gamma (90-150 Hz) and found that the coherence decreases as function of increases in frequency during the T1 interval (ANOVA, $F_{(2,87)}=835.37$, $p<0.001$; followed by post hoc Scheffe test, $p<0.05$) as well as during the T2 interval (ANOVA, $F_{(2,87)}=193.81$, $p<0.001$; followed by post hoc Scheffe test, $p<0.05$). Therefore our results show that for T1 and T2 periods, alpha and beta frequency ranges (<30 Hz) have a higher coherence than gamma frequency ranges (30-90 Hz) which have a higher coherence than high gamma frequency ranges (90-150 Hz).

Spike train and LFP coherence analysis

The coherence analysis strongly suggests that the increase in synchrony in response to tone is caused by a neuronal synchronization of local networks. To further explore this possibility, I analyzed the unfolding of the coherence between the LFP signal (continuous process) and the spike train (point process) over time by computing coherence spectrograms (coherograms). I used an overlapping 125 ms window that was offset by 10ms steps of the cross-spectrum of the two signals (a point process and a continuous signal). Figure 2.9A shows the result of 49 MUA-LFP coherence analysis pairs. I observed that there is a high coherence level of low frequencies (<15 Hz) in the baseline activity. Moreover, there is a high coherence peak specifically at beta range 25-

30 Hz throughout baseline. The coherence in this frequency range greatly increases and expands for higher frequency ranges (up to 60 Hz) in the first 100 ms after the tone onset. After this sharp increase, the coherence values apparently decrease to below baseline levels at 100 ms to 300 ms following the tone onset. Auditory stimuli induce increases in coherence in frequencies of up to 60 Hz between the LFP and the spike spectrum in the first 100 ms after the tone. However, the coherence apparently reaches its peak at the same 25-30 Hz frequency range that displayed a high coherence at the baseline levels. Therefore, it seems that tones amplify ongoing baseline coherence at this specific frequency range.

In order to further quantify the observed dynamics in the coherogram between the LFP and the spikes we computed the coherence and its 95% confidence intervals. I compared the 150 ms after tone onset (time T1) to the baseline coherence (150 ms to 300 ms before tone onset). The coherence value is statistically different between these two time periods (Jackknife U test, $p<0.001$) and is higher for the T1. Figure 2.9B shows the coherence values for a wide range of frequencies (1-150 Hz), including their 95% confidence interval, which was calculated using the jackknife methodology (Mitra & Bokil, 2008). This analysis confirms that there is an increase in coherence between spike trains and the LFP signal in relation to the baseline at the gamma ranges (30-60 Hz), but not at high gamma frequency ranges (90-150 Hz) (Figure 2.9B). I further quantify this observation by comparing frequency differences within the T1. During this time period the mean coherency distribution is different among the alpha/beta (1-20 Hz), low gamma (30-60 Hz), and high gamma (90-150 Hz) frequencies (ANOVA, $F_{(2,57)=}392.07$, $p<0.001$). The highest value for coherence is at the low end of the gamma range

frequency (30-60 Hz), followed by low frequencies (<20 Hz), and then by high gamma frequencies (90-150 Hz) (ANOVA followed by a post hoc Scheffe test, $p<0.05$). I also compared mean coherence values for alpha/beta, low gamma, and high gamma frequency ranges at the baseline. The coherence values for the SPK-LFP during baseline is different among these frequencies (ANOVA, $F(2,57)=425.79$, $p<0.001$), and is higher for the alpha/beta range, followed by the low gamma range and high gamma frequency range (Scheffe, post hoc test, $p<0.05$).

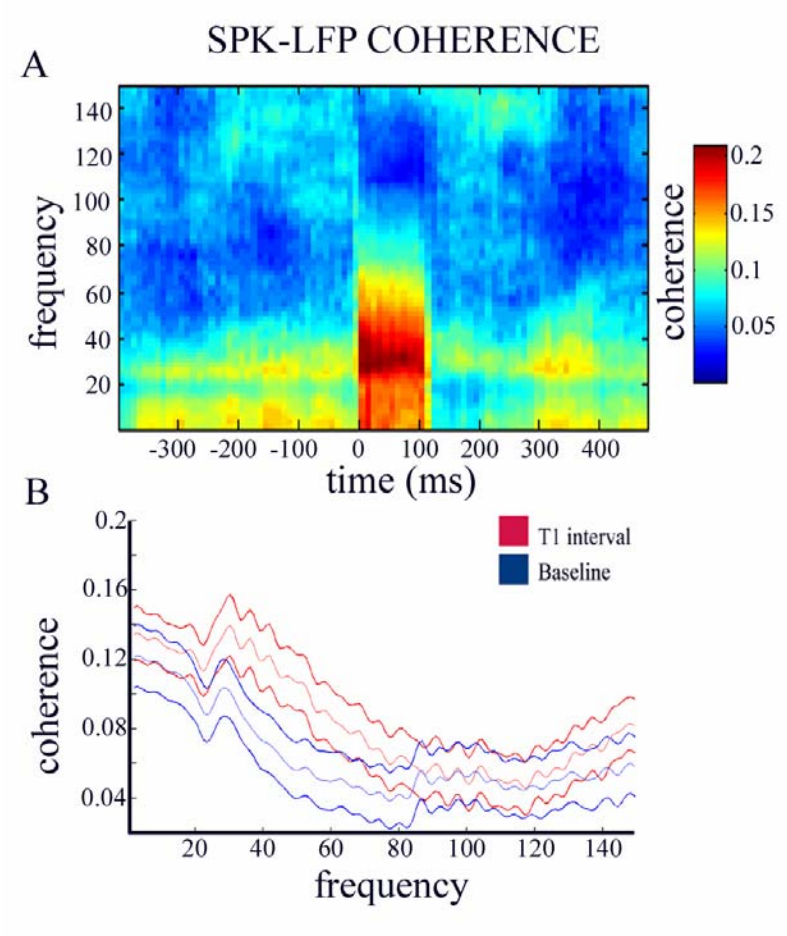

Figure 2.9. Auditory stimuli synchronize small neuronal networks at gamma frequency range. A) Top figure shows the averaged 49 pairs of spike-LFP coherogram (Ordinate: frequency (Hz); Abscissa: time (ms); Z axes: coherence (0-1 range). B) Bottom figure shows of the quantification of the spike-LFP coherency by plotting the coherence along with 95% confidence interval of 150ms intervals during T1 (50ms to 150ms, red trace) and baseline period (-150ms to -300ms, blue trace).

The SPK-LFP coherence results show that auditory stimuli change the dynamics of neuronal coherence between spikes and the LFP signal throughout the auditory cortex. At the baseline this coherence smoothly decreases as a function of frequency, and is highest at low frequency ranges. The processing of tones by the auditory cortex increases the coherence at low gamma frequency range (Figure 2.9A and 2.9B) without, however, changing the coherence at the high gamma frequency range (90-150 Hz).

Spike train synchrony analysis

To further explore if simple auditory induces widespread synchrony in the A1 neuronal network I measure the synchrony among MUA. It is important to note that these MUA are separated by 250-300 μm. I order to test whether neurons synchronize their firing rate, we primarily performed a cross-correlation analysis (CCH) of 190 spike train pairs after and before the tone onset. The CCH analysis shows that neurons in A1 synchronize their activity in order to process sensory information (Figure 2.10). Figure 2.10A shows an example of one experimental session in which we averaged the CCH during the T1 interval and compared it to the baseline from a total of 10 neuron pairs in 60 trials each. I observed a single positive peak around the origin of the ACH during T1 and baseline. The increase in spike train synchrony was quantified by computing the CCH coefficients at half height peak after and before the tone onset. This analysis is shown in Figure 2.10B, which shows mean and SEM coefficients of 190 CCH pairs. This figure shows that the correlation strength across the population is higher during the time period T1 than during the baseline (t student test, $p<0.001$). Moreover, we quantified the degree of temporal dispersion of spike trains around the CCH origin by computing the peak width at the half height of the CCH for each pair and then averaged them. Figure

2.10C shows that the averaged width at half height peak during T1 is broader than baseline levels (t test, $p<0.001$). Therefore, tones induce neurons to increase the probability of synchronous firing as well as the temporal dispersion of the firing. Moreover, we observed a symmetric secondary peak around 60 ms in the averaged CCH in 10 of the 11 experiments analyzed. This result suggests that neurons separated by at least 250-300 μm have a degree of synchrony at beta frequency ranges (see red trace at Figure 2.10A).

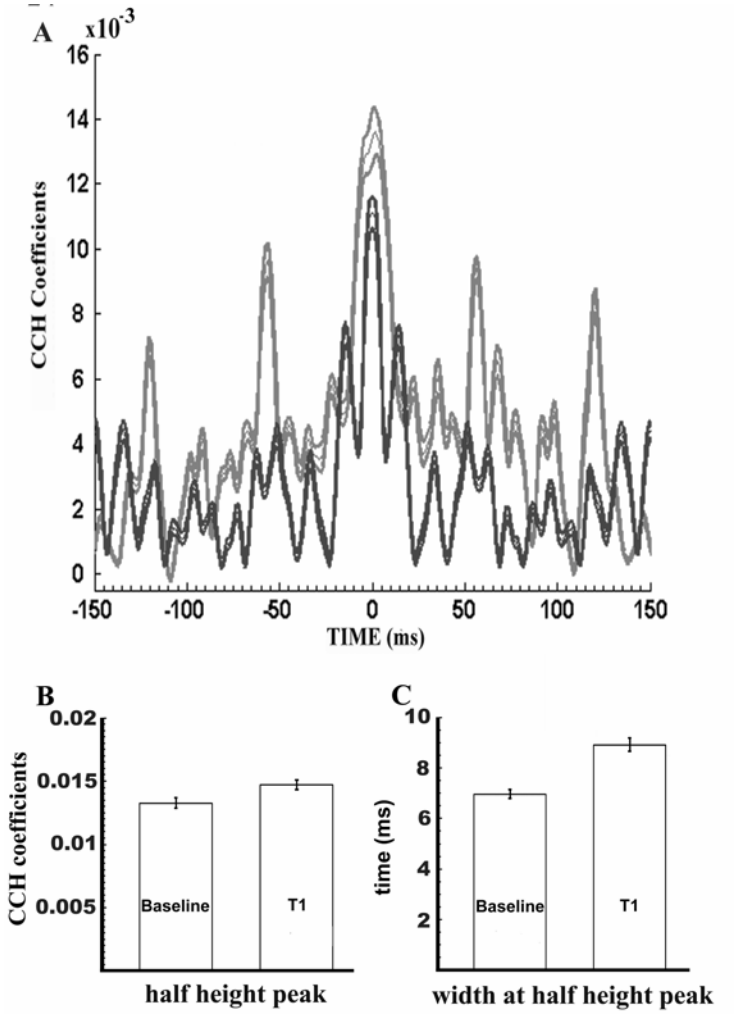

Figure 2.10. Auditory stimulation increases the synchrony of MUA sites and increases their temporal dispersion. A) Top figure shows the mean cross-correlograms (CCH) from 190 MUA pairs (63 MUA across 7 rats) over 20 trials for each MUA during 200ms interval after tone onset (T1, gray trace) and baseline (Baseline, black trace). B) Bottom right figure shows the mean ± SEM of the CCH coefficients at half height peak for T1 interval and Baseline interval. C) Bottom left figure shows the mean ±SEM of the width at the half height peak (ms) for T1 and baseline intervals.

The previous analysis reveals that neurons in A1 increase their synchrony after tone onset. To further explore if this increase in synchrony occurs at some specific frequency band I measure the spectral coherence among the spike train of the simultaneously recorded MUA sites. The measurements of coherence among the population of MUA show that neurons in the auditory cortex synchronize their firing at alpha/beta frequency ranges. The coherogram in Figure 2.11A shows the coherence among simultaneously recorded MUA pairs averaged across different rats unfolding in the time axes. This figure demonstrates that neurons in A1 have a coherent firing below 30 Hz frequency ranges at baseline levels. After the tone onset, coherence increases at these low frequency ranges and apparently also increases in frequencies ranging from 1 to 60 Hz. This increase in coherence lasts approximately 100 ms. Figure 2.11B shows the coherence values along with its 95% confidence during T1 (0-200 ms post tone onset) and baseline (-100 ms to -300 ms before tone onset) periods are significantly different (Jackknife U test, $p<0.001$). Moreover, during the T1 interval the coherence values are significantly different among alpha/beta ranges, gamma and high gamma ranges (ANOVA,$F_{(2,90)=}390.6$,$p<0.001$). Additionaly, the coherene during T1 is significantly higher for alpha/beta ranges (post hoc Scheffe test, $p<0.05$) and are not statistically different between gamma and high gamma ranges. This result shows that neurons dispersed through 1.0 mm^2 of the A1 synchronize their action potentials at the alpha and beta frequency range. However, these neurons do not synchronize their firing rate at the gamma or high gamma frequency range in response to a simple pure tone stimulus.

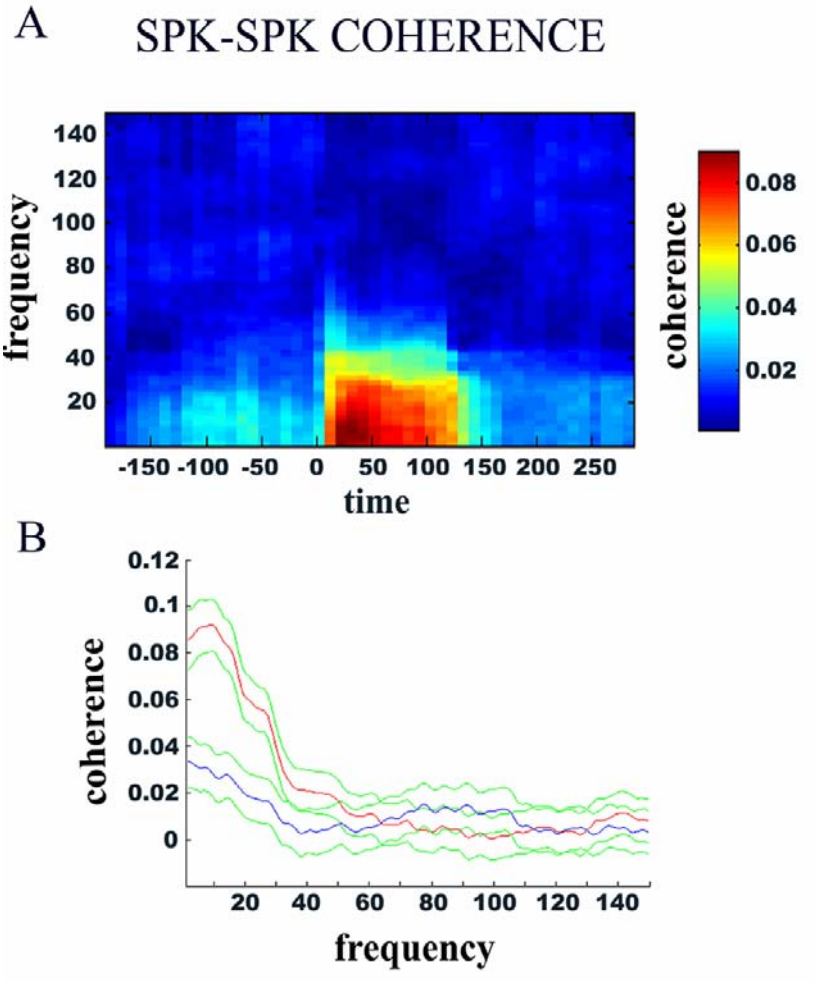

Figure 2.11. Spike train spectral coherence in the auditory cortex increases upon auditory stimulus. A) Top figure shows the averaged coherogram of 150 neuron pairs simultaneously recorded during a 200 ms time period after auditory stimulation. B) Bottom figure shows coherence of these 150 neuron pairs during baseline (blue line) and after tone onset (red line). It shows the coherence plotted (Ordinate) against frequency (Abscissa) along with the 95% confidence interval.

2.4 Discussion

General findings

The experiments performed in this chapter demonstrate the occurrence of gamma and high gamma oscillations induced by the processing of auditory stimuli in awake rats. I extended previous observations by showing that neurons in the auditory cortex show oscillatory spiking at a wide range of frequencies upon tone stimulation. In addition, results from the coherence between the LFP and MUA, strongly suggest that small neuronal assemblies in the auditory cortex have intrinsically coherent activity around 20 Hz that is amplified and extended to a higher synchronous activity at the low gamma range, but not at the very high gamma range. I also show that the coherence among the LFP signals in ongoing baseline levels of activity is dynamically complex and constantly extending up to 40 Hz, with occasional high coherent activity at high frequencies. This coherent ongoing LFP signal is modified by auditory stimulation. It shows a high level of brief coherence below 25 Hz. I also measured the spike-spike coherence among the simultaneous MUA recordings after auditory stimulation. Surprisingly, this analysis shows that despite the increase in the LFP-spike coherence at low gamma frequency ranges (up to 60 Hz), the MUA did not show such coherence. It acts as a low pass filter, in which the MUA is only coherent at low frequency ranges (up to 40 Hz).

High frequency oscillations

I found that neuron clusters in the auditory cortex of the awake rat passively listening to tones show oscillatory patterns that are significantly different from neurons with a poisson distribution. This oscillatory pattern is encountered in nearly 50% of the neurons for the alpha/beta frequency range and in 37% of the neurons at higher frequency

ranges. However, I also noted that while the oscillatory behavior of the neurons studied consistently showed significant differences around 10-25 Hz, the increases in gamma and high gamma ranges were not consistently found at one particular frequency. Some neurons could show oscillatory behavior at 30-50 Hz while others show this oscillatory behavior at 70-90 Hz. One might wonder if this irregular oscillatory behavior could be explained by the fact that we have used sub-optimal sensory stimuli. In this regard, it is important to point it out that previous reports suggested that auditory neurons in the anesthetized monkey have an optimal oscillatory response to tones inside of their receptive field (Brosch et al, 2002). Further experiments should be designed to address whether the occurrence of high frequency oscillations depends on receptive properties.

Our results are in contrast to previous results that did not find any evidence for oscillatory behavior in the MUA spike trains from awake rats in different behavioral states (Cottilon-Williams & Edeline, 2003). It is possible that such a discrepancy could be explained by the different experimental settings and analysis. They defined their oscillations by looking at the main peak in the spectrum after the tone onset or by looking at the PSTH, while we compared the whole spectrum of the ACH after the tone onset to the spectrum of an artificially created poisson spike train with the same mean firing rate of the neuron being studied during a brief time period (200 ms). I chose this approach because the induction of oscillation by tones might be quite subtle, but it is still statistically significant. I showed that the structure of the interspike interval of the spike train after tone stimulation is different from a random distribution. Moreover, we selected a relatively short time period to perform our analysis. The absence of oscillatory neuronal behavior during the ACH might be accounted for by the inclusion of large time periods in

the analysis. There are more periods of no-oscillatory behavior than oscillatory behavior. Therefore, large stretches of no-oscillatory periods tend to "wash out" the side peaks of the ACH. Thus, a combination of stimulus configuration and/or internal states could be the cause of why such variability is encountered in the oscillatory behavior of neurons to auditory stimulus.

The oscillatory behavior of the neurons reported here corroborate initial studies in anesthetized rats (Kelly, 1988; Cotillon & Edeline, 2000a, 2000b; Maldonado & Gerstein 1996) and in anesthetized cats (Eggermont, 1992, 1994) which detected low frequency oscillations at alpha frequencies (8-16 Hz). Previous findings in anesthetized moneys also showed the occurrence of gamma oscillations in the MUA clusters (Brosch et al., 2002). In addition, *in vitro* intracellular recordings from neurons of isolated auditory cortex slices (Metherate et al., 1992; Cunningham et al., 2004), and from the auditory cortex containing intact thalamo-cortical projections in mouse and rats (Metherate & Cruikshank, 1999), as well as intracellular recording in anesthetized rats in vivo (Sukov & Barth, 2001) show that a variety of neurons (fast spike neurons (FS), regular spike neurons (RS) and fast rhythmic bursts (FRB, also known as chattering cells) generate fast sub-threshold and spike train oscillations at gamma ranges in the auditory cortex. These oscillations were generated after intracortical stimulation or after electrical stimulation of the fiber tract. The results presented in this chapter extend these previous observations by demonstrating that tones induce oscillations at beta and gamma frequency ranges in neurons of the auditory cortex in awake rats as well.

The LFP recorded in parallel to the MUA signal showed a clear oscillatory pattern in response to the tones. Previous results have also shown that tones drive oscillatory

activity in neurons of the auditory cortex in anesthetized monkeys (Brosch et al., 2002), and clicks induced gamma oscillations in anesthetized rats (Franowicz & Barth, 1995). However, our results have some differences concerning latency and frequency of the induced gamma frequency range seen previously in anesthetized rats (Franowicz & Barth, 1995) and latency of oscillations in monkeys (Brosch et al., 2002). Previous reports in anesthetized rats show that auditory stimuli induce gamma oscillations 300 ms after the stimuli onset (Franowicz & Barth, 1995). In fact, clicks inhibit ongoing gamma oscillations, and moreover, electrical stimulation of the MGBv also inhibits gamma oscillations during a period of 300-400 ms after a stimulus onset (MacDonald & Barth, 1995; Franowicz & Barth, 1995; Barth & MacDonald, 1996). I show here that bursts of gamma oscillations occur in the first 100 ms and extend up to 300 ms after the tone onset (Figures 2.2 and 2.3), which also has been reported in awake moneys (Steinschneider et al., 2008) and awake mustached bats (Medvedev & Kenwall, 2008). Moreover, tones induce a high frequency response (40-150 Hz) which is comparable to the high frequency response seen in awake monkeys (Steinschneider et al, 2008). The studies in anesthetized preparation are important to establish the existence of high frequency oscillations. However, experiments using simultaneous intracellular and/or extracellular recordings coupled with electrical stimulation in the posterior intralaminar nucleus of the thalamus (PIL) (Sukov & Barth, 1998, 2000; MacDonald et al., 1998; Barth & MacDonald, 1996), electrical stimulation of the thalamic reticular nucleus (TRN) (MacDonald et al., 1998), and nucleus basalis of the basal forebrain (Metherate et al., 1992) demonstrate that those structures strongly modulate the occurrence and latency of gamma oscillations. Therefore, it is likely that in the awake rat these nuclei modulate the oscillatory behavior

of the neuronal population of the auditory cortex caused by auditory stimulation. Thus, the similarity of latency and frequency of induced gamma frequencies in response to sensory stimuli among recordings in awake animas (rats: this report, monkeys: Steinschneider et al., 2008; Fries et al., 2001; bats: Medveded & Kanwal, 2008; and intracranial recordings in humans: Edwards et al., 2005, Tratner et al., 2006) stress the importance of using awake preparations to study gamma oscillations evoked by sensorial stimulus given the effects of anesthesia in the strength and timing of neuronal responses (Zurita et al., 1994; Syka et al., 2005) and oscillations (Faulkner et al., 1998).

Previous studies in anesthetized monkeys suggested that the gamma oscillations could be an artifact of the broadband increase in power of the stimulus-evoked field potential (Galambos et al., 1992; Brosch et al., 2002). However, results utilizing naturally occurring complex vocalizations to study the role of gamma oscillations in processing communication calls in mustached bats have suggested that gamma oscillations likely represent complex acoustic features of these vocalizations because they are highly sensitive to the spectrotemporal structure of communication calls (Medveded & Kanwal, 2008). In addition, these authors also suggested that, in different trials, the frequencies at the gamma range and low frequencies have an independent covariance in power. Thus, the distribution of power for the low and high frequency likely do not come from the same broadband process (Medveded & Kanwal, 2008). In the results presented here, I avoided including the sharp transitions of the MAEP during the power spectrum analysis. Therefore, the increase of power at gamma and high gamma frequency ranges can not be explained by a broadband increase across frequencies caused by fast evoked potentials caused by tones.

The occurrence of a high gamma frequency (>90 Hz) in response to tones in this study is also seen in studies in humans (Crone et al., 2001; Edwards et al., 2005), in which these high frequencies were reliably induced by passively listening to auditory stimuli or by actively discriminating sounds. Studies in humans suggested that the high gamma range could be reliably induced by auditory stimulation while the low gamma range shows more variance of response to sensory stimulus. Thus, this suggests a functional role for high gamma oscillations in the processing of tones and phonemes (Edwards et al., 2005). More recently, another report using depth EEG recording and biofeedback techniques provided striking evidence that the high gamma range (60-140 Hz) is induced by speech comprehension and music in the superior temporal sulcus and by complex acoustic patterns in the Heschl's gyrus which corresponds to the primary auditory cortex (Lachaux et al., 2007). Moreover, studies in monkeys extended this previous observation by suggesting a strong correlation between high frequency power and tonotopic organization (Steinschneider et al., 2008). I am now providing evidence that the occurrence of high gamma oscillations induced by auditory stimulation occurs in rats, and thus, it seems to be a widespread phenomenon in the auditory cortex of mammals. This finding is important because rats are an species amenable to study high frequency oscillations at a systems level as well as at a cellular level.

Global coherence

The LFP from each channel signal provides a macro-description of neuronal ensembles around the electrode tip. It is thought to be composed mostly of the summed EPSP currents from hundreds of neurons distributed in parallel in the case of the layered cortex (Miztdorf, 1985; Logothetis, 2002). The spectral analysis of the LFP traces

demonstrate that this relatively small neuronal network surrounding the electrode tip oscillates at a wide range of frequencies, and thus has a certain degree of synchrony. However, it could be that this synchronic behavior is only restricted to a relatively small neuronal network around each electrode tip. I directly measured this synchronous behavior across the auditory cortex by calculating the coherence values among electrodes spread in a 1.0 mm^2 cortical area. I show here that during baseline levels the coherence between sites in a 1.0 mm^2 range is highly complex; it is high at approximately <30 Hz frequencies and sharply drops at higher frequencies (>40 Hz). However, peaks of high coherency reappear at high frequencies for short periods of approximately 100-300 ms. This result complements previous results aiming to study spontaneous gamma oscillations in the auditory cortex of rats (Franowicz & Barth, 1995). It was found that there is an intermittent increase in power at the gamma range that appears to be widespread in the auditory cortex which has highly complex dynamics (Franowicz & Barth, 1995). We do not know if the dynamics of this ongoing coherence pattern influence the processing of incoming auditory information. However, there is some experimental evidence that suggests that ongoing baseline delta oscillations modulate the activity of auditory neurons to upcoming sensory events (Lakatos et al., 1995, Canolty et al., 2006). In addition it seems that there is a hierarchical control of high oscillations by delta oscillations, in which the probability of finding high oscillations is higher at specific phases of low oscillation (Lakatos et al., 1995; Canolty et al., 2006). Thus, it seems probable that the constant high coherence of low frequency bands during the baseline might entrench the coherence of high frequency oscillations at specific time periods which then would influence the processing of sensorial information.

I show here that in the awake rat the tone induces a high degree of synchrony across a wide range of frequencies during the first 100 ms after stimulus. It disrupts the ongoing coherency dynamics of the baseline which regain its characteristic pattern 100 ms after the tone onset. One might wonder whether the increase in coherence is due to the MAEP which would eskew the coherence spectrogram because of the power caused by the N1/P1 MAEP components. It is hard to rule out the contribution of the MAEP for the coherence among the LFP sites. However, if the coherence is only explained by a "broadband effect" in the spectrum then we would expect the coherence at low and high frequencies to be the same. However, I found that the coherence decreases as a function of frequency. Higher frequencies have lower coherency during the baseline and after the tone onset. These results seem to contradict the argument that the increase in coherence in the first 100 ms post stimulus is only a function of the MAEP.

Local networks and high frequency oscillations

The results presented in this chapter indicate that the increase in high frequency power at longer latencies is caused by synchrony at local neuronal networks. It occurs because small neuronal networks have synchronous activity that is likely independent from neighbor to neighbor networks. The combination of the results gained from measurements of power and coherence show that while auditory stimuli increases the occurrence of high frequency oscillations (>90 Hz) in up to 300 ms after the tone onset, this increase is not accompanied by a concomitant increase in coherence at this high frequency range in an area of 1.0 mm^2. The increase in coherence only occurs within 100 ms after the tone onset and it is restricted to a low frequency range (<25 Hz). Technical constraints prevented me from being certain of the exact relative position of the electrode

sites (see discussion of methods). Therefore, although desirable, a more thoughtful examination of the correlation between the position of the electrodes and the distance was not possible. However, studies in anesthetized monkeys (Brosch et al., 2002) suggest that there is a high increase in coherence at the high frequency range (up to 100 Hz) for the LFP sites that are up to 1000 μm apart. Both results suggest that high frequency oscillations are restricted to a small set of neuronal networks. However, both studies used tones which will optimally activate only a fraction of the auditory cortex population. It would be important to use complex species-specific vocalizations to explore whether these local neuronal oscillators change their coherence in order to extract meaningful acoustic features of the complex spectro-temporal pattern of vocalizations.

The LFP results suggest that large neuronal populations synchronize their activity at the gamma and high gamma frequency ranges after the tone onset. However, the LFP synchronous activity is only translated in spike train neuronal output at the lower end of the gamma range frequencies. Thus, the estimate of coherence between the LFP and spike trains suggests that neurons embedded in a network that have synchronous activity at gamma and high gamma ranges, integrate gamma range oscillatory input and fire action potentials at this frequency range, but filter out very high frequency oscillations. In this regard, it is important to point out that my results are similar to the results of Metherate & Cruikshank (1999). They measured the spectrum of the CCH between intracellular recordings in unspecified neuronal cell types and extracellular recordings which show peaks at the same range (10-60 Hz) that I observed in my spike-LFP coherence analysis (Metherate & Cruikshank, 1999). It has been shown that thalamic neurons show synchronous spiking in response to 100 Hz amplitude modulated tones

while cortical neurons do not follow such a fast synchronic response (Creutsfeldt et al., 1980). Thus it is conceivable that the fast oscillations detected in the LFP signal might be caused by inputs from thalamic neurons. Experiments using ablation of thalamic nuclei that modulates gamma oscillations in the auditory cortex (Barth & MacDonald, 1996; Brett & Barth, 1996) and experiments using intracellular recordings in the auditory cortex of anesthetized rats (Sukov & Barth, 2001) strongly suggest that the gamma frequency oscillation can be generated intracortically (Sukov & Barth, 2001). Moreover, experiments in vitro have shown that a variety of neurons (Regular Spiking, RS; Fast Spiking, FS; and Fast Rhythmic Bursting, FRB) in the auditory cortex have oscillatory behavior at the gamma range (Cunningham et al., 2004). These results suggest that an ensemble of cortical neurons can be synchronic and/or oscillate at the gamma range; however, none of these papers report oscillatory neuron behavior at the high gamma range. Therefore, further experiments exploring the coherence of the activity between thalamic and cortical neurons should shed some light on explaining the origin of the fast oscillations in the LFP of cortical neurons.

The results from spike-spike synchrony measurements demonstrate that simple auditory stimuli change the synchrony among neurons in the auditory cortex. I used a cross-correlogram (CCH) as well as a spectral coherence to determine whether tones changed the synchrony of the neurons recorded in this study. As seen in other studies (Dickson & Gerstein, 1974; Frostig et al., 1983; Espinosa & Gerstein, 1988; DeCharms & Merzenich, 1996; Brosch & Schreiner, 1999), I saw that the majority of the neuronal pairs have a CCH with a symmetrical positive peak (or negative peak) centered at the CCH origin. Additionally, I observed that tones increase the synchrony of the neurons in

the auditory cortex by measuring the peak at the half height of the CCH. The tones also slightly increase the temporal dispersion of these neurons (from 7 ms to 9 ms), which was measured by the peak width at the half height of the CCH.

There is some evidence that neuronal synchrony depends on stimuli and receptive field properties in the auditory cortex. Although previous studies have reported that the stimulus configurations change the synchronicity dynamics of neurons in the primary auditory cortex (Frostig & Gerstein, 1983; Espinosa & Gerstein, 1988; DeCharms & Merzenith, 1996, Brosch & Schreiner, 1999), I did not focus on the spike synchrony and receptive field properties among the neurons recorded in this report. Therefore, my measurements of synchrony among auditory neurons might be underestimated. However, I analyzed the averaged CCH combinations for each experimental recording session in order to uncover any possible consistent secondary peaks in the CCH. Indeed, I detected that most of our averaged CCH show a secondary peak around 60 ms and 100 ms from the origin as depicted in Figure 2.9A. My results are similar to the results of Brosch & Schreiner (1999) and Eggermont (1992, 1994) in which they detected secondary peaks ranging from 60 ms to 100 ms of the CCH origin. Additionally, to find secondary peaks around 60 ms in the averaged CCH, I further explored whether synchronous activity among the neurons in the auditory cortex also occurs at the higher frequency range. My results demonstrate that simple auditory stimuli increase the synchrony among neurons in the auditory cortex at the low frequency range in the auditory cortex of the awake rat (<30 Hz). It is described that neurons with similar receptive field properties synchronize their firing for continuous auditory stimulus (DeCharms & Merzenich, 1996). Moreover, Brosch and collaborators also demonstrated that in approximately 20% of neuron pairs in

their study show synchrony at the gamma range (Brosch et al., 2002). Additionally, this synchronicity appears to depend on the similarity of the receptive fields. It is possible that the lack of finding synchronicity at these high frequency ranges in my data set could be explained by the fact that I likely recorded neurons with different receptive field properties.

Previous reports using repetitive clicks and AM stimuli in anesthetized cats have proposed that neurons (Schreiner & Urbas, 1998; Eggermont, 1991, 1992a, 1992b, 1994) and LFP sites recorded in parallel to neurons stimulated by repetitive clicks (Eggermont & Smith, 1995) synchronize their action potentials to clicks played optimally around 10 to 15 Hz. However, some of these neurons fire to stimulus presentation rates of up to 30 Hz (Eggermont and Smith, 1995) and others have reported increases in synchrony in up to 100 Hz (DeRibaupierre et al., 1972). Like others have described (Creutzfeldt, 1980; Eggermont & Smith, 1995) my measurements of spike coherence appear to suggest that neurons in A1 do not follow fast varying auditory stimuli and act as a low-pass filter. However, more recent papers using complex stimuli combining fine, fast temporal structures and slow, modulated spectro-temporal envelops suggested that neurons in A1 are capable of synchronizing their activity to these fine temporal fast structures (Elhilali et al., 2004). Recent studies also claim that a small subset of neurons in A1 display a non-synchronous increase in firing rates to auditory stimuli played at a very repetitive rate (>100 Hz) thereby transforming a temporal neuronal code into a rate based code (Lu & Wang, 2002; Lu & Wang, 2004; Lu et al., 2001a, 2001b). Here, I show that neurons show low synchronization in their spike train (around 0.1) and only at low frequencies (up to 30 Hz). Moreover, I detected that the phase of the coherence for the low frequency range

is nearly close to zero (not shown). Therefore, neurons in the auditory cortex fire almost simultaneously at these low frequency ranges and they will likely affect the neuronal processing of neurons that they project to.

Studies using spectral coherence techniques to explore whether neuronal synchrony in the visual area 4 (V4) is modulated by attention have found neuronal synchrony around the same range as described here (0.1 coherence) (Fries et al., 2008). However, unlike our studies, Fries and collaborators also found significant coherence values at the gamma frequency range which are modulated by visual attention. Perhaps, attention and/or a combination of more complex stimuli might modulate the coherent activity of neurons in A1 at the gamma range as well. Moreover, auditory perception is likely not a passive process in which the sounds present in the environment impinge a passive response from the auditory cortex which would behave as an auditory filter (Nelken, 1999). It is quite possible that the activity of the auditory cortex is concerned with the representation of sounds as auditory objects, and as such, they are likely built into complex cognitive processes like attention, memory and expectations caused by timely regularities of the perceptual objects. Furthermore, because the auditory stimuli used in my experiments were pure tones, which do not have complex temporal modulations, the complex oscillation patterns that I observed might not be related to any faithful representation of the physical temporal modulations present in sounds encountered in the environment. Therefore, I further explored whether high frequency oscillations are modulated by perceiving acoustic objects in the following chapters to test the hypothesis that auditory perception modulates intrinsically generated oscillations in A1.

Chapter 3

High frequency oscillations are modulated by actively perceiving tones

3.1 Introduction

It is thought that the sensory primary cortices do not act like a passive filter of the environment, but their activity is built by expectations from previous experiences (reviewed in Engel et al., 2001b; Nicolelis, 2006; Fritz et al., 2007). For instance, it is proposed that attention modulates parsing and grouping of acoustic features (review in Bregma, 1990; Alain & Arnott., 2000) and there is evidence that the activity of the primary auditory cortex (A1) reflects perceptual grouping in monkeys (Micheyl et al., 2005). Moreover, early reports strongly suggested that attention modulates the firing rate of A1 neurons in cats and monkeys (Hubel et al., 1959; Miller et al., 1972; Hocherman et al., 1976). More recently, it was found that the receptive properties of A1 neurons are also modulated by active listening (Fritz et al., 2003, 2005, 2007) and the neuronal activity in A1 reflects categorization of simple acoustic attributes (Ohl et al., 2000). Therefore, A1 does not behave as a passive filtering device, but it uses sensory memory and attention in order to process sensorial information (Ohl et al., 2000; Nelken et al., 2003, 2004; Fritz et al., 2003, 2005, 2007; Scheich et al., 2007). Thus, the idea that A1 processes acoustic objects and that active listening is required in order to allow thorough processing of sounds has gained considerable experimental support.

Theoretical and modeling work has suggested that neuronal network synchronization would be a possible neuronal mechanism by which the auditory cortex

could implement acoustic grouping (Von Malsburg, 1985; Wang & Chang, 2008). Neuronal synchronization is often reflected by high frequency oscillations at the gamma range (40-70 Hz) (Gray & Singer, 1995; Singer, 1999). However, experimental evidence from epipial recordings in anesthetized rats suggests that auditory stimulus induced gamma oscillations at long latencies, and the stimulation of the main thalamic sources that projects to A1 (i.e. the ventral and medial MGB) inhibits these oscillations (Franowicz & Barth, 1995; Barth & MacDonald, 1996). Other results have shown that stimulation of thalamic nuclei related with arousal (TRN and PIL) strongly induces high frequency oscillation in the primary auditory cortex (Brath & MacDolnald, 1996; Breth & Barth, 1997; Sukov & Barth, 1998; Sukov & Barth, 2001).

Sensory perception is inextricably related with attention. If high frequency oscillations play a role in perception, then it should be modulated in behavioral paradigms in which experimental animals can actively report hearing a sound. Indeed, there are several papers that show these oscillations are modulated by attention and discrimination of tones, phonemes and language perception in human subjects (Galambos et al., 1981; Tiitinen et al., 1993; Crone et al., 2001, 2006; Canolty et al., 2001, 2007; Edwards et al., 2005, Lachaux et al., 2007). However, the precise cortical origin of the attention-related modulation of the high frequency oscillations it is not known. It is unclear if these oscillations are the result of A1 activity, or if they are a consequence of auditory processing at high hierarchical areas of the temporal lobe. Moreover, the attentional modulation of gamma oscillations could be a particular feature of the human temporal cortex to process speech perception, group acoustic features of speech in acoustic objects to be followed over time and/or to attach meaning to it.

Modulations of high frequency oscillations at cellular and small neuronal clusters in the temporal cortex by active listening have yet to be explored. There are not enough data to suggest that these oscillations play a role in auditory perception in awake behaving experimental animals actively listening to auditory stimuli in A1. Although it has been reported that auditory stimuli induce high frequency oscillations in the auditory cortex of awake animals (rats: Chapter 2; monkeys: Steinschneider et al., 2008; bats: Medvedev & Kanwall, 2008), it is unclear if these oscillations are a possible neuronal mechanism underling auditory perception. If the high frequency oscillations are related to the generation of the perceptual experience, then modulations of these oscillations should occur in animals actively listening to auditory stimuli. Therefore the aim of this chapter was to test the hypothesis that high frequency oscillations are modulated by active listening to tones in the primary auditory cortex in awake behaving rat.

3.2 Methods

Experimental groups

In order to test whether active listening modulates high frequency oscillations in the primary auditory cortex of awake rats, trials in which rats attended to a single tone were compared to trials in which rats passively listened to a single tone. In order to perform such experiment, the LFP of rats that were trained in a instrumental conditioning paradigm were compared to LFP of un-trained rats. This instrumental conditioning paradigm was used to train rats in a two-tone discrimination task, in which they had to discriminate two-tones played in a rapid 200 ms succession from one single tone in order to receive a reward. The behavior by which I detected whether rats had learned this

discrimination task was protrusion of their tongue towards a stainless steel tube which delivers water reward.

Rats quickly learned the two-tone discrimination task, as the percentage of licking behavior was much higher during the two-tone trials than the one-tone trials (see following chapter). However, they still licked the metal tube in order to receive water after hearing one-tone trials in approximately 25% of these one-tone trials (see following chapters). Therefore, in the one-tone trials in which rats licked the metal tube wrongly anticipating water, they were actively listening to the tone. Those trials are very useful to test whether active listening modulates the occurrence of high frequency oscillations in the auditory cortex of awake rats. Therefore, in this chapter, I will focus only on the comparison of the two experimental groups. The first experimental group was the active listening (the one-tone trials in which rats mistakenly licked in order to receive water) and the second experimental group is rats that were not trained in the two-tone discrimination task, but were listening to single tones.

Behavior apparatus

The behavioral apparatus in which rats were trained consisted of 4 acoustically insulated chambers. Each one of these chambers contained speakers in which auditory stimuli were generated and played by a programmable function generator controlled by a PC workstation. Rats were put in a water restriction regimen prior the start of the training protocol (40 minutes of water access/day). This procedure ensured that they were highly motivated to perform the behavioral task. Before each training session rats were placed into a restrainer custom black Plexiglas box which was immediately transferred to the chamber after the rat entered it. Upon the correct behavioral conditions, a water reward

was delivered through an 18'' metal tube localized 10 mm in front of the rat's snout. Water was not given to rats in the one-tone trials. Moreover, no negative reinforcement, such as electrical shock, was given to rats if they wrongly licked the metal tube to receive water in the one-tone trials. Additionally, the occurrence of the trials as well as the two-tone and one-tone trials was randomized. Therefore, rats could not anticipate when and whether two or one-tone trials would occur. After rats reached a 75% of correct two-tone discrimination performance, they underwent a surgery to implant a cemented cap in order to perform the electrophysiological recordings.

Animal preparation.

The animal preparation is virtually identical to the procedures described in Chapter 2 (page 25), except that after recovery from the craniotomy, trained rats were placed daily in the atraumatic head holder and then submitted to 2 to 4 training sessions per day for 2 to 4 days before the recording session. This step ensured that rats performed the discrimination task that they were trained during the training sessions, and that they were accustomed to the electrophysiology recording environment.

Signal selection

In order to test the hypothesis that active listening modulates the temporal characteristics of the neuronal activity in the auditory cortex, multiple clusters of single-units (MUA) and LFP were recorded in awake untrained and in awake trained behaving rats that licked a metal tube after they heard a single tone. I restricted my analysis to LFP sites that show the classic middle auditory evoked potential (MAEP) and in multi-unit clusters of single units comprised of well isolated neurons that had short response latencies (10 ms to 20 ms) to the 10 kHz tones.

The experiment and analysis described here were performed in a total of 6 experimental recording sessions of 3 rats trained in the behavioral paradigm and in 11 experimental recording sessions of 7 untrained rats. A total of 20 trials for each of the 57 LFP sites (and 67 spike trains) of the active listening experimental group and a total of 53 LFP sites (and 64 spike trains) of the passive listening experimental group are analyzed in this chapter. All surgical procedures and experimental protocols were in accordance to NIH guidelines and were approved by OHSU Institutional Animal Care and Use Committee (IACUC).

Stimulus generation and recording session

The auditory stimuli generation and recording session were performed exactly as previously described in Chapter 2.

Data Analysis

The data selection and off-line data analyses were performed with NEX and MATLAB (The MathWorks, Inc., Natick MA, USA). Peri-event histograms (PSTH) of 1 ms bins were computed to select short latency MUA clusters time-locked to the acoustic stimulus. Then, custom programs were written in NEX language to select 1600 ms data segments containing trials of the active and passive listening experimental groups. These data segments were then exported to the MATLAB environment in order to perform the analysis described in this dissertation.

The firing rate was computed with a 1 ms bin and smoothed by a 5 ms gaussian window for a period ranging from 100 ms before to 300 ms after the tone onset. The firing rate was computed using 20 random trials for each neuron and then averaged across

the population (67 neurons for active and 64 for passive listening). Figure 3.2 displays the mean and SEM of the averaged firing rate of the active and passive listening condition.

As a preliminary analysis, the mean and standard error of the mean (SEM) of the LFP trials across rats were computed to study the effect of active listening in the LFP. The increase of the N1 component in the LFP amplitude response was further measured by selecting the period of 10 ms to 50 ms after the tone onset and computing the mean and SEM of the LFP absolute value amplitude from the active and passive listening.. Additionally, the latency of the active and passive listening LFP response to tones was also compared. The average of 60 trials from each one of the LFP channels across animals was computed and the time of the N1 peak response was selected. The null hypothesis that there are no differences in the absolute value or latency of the LFP response for active and passive listening was tested by a student t test at $p<0.01$.

After verifying that there were statistical differences in amplitude but not latency between active and passive listening, I then proceeded to detect high frequency oscillation differences in these conditions. In order to detect any oscillatory pattern that could indicate synchronized activity of the neurons that contribute to the LFP signal, the LFP signal of each single trial was filtered at 40-70 Hz and at 90-150 Hz using a 5 pole Butterworth filter. Then this signal was visually inspected for the active and passive listening conditions. Example of this analysis is shown in Figure 2.4. After this preliminary analysis, I then quantified any oscillatory behavior by computing the spectrogram and power spectrum of the LFP.

In order to test whether active listening modulates synchronization of neurons in A1, the cross-correlogram function (CCH) of neurons was quantified using the NEX

built-in CCH analysis. The CCH of simultaneous recorded MUA counted the number of spike coincidences for various time shifts (-150 ms to +150 ms) of each MUA train pair in a 1 ms bin size smoothed with a 5 ms gaussian window during a 500 ms time period ranging from -100 ms before to 400 ms after tone onset. The CCH was normalized by dividing the spike coincidences by the total number of bins, which gives a probability of coincidences during the interval analyzed (CCH coefficients). In order to verify that the CCH peak coincidences around zero lag are not due to change, the CCH algorithm also computed the 95% interval confidence intervals. These 95% confidence intervals are based on the assumption that spike trains have an independent poisson distribution (Abeles, 1982). The peak at half height of the CCH coefficient for each pair was selected to statistically test for significant neuronal synchrony differences between active and passive listening conditions using a student t test. The peak width at half height was computed to measure the degree of temporal dispersion of the neuronal coincidences, and a student t test was used to detect significant differences between the experimental groups.

Spectral analysis.

In order to study whether active listening to tone modulates the neuronal synchronization in the auditory cortex, I analyzed the spectrogram, power spectrum, coherence spectrogram and the coherence spectrum of simultaneous LFP and multi-unit activity recordings (MUA). The spectral analysis was described in Chapter 3. In order to compute the spectrogram and power spectrum of the LFP I used a time-frequency bandwidth of 3 and 5 Slepian taper functions in 125 ms overlapping windows of 10 ms steps. For the coherence spectrograms and coherence of the spike signal i used a time

bandwidth product of 5 and 9 Slepian taper functions in 125 ms overlapping windows in 10 ms steps. The chronux software provides measurements of 95% confidence interval of the spectrum and coherence which can be used to test significant differences of coherence values between time intervals. The jackknife statistical test used to compare significant differences of power or coherence spectrum between two time series is based on resampling statistics. For each coherence estimate across tapers the jackknife method leaves one taper estimation out of the estimate and resamples the coherence estimate. This creates a set of spectrum and coherence estimations in which a variance can be computed and tested for difference of means by using a non-parametric Arvesen's Jackknife U statistical test implemented in MATLAB (Thomson & Chave, 1991; Efron & Tibshirani, 1993; Hesterberg et al., 2008) available in the chronux package MATLAB library at www.chronux.org.

3.3 Results

Active listening modulates the MAEP

This chapter tests the hypothesis that active listening increases the occurrence of high frequency oscillations in the primary auditory cortex of awake rats. I compared rats actively listening to a tone (10 kHz, 75 dB, 20 ms) to rats passively listening to one tone. Rats lick the spout in 75% of the two-tone trials while they lick the spout in 30% of the one-tone trials. Therefore, they are actively listening to the one tone. Moreover, the physical attributes of this tone are exactly the same as the stimulus used to study induction of high frequency oscillations in the awake un-trained rats in the previous chapter. Note that we have two experimental groups processing the same sound. However, while the naïve rats passively listen to the tone, trained rats actively listen to

the same tone. Therefore, these experimental groups were compared in order to study whether high frequency oscillations are modulated by active listening.

The short latency, sharp onset response to tones, the use of consistent stereotaxic coordinates, the consistency of the arteries and veins of the temporal cortex which can be used as anatomical landmarks, and the small craniotomy (~1.3 mm^2) in relation to the extent of the primary auditory cortex (~3.0 mm^2) indicate that the recordings performed in this and following chapters were from the primary auditory cortex. I did not detect any differences in the average firing rate of the neuronal population recorded in the passive and active listening rats. Figure 3.12A shows that mean firing rate for active and passive listening is 40 spikes/s for both experimental groups, and they have mean latency peaking at approximately 15 ms. Thus, neither the average latency nor the average firing rate was different between active and passive listening. Figure 3.12B shows the grand averaged middle auditory evoked potential with a typical latency encountered in the primary auditory cortex (15 ms). Several components of the MAEP are modulated by active listening. The rats actively listening to the tone had a greater evoked response corresponding to the N1 component of the MAEP. Moreover, there was a second negative peak (N2) around 50 ms after the tone onset that was seen in the active listening context but was not observed in the passive listening rats. Additionally the positive P70 component of the MAEP (around 70 ms to 100 ms) is also modulated by active listening. Latter components (200 ms to 300 ms) appear to be modulated differently in both conditions as well. The active listening effect in the MAEP was further quantified by comparing the N1 strength and latency between passive versus active listening (graph 3.12C). The absolute value of the LFP evoked responses of all trials (940 trials of passive

and 1020 of active listening) between intervals encompassing 10 ms to 30 ms after tone onset were taken and their values were compared using a student t test. The N1 evoked response (N.E.R.) during active listening was higher then the evoked responses during passive listening (t test, $p<0.001$). Although the mean latency was slightly higher for the passive listening condition it was not significantly different from the active listening condition (t test, $p= 0.1839$).

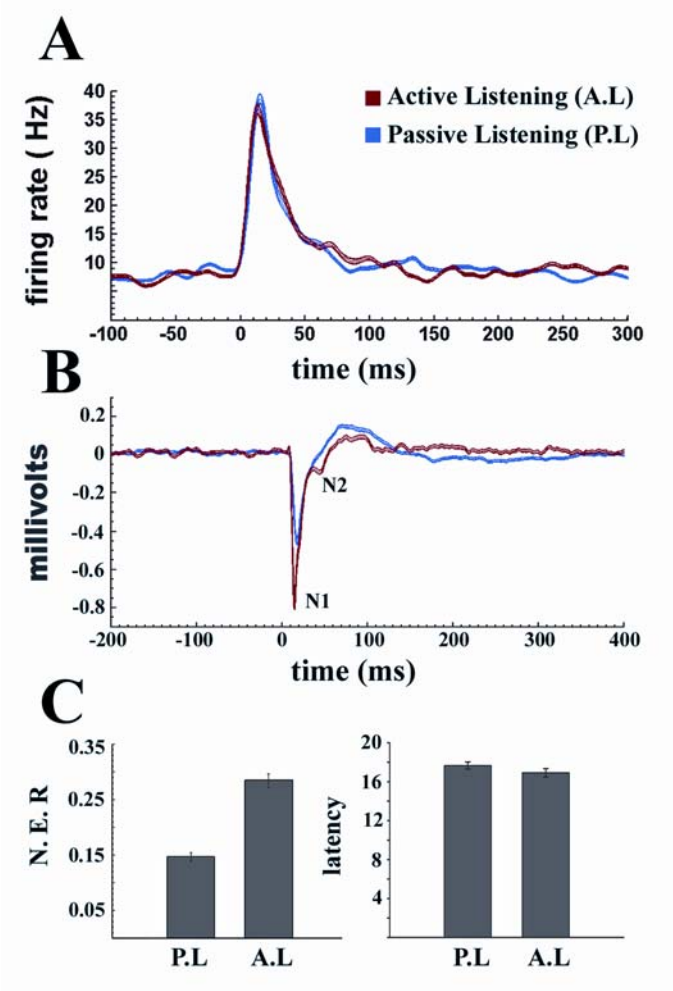

Figure 3.12. Active listening modulates the activity of the primary auditory cortex. A: Top graph shows the PSTH of the active listening (red line) and passive listening (blue line) experimental groups in which it displays the mean population firing rate ± SEM smoothed with a 5 ms gaussian window (active listening: 67 neurons, n=3 rats, 6 experimental sessions; passive listening: 64 neurons, n=7 rats, 11 experimental sessions). The time 0 is tone onset (10 kHz, 20 ms, 70 dB SPL). B: In the middle graph the blue trace indicates the averaged evoked responses (53 LFP sites from 3 rats) of the un-trained rats to one tone stimulus. The red trace shows the averaged evoked responses (57 LFP sites from 3 rats) of the rats active listening to the one tone stimulus. The ordinate is in millivolts and the abscissa is time in milliseconds. Tones are 10 kHz, 75 dB, 20ms. The thin traces are the mean and the thick traces are the standard error of the mean (SEM). C: The bottom left graph shows the mean amplitude of the N1 responses (mv^2) plus SEM during 10 ms to 30 ms after tone onset for the passive (53 LFP sites in 3 rats) and active (57 LFP sites in 3 rats) . The right bottom graph shows the mean and SEM of the N1 peak latency responses after the tone onset for the active versus passive listening.

Active listening modultes high frequency oscillations

After having demonstrated that active listening changed the MAEP responses, i switched my attention to the high frequency oscillations themselves. Figure 3.13 exemplifies that active listening to sounds modulates the amplitude of time-locked oscillations as well as induced high frequency oscillations. Figure 3.13 shows a LFP trace example where oscillations are clearly seem after the N1 evoked response to tones. These induced oscillations are more apparent when the signal was filtered at high frequency ranges. Note the burst of oscillations after the oscillatory time-locked response for both conditions: passive and active listening. This figure also shows that the high frequency oscillations often have high amplitude and longer duration in the active listening condition. These measurements were quantified by calculating and comparing the spectrogram and normalized power spectrum for the active and passive listening conditions.

The spectrogram of the 57 LFP traces recorded during the active listening is very similar to the spectrogram of the 53 LFP traces recorded during the passive listening condition. This analysis shows that there is an increase in power at low frequencies (<20 Hz) for both conditions just after the tone onset. The detail of the spectrogram filtered at a high frequency range (40-150 Hz) also shows that in either, passive and active listening, there is an increase in power for these frequencies that lasts approximately 100 ms after the tone onset. However, some differences are clear. There is an overall increase in power during the baseline and after the tone onset in the active listening condition. This increase in power is augmented after tone onset for low and high frequencies.

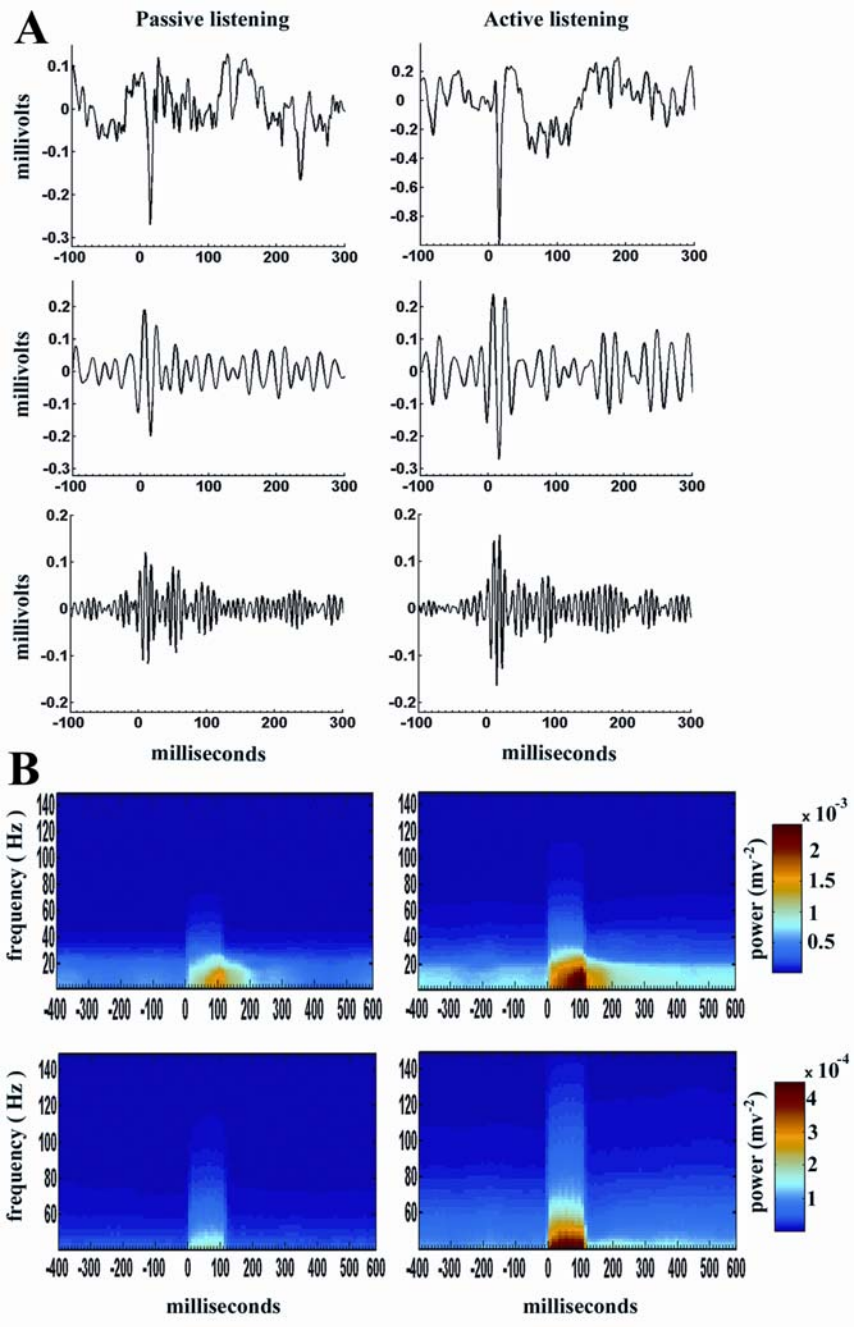

Figure 3.13. Active listening modulates the amplitude of high frequency oscillations in the auditory cortex of the awake rat. A) The two upper traces are wide band LFP from the passive (left column) and active listening (right columns), the middle traces show the filtered LFP trace between 40-70 Hz, and the bottom traces show the filtered LFP at high gamma ranges (90-150 Hz). The ordinate are in millivolts and the abscise are in milliseconds. B) Spectrogram of the passive listening (left spectrograms) and active listening rats (right spectrograms) showing wide frequency range (1-150 Hz, top) and detail of the high frequencies (40-150 Hz, bottom). Ordinate: frequency (Hz), abscissa: time (ms).

The spectrogram demonstrates that there is an overall increase in power of the LFP traces during the baseline and after the tone onset. However, because the fast MAEP to tones could skew the power estimate, the power spectrum after the tone onset (30 ms to 330 ms after tone) was computed and normalized by the power spectrum of the baseline (-100 ms to -400 ms before tone onset).. Figure 3.14A shows that the power normalized by the baseline increases after the tone onset during the passive and active listening conditions. Interestingly, the shape of the normalized power is similar between these two conditions. There is a peak in power for frequencies at 10 Hz, sharp decrease for 20-25 Hz frequencies, and an increase of power for high frequencies. However, this power increase is more pronounced for the active condition in low and very high frequencies. The comparison of alpha/beta, gamma and high gamma frequency ranges between passive and active listening showed the highest increase in power for all frequencies during the active listening condition (t student test, $p<0.001$; Figure 3.14B). Additionally, because the increase in the normalized power was apparently not uniform for all frequencies analyzed, the normalized power for frequencies encompassing the alpha/beta, gamma and high gamma frequency ranges were lumped together and statistically compared. This analysis is shown in Figure 3.14B. The increase in power is higher for the low frequency range for the passive listening condition, followed by the high gamma and gamma frequency ranges (ANOVA, $F_{(2,140)} =3.12$, $p=0.0474$; followed by Scheffe post-hoc, $p<0.05$). The same was not true for the active listening condition. The highest increase in normalized power was in the high gamma range, followed by the low alpha/beta and gamma frequency ranges for this experimental group. (ANOVA, $F_{(2,152)}=0.0009$, $p<0.05$; followed by Scheffe post-hoc, $p<0.05$).

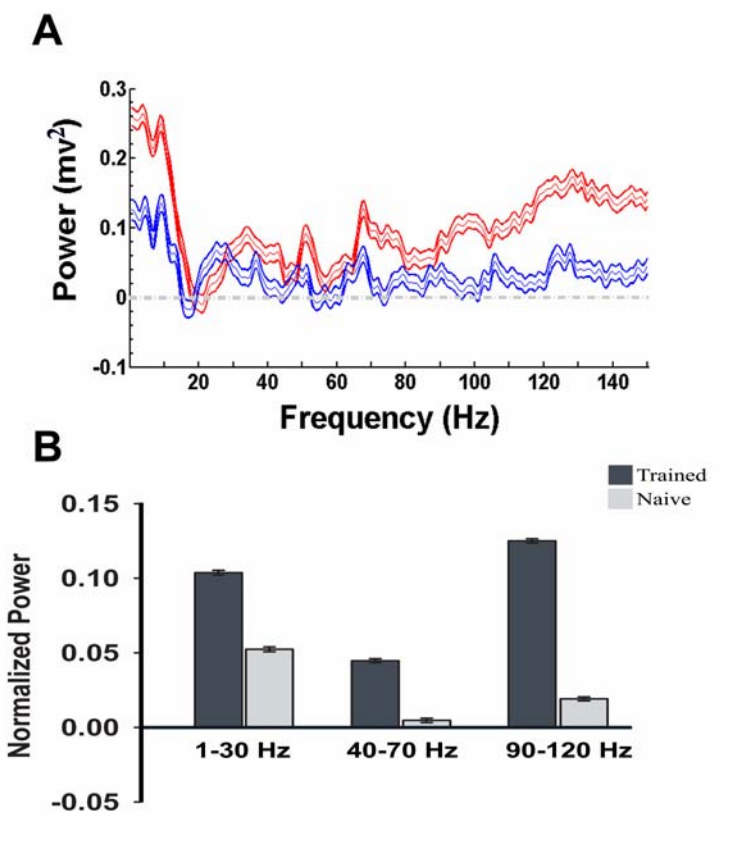

Figure 3.14. The normalized spectrum of passive and active listening shows an increase in power during active listening. A) The top figure shows the normalized power of the active (red lines) versus passive (blue lines) throughout all frequencies analyzed (1-150 Hz), (the thin line is mean and thick lines are SEM). B) The bottom graph shows the normalized mean ± SEM power for alpha/beta (1-30 Hz), gamma (40-70 Hz) and high gamma (90-120 Hz) of combined frequency ranges during active(black bars) and passive listening (gray bars).

The previous analysis shows that active listening to simple acoustic events changes the dynamics of the auditory cortex response to these events. It changes the excitability of the network, in which it is more synchronic at all the frequencies analyzed. Importantly, this increase in power is not uniform. The highest increase in power is in the high frequency range (90-150 Hz) during the active listening condition, which is not the case for the passive listening condition. This result suggests that small neuronal networks in A1 become synchronized at these high frequency oscillations. The synchrony among LFP sites was directly measured by computing the spectral coherence among simultaneous recorded LFP having an average distance of 300 μm among them.

Active listening modulates LFP coherency

The comparison of the coherence spectrogram (Figure 3.15A (top) and 3.15B (middle)) between active and passive listening reveals that the baseline synchrony of the neuronal population in A1 is higher for the active listening condition. The coherence spectrogram of the Figure 3.15 shows that even before the tone onset (-100 ms to 0 ms) the coherence of the active listening condition is high at frequencies ranging from 30 to 100 Hz. This is not the case for the passive listening condition. In this experimental group, the baseline coherence drops sharply around 30-40 Hz and has a rebound between 60-80 Hz. However, at these high frequencies, the coherence is higher for the active listening condition. Tones greatly skew the coherence spectrogram for both conditions. There is a high increase in coherence at all frequency ranges measured after tone onset. The increase in coherence lasts for approximately 100 ms for active and passive listening. After this period, the coherence spectrogram is similar to baseline levels for the passive

listening condition. However, for the active listening condition, the coherence spectrogram pattern after tone onset is not exactly the same as before tone onset. The coherence appears to have a decrease between 30-40 Hz frequency ranges between 100-150 ms after tone onset, and afterwards (150-300 ms), it appears to have a rebound specifically at the gamma frequency range (40-70 Hz).

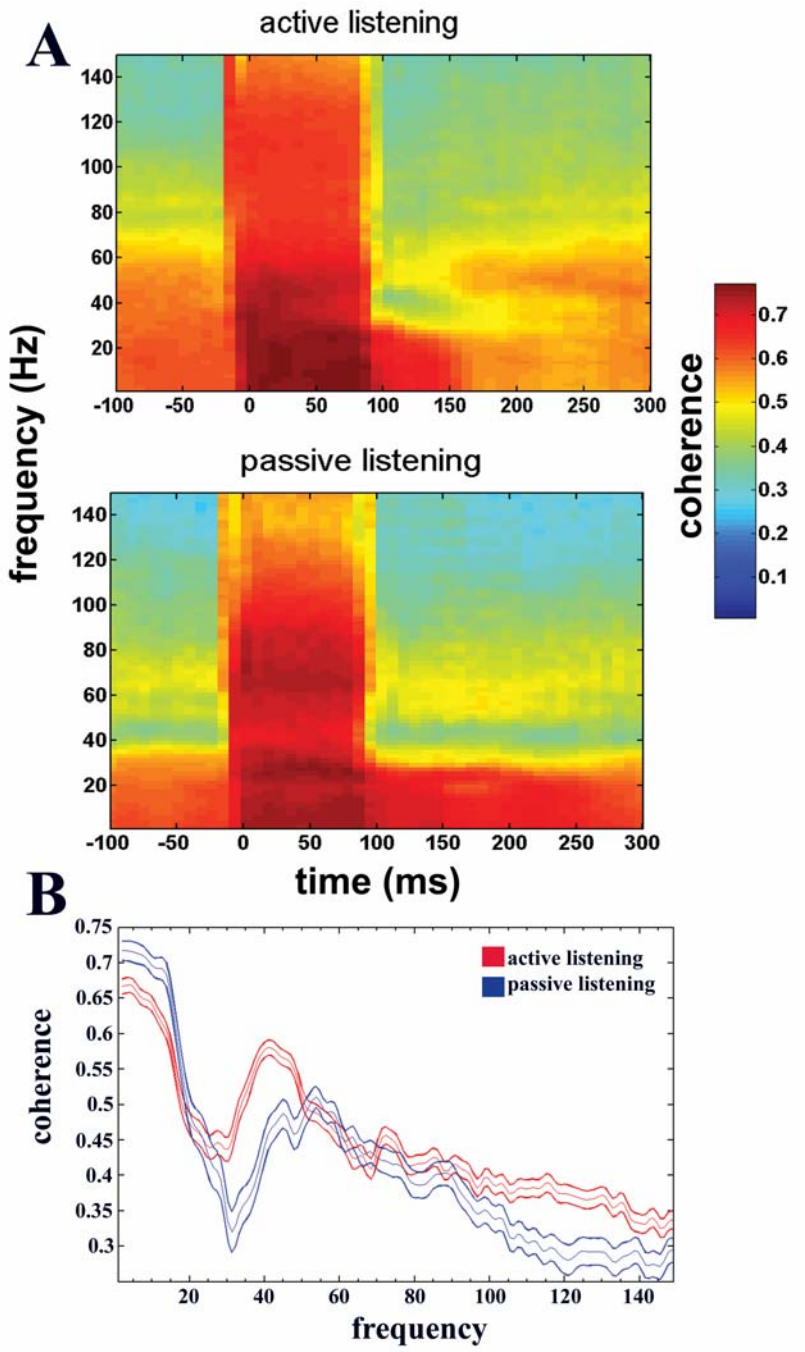

Figure 3.15. Active listening increases the coherence among LFP sites at gamma and high gamma ranges. A) Top graph shows the coherence spectrogram during active listening (n=3 rats; 57 LFP sites; 189 pair combinations. B) Middle graph shows the coherence spectrogram during passive listening (n=5 rats; 51 LFP sites; 178 pair combinations). The ordinate is frequency (Hz), abscissa is time (ms) and the z-axes is coherence. C) Bottom graph shows the mean coherence plot (thin line) plus its 95% confidence intervals (thick line) from a 50 ms to 350 ms time period. Red line = active listening; Blue line = passive listening. The ordinate is coherence and the abscissa is frequency (Hz).

The effects seen in the coherence spectrogram were further quantified by computing the coherence and its 95% confidence intervals during 30 ms to 330 ms after tone onset. This time period was selected because the differences seen in the coherence spectrogram after tone onset likely reflect important cognitive processes that might be happening in the active listening condition. As previously detected in the coherence spectrogram, there is a peak in coherence at the low end of the gamma frequency ranges (35-55 Hz) during active listening as compared to the passive listening condition (student t test, $p<0.001$). There are also differences at low frequency range (1-30 Hz ; $p<0.001$) and at high frequency ranges (90-150 Hz; $p<0.001$) between active and passive listening. At low frequency range (1-30 Hz), there is more coherence during the passive listening. At high frequencies, the opposite occurs.

The LFP signal is constituted by the thousands of synaptic contacts received by the neurons in their dendrite tree and neuronal body (Mizdorf, 1985; Logothetis, 2002). The neuronal output will only occur after the spatial and temporal integration of the net EPSP depolarization reaches a threshold in which the neuron fires an action potential (Nicholls et al, 1992). Thus, oscillations in the LFP aspecific frequency only reflects synchronic activity caused by the integration of synaptic inputs received at the dendrite trees from a large neuronal network dispersed in a few hundreds of microns around the electrode tip (Katzner et at., 2009). The MUA-LFP coherence and also the MUA-MUA coherence was measured, in order to further explore whether active listening not only changed the synchrony of inputs received in A1 but also affected the spike train synchrony.

Active listening modulates local neuronal network synchrony

The next figure (Figure 3.16) shows the comparison of the MUA-LFP coherence spectrogram of the active and passive listening. This figure demonstrates that the average coherence between the spike train of a particular neuron and the LFP signal around it drastically increases after tone onset. This increase occurs during active and passive listening. However, during the active listening, it appears that there is an even higher increase in MUA-LFP coherence as compared to the passive listening condition. Additionally, this increase is restricted in time and, to some extent, in frequency. The increase in coherence only occurs during the first 100 ms after the tone onset during active and passive listening. Figure 3.16 shows the coherence spectrogram analysis which suggests that coherence increases at low and high frequencies during active listening as compared to the passive listening condition. The coherence spectrogram also suggest that this increase in coherence during active listening is higher in the first 100 ms after the tone onset, but also appears to be higher at high frequencies (40-100 Hz) during 150-300 ms after tone onset. The coherence spectrogram shows that the MUA-LFP coherence increases after tone onset. Moreover, the MUA-LFP coherence increases in the active listening condition across all frequencies. The coherence was further quantified during a period of 30 ms to 330 ms after the tone onset. The graph of the Figure 3.17 shows the estimate coherence mean and its 95% confidence interval. This figure demonstrates that there is a peak in coherence around 20 Hz, but also the coherence increases around 40-60 Hz frequencies (Jackknife U test; $p<0.01$).

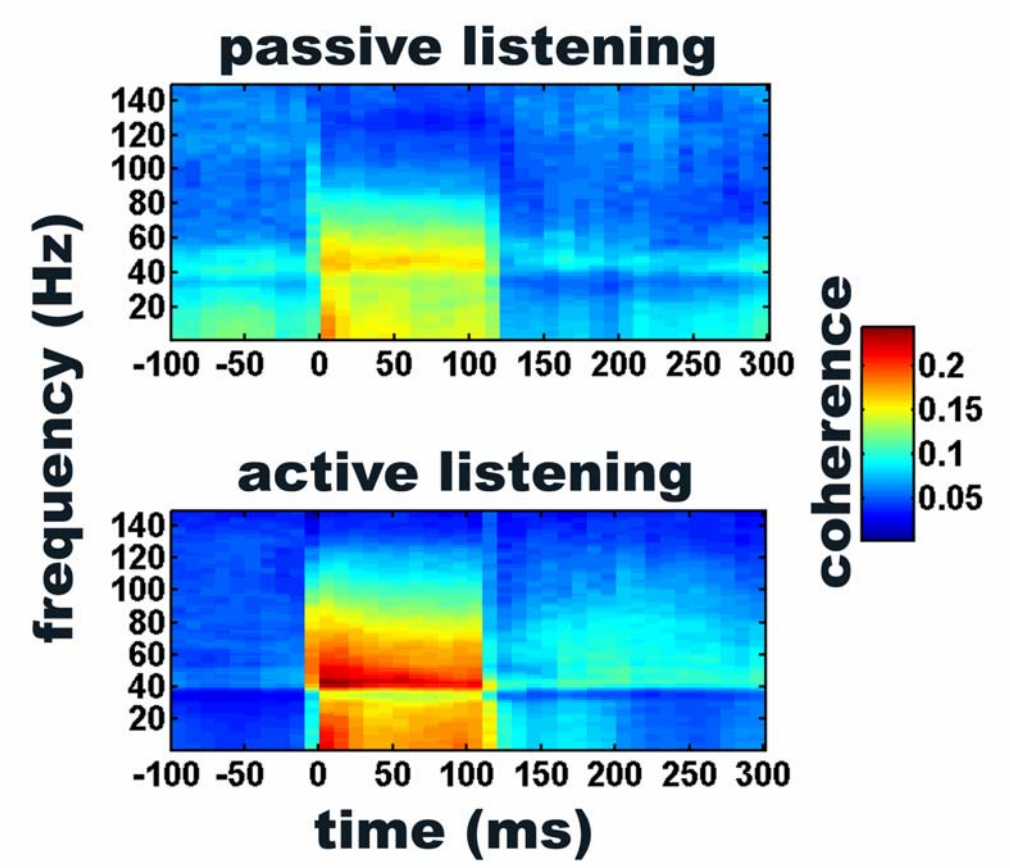

Figure 3.16. Active listening amplifies the MUA-LFP coherence after the tone onset. A) Top panel shows the averaged coherence spectrogram during passive listening (20 trials of 49 simultaneously MUA-LFP sites; n=5 rats). B) Bottom panel shows the averaged coherence spectrogram during active listening (20 trials of 51 simultaneously spk-lfp sites; n=3 rats). Ordinate is frequency (Hz), abscissa is time (ms), and z axes is color coded coherence.

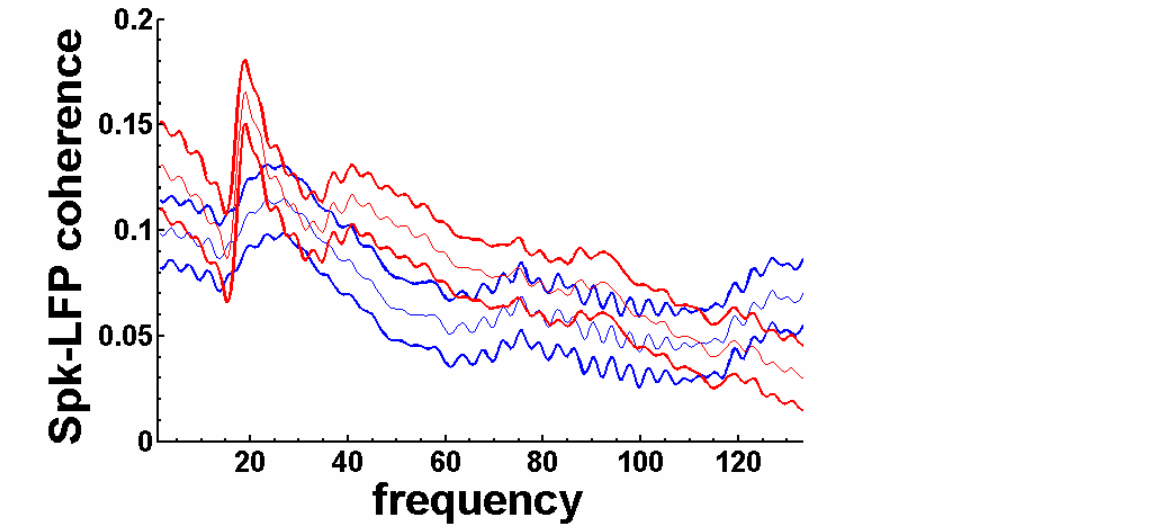

Figure 3.17. Active listening increases local coherence across at beta and gamma frequencies. This graph shows the mean coherence (thin line) and 95% confidence interval (thick line) of a 30 ms to 300 ms after the tone onset for active (red line; 20 trials of 51 MUA-LFP pairs) and passive (blue line; 20 trials of 49 MUA-LFP pairs) conditions. Ordinate is coherence (0-1) and abscissa is time (ms).

Modulation of spike train synchrony by active listening

After measuring the coherence between the spike train and the LFP from the same electrode the synchrony among spike trains was analyzed. The first analysis performed was a cross-correlogram between neurons in the active listening and from neurons in the passive listening condition. I found that 31.5% (60/190) of the possible pairs in the passive listening condition showed significant CCH coefficients above the 95% interval confidence. The active listening condition had 42% (183/434) of the possible pairs showing significant CCH coefficients above the 95% confidence intervals. Figure 3.18 shows the average peak at half height and the peak width at half height of all CCH pair who has CCH coefficients above the 95% confidence interval. This analysis shows that active listening increases the synchronization of neurons in A1 (permutation t test; $p<0.01$; 1000 permutations). Moreover, this figure also shows that there is an increase in the temporal dispersion of the neurons in A1 during the active listening condition (permutation t test; $p<0.01$; 1000 permutations).

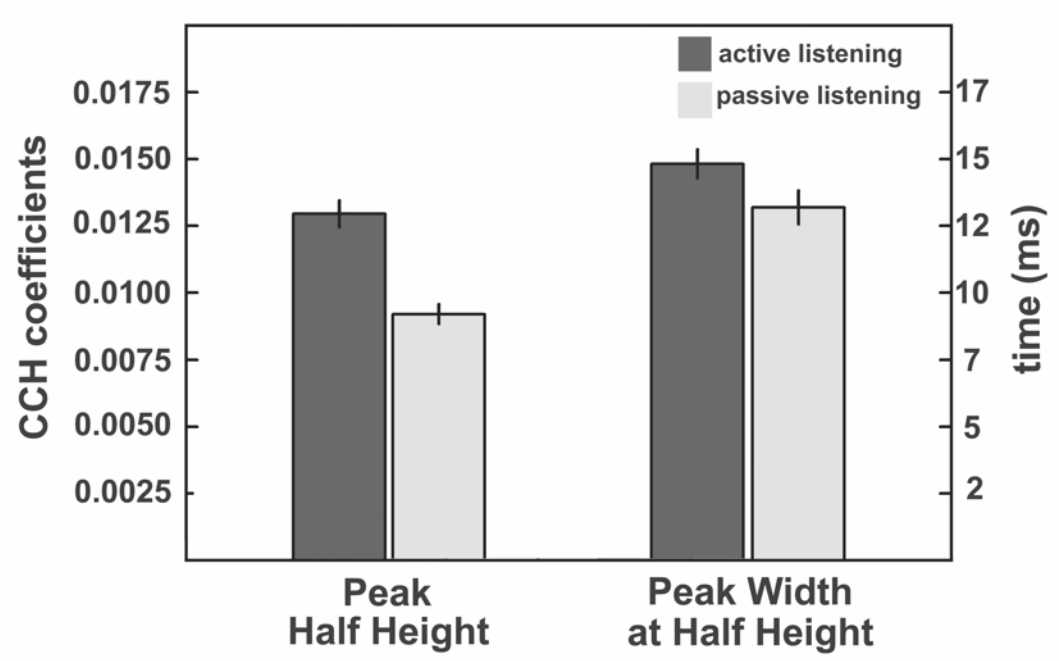

Figure 3.18. Active listening modulates the synchrony strength and time dispersion among neurons in A1. The left bars represent the peak at half height of the CCH coefficients in active (dark gray) and passive (light gray) listening. The right bars represent the peak width at half height of the CCH during active (dark gray) and passive (light gray) listening. The left ordinate is the CCH coefficient at their half height peak, whereas the left ordinate is the time (ms) of the CCH.

The mean coherence of frequencies ranging from 1-150 Hz among all multiple single-unit along time was analyzed by plotting the coherence spectrogram. The coherence spectrogram is shown in Figure 3.19. This figure suggests that the coherence increases after the tone onset for passive and active listening and lasts for approximately 200ms. However, the active listening condition has a higher coherence than the passive listening condition within this 200 ms. It also appears that the coherence is higher at baseline levels in the active listening condition than in the passive listening condition. Additionally, the coherence is higher at lower frequencies (<20 Hz) and gradually decreases at high frequency ranges (> 60 Hz). It also seems that the coherence in the active condition extends to higher frequency ranges as compared to the passive listening condition.

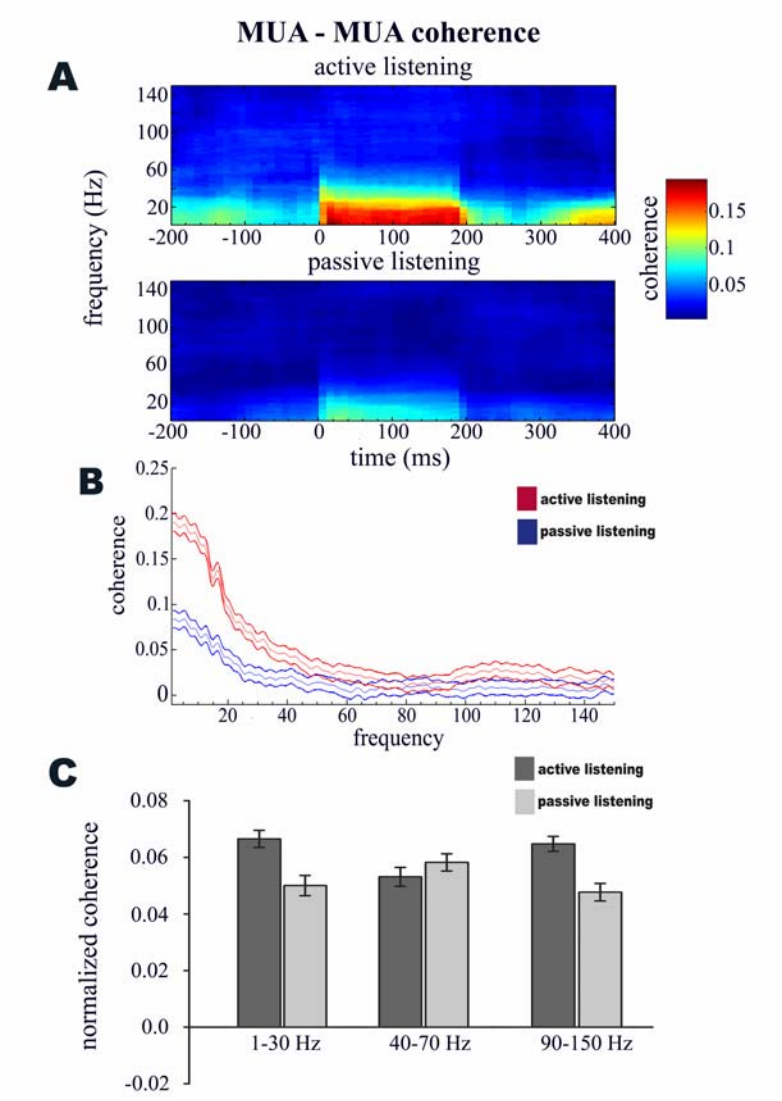

Figure 3.19. The coherence spectrogram shows that there is more coherence among neurons after the tone onset in the active than in the passive listening condition. A) Top graph is spike train coherogram of active listening (67 multiple single-units; 3 rats; 200 combination pairs). Bottom graph is the coherogram of passive listening (64 multiple single-units; 5 rats; 185 combination pairs). Ordinate is frequency (Hz), abscissa is time (ms) and the color coded z-axes is coherence. B) Middle figure shows the mean coherence (thin line) and its 95% confidence interval (think line) for spike train coherence of the active listening (red line; 67 MUA, 200 pairs) and passive listening (blue line; 64 MUA, 185 pairs). C) The bottom figure shows the mean normalized coherence (± SEM) for active listening (dark gray bars) and passive listening (light gray bars) in the alpha/beta (1-30 Hz), gamma (40-70 Hz), and high gamma (90-120 Hz) frequency ranges.

In order to further quantify and compare the coherence between active and passive listening, the mean coherence and its 95% confidence interval was measured during 0 ms to 300 ms after the tone onset. Moreover, the coherence of this time interval was computed for each MUA pair and normalized by the baseline coherence (-400 ms to -100 ms before tone onset).

The coherence analysis displayed in Figure 3.19 demonstrates that active listening modulates the MUA-MUA coherence up to 40 Hz (Jackknife U test, $p<0.01$). Figure 3.19B shows the mean coherence and its 95% confidence interval of the active (red line) and passive (blue line) listening conditions. I observed that low frequencies have a higher coherence during the active listening as compared to passive listening. After 50 Hz the coherence for both conditions is virtually zero, except for a slightly increase in coherence at frequencies around 90-150 Hz in the active listening condition only.

The active listening modulation in coherence was further explored by normalizing the coherence after the tone onset by the baseline levels and comparing both experimental groups. Figure 3.19C shows the normalized coherence of the 0-300 ms after the tone onset by the coherence at the baseline levels. This analysis was performed for each individual trial of the neurons analyzed. However, in order to compute the coherence, sufficient spikes at the baseline levels were only available in a subset of these trials. Nevertheless, the averaged coherence at the alpha/beta (1-30 Hz), gamma (40-70 Hz), and high gamma (90-120 Hz) shows that active listening modulates the coherence at alpha/beta (Wilcoxon paired t test, $p<0.01$) and high gamma ($p<0.001$), but not at gamma frequency ranges (Wilcoxon paired t test, $p=0.2826$).

The coherence is a complex quantity composed of both phase and amplitude of two Fourier transform signals, whether these signals are LFP or spike trains. The relative phase of the coherence allows us to estimate whether two multiunit spike trains fire simultaneously. The increase in coherence at low frequency ranges indicates that neurons might fire at a precise lag or that they fire simultaneous action potentials. The average coherence phase of each frequency for each pair is plotted in polar plot coordinates. This analysis gives an idea of the effectiveness of the synchronous activity at particular frequencies of the A1 neurons in activating postsynaptic neurons.

The polar plot displayed in Figure 3.20 shows the coherence phase of neurons in the auditory cortex. Each arrow represents the averaged coherence for each of the MUA clusters (200 MUA pairs for active and 185 pairs for passive listening) of a particular frequency. Note that any one recording site of a given pair can be taken as a reference, thus the sign of the coherence is arbitrary. Figure 3.20 shows that at low frequency ranges the mean coherence of the combination pairs is consistently around the zero phase. Thus, at these low frequency ranges the neurons in A1 are likely simultaneously activated and they will likely activate the neurons which they are projecting to. Additionally, this simultaneous activity occurs during active and passive listening. However, while for active listening most of the averaged pairs have a nearly zero phase lag, the coherence phase in the passive listening do not.

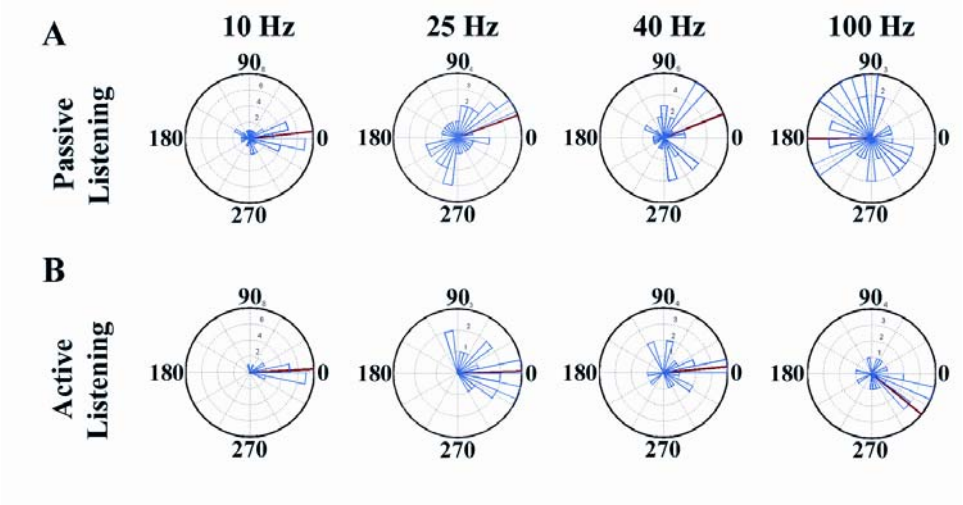

Figure 3.20**.** Polar plot histogram of the coherence phase during active and passive listening. A: The blue histograms of the polar plot shows the averaged coherence phase of passively listening rats at alpha (10 Hz), beta (25 Hz) gamma (40 Hz) and high gamma (100 Hz) frequencies during 300ms after tone onset. B: Polar plot histograms showing the averaged coherence phase of neuronal pairs at the same frequencies during a 300ms interval after tone onset in the active listening condition. The red trace is the mean averaged angle.

3.4 Discussion

Attention-related processes modulate the MAEP components

The LFP recordings presented here showed a very short latency to tones with a positive peak (P1) around 10ms, a negative peak (N1) at 15 ms eventually followed by a N2 (30 ms to 50 ms) component, and by another positive peak starting at 45-100 ms (P3) after the tone onset. This response pattern is highly consistent across channels and it has been described before as characteristic from the primary auditory cortex (Barth & Di, 1990, 1991; Di & Barth, 1992; Eggermont and Ponton, 2001). Moreover, there is a clear attention modulation of the N1 component (15-17 ms) and a second N2 component (30 ms to 50 ms) as well as the second positive (P2) MAEP component that occurs around 70-100 ms after the tone onset response. It seems that perception of the tone modulates the amplitude but not the latency of early MAEP components.

The results presented in this chapter are in agreement with EEG and MEG recordings in human subjects in which spatial-attention modulates the N1 (N1m) and P1 (P1m) components of the MAEP (reviewed in; Herrmann & Knight, 2001; Näätänen & Alho, 2004; Anllo-Vento et al., 2004), and this modulation starts as early as 20-50ms (Woldorff et al., 1993) and it is estimated to be located in A1 (Rademacher, 2001; Poghosyan, 2008). The result presented in this chapter extends these previous data by directly recording LFP in A1 and showing that perception of an auditory event modulates the amplitude of MAEP components in A1.

Perceiving tones modulates high frequency oscillations

It has been shown that high gamma frequency oscillations (>90 Hz) in the temporal lobe are induced by selective attention perception and discrimination of tone

and phonemes, perception of music and speech comprehension (Crone et al., 2001, 2006; Canolty et al., 2001; Edwards et al., 2005, Lachaux et al., 2007; Ray et al., 2008) Therefore, these studies were very important to establish that high gamma oscillations are induced by perception of simple and complex auditory stimuli. However, all of these results are collected with ECoG or MEG techniques, which prevented a detailed description of where the high frequency oscillations are generated. Previous results in experimental animals complemented the human data by showing that the latency and amplitude of high frequency oscillations are modulated by the activity the of nucleus basalis of the anterior forebrain (NB), the thalamic reticular nucleus (TRN), and the posterior intralaminar nucleus of the thalamus (PIL) (Metherate et al., 1992; Barth & MacDonald, 1996; Sukov & Barth, 1998, 2001; MacDonald, et al., 1998;). Both the TRN and the PIL, this latter nucleus being considered part of the intralaminar/midline thalamic nuclei (Van der Werf et al., 2002), receive projections from the brainstem reticular formation (Pare et al., 1988; Hallanger et al., 1987). Thus, the activity of these nuclei is modulated by the ascending arousal system (Sarter et al., 2006; Steriade & Pare, 2007; Jones, 2008). These results suggest that these high frequency oscillations in the primary auditory cortex could be modulated by arousal, vigilance, or attention. I directly tested this hypothesis by maintaining the physical attributes of the auditory stimuli constant while manipulating the goal-directed behavior of the rat.

The results showed here demonstrated that perceiving a tone changes the intrinsic temporal dynamics of the primary auditory cortex. These results are consistent with the finding that visual scene selection in binocular rivalry experiments induces local neuronal synchronization at the gamma band in V1 (Fries et al., 1997; 2001a). It is also consistent

with the finding that selective spatial based attention and selective feature based attention modulates the neuronal synchrony at the gamma range in V4 (Fries et al., 2001b, Womesdorf et al., 2006; Fries et al., 2008; Bichot et al., 2005). However, we performed an across-group comparison in which one of the experimental groups has undergone an extensive training protocol (active listening group). It is well established that temporal as well as spectral discrimination training protocols change the topographic organization in A1 (Weinberger and Diamond, 1987; Recanzone et al., 1993; Bao et al., 2004; Kilgard et al., 1999). Therefore, it is possible that our results could be a bi-product of topographic organization instead of a result of active listening per se. Our experimental setting does not allow us to completely rule out this explanation; however, some observations have to be taken in consideration. First, I used relatively loud sounds (75 dB SPL) which likely saturate the neuron response, thus neurons with different CF are likely stimulated by the stimuli condition. Second, I excluded sharp neuronal onsets which are the response utilized to generate the tonotopic maps of A1 from the spectral analysis. Thus the analysis used in this chapter might not be contaminated by the sharp neuronal transitions used to construct tonotopic maps which are likely the mechanism by which feature extraction of simple sounds is achieved. Third, the recordings performed in this experiment spread to a cortical area of 1.0 mm^2. Since A1 has a characteristic frequency gradient of ≈ 500 μm/ octave and a bandwidth of 1.4 octaves at 40db SPL above threshold (Rutkowski et al., 2003; Sally and Kelly, 1998), it is probable that I am recording from neurons with similar spectral characteristics in passive and active listening as well. However, further chapters will address the question of attention modulation in A1 using within-group comparisons. Thus, still remains the possibility that

the attention modulation of A1 observed here could be explained by anatomical structural changes in the auditory cortex caused by extensive training.

Perception increases coherence among LFP sites

It is thought that the LFP signal collected with high impendence electrodes measures synaptic potentials with an estimated 250-450μm diameter in a relatively small population of neurons (Abeles, 1982; Engel et al., 1990; Katzner et at., 2009). Thus the increase in amplitude in a LFP site at specific frequency bands does necessarily show an increase in synchronization across LFP sites. In order to further explore whether the increase in LFP amplitude reflects synchronization among the LFP sites, we computed the coherence spectrogram and coherence spectrum. Our results showed that there is more coherence at low frequency bands for passive than active listening group, while the opposite was true for high frequency bands. This result shows that coherence among LFP sites is modulated in the active listening condition at both the gamma band and high gamma band.

Attention-related processes modulates local synchrony

I also measured synchrony at local neuronal populations by computing MUA-LFP coherence. This measurement shows that active listening to tones generates a distinctive coherence peak at 20 Hz, followed by a second less conspicuous peak at the low end of gamma frequency band (40-60 Hz) at local neuronal networks. Importantly, this increase in coherence is not caused by the short response onset of the LFP and action potentials to the stimulus, because the window of analysis was 30 to 330 ms after the stimulus onset. Therefore, perception of simple acoustic event modulates the synchronization of local neuronal networks in the primary auditory cortex which is induced to synchronize their

spike train at specific frequency bands. Note, however, that while the LFP power spectrum analysis showed an increase in power at high gamma frequency bands, the MUA-LFP coherence analysis did not. These results suggest that oscillations at beta and gamma bands are caused by local neuronal networks. Thus, the MUA-LFP coherence results suggest that active listening appears to increase neuronal synchronicity in local neuronal networks at specific frequencies. Therefore, neuronal networks that are relatively close in space and are engaged in sensory processing will likely fire action potentials at specifically 20 Hz and at 40-60 Hz frequency bands. Moreover, because the auditory stimuli used here are 10 kHz tones in both conditions, this increase in coherence is not due to the response to stimulus characteristics. A caveat of this study, however, is that it is possible that these results could be explained by an electrode sampling bias of our recording setup to a particular class of neurons in the primary auditory cortex. Studies with larger sampling using single-units would be necessary to further explore this possibility.

It is important to consider that A1 has a modular organization in which a particular modular neuronal network is tuned to subsets of the sound features (reviewed in Read et al., 2003; Schreiner, 2000). Additionally, in the visual system, it has been shown that gamma oscillations show a strong correlation to micro-columns of neuronal processing such as neuronal clusters of speed processing in MT (Liu and Newsome,2003; 2005; 2006) and orientation tuning of V1 (Gray & Singer, 1989; Frien et al., 2000). Therefore, it is possible that these oscillations could be a neuronal mechanism that links neurons processing features of the acoustic scene.

Attention could enhance the processing of relevant acoustic features in order to label neurons that in A1 are relevant for processing the acoustic scene at hand and, therefore, facilitate auditory scene analysis. Note, however, that in the experiments of this chapter the physical attributes of the sound are exactly the same in active or passive listening, and moreover, they are pure tones. Thus, our results could be interpreted as an indicator that high frequency oscillations are not exclusively a neuronal mechanism that enables acoustic feature extraction, but instead, a bi-product of a general vigilant state in A1 which increases synaptic activity in this region. However, because the results show that perception of relevant sound with simple acoustic features induces neuronal synchronization at high frequency bands, it does not rule out the possibility that high frequency oscillations may be a neuronal mechanism of auditory scene analysis (ASA). Additional experiments, in which the auditory stimulus configuration are manipulated, are warranted to further clarify what is the role, if any, of synchronization in ASA.

In conclusion, the results of this chapter demonstrated that gamma and high gamma oscillations are enhanced in rats engaged in actively perceiving a simple acoustic stimulus. Moreover, it suggests that in a vigilant state in which sensation leads to perception, these high frequency oscillations might be a neuronal mechanism by which neuronal networks processing incoming auditory stimuli can be coordinated in order to optimize sensorial processing. Therefore, our results complement recent findings suggesting a high correlation between the tonotopic organization of the primary auditory cortex and the occurrence of high gamma oscillations (Steinschneider et al., 2008). This correlation suggests that these oscillations might be important to extract sound features. Our results are important in establishing that not only high frequency oscillations are

correlated to auditory stimulus processing, but that they are in fact, modulated by actively perceiving them. Importantly, these high frequency modulations reflect cognitive process in the primary auditory cortex.

Chapter 4

Attending to two-tones played in a fast time interval modulates the neuronal activity of the auditory cortex.

4.1 Introduction

The auditory system has to code highly dynamic patterns of frequency and amplitude modulations to assign what the sound is and where it came from. In addition to coding such complex and dynamic temporal patterns varying over time, it also has to disentangle meaningful foreground information from background acoustic noise. This is especially important for animals living in complex large groups. For instance, in a noisy party, we are able to follow a conversation even though there is an overlapping spectral pattern from the speech produced by different individuals in the party.

The process by which several species including humans (Bregman, 1990), songbirds (MacDougall-Shackleton, 1998), and monkeys (Izumi, 2002) achieve this feat is called auditory scene analysis (ASA) (Bregman, 1990). The sound sequence pattern composed by acoustic events that is followed as a separate entity amid other sounds over time is defined as an acoustic object or an auditory stream (Bregman, 1990; Cusack & Carlyon, 2004; Snyder & Alain, 2008; and Bee & Micheyl, 2008). Psychophysical data suggest that the auditory system uses time regularities as invaluable information to group sounds in auditory perceptual streams (Bregman, 1990; Handel 1989; Moore, 2003). For example, studies using complex tones with unresolved frequencies (Roberts et al., 2002) or amplitude modulated noises (Grimault et al., 2002) demonstrate that the auditory system is capable of forming auditory stream by using only temporal cues (Dannenbring & Bregman, 1976; Bregman, 1990; Bregman et al., 2000). Moreover, it is documented

that individual acoustic events presented in a context of metrical regular sequences (rhythms) are easy to perceive and to remember (Large & Jones, 1999).

Lesions studies in regions of the temporal cortex encompassing A1 suggest that this area is necessary for acoustic temporal processing since they lead to impairment of acoustic temporal discrimination (monkeys: Cowey & Weiskrantz, 1976; Colombo et al., 1996; humans: Griffiths et al., 1997; Liegeois-Chauvel et al., 1998; rats: Syke et al, 2002, Cooke et al., 2007). These psychophysical results greatly suggest that A1 processes temporal cues to form an auditory object. However, most of the single-unit recording studies focused on spectral cues to study the correlation of A1 activity with auditory stream formation in awake monkey (Fishman et al., 2001; 2004; Micheyl et al., 2005, 2007).

Experimental evidence in monkeys performing tone sequence discrimination suggested that A1 activity is modulated by the sequence in which a particular set of tones are heard (Phan & Recanzone, 2007; Yin et al., 2009). For instance, neurons in A1 are modulated by the order in which fast tone sequences (interval of ≈ 20 ms) were played (Phan & Recanzone, 2007). In one study in which trained monkeys immediately received a reward after releasing a bar upon hearing a specific melody, the activity of A1 is strongly modulated by the order in which the tones were presented, thereby suggesting that A1 is processing melodies (Yin et al., 2008). In this study, monkeys were trained to respond to a specific tone sequence, and once trained, they were very proficient at anticipating the melody. Importantly, the same tones heard separately did not elicit as strong a neuronal response as when played in the specific sequence (Yin et al., 2008). In addition, this effect was not observed in untrained monkeys (Yin et al., 2008).

It has been known for quite some time that attention to relevant acoustic cues strongly modulates the activity of a subset of neurons in the primary auditory cortex in cats and monkeys (cats: Hubel et al., 1959; monkeys: Miller et al., 1972; Hocherman et al., 1976). Attention to relevant acoustic cues not only modulates the firing rate of A1 neurons, but also modulates the receptive properties of its neurons in a scale of a few minutes (ferrets: Fritz et al., 2003; 2005; 2007). These studies showed that receptive field plasticity is highly dynamic and it is sensitive to attentional demands to correctly perform the task at hand (Fritz et al, 2003; 2005; 2007). Moreover, it is hypothesized that the acoustic streams are formed by attentional demands, spectral and temporal cues at A1 and secondary auditory cortices (Alain & Arnott, 2000; Alain et al., 2001; Carlyon et al., 2001; Cusack & Carlyon., 2004; Snyder et al., 2006; Gutschalk et al., 2007).

Additionally, recent experimental evidence suggests that the activity of A1 might not be only related with acoustic feature extraction. For instance, it has been shown that approximately 13% to 14% of A1 neurons display non-auditory responses that correlated with features of the task being performed (Brosch et al., 2005; Yin et al., 2008). In these studies monkeys were required to grasp a bar throughout a discrimination task. Their task was to release the bar once they heard a specific tone sequence (Yin et al., 2008) or release the bar once they heard a direction of frequency change (Brosch et al., 2005) to receive a reward. The activity of a small population of A1 neurons was related to the time of the reward or to non-acoustic cues, such as light, which signaled the beginning of the trial (Brosch et al., 2005). Thus, there is evidence that neurons in A1 are activated by non-acoustic cues that are relevant for a good performance in an acoustic task in order to receive a reward (Brosch et al., 2005; Yin et al., 2008). Therefore, there is some

experimental data suggesting that the activity of A1 is not only correlated with acoustic physical feature extraction, but also with abstract acoustic object formation that is relevant to goal-directed behavior

The study of Yin et al., 2008 showed that the activity of A1 is modulated by temporal cues as well as spectral cues, and moreover, they suggest that attention to temporal cues shapes the neuronal response of A1. Perhaps more importantly, their results also suggest that A1 extracts acoustic cues that are useful in anticipating relevant environmental information. Despite the importance of that study in showing that the activity of A1 is modulated by the temporal cues in which a sound is played, a direct analysis of the correlation of A1 activity with behavioral performance by utilizing psychophysical measurements was not performed. Such analysis could shed some light on deciding if the activity of A1 is mainly related with primitive grouping of tone sequences in melodies or if it has a dynamic role in implementing goal-directed behaviors.

The correlation of A1 activity with behavioral performance requires the analysis of neuronal activity during correct and incorrect trials. However, this type of comparison between correct and incorrect trials and their correlation with behavioral performance is rarely seen, perhaps because when a monkey is proficient in a given behavioral task, there are relatively few incorrect trials which could be used to correlate the neuron properties with behavioral performance. Experimental settings and spike train analysis in which the activity of A1 is correlated with animals' behavior could shed some light in the role of the primary auditory cortex in processing acoustic relevant information for goal-directed behavior.

In this chapter I aim to test two correlated hypothesis. First, that paying attention to reliably predictive acoustic patterns modulates the activity of the auditory cortex. Second, that the activity of the auditory cortex predicts behavioral performance. Therefore, in this chapter I specifically aim to use signal detection theory to test the hypothesis that the activity of neurons in A1 predicts behavioral outcome. In order to test this hypothesis, I developed a simple two-tone discrimination task, in which rats have to attend to two tones played in fast succession in order to receive a reward.

A second aim of this chapter was to test whether neuronal synchrony is also modulated by attention to temporal cues. It has been shown that neuronal synchrony in the primary visual cortex (V1) is strongly modulated by visual perception in binocular rivalry experiments (Fries et al., 1997, 2002). These results implied that V1 neurons processing different features of the visual scene are bound together by neuronal synchrony in order to form a coherence percept (Fries et al., 1997, 2002a, 2002b; Singer, 1999). Moreover, selective spatial attention also modulates neuronal synchrony in the extra-striate visual cortex (Fries et al., 2001, 2008; Womesdorf et al., 2006). In the previous chapter, I also showed that neuronal synchrony is apparently modulated by perception of a tone in A1. Therefore, because neuronal synchrony may be a neuronal mechanism to form coherence percept and because it is also modulated by attention, I also tested if neuronal synchrony might be modulated by attending to temporal cues in A1.

4.2 Methods

Behavioral apparatus and training

I trained 17 rats to discriminate one versus two-tones played at 200 ms interval in order to correctly receive a water reward. After completion of the training, multiple single-units were recorded in the primary auditory cortex (A1) of awake behaving rats in order to test the hypothesis that the activity of A1 is, not only modulated during the tone onsets, but also modulated during the interval between tones.

The behavioral apparatus used to train rats consisted of 4 chambers (dimensions of 53 x 39 x 26 cm) each one acoustically insulated with layers of foam and lead. These chambers were also ventilated and lighted by 4-W light bulbs. This behavioral apparatus contained speakers located 20 cm in front and 10 cm above the rat's head. Auditory stimuli were generated by programmable function generator (33120A, Hewlett Packard, Denver, CO, USA) and played through this speaker. Before each training session, rats were weighed and placed into a restrainer custom 23 cm box made of black Plexiglas which rats voluntarily entered. The black Plexiglas Box was immediately transferred to the chamber after the rat entered it. The box has a trap back door which prevented rats from backing out. The front wall contained a 2 cm-wide hole through which the rats could poke their nose to contact a metal 18-gauge stainless steel tube with their tongue.

The target behavior by which I detected whether rats have learned the two-tone discrimination task was protrusion of the tongue out of the mouth toward the 18-gauge stainless steel tube. Water reinforcement was delivered through this tube which was precisely positioned 10 mm away from the rat's snout. Calibrated water drops (approximately 40 µl) were delivered to each rat by opening of a miniature solenoid

valves (LFAA1201516H, The Lee Co, Essex, CT. USA) which gate pressurized water streams. A photodarlington optical switch (No. H21B2, Fairchild Semiconductor) was positioned around the tip of the tube so that the interruption of an infrared photobeam signaled the protrusion of the tongue. A 10 ms interruption of the photobeam was considered a response. Photobeam interrupts were recorded by a personal computer via a 16 separate threshold circuits and a 16-channel analog-to-digital converter (DAS-16, Keithley Metrabyte, Cleveland, OH, USA) which sampled each channel at 200 Hz. Software performing timing control, stimulus control, and data acquisition was written using the ASSYT scripting language (Keithley-Metrabyte Inc. version 4.01). The rat's motivation was ensured by controlling daily water intake for 30-45 minutes in their home cage immediately after each daily conditioning session. Rats were weighed to ensure that their body weight did not fall below 80% of matched age control rats with ad libitum access to water.

Behavioral paradigm and training

Rats were trained in an instrumental operant paradigm in which they had to learn a two-tone discrimination task. Prior to training, rats were put on a water restriction regimen in which they had daily access to water for a 30-45 minutes for approximately 7 days. The same water restriction regimen was maintained throughout the duration of the training period. The target behavior was a protrusion of the tongue. In another words, the rats licked an 18'' gauge stainless tube which was used to deliver water when the behavior was correctly performed. This licking behavior allowed us to quantify the acquisition of the two-tone discrimination behavior. The rats had to discriminate between one and two 10 kHz tones played at 75 dB for a duration of 20 ms and with a 200 ms

interval in order to receive a water reward. The water reward (unconditioned stimulus, US) was given to these highly motivated thirsty rats upon correctly licking a spout after they heard the two tones (positive conditional stimulus, CS+). A water drop (40 µl) was delivered to them immediately after they licked the spout. No water reinforcement was given in the one tone (negative conditional stimulus, CS-) trials. Note that neither negative reinforcement nor punishments were given to rats that licked the spout after hearing one tone or that did not lick the spout after hearing two tones. The behavioral paradigm is depicted in the top graph of Figure 4.21, which shows a scheme of one training session of approximately one hour with 120 random one and two-tone trials. Observe that each trial was randomly inter-spaced by an average of 30 seconds (± 5 s), which minimize anticipation of the trials.

After the rats learned the two-tone discrimination task, they were tested in a psychophysical test. This test was designed to test the temporal discrimination acuity of the rats. Each psychophysical test session consisted of 140 trials in which 60 trials were the CS+ two-tone trials (200 ms inter-tone interval), 60 trials were the CS- one-tone trials, and 20 trials consisted of 4 short inter-tone interval types with 5 trials each. The two-tone trials with short inter-tone interval could be any 4 combinations of the 10 , 15, 20, 25, 30, 35, 40, 45, 50, 55, or 100 ms intervals. Note that the tones had a 8 ms duration in the psychophysical test. Three precautions were taken in order to prevent behavioral decrements of the acquired two-tone discrimination that could be caused by the psychophysical test. First, there were very few short inter-tone intervals intermixed within the psychophysical test, which otherwise would be the same as the acquisition of phase 1. Second, there was no water reward given in the short inter-tone intervals. Third,

each psychophysical test session was separated by, at least, eight acquisition type sessions. Therefore, no more than one psychophysical test was performed in an approximately 10 day period. The bottom graph of Figure 4.21 shows one psychophysical test session.

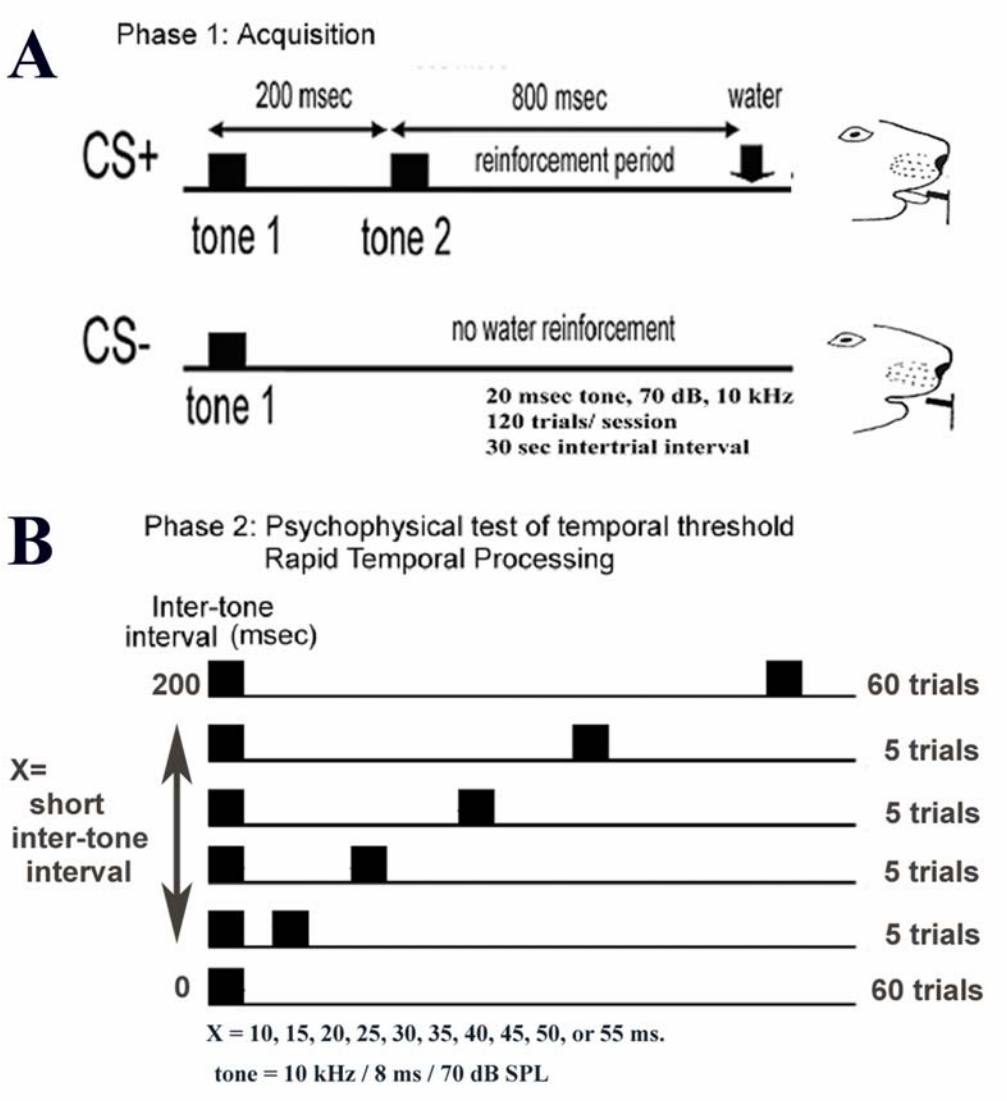

Figure 4.21. Behavioral paradigm. A) Top figure depicts acquisition phase 1 which shows the positive conditional stimulus (two-tone trials, CS+) and the negative conditional stimulus (one-tone trials, CS-). B) The bottom figure describes the phase 2 psychophysical test, which is basically the same as the acquisition behavioral paradigm, except that it adds 5 trials for each of the 4 short inter-tone interval types.

The CS+ consisted of two-tone trials, in which two 10 kHz tones with a 20 ms duration played at 70 dB SPL were separated by a 200 ms silence interval. Any time that the rat licked the spout during the reinforcement period (within 800 ms after second tone onset) he received 40 µl water drop and the trials restarted. The bottom drawing of the graph shows the negative conditional stimulus (CS-), which consisted of a one tone trial, in which one 10 kHz tone with 20 ms duration was played. Any time that rats licked the spout within 1000 ms after the tone onset (the no water reinforcement period) the trial ended and a new trial restarted. I computed the licking percentage in the correct two-tone and in the incorrect one tone trials as well as the time in which rats licked the spout. This time was computed as latency in relation to the first tone and it is shown in Figure 4.23. After the animals reached an asymptote of 75% correct two-tone trial responses they were tested in a psychophysical test. This test consisted of randomly varying the silence interval in few of the two-tone trial. After completing the psychophysical test, rats were prepared for a cap implant for multiple single-unit recordings. Behavioral data also was collected during the recording procedure sessions in order to investigate whether the two-tone discrimination paradigm learned in the training sessions was maintained during the electrophysiological recording conditions. Additionally, to investigate if the motivation to lick the spout maintained constant during the recording session, the time of each recording session was subdivided in evenly 10 bins throughout the experimental sessions. Then, the number of trials in which rats responded, did not responded to the two-tone trial type (CS+), or responded to the one-tone trial type (CS-) was collected for each bin. I reasoned that if the motivational level is maintained constant throughout the recording, then the different trial types would have a uniform distribution along the time axes.

Animal preparation

The experiments were carried out in a total of 17 Sprague-Dawley albino rats (Taconic Farms, Germantown, NY). A large number of these experiments were not analyzed in this dissertation, but were necessary steps in order to acquire the skills to perform extracellular recordings in the awake animals and in the awake behaving rats, to optimize the conditions of recording in the auditory cortex, to optimize the conditions for behavioral training. All surgical procedures and experimental protocols were in accordance to NIH guidelines and were approved by OHSU Institutional Animal Care Use (IACUC). All the animal preparation procedures were described in Chapter 2. The only modification of that protocol was that two days after recovery from the craniotomy rats were daily placed for 2 to 3 hours in the atraumatic head holder. Rats were then submitted to 2 to 4 training sessions per day for 2 to 4 days before the recoding session. This step was necessary in order to ensure that rats would perform the discrimination task that they were trained for during the recoding session.

Stimulus generation and recording session

The auditory stimulus consisted of a 20 ms tone at 10 kHz frequency presented in a 30 second semi-random intervals. The stimuli generation and recording sessions were essentially the same as described in Chpater 2.

Recording procedures, preliminary analysis and data set

Multiple single-units (MUA) were recorded in awake and trained awake behaving rats listening to simple auditory stimuli in order to test the hypothesis that attentional expectations sharpen the auditory cortex activity at the single cell level. The auditory stimuli during searching and isolation of MUA consisted of 50 ms tones ranging from 1

to 30 kHz presented every 500 ms at 1 kHz random steps at 70 dB SPL. Once acceptable simultaneous MUA were isolated (ranging from 5 to 15 simultaneously MUA recordings/session) the two-tone discrimination protocol was initiated. After the experimental session was over, a similar 50 ms tone pip protocol used to isolate MUA, was utilized to define the MUA characteristic frequency. This protocol consisted of ten iterations of 1 to 30 kHz tones with a 50 ms duration, ranging from 70 dB to 20 dB SPL.

The data selection and off-line data analyses were performed with NEX and MATLAB (The MathWorks, Inc., Natick MA, USA). The NEX spike train analysis software was used to compute peri-event histograms (PSTH) of 1ms bins to select neurons that were time-locked and had a short latency (<20 ms) to the acoustic stimulus. It is known that A1 neurons have a short latency and sharp tuning curves (Sally & Kelly., 1988). I restricted our analysis to well isolated MUA that had short response latencies (<20 ms) to the 10 kHz tones. This criterion for selecting these neurons was based on the pattern of neuronal responses to tones in A1. Therefore these neurons had a latency response to tones ranging from 10 ms to 17 ms. Additionally, I collected the LFP responses which had to have the characteristic middle auditory evoked potentials (MAEP) consistent to the A1 response reported in the literature (Talwar et al., 2001; Barth & Di., 1990,1991; Franowicz & Barth., 1995). Then, the NEX programming language was used to select 20 attended, unattended, and aroused tone trials of 1600 ms each. Each of these data segments had 500 ms of baseline and 1100 ms after stimulus onset. After these preliminary analyses a total of 86 MUA were used in this study. These MUA were selected from a pool of 8 experimental sessions in 3 rats

Behavioral Index

The PSTH was used as a preliminary analysis to detect attention modulations in the firing rate of the attentive and inattentive trial types. After this first analysis, each neuron PSTH was normalized by its averaged baseline firing rate to create a normalized PSTH. This normalized PSTH was used to generate a behavioral index. This behavioral index which compares the normalized firing rate of the attentive versus inattentive trials was generated during the T1 (0-200 ms after first tone onset) and the T2 (200-400 ms after first tone onset) time periods. The formula xFR- yFR/ xFR+yFR was used to create the behavioral index. The xFR represent the normalized firing rate of the attentive TT, and the yFR represent the normalized firing rat during the inattentive TT trial types. I computed this behavioral index during the T1 and T2 time interval. The behavioral index generates a value between -1 to 1 in which a value towards 1 signals an increase in firing rate during the T1 or T2 intervals, whereas a value toward -1 signals the opposite. A value of 0 signals no increase in firing rate. Moreover, a paired non-parametric statistical test (Wilcoxon signed rank test) was used in order to test the null hypothesis that there is no difference between the behavioral index of the T1 and T2 intervals.

The Receiver Operator Characteristic (ROC) analysis

The results obtained with the behavioral index strongly suggest that it is possible to classify whether the rat will attend to or will not attend to the second tone and receive water based solely in the neurons' firing rate. The *receiver operator characteristic (ROC)* analysis was employed to quantify the reliability of classifying an attentive and an inattentive trial type based in their firing rate. The ROC analysis is based on signal detection theory, which is a means to quantify the ability to discern between signal and noise (Green & Swets, 1966).

The ROC analysis is base on a binary classification which is the task of classifying the members of a given set of objects into two categories. There are four possible outcomes in a binary classification. In our case, we can classify the firing rate of a neuron as belonging to the class *attentive TT* when the firing rate of the neuron correctly belongs to the category *attentive TT*. In this case, we have a *true positive* (TP). However if the firing rate of the neuron in fact belongs to the *inattentive TT* category, then we have a *false positive* (FP). Conversely, we can classify the firing rate of a neuron as belonging to the *inattentive TT* category. If the firing rate of the neuron correctly belongs to this category, then we have a *true negative*. Otherwise, if the firing rate of the neuron belongs to the attentive TT category, then we have a *false negative*.

Therefore, a given ROC value is the probability by which, based in the firing rate, an ideal observer can reliably classify a trial as being attentive TT (rat licks the spout in the two tone trial to receive water) or inattentive TT (rat did not lick the spout in the two tone trial to receive water). Thus, we have a relative frequency of True Positive Fractions (TPF), False Possitive Fractions (FPF), False Negative Fractions (FNF), and the True Negative Fractions (TNF) which is showed in the table of Figure 4.22A.

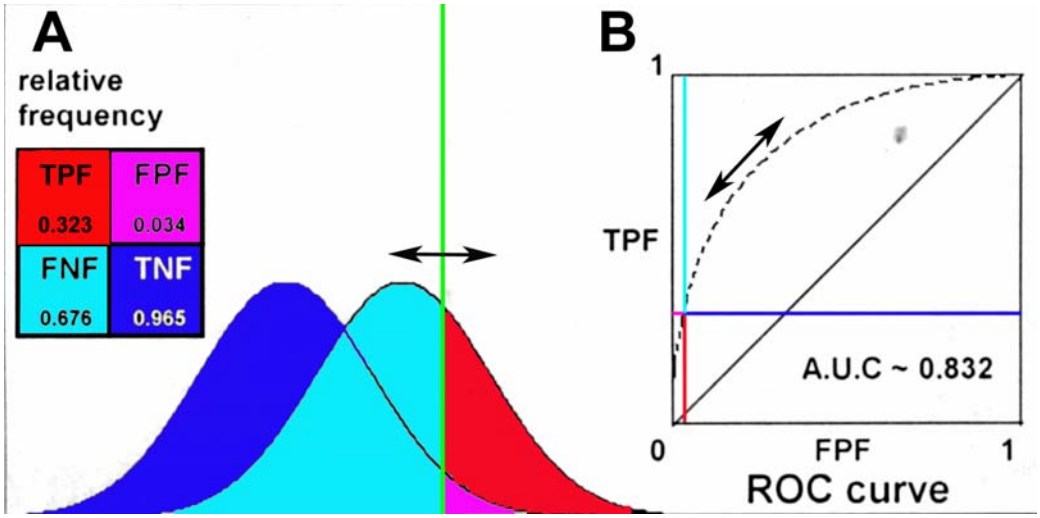

Figure 4.22. ROC principle. Two different but overlapping bell-curve distributions (i.e, the firing rate of the attentive and inattentive trials) are labeled as the right POSITIVE bell-curve (which includes the True Positive Fractions (red) plus False Negative Fractions (light blue)) and the left NEGATIVE bell-curve (which includes the True Negative Fraction (dark blue) and the False Positive Fractions (pink)). The distributions are separated using a threshold (vertical green line). The insert graph shows a plot of the TPF and FPF as the threshold is varied through the data set values. The TPF and FPF values are expressed as fractions ranging from 0 to 1, but they could be also expressed as percentages of True Positives and False Positives.

The ROC method is based on the idea of an adjustable cut-off threshold level which separates two overlapping categories (Fawcet, 2006). The ROC principle is illustrated in Figure 4.22. In my case, the categories are attentive and inattentive TT trials. The adjustable threshold is represented by the green vertical line, whereas the perpendicular arrow represents that this threshold is adjustable. At a high threshold level the vertical green line will be at the far right of the left gaussian curve. This represents the point 0,0 at the far left in the graph 4.22B. At this point there is no TPF or FPF. However, as we move the threshold from right to left, the number of True and False Positives initially increases. Thus, we plot points moving up in the graph 4.22B, which represents the True Positive values, but we also plot points moving to the right which represents the False Positives. These two values will draw the dash-line curve running from the point (0,0) to the point (1,1). If this dash-line curve approaches the diagonal line in graph 4.22B, then there is a big overlap between the two bell-shape curves representing the two categories in graph 4.22A. In this case, the parameters used to construct the bell-shape curve are not reliable to separate the two categories. If the bell-shape curves shown in graph 2.2A had little overlap, then the dash-line curve showed in 4.22B would approach the value of 1 in the Figure 4.22B. This is a case of a perfect classifier. This value represents that we have 100% of TPF and 0% of FPF. Thus, the value of the area under the ROC curve (AUC) signals how good the parameter used to construct the curve is. For the perfect classifier (little overlap) the AUC has a value approaching 1 and the parameter used to construct the ROC is a good one. Thus, if this value is close to 0.5, then this parameter is not reliable to classify the two categories.

The normalized firing rate (N.F.R.) was the parameter choose to perform the ROC analysis. The N.F.R. was computed by dividing the firing rate by the average baseline firing rate. In our case, in order to construct the ROC, I first rank the normalized firing rate.Then I set the threshold to the highest value and determine whether the value found for the firing rate belongs to attentive TT trial. That being the case, then we have a True Positive and we plot the first ROC point by moving up in the TFP shown in the graph 4.22B. Conversely, if the highest firing rate value does not belong to the attentive TT trial, then we have a False Positive. Thus, we move to the right to plot our point in graph 4.22B. The AUC of the ROC is constructed by repeating this process throughout the rank firing rate values. Moreover, it is important to observe that graph A is symmetric in relation to the two category values. The graph 4.22B is also symmetric in respect to the diagonal. Thus if the values of the two-bell curves are switched, the ROC curve will be traced in the other side of the diagonal, which will result in AUC value between 0 and 0.5.

The ROC analysis that I performed in my data set has a clear interpretation. A value of 0.5 indicates that a given firing rate could be elicited with equal probability for the attentive and inattentive trials. Values approaching 1 indicate that the firing rate responses to the attentive trials are always greater than the inattentive trials. Values approaching 0 indicate the opposite. In order to construct the AUC, I normalized the firing rate of the attentive TT and inattentive TT trial types by their respective baseline. Then, the firing rate was calculated with a 5 ms gaussian window running from 200 ms before to 400 ms after the first tone onset. Additionally, I tested the hypothesis that the AUC collected from the comparison of the experimental groups is statistically different

from a random AUC with an average value of 0.5 (Control AUC in figures 4.28C and 4.30C). In order to compute this random AUC, the spike trains belonging to the attentive and inattentive trial types were switched and shuffled. This procedure generated a spike train without any correlation to the behavior of the animals. Then, the ROC analysis was performed for these switched and shuffled spike trains, which yields a 0.5 AUC value. The experimental AUC were statistically compared to the control AUC by a permutation statistical t test with 1000 permutations of the data set.

Time series analysis

The synchronization of spike trains during the attentive and inattentive trials was quantified by calculating the cross-correlogram functions (CCH) of simultaneous recorded MUA during 200 ms intervals of the T1 and T2 interval. The CCH was calculated using the NEX software which has a built-in CCH function that counts the number of spike coincidences for various time shifts (-200 ms to +200 ms) of each MUA train pair in a 1 ms bin size. The CCH was normalized by dividing the spike coincidences by the total number of bins, which gives a probability of coincidences during the interval analyzed (CCH coefficients). The NEX program also calculates the 95% interval confidence limits for the CCH function. These confidence intervals are based on the assumption that spike trains have an independent poisson distribution (Abeles, 1982). Figure 4.32 shows a CCH neuron pair in which the gray area is the 95% confidence interval. In order to know if the degree of synchrony is higher for the attentive TT versus inattentive TT trials, I simply counted the number of neuron pairs that had spike coincidences peaking above the expected 95% confidence interval for each experimental session. I then selected the highest value of the half height peak for all of these neuron

pairs during the T1 (0-200 ms) and T2 (200 ms-400 ms) intervals of the attentive TT and inattentive TT trials. All neuronal pairs that had values above the 95% confidence interval were then z-score normalized (the peak CCH coefficients of each neuronal pair minus the mean of all CCH coefficients divided by the standard deviation) and expressed as percent of the highest value. These z-score normalized values of the CCH were then plotted in a color-coded matrix (shown in Figure 4.32) for each experimental session. Additionally, in order to have a measurement of the correlation strength of the CCH across experiments, I compared the CCH coefficients at half height peak during the T1 and T2 interval of the attentive TT and inattentive TT trial types for averaged CCH pairs. In order to have a measurement of the temporal dispersion between the correlated spikes train pairs, I also computed the width at half height peak for each CCH pair and averaged them during the T1 and T2 interval of the attentive and inattentive trials. The strength (or temporal dispersion) values of the T1 (or T2) intervals during attentive and inattentive trials were statistically compared using a paired t student test.

Spectral analysis.

In order to study whether pure tones induced neuronal synchronization in the auditory cortex of the rat, I also analyzed coherence spectrogram and the coherence spectrum of simultaneous multi-unit recordings. The spectral analysis was performed with the Chronux data analysis toolbox for Matlab (www.chronux.org) which uses multitaper methods to estimate the power spectrum of the spike train (point process) and derivate the spike spectrogram and coherence. The multitaper method has been extensively used and described in a variety of cortical regions (Prechtl et al., 1997; Mitra & Pesaran., 1999; Halliday & Rosenberg., 1999; Jarvis & Mitra., 2001; Pesaran et al.,

2002, Mitra & Bokil., 2008) and was discussed in chapter 2 and 3. The spike can be treated as a point process in which each sequence of spike trains is binned in 1 ms width, tapered by the slepian functions and Fourier transformed. After computing the spike spectrum, I proceeded to compute the coherence between spike train pairs.

The coherence is the cross-spectrum of two signals normalized ($S_{yx}(f)$) by the spectrum of each signal ($S_x(f)$) and ($S_y(f)$) (see chapter 2). The coherence value provides a normalized linear association of phase and amplitude between two signals ranging from 0 to 1. A value of 1 indicates that two signals have a constant phase and amplitude co-variation while a value of 0 indicates that two signals are independent, not having any phase or amplitude relationship (reviewed in Halliday & Rosenberg,1999; Mitra and Bokil, 2008).

In order to compute the coherence spectrogram of the spike signal, I used a time bandwidth product of 5 and 9 Slepian taper functions in 125 ms overlapping windows in 10 ms steps (180 ms time window for coherence only). The Chronux software provides measurements of 95% confidence interval of the spectrum and coherence estimation which can be used to test significant statistical differences of coherence values between experimental groups. The confidence interval is computed by using a jackknife resampling procedure, in which for each coherence estimate across tapers, the jackknife method leaves one taper estimation out. This creates a set of coherence estimations in which the variance and confidence intervals can be computed and tested for difference in means by using a Jackknife U test (Thomson & Chave, 1991; Efron & Tibshirani, 1993; Pesaran et al, 2002).

4.3 Results

Behavior results

In order to study the effects of attention-related processes in the activity of the auditory cortex, I envisaged a behavioral paradigm in which rats had to discriminate one versus two tones played in a relatively fast succession. I trained rats to respond to two 10 kKz brief tones (20 ms durations) separated by a 200 ms silence interval and ignore a single 10 kHz tone (20 ms durations). The target behavior was a protrusion of the rat's tongue within a 800 ms time interval after the second tone onset.

Rats learned to discriminate between one and two-tone trials after approximately 3 weeks of training. This result is depicted in the top right graph of Figure 4.23, in which the abscissa shows training days in which each data point is the mean of the percentage of correct response in 2 sequential days. The ordinate shows the percentage of licking response to one or two-tone trials. Note that rats quickly learned to discriminate between one or tone tones and their performance steadily increase in the course of the training sessions (see day 10 data point). That is, while they retained their response to the two tone trials in 75% of the trials, they also responded to aproximately to 25-30% the one tone trials. I also computed the latency of response in relation of the first tone. The result is shown in the Figure 4.23B. This graph shows the latency response in milliseconds (ordinate) along the training sessions (abscissa) in 2 day session blocks. Figure 4.23C details the latency response during the first and second training session. Rats very quickly learned to anticipate the water reward. From the first to the second training session their latency response dropped from 900 ms to 450 ms and remained at this level throughout the training days.

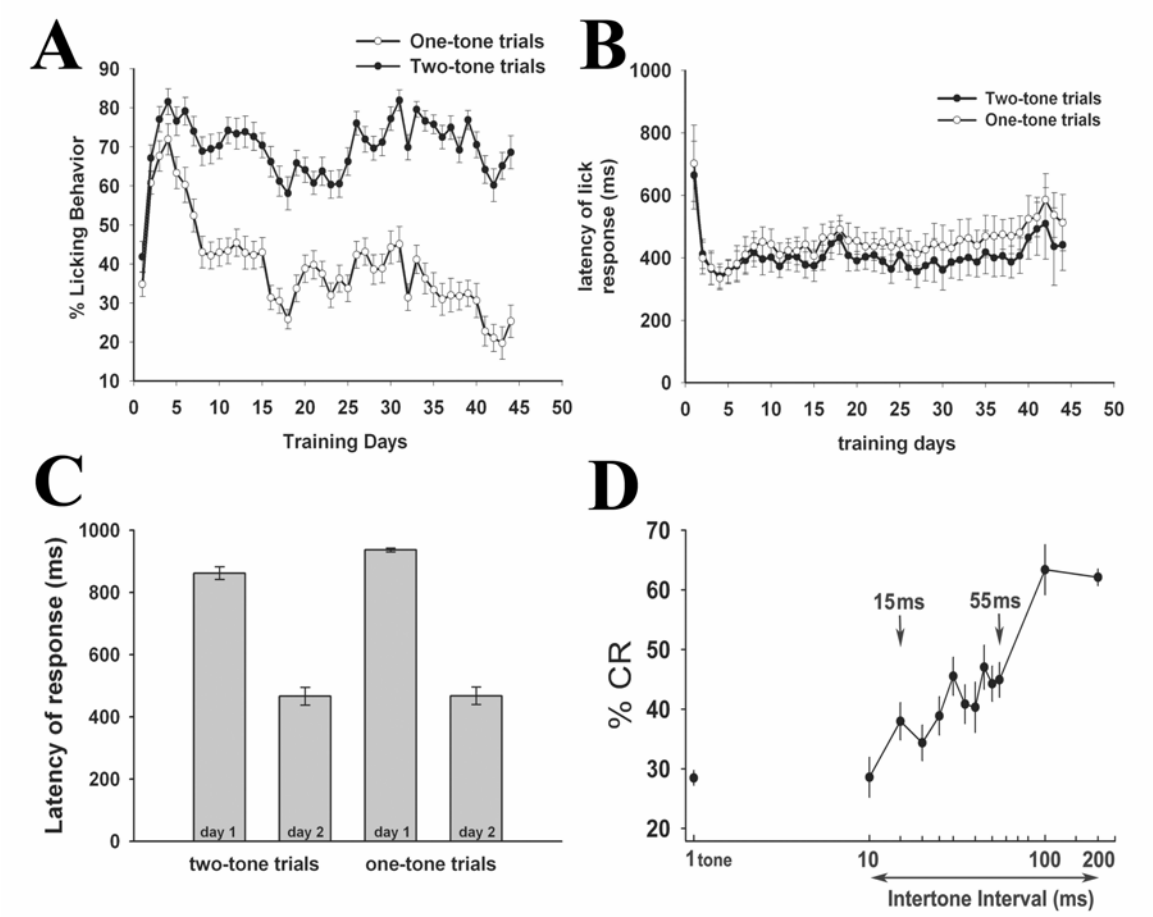

Figure 4.23. Rats learned to discriminate between one and two-tone. A) Figure 23A shows the average of percentage of licking responses (ordinate axes) to two-tone trials (black circles) and to one-tone trials (white circles) along with training days (abscissa axes). B) Figure 23B shows the latency of response in relation to the first tone for the two-tone trials (black circles) and for the one-tone trials (white circles). Each data point in the training days represent 2 days blocks. C) Figure 23C shows the latency of the first and second training day for one and two-tone trials. D) Figure 23D shows the percentage licking response for the inter-tone intervals tested in the psychophysical test. All graphs show the mean and SEM of 17 trained rats percentage responses or latencies.

The psychophysical test confirmed that rats used the time between tones to guide their decision about licking the spout to receive water. This is because when tones are played in a continuously faster succession it becomes more difficult to accurately perceive them as a separate acoustic object having a particular sequence that is different from a simple acoustic object without two acoustic element in it. Figure 4.23D shows the results of the psychophysical test. Note that there is no difference between the percentage of the licking behavior between one-tone trials and the two-tone 10 ms short inter-tone trials. However, this was not the case for the other two-tone short inter-tone intervals (15 ms to 55 ms; student t test, $p<0.05$). Additionally, the %CR was not different between inter-tone intervals of 100 ms and 200 ms. These results demonstrated that the interval between tones is a very important feature for rats to discriminate between two acoustic objects, and to anticipate if they will receive water.

The two-tone discrimination behavior is maintained during the recording sessions, as can be observed at Figure 4.24D. This figure shows that there are more trials in which rats lick to the two-tone trials (attentive TT) than trials in which rats lick to the one-tone trials (attentive OT) (wilcoxon paired ttest, $p= 0.00486$). The same is also true for the trials in which rats are attentive to the second tone and lick to receive water (attentive TT trial types) compared to the trials in which they ignore the second tone (inattentive TT trial types; wilcoxon paired ttest, $p= 0.0439$). Figure 4.24B displays this result.

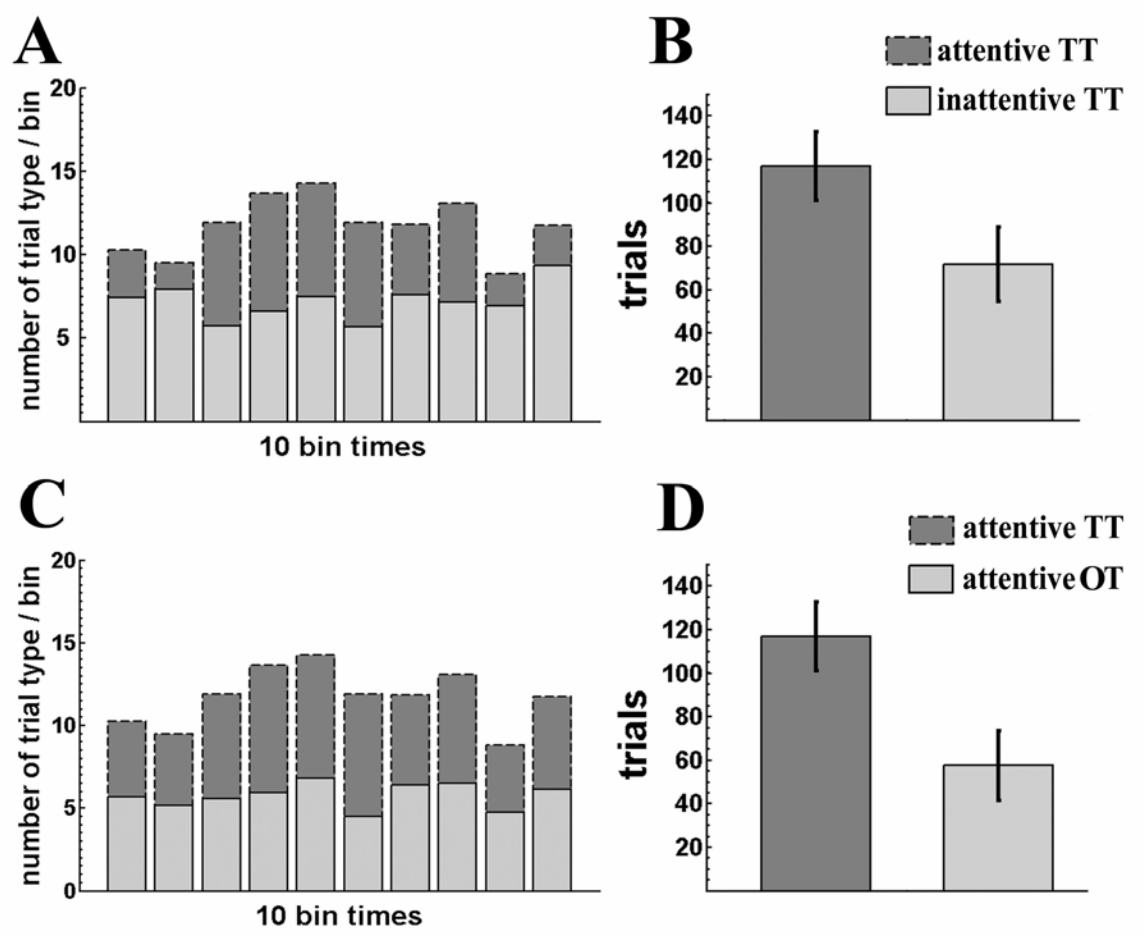

Figure 4.24. Rats maintained the learned behavior during recording sessions. A) Figure displaying the average number of trials in 10 evenly distributed bins throughout the experimental sessions (dark gray = trial types in which rats lick the spout to receive water after hearing two tones (attentive trials); light gray = trials in which they ignore the second tone (inattentive trials); n=11 rats)). The foremost left bar is the beginning of the recording session and the foremost right bar is the end of the recording session. B) Figure comparing the number of trials in which rats attended (dark gray) or did not attend (light gray) to the second tone. C) Figure showing average number of trial type in 10 evenly distributed bins throughout the experimental sessions (dark gray = trial types in which rats licked the spout to receive water after hearing two tones (attentive TT); light gray = trial types in which rats lick the spout after hear one tone (inattentive TT). D) Figure showing the comparison of trial types displayed on figure 4.24C.

One could argue that the motivation for licking the spout could be variable throughout the recording sessions. Therefore, I divided the time of each recording session in 10 evenly distributed bins in which the different trial types were counted. This analysis is shown at Figure 4.24A and Figure 4.24C. The foremost left bar indicates the beginning of the recording session and the foremost right bar indicates the end of the recording session. Figure 4.24B shows the average of two-tone trial types that rats lick to the spout (dark gray), and the average of two-tone trial types in which rats did not lick to the spout (light gray). Figure 4.24D shows the average of two-tone trial types (dark gray), and the average of one-tone trial types in which rats licked the spout (light gray). These two graphs show that the probability of licking or not licking behavior is maintained constant throughout the recording session. These results are consistent with a constant motivational state throughout the recording sessions. Thus the mistakes that rats made in the two-tone discrimination task are not due to fluctuations in motivational state.

It is very important to note that despite the fact that rats learned to discriminate between one and two tones they still made mistakes. In approximately 25% to 30% of the two tone trials they did not lick the spout and therefore did not receive water. The same level of mistakes was made for the one tone trials. Rats licked the spout after hearing one tone in approximately 20 to 30% of the trials. Obviously what I call mistakes might have a variety of complex causes and explanations. These rodents might have developed philogenetic adaptations in order to survive in an uncertain environment: an ever-changing environment in which they do not know the availability of water resources, food or sexual partners in order to reproduce. Therefore, they will respond or stop to respond to tones even though the certainty of the reward did not vary. We do not know

the extent to which the nervous system is wired to respond to uncertainty. However, I can use this response pattern in order to ask whether attending to two-tones changes the neuronal activity in the primary auditory cortex. In order to study the effects of attention-related processes in auditory processing, I decided to focus my analysis on the two-tone trials only. I rely on the fact that even well trained and motivated rats performing correctly in 70% of the two-tone trial types did ignore 30% of the two-tone trial types which they were trained to attend.

A1 activity is modulated by attention-related processes

In this session I measured the spike trains of A1 in the attentive and inattentive TT trials. The comparison of A1 activity between these trials can indicate if attention-related processes are modulating the activity of a primary cortical area. Recording were performed in 86 multi-unit clusters in the auditory cortex of 3 rats (3 recordings sessions in 2 rats and 2 recording sessions in 1 rat) engaged in the two-tone discrimination task in order to study the effects that attention-related processes might have in the primary auditory cortex.

The first observation to be noted is the very short response latency to tones. The peak for both tones in both trials ranged between 10 ms to 17 ms which is consistent with the latency from the primary auditory cortex previously reported (Kelly et al, 1988; Doron et al., 2002; Rutkowski et al, 2003; Kilgard et al, 2006). Second, there was forward masking effect, which is characteristic of the primary auditory cortex response, for attentive and inattentive TT trial types. The firing rate response is higher for the first tone, (Figure 4.25). Third, apparently, there were differences in the mean firing rate of these neurons after the second tone. It was observed that the mean firing rate of the

neurons were higher for rats that attented the second tone, and that effect occurs 100 ms after the second tone. Therefore, this enhanced firing rate occured before animals licked to receive water). Moreover, the baseline firing rate was apparently higher for the trials in which rats did not attend to the tones. This reduction of the baseline neuronal activity in the trials in which rats attended to the second tone could have enhanced the signal/noise ratio during the first tone onset and/or the inter-tone interval.

In a preliminary analysis to detect whether attending to the second tone in a fast two-tone sequence modulates the activity of A1, the averaged PSTH for all neurons in the attentive and inattentive TT trial types was computed. Figure 4.25 shows the average PSTH of all neurons (1ms bins). I see a clear attentional modulation of the activity during 200 ms after the second tone onset. Attentional modulations during or between tone onset was not clearly observed for the average population.

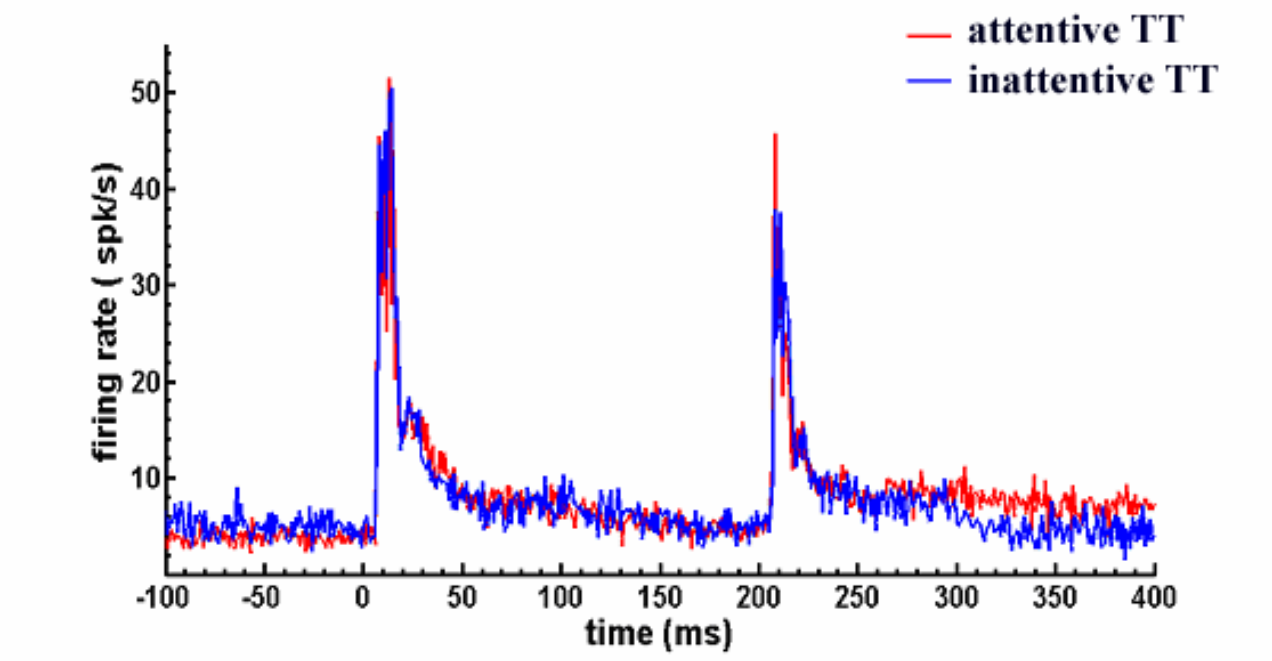

Figure 4.25. Attending to the tones modulates firing rate in the auditory cortex. This figure shows the averaged firing rate (1ms bins) for 86 neurons in 3 rats during attentive TT (red line, total of 20 trials) and inattentive TT trials (blue line, total of 20 trials). Time t=0 ms is first tone onset and t=200 ms is second tone onset.

Despite the observations reported in the previous paragraph, there was a great variability in the neuronal response in A1. Figure 4.26 shows a panel with three examples of neurons encountered in A1. This figure exemplifies the fact that the population recorded in A1 has a heterogeneous activity pattern. For instance, the Figure 4.26 shows the raster plot, the firing rate, and the normalized firing rate (N.F.R.) of a neuron that has its activity modulated by attention in the first and second time onset. The firing rate is computed by 5 ms gaussian curve. The N.F.R. was computed by dividing the firing rate by the averaged baseline firing rate. Moreover, the activity of this neuron is modulated after the first and second tone onset. This neuron had a modest forward masking effect during both attentive and inattentive TT trial types. Figure 4.26B shows a neuron with a strong forward masking and a strong modulation of its activity in the response to the first tone onset, but not following the second tone onset. Figure 4.26C shows a third neuron with no forward masking effect and no attentional modulation in the tone onset response, but shows attentional modulation after the second tone onset. I further studied the forward masking effect by normalizing the firing rate by the baseline, integrating the N.F.R. activity between 0 to 20 ms post tone onset, and comparing the N.F.R. for each neuron separately.

I compared the neuronal response elicited by the first and second tone in the attentive as well as in the inattentive trials (Wilcoxon paired t test, significance at $p<0.05$). In the attentive TT trial types, 51.1% of the neurons showed more activity in response to the first tone, 16.8% of the neurons showed more activity to the second tone, and 32.5% of the neurons did not show difference. In the inattentive TT trial types, 59% of the neurons showed more activity to the first tone, 14% to the second tone, and 26%

did not show any differences. Therefore, the forward masking effect was similar in the attentive and inattentive TT trial types. However, this is not the case for the interval immediately after the first and second tone onset. The firing rate of the interval between 20 to 200 ms after the first tone onset was compared to the firing rate of the 20 to 200 ms after the second tone onset interval in attentive and inattentive trial types. The activity of A1 increased in 46.5% of the neurons after the second tone onset interval, decreased in 31.4% and maintained the same in 22% of the neurons in the attentive trial types. In the inattentive trial types, only 15% of the neurons showed an increase in firing rate after the second tone onset, while 50% showed a decreased firing rate and 34.8% did not show any differences. These results demonstrate that the activity of the neurons in A1 is differentially modulated during the interval after second tone onset in the attentive and inattentive TT trial types.

Attention-related processes modulate the normalized firing rate response to the first tone onset in A1. By comparing the attentive versus inattentive TT trial types I saw that 41.8% of the neurons showed higher normalized firing rate during the attentive trials, 32.5% showed higher activity in the inattentive trials, and 26.7% of the neurons did not show differences between these trial types. Thus, attention-related processes either enhance or inhibit the activity of A1 to tone onset. Moreover, I measured the inter-tone interval activity by averaging the normalized PSTH between 20 ms to 200 ms after the tone onset for attentive and attentive trial types. There is a higher activity in 41.8% of the neurons during attentive trials, while 30.2% display the opposite trend and 27.9% did not show any differences between attentive and inattentive TT trial types. After the second tone onset, attention-related modulation in A1 is more pronounced, since 67.4% of the

neurons increase their firing rate during the attentive trial types in comparison to the inattentive trials, while 8.1 % did not show any differences between these groups, and 24.4% of the neurons showed increased firing rates during inattentive TT trial types. These results demonstrate that the activity of the neurons in A1 is modulated by attending to the two-tone discrimination task. Moreover, the attentional modulation is more pronounced after the second tone, but it also occurs during the inter-tone interval, and during the first and second tone onsets.

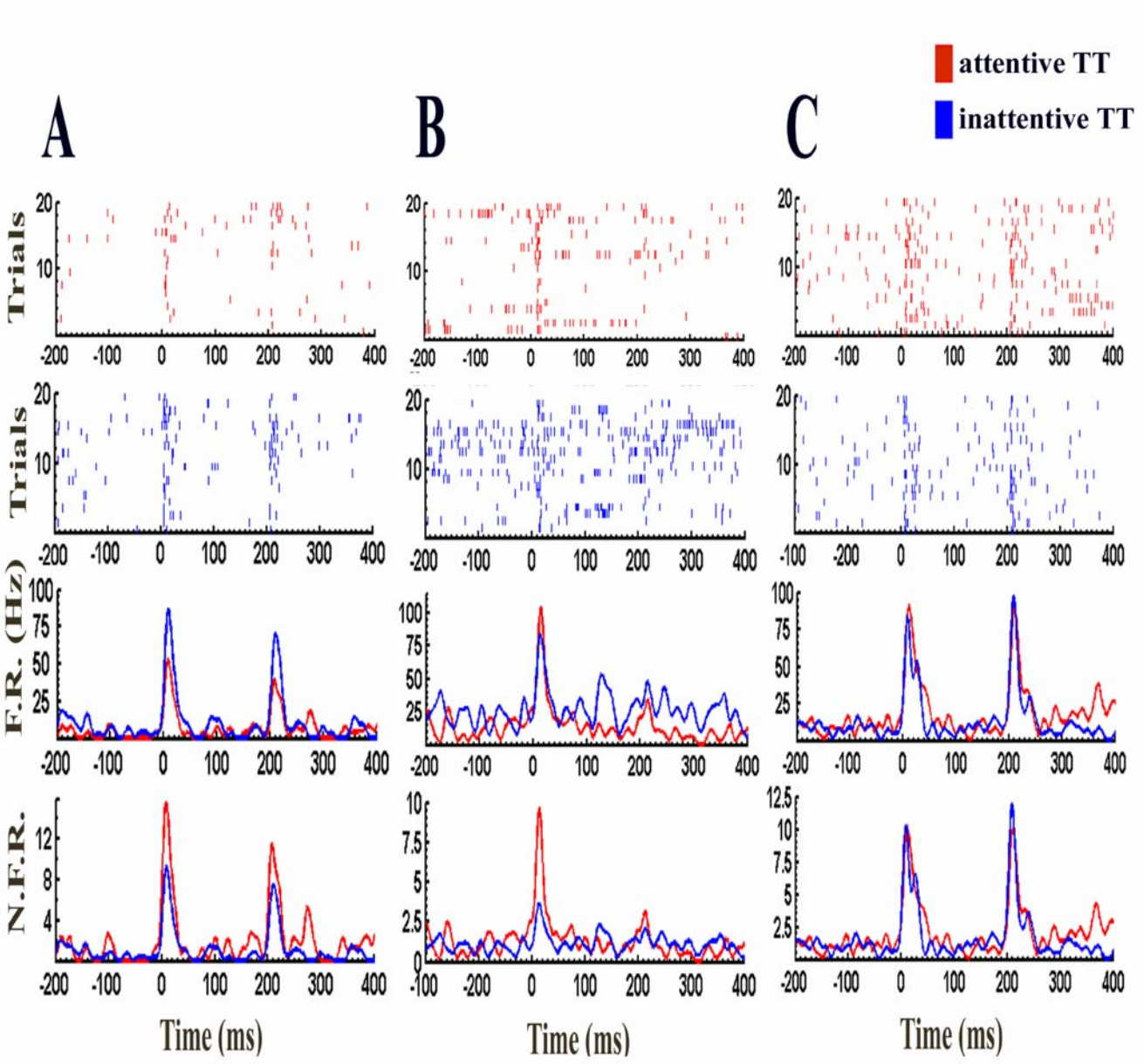

Figure 4.26. Examples of neurons modulated by attending to two-tones. Figures 4.62A, 4.26B, and 4.26C show examples of neurons in A1 that have different patterns of activity.First top row shows the raster plot of attentive trials, while the second top row shows the raster plot during inattentive trials (red and blue ticks signals spike times). Third row shows the PSTH, and the fourth row shows the baseline normalized PSTH (red trace signals attentive and blue traces inattentive trials). F.R. (firing rate in spikes/s); N.F.R. (normalized firing rate by baseline).

In order to further explore any differences in the firing rate that might be accounted for attention-related modulation of the neuronal activity in the primary auditory cortex, I decided to focus on two intervals: 0-200 ms (T1 interval) and 200-400 ms (T2 interval) after the first tone onset. The reasoning was that if attention-related processes modulate the activity of the auditory cortex, it would likely occur not only after rats have the information to make a correct decision about the water reward, but also before the second tone onset. Moreover, the behavior index between T1 and T2 intervals was compared to find whether neuronal activity is differently modulated along the course of the attentive and inattentive TT trial types. Figure 4.26 shows the behavior index for the normalized averaged activity of the 86 neurons during intervals T1 and T2.

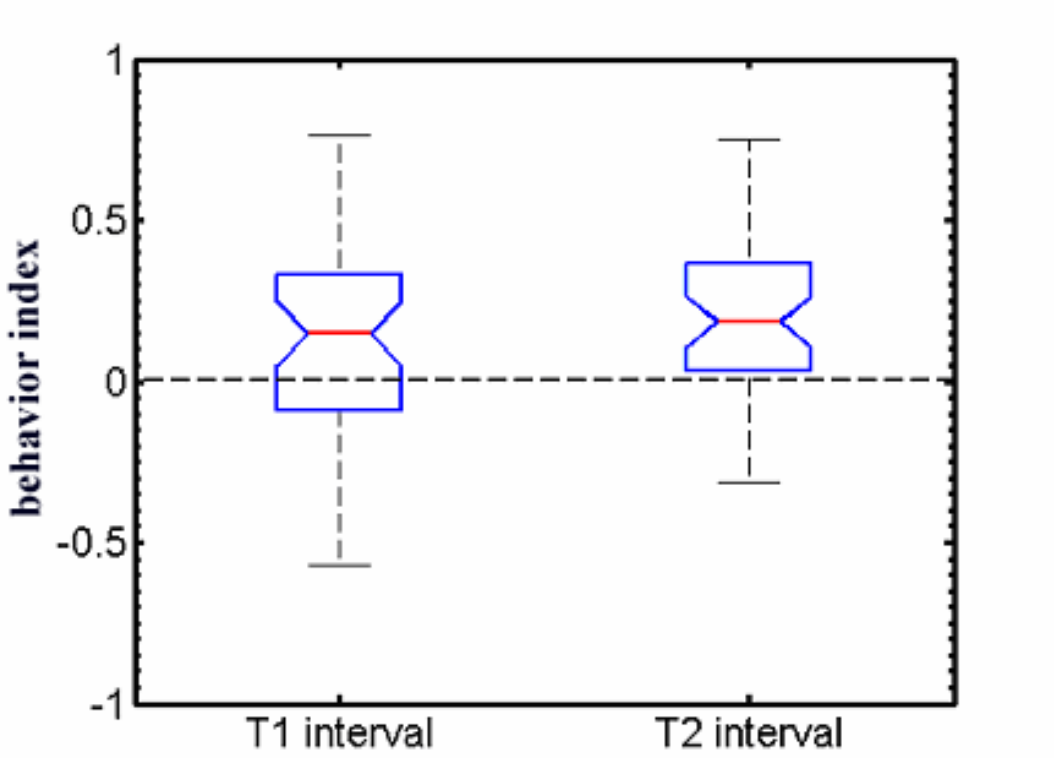

Figure 4.27. The firing rate is modulated by attention demands. The ordinate shows the behavioral index, in which values toward -1 signals increasing in firing rate for inattentive trials and values toward 1 signals an increasing firing rate for the attentive trials. The abscissa shows the box plot of the normalized firing rate average for 86 neurons during 0 to 200ms post tone onset (T1 interval), and during 200 to 400ms after first tone onset (T2 interval). The dash line represent the firing rate value in which there is no differences between attentive and inattentive trials.

Attention-related processes occuring during correctly performing the two-tone discrimination modulate the activity of neurons in the auditory cortex. Figure 4.27 shows a box plot in which the boxes represent quarcentiles, the whiskers the full extent of the data set, and the notch represents the 95% confidence interval. Notches that do not overlap indicate significant statistical differences. Thus, this box plot is very useful to detect statistical differences between the attentive and inattentive trials as well as between T1 and T2 intervals. A behavioral index values around zero signalizes that there is no difference in firing rate. This value is depicted by the dash line in Figure 4.27 . The values of this index show that firing rates tend to be higher for the attentive trials during T1 and T2 intervals. Thus it seems that neurons fire more action potentials in the trials in which they attend to the two tones.

In order to further explore the effects of attention in A1 I decided to reanalyze the normalized firing rate. This is because the behavioral index integrated 200 ms of neuronal activity which encompassed neuronal responses to tone onsets. Thus, the behavioral index could be contaminated by differences in firing rate due to neuronal responses related to the tone onset or forward masking effects. However, these two neuronal responses could still be differentially affected by the attentive and inattentive TT trial types . I used signal detection theory to further analyze attentional modulation in A1.

The activity of A1 reliably predicts performance.

In this session i will describe the results of the ROC analysis. This analysis was used to classify a given behavior based on the spike train. Therefore, this analysis directly associates the neuronal activity with behavior outcomes. I used the ROC analysis to ask the following question: Can the neuronal activity of A1 reliability predict the behavior

outcome? Our experiment allows us to use signal detection theory to investigate this possibility. If the activity of A1 has predictive power, then by measuring the firing rate alone we should be able to judge if rats will or will not lick the spout to receive water. The attentive and inattentive TT trials can be thought of as two categories in a two-alternative forced task. I utilized the receiver operator characteristic (ROC) analysis in order to quantify how reliable the firing rate is in order for a ideal observer to classify the attentive TT (correct trials category) and in attentive TT (incorrect trials category).

I computed the area under the ROC curve (AUC) generated by comparing the baseline normalized firing rate between 20 trials of attentive TT and inattentive TT categories along the time axes. An AUC value is the probability with which, based on the firing rate, an ideal observer can reliably classify the trials category as being attentive trials (correct trials) or inattentive trials (incorrect trials). A value of 0.5 indicates that a given firing rate at a particular time has an equal probability to be elicited by the attentive and inattentive trials. Values tending to 1.0 indicate that firing rates can be reliably utilized to classify the trials as being attentive TT trials, whereas strong firing rate responses for the inattentive TT trials will have a value tending to 0.0 (see methods). Moreover, I computed a ROC curve from a random spike train of the attentive and inattentive TT trial types. This ROC curve has an AUC value with average value of 0.5 (AUC control, see methods). Then, I selected the AUC value of interest (either the T1 or T2 interval) and compared to the AUC control values by using a non-parametric permutation t test (1000 permutations, $p<0.05$ to reject the null hypothesis that these AUC value are not different). Figure 4.28 shows the result of this analysis.

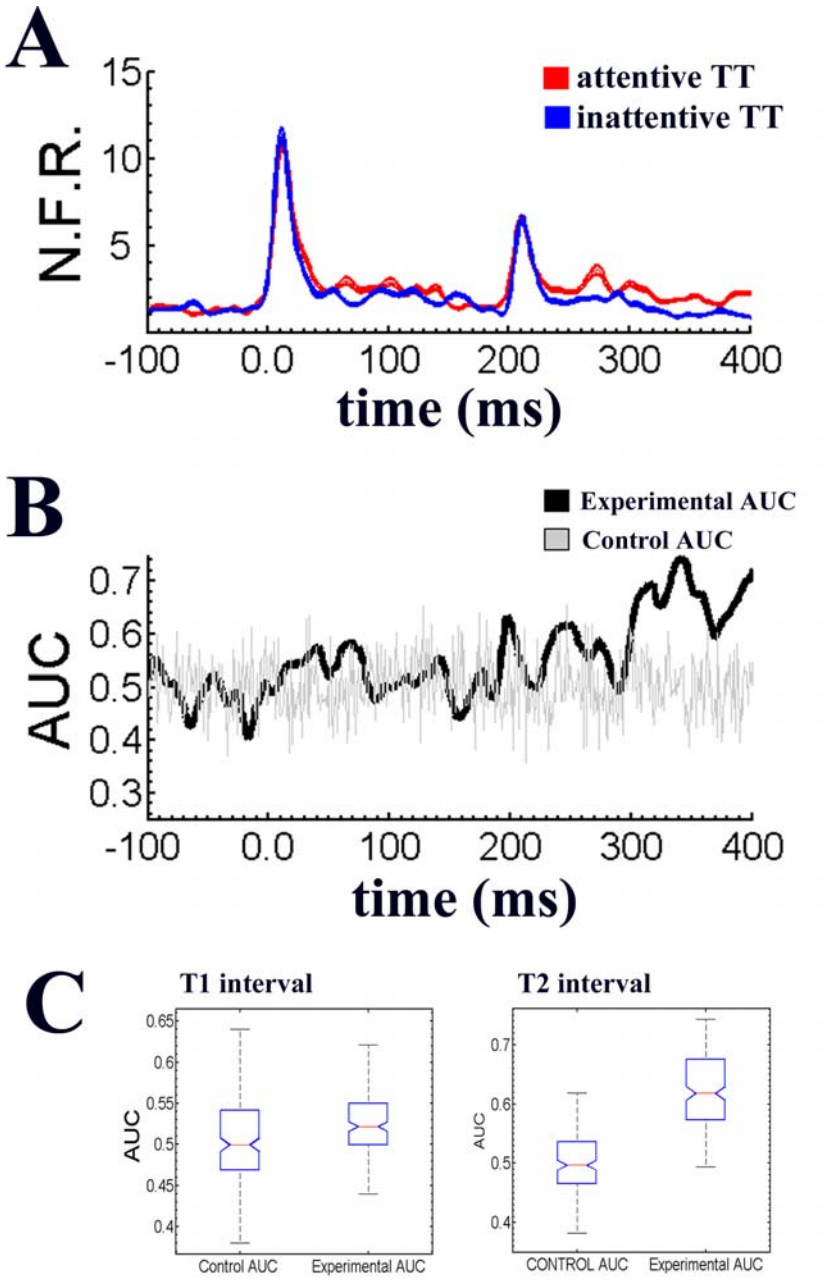

Figure 4.28. The firing rate of neurons in A1 reliably predicts behavior outcomes. A) This graph shows the baseline normalized firing rate (Hz; Ordinate) of attentive two-tone trials (red) and inattentive two-tone trials (blue) for random selected 20 trials of each condition over time (ms; Abscissa). B) Middle graph showing the ROC quantification where the black thick line shows the AUC values of the experimental groups over time. The gray line is a control random AUC with mean value of 0.5. The ordinate is the AUC values for attentive (values toward 1.0) and inattentive (values toward 0) categories. C) Box plot comparing the AUC during T1 interval (left box plot), and during T2 interval (right box plot) with a control AUC with mean value of 0.5.

There are several important observations that can be drawn from the analysis displayed in Figure 4.28. Figure 4.28A shows the average normalized firing rate for attentive and inattentive TT trial types. This figure shows that the averaged normalized firing rate is higher for trials in which, attending to the second tone, rats licked the spout anticipating a water reward. This increase in normalized firing rate (N.F.R.) occurs in the inter-tone interval, therefore, before the second tone onset. There is an increase in firing rate between 25 to 40 ms after first tone onset. Moreover, this increased firing rate seems to continue throughout the inter-tone interval, since that N.F.R. is higher during attended trials. Additionally, there is an increase in the firing rate immediately after the second tone (200 ms in time axes). This increase in firing rate is well before rats licked the spout because the latency of the licking response is around 400-450 ms after first tone onset (Figure 4.23).

The thick black line in Figure 4.28B shows the AUC values of the ROC analysis computed between attentive and inattentive TT trial types, whereas the gray thin line shows the AUC value computed from the ROC analysis from the shuffle and switched spike trains from attentive and inattentive trials. The gray thin line shows that the AUC control value fluctuates around 0.5. It is important to note that the AUC reach values closely to 0.6 at 30-40 ms, 70-80 ms. Moreover, AUC values reaches above 0.6 immediately before the second tone onset, at approximately 190 ms after the first tone onset. This result strongly suggests that the activity of A1 during the inter-tone interval signals the processing of fine temporal cues that are likely important to anticipate the presence of the second acoustic event. For instance, the second tone onset could peaks at an earlier latency.

The AUC analysis demonstrated that the A1 activity to tone onset was not a good parameter to classify the attentive or inattentive TT trials. We can clearly see that the peak of response for the first and second tone lies within 0.5 to 0.55 AUC value (Figure 4.28B). Note that the peak response was not different between attentive and inattentive TT trials for the first and second tone onset. Thus, the onset response is likely not related to the behavioral task demands, but with the processing of the physical attributes of the sound. However, as described before, strong responses occur immediately after the first and second tone onset. AUC values of 0.6 indicate increased firing rate responses in attentive TT trials occurring immediately after first tone onset An AUC value higher than 0.6 also occurs between 40-60 ms after second tone onset. Between 100 ms to 200 ms after the second tone onset, this value is above 0.75, which was the highest value of the AUC. Figure 4.28C shows a box plot graph which indicates the statistical comparison between the experimental AUC and the control AUC values during T1 interval (0-200 ms) and during T2 interval (200-400 ms). The AUC value between tones (T1 interval) were statistically significant different from a 0.5 value computed from a random AUC curve (permutation t test; p=0.0019; 1000 permutations). The same was also true for the T2 interval (permutation t test; p=0.0009; 1000 permutations). The AUC value during the first tone onset (0-20 ms interval) was not statistically significant (permutation t test; p=0.0519; 1000 permutations), and neither was the AUC during the second tone onset (200-220 ms interval; permutation t test; p = 0.065774; 1000 permutation). Moreover, the comparison between the AUC of ROC control and ROC experimental curve during the baseline did not show statistical differences (permutation t test, p=0.96205; 1000 permutations). Therefore, the results showed that the activity of

A1 was modulated by attention-related processes to correctly perform the task during the inter-tone. Therefore, even before the rats have the information that there will be a reward. Moreover, the attentional modulation of A1 activity is much more pronounced just after second tone onset, but likely before the protrusion of the tongue that signals the licking behavior (see Figure 4.23).

The activity of A1 can reliably predict correct performance.

In this result section I will first present data showing that the firing rate is differently modulated in trials in which rats correctly discriminating the two-tones from trials in which rats respond to one tone. Then, I will further use the ROC analysis to investigate if A1 activity can predict the correct behavioral outcome. For instance, it could be possible that the A1 activity could be predicting a general arousal state in reponse to the tones, but not necessarily a correct performance of the rats.

Figure 4.28 demonstrates that the neuronal activity of A1 in the attentive TT trials is a good indicator of behavioral outcome during a short period of time after the tone onset. However, is the neuronal activity of A1 computing temporal cues? The behavioral data suggests that temporal cues, i.e. the silence interval between tones, is essential to distinguish between acoustic objects in order to guide their decision making process. However, the higher activity of A1 in the attentive compared to the inattentive two-tone trials does not allow us to claim that A1 activity between tones is related to processing of temporal cues. For instance, it can be argued that the A1 activity could be related to general arousal caused by the tone itself. To control for this possibility, I compared the normalized firing rate of attentive two-tone trials (attentive TT) with the normalized firing rate of the attentive one-tone trials (attentive OT). Rats attending to a

one-tone trial are in a vigilant state, they are not correctly processing the auditory stimulus to guide their goal-directed behavior. In this case, the time between the two tones becomes irrelevant for guiding their decision. Comparing the activity of A1 in trials in which rats lick the spout after hearing one and two-tones could shed some light on the role of A1 in processing temporal cues.

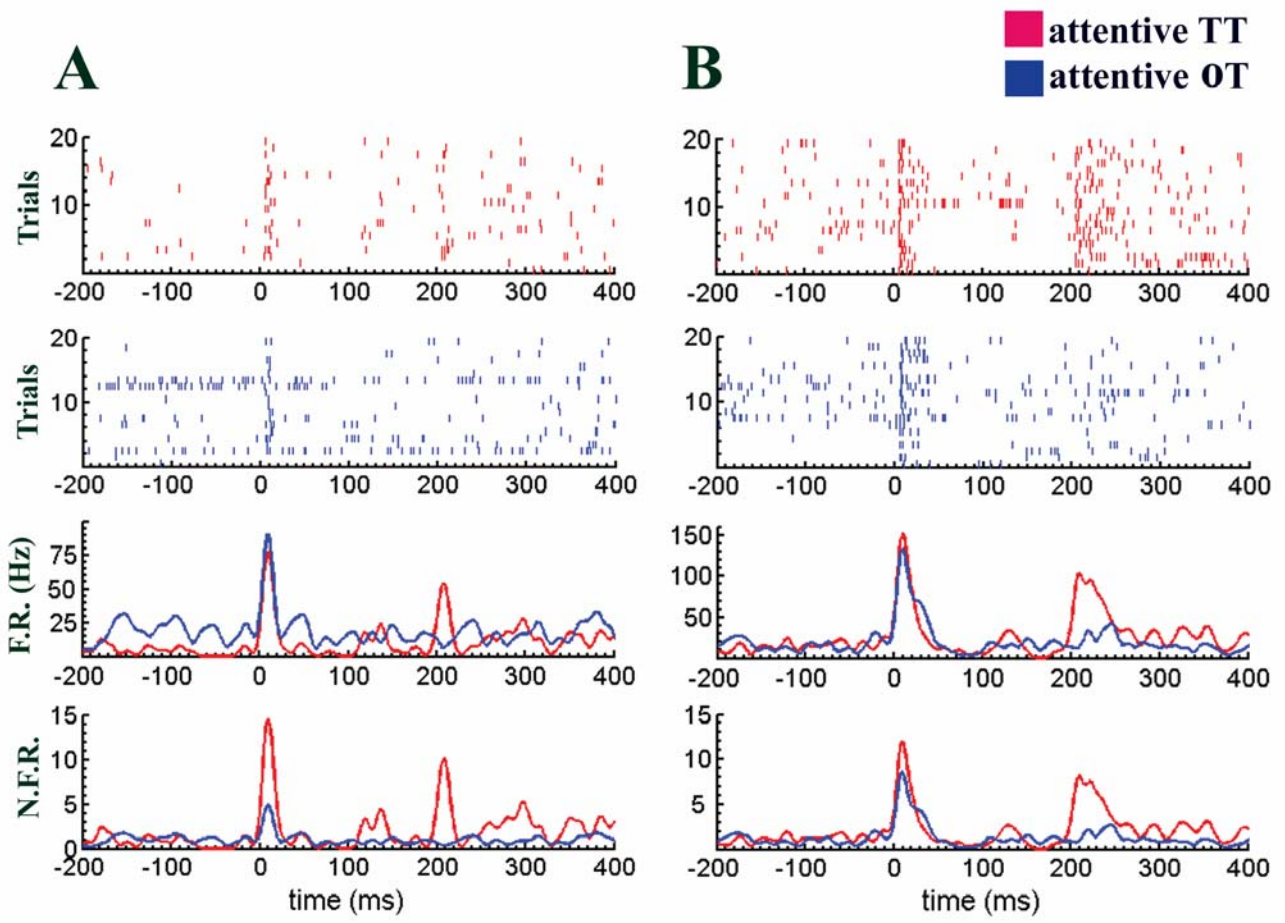

Figure 4.29. This figure shows two examples of neurons (columns A and B) during attentive TT (red lines) and attentive OT (blue lines) trials types. The first top row shows the raster plot of attentive TT trials, while the second top row shows the raster plot during attentive OT trials (red and blue ticks signals spike times). Third row shows the PSTH, and the fourth row shows the baseline normalized PSTH. F.R. (firing rate in spikes/s); N.F.R. (normalized firing rate by baseline).

I computed the raster plot, the PSTH, and the normalized PSTH of A1 neurons during trial types in which rats were attending to the two-tone trials and during trial types in which rats were attending to the one-tone trials. I called the trials in which rats attended to the one tone trials as attentive OT trial types. Figure 4.29 displays two neuron examples commonly found in our data set. This figure shows the raster plot in the first two rows, the firing rate (spikes/s) in the third row, and the normalized firing rate (N.F.R) in the fourth row. The N.F.R. was computed by dividing the firing rate by the average baseline firing rate. The example in Figure 4.29A shows that this neuron has a higher baseline firing rate during the attentive OT trial types than during the attentive TT trial type (see third row). The normalized firing rate shows that the neuronal response to tone onset in the attentive TT trials has a much higher signal to noise relationship (fourth row). Moreover, there is an increase in the firing rate at 100-140 ms after the first tone onset in the attentive TT trial type. Additionally there is an increase in the firing rate after the second tone onset. The second example (Figure 4.29B) shows exactly the same trend, however, the signal to noise relationship during first tone onset is less pronounced for this particular neuron. Note that these two examples are from different animals.

I found that 14% of the neurons did not show differences in N.F.R. between attentive TT and attentive OT during the first tone onset. However, 20% of the neurons showed a higher N.F.R in the attentive OT trials and 64.3% showed higher N.F.R. in the attentive trials. After the second tone onset, I found that 81.6% of the neurons had a higher N.F.R. for attentive TT trials as compared to attentive OT trials, while 18.4% did not display clear differences between attentive TT and attentive OT trials types. The

normalized activity of the interval between tone onsets was also measured. Nearly half of the neurons (46%) showed higher activity during attentive TT than attentive OT trial types. Only 27 % of the neurons showed the opposite trend, and 27% of the neurons did not show differences.

The ROC analysis was used to further measure differences in A1 neuronal activity between attentive TT and attentive OT trial types. This analysis is displayed at Figure 4.30. Figure 4.30A shows the normalized firing rate (NF.R.) , Figure 4.30B shows the AUC throughout the time axes (think black line), and Figure 4.30C shows the non-parametric permutation t test between AUC experimental data set and AUC control data set during T1 (left figure) and T2 (right figure) intervals.

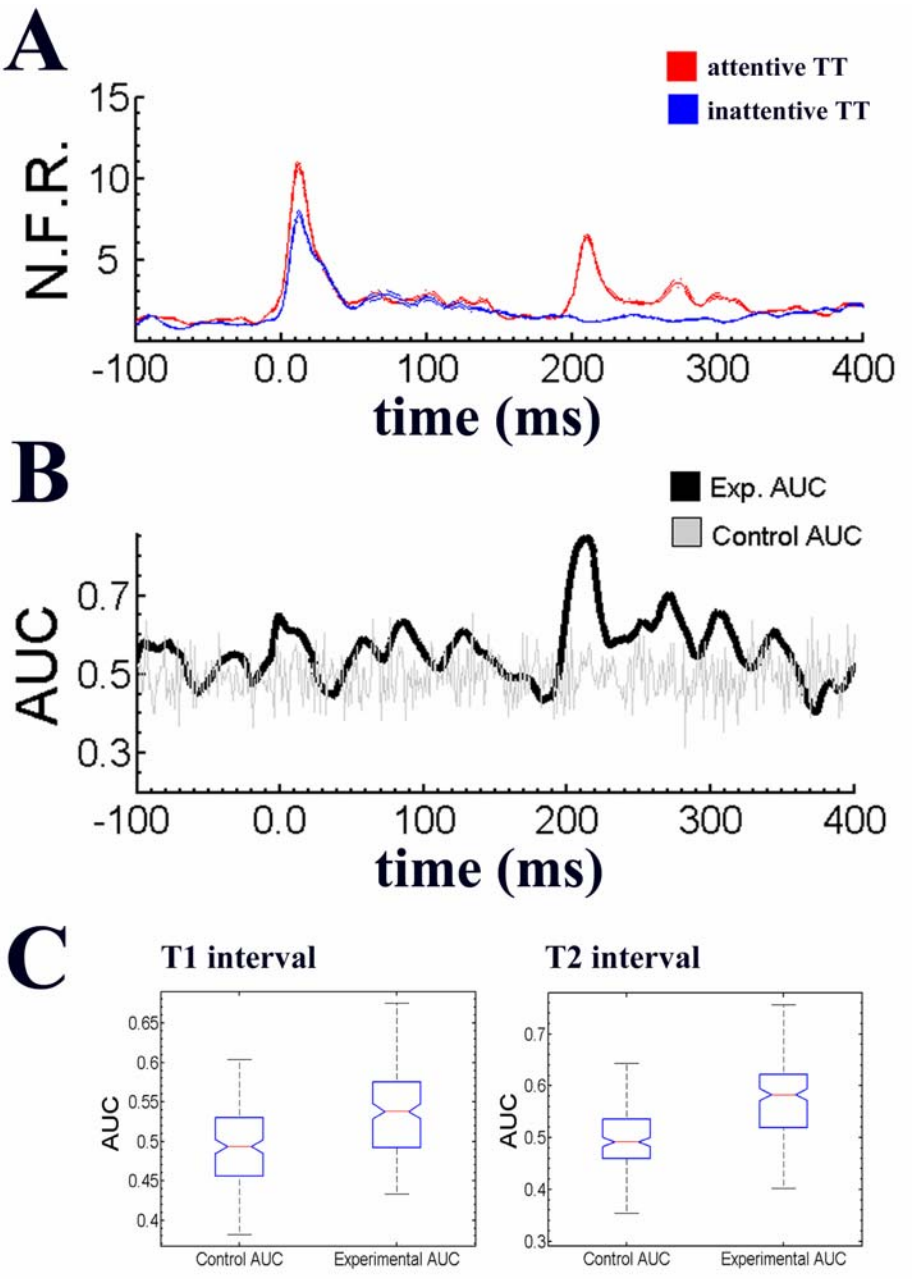

Figure 4.30. Correctly performing the two-tone discrimination task changes the firing rate of neurons in the auditory cortex. A) This graph shows the baseline normalized firing rate (Hz; Ordinate) of attentive two-tone trials (red) and attentive one-tone trial types (blue) for random selected 20 trials of each condition over time (ms; Abscissa). B) Middle graph showing the ROC quantification where the black thick line shows the AUC values of the experimental groups over time. The gray line is a control random AUC with mean value of 0.5. The ordinate is the AUC values for the attentive TT (values toward 1.0) and attentive OT (values toward 0) categories. C) Box plot comparing the AUC during T1 interval (left box plot), and during T2 interval (right box plot) with a control AUC with mean value of 0.5.

The ROC analysis displayed in Figure 4.30 demonstrates that the firing rate during the first tone onset, during the time immediately after the first tone onset, and during the time period after second tone onset predicts whether there will be a correct response to the two-tone trial type. For instance, during the inter-tone interval the AUC values for the time periods of 70-80 ms and 110-130 ms post the first tone onset is 0.6. The box plot of Figure 4.30C (right figure) indicates that during the T1 interval the AUC values of the experimental groups are not due to chance, since they have a value above 0.5. The comparison between the experimental AUC values and control AUC values during the T1 interval showed that they are statistically different (permutation t test; $P<0.001$; 1000 permutations).

The AUC experimental values were obtained from the experimental spike train of the attentive TT and the attentive OT experimental groups. The spike train of these two groups were shuffled and switched to obtain the AUC control that has an average 0.5 value. Figure 4.30A showed that the AUC value for intervals between 60-80 ms and 100-120 ms after the second time onset is around 0.7. Figure 4.30C (left figure) shows the comparison between attentive TT and attentive OT during the T2 interval. The averaged AUC during the T2 interval is also statistically different from a 0.5 value (permutation t test, $p<0.001$; 1000 permutations). The statistical comparison of the AUC experimental value and AUC control value during the first tone onset also showed that they are different (permutation t test, $p=0.0009$; 1000 permutations). However, the comparison between the AUC of these two ROC curves at baseline did not show any statistical differences (permutation t test, $p=0.5934$; 1000 permutations). The results

clearly demonstrate that the spike trains of the attentive TT and attentive OT experimental groups are tightly correlated with a future behavioral outcome.

Synchrony results

In this result section I will investigate if the neuronal synchrony is also modulated by attention-related processes. I will first quantify synchrony by computing cross-correlograms, and then, i will compute the spectral coherence between spike trains. The spactral coherence was used to investigate if the synchrony observed between neurons occurs at a particular firing rate frequency.

It has been proposed that attention also modulates activity by synchronizing action potentials of neuronal networks in order to label and/or enhance neuronal ensembles that are functionally related in order to process relevant perceptual information (Singer, 1999; Fries et al, 2008). Thus, besides a rate neuronal code, there is a temporal neuronal code that can be modulated by high hierarchical centers in order to convey perceptual information to perform cognitive tasks. Our behavioral paradigm offers the opportunity to ask if attending to temporal cues in a two-tone discrimination task modulates synchronization. In order to explore the latter possibility, a cross-correlation analysis (CCH) of the simultaneous recorded multi-unit clusters during attentive and inattentive trials was performed.

The time periods T1 (0-200 ms) and T2 (200-400 ms) post the first tone onset were selected, and the CCH was computed for attentive TT and inattentive OT trial types. The CCH pairs that have spike coincidences above the 95% confidence interval were selected (see Figure 4.32 for an example). The CCH coefficients from each experimental session were normalized by the highest CCH value across time

periods/trials. Then, they were transformed to z-scores followed by a cumulative normal distribution transformation. Then, the CCH coefficients were finally plotted in a CCH matrix as percentage relative to the highest CCH coefficient. These normalized values are shown in the four color-coded matrixes in Figure 4.31.

The spatio-temporal CCH analysis was performed for each experiment and one particular example is shown in Figure 4.31 (Rat 1A shown in red in table 1). The top row of this figure depicts two color-coded matrixes showing the CCH pairs at the attentive (matrix in the first column) and inattentive trials (matrix in the second column) during the T1 interval (0-200 ms after tone onset). The colors at each square indicate the normalized CCH coefficient of each neuron pair expressed as a percentage of the highest z-score. The black diagonal squares indicate the auto-correlation, the dark blue indicate CH coefficients below 95% confidence interval, and the scale showing low blue to dark red indicates the strength of the CCH correlation coefficients. The high red squares in the matrixes of the third, fourth and fifth columns shows significant neuronal pairs present in: 1) the attentive trials only ((a)-(u) matrix in the third column); 2) in the inattentive trials only ((u)-(a) matrix in the fourth column); 3) or neuronal pairs present in attentive and inattentive trials (a U u matrix in the fifth column). The second row in Figure 4.31 shows the same analysis performed during the T2 interval (200-400ms after the first tone onset).

The CCH matrix analysis showed in Figure 4.31 was performed in rat 1 of the experimental session A (rat 1A; table 1). In this experimental session I was able to record from 15 simultaneous MUA. The four first columns in this figure suggest that there are more synchronized neurons during the attentive than the inattentive TT trial

types during the T1 interval. Matrix ((a)-(u)) shows 21 synchronized neuron pairs present only in the attentive trials. Matrix ((u)-(a)) shows 3 synchronized neuron pairs present only during inattentive TT trials. Matrix (a U u) shows 22 synchronized neuron pairs present in both trials. During the T2 interval there are 12 synchronized pairs present only during attentive TT trials, 10 pairs only during inattentive TT trials, and 12 pairs present in both trials. By carefully analyzing the two-color coded matrixes in the top row of Figure 4.31, it is apparent that the same neuron pairs showing high synchronization strength are present in both attentive and inattentive TT trials. Moreover, the increase in the number of synchronized neuronal pairs during the attentive TT trials in the T1 interval is due to neurons with low synchronization strength. I did not observe the same trend for the T2 interval period. The same CCH matrix analysis performed in rat 1A was also performed in all rats across all experimental sessions and the percentage of neuronal pairs with statistical significant CCH coefficients is shown at table 4.1. Table 4.1A and 4.1B show the percentage of neuron pairs showing significant synchronous spikes during the T1 and T2 interval respectively. These two tables (4.1A and 4.1B) suggest that there were a higher percentage of neurons displaying synchrony during attentive versus inattentive trials during the T1 interval. During the T2 interval the opposite was true.

The CCH coefficients were computed from 86 MUA clusters which could yield a maximum of 418 CCH pairs during T1 and T2 interval. During the T1 intervals 135 pairs (32.3%) show statistically significant peaks at origin of the CCH during the attentive trials, while 117 pairs (28%) show peaks at the origin of the CCH in the inattentive TT trials. During the T2 interval, there were 46 pairs (11%) showing

significant peaks for attentive trials, while there were 27 pairs (6.7%) showing significant peaks for the inattentive TT trials. However, neither of these effects was statistically significant (paired t test, $p>0.05$). The table 4.1C compares the percentage of neurons with significant CCH coefficients during T1 versus T2 time periods in the attentive (three first columns in the table) and also in the inattentive trials (three last columns in the table). Although the percentage of synchronized neurons seems to be higher in the T1 interval for attentive than unattentive trials, it did not show a statistical significant effect (paired t test, $p>0.05$).

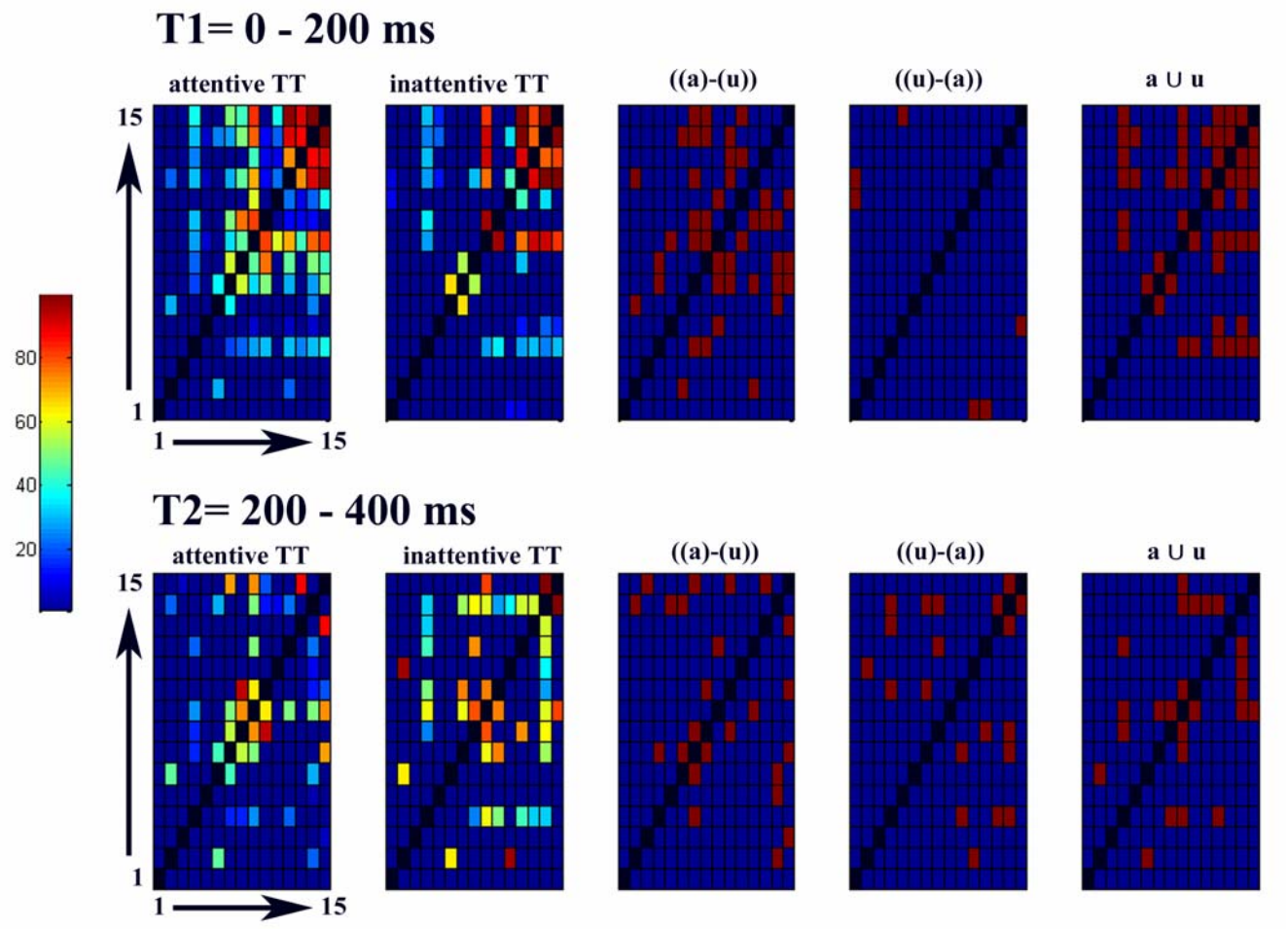

Figure 4.31. The number of synchronous neurons is higher in attentive than inattentive TT trials. Top row show CCH matrixes during attentive and inattentive trials for the T1 intervals, whereas bottom row shows CCH matrixes for T2 intervals. Neurons 1 to 15 (arrows) are displayed in the vertical and horizontal axes. The squares of the matrixes in the first and second columns show color-coded normalized CCH which is expressed as percentage of the highest CCH value across neurons. The diagonal black squares show the auto-correlation whereas the blue squares indicate no-correlations and the colors toward red indicate high correlation. The third, fourth, and fifth columns show the CCH coefficients for neuron pairs (red squares) that are present in the attentive trials only ((a)-(u)), in the inattentive trials only ((u)-(a)), or present in both (a U u).

Table 4.1. Percentage of significant CCH coefficients for each experimental session during attentive and inattentive trials. Table 4.1A shows the percentage of synchronous neuronal pairs during the T1 interval, and table 4.1B during the T2 interval. The first column is experimental session, the second column is all the neuronal pairs in attentive trials, the third column is all the neuronal pairs in inattentive trials, the fourth column is all the neuronal pairs present in both trials, the fifth column is the neuron pairs present only during the attentive TT trials, the sixth column is neuron pairs present only in inattentive TT trials. The table 4.1C compares the neuronal pairs in intervals T1 and T2 during attentive (black columns) and inattentive TT trials (dark gray columns). Columns T1 and T2 describe percentages of neuron pairs present in both intervals, T1 describes percentages of neuronal pairs present in T1 only, and T2 describes percentages of neuronal pairs present in T2 interval only. Each row shows the percentages of neuron pairs in relation to all possible neuronal pair combinations for each individual experimental session. The $\sum$ all sessions row is the percentages of significant CCH coefficients in all possible combinations for all experimental sessions (including rats that did not show any CCH significant pair). The total possible combination was 418 neuronal pairs.* **The matrix of Figure 4.31 is from RAT 1A**

Neuron pairs showing significant CCH coefficients

Across trial comparison (T1 interval: attentive TT versus inattentive TT)

Tab

T1 Interval (0-200 ms)

Exp. sessions	attentive	inattentive	both	only attentive	only inattentive
Rat 1A*	47.8%	29.7%	25.5%	22.3%	3.2%
Rat 1B	22.3%	30.8%	18%	4.2%	12.7%
Rat 1C	87%	65.4%	58.1%	29%	7.2%
Rat 2A	18%	25%	15.3%	2.5%	10.2%
Rat 2B	20%	20%	20%	0%	0%
Rat 2C	11%	3%	3%	8.3%	0%
Rat 3A	--	--	--	--	--
Rat 3B	--	--	--	--	--
∑ all sessions	**32%**	**28%**	**21.3%**	**11%**	**6.4%**

Across trial comparison (T2 interval: attentive versus inattentive)

Table 4.1B

Exp. sessions	attentive	inattentive	both	only attentive	only inattentive
Rat 1A*	25.%	23.4%	12.7%	12.7%	10.6%
Rat 1B	11.7%	21.2%	9.5%	2.1%	11.7%
Rat 1C	29%	27.2%	12.7%	16.3%	14.5%
Rat 2A	11.5%	19.2%	7.7%	3.8%	11.5%
Rat 2B	33%	20%	13.3%	20%	6.6%
Rat 2C	8.3%	5.5%	2.7%	5.5%	2.7%
Rat 3A	--	--	--	--	--
	--	--	--	--	--
∑ all sessions	**16%**	**18.4%**	**8.8%**	**7.4%**	**8.8%**

Within trial comparison

Table 4.1C

Exp. sessions	T1 and T2	only T1	only T2	T1 and T2	only T1	only T2
Rat 1A*	22.3 %	25.5 %	3.2 %	13.8 %	14.9 %	9.57 %
Rat 1B	9.57 %	12.7 %	2.1 %	17 %	13.82 %	4.25 %
Rat 1C	29 %	58 %	0 %	25.4 %	41.8 %	2.13 %
Rat 2A	7.7 %	10.25 %	3.8 %	10.25 %	15.4 %	8.97 %
Rat 2B	6.6 %	13.3 %	26.6 %	13.3 %	6.6 %	6.6 %
Rat 2C	2.7 %	8.3 %	5.5 %	0 %	2.7 %	5.5 %
Rat 3A	--	--	--	--	--	--
Rat 3B	--	--	--	--	--	--
∑ all sessions	**13 %**	**19.37 %**	**2.87%**	**12.67 %**	**15.3 %**	**6 %**

The analysis of CCH coefficient matrixes in each separated experimental session shows that there are a higher number of synchronous neurons in attentive trials. However, their CCH coefficient strength appears to be higher in inattentive trials. Therefore, further comparisons of the strength and temporal dispersion of the CCH neuronal pairs during the T1 and T2 interval of the attentive and inattentive trials were performed. The strength of the synchronous neurons during attentive and inattentive trials was compared by using a box plot of the half height peak of all pairs that showed significant increases in the probability of spike coincidences. The box plot shows the median, quarcentiles and 95% confidence intervals of the half height peaks of the attentive and inattentive trials. Surprisingly, obvious differences in the strength and temporal dispersion of neuronal pairs analyzed during T1 interval were not found. Figure 12 shows an example of typical CCH pairs that show statistically significant spike coincidences (spike coincidences above 95% confidence intervals) around the origin. This analysis is shown in the top left (T1 interval) and top right (T2 interval) graphs of Figure 4.32. Significant differences in the strength of the spike coincidences between attentive and in attentivetrials during T1 intervals were not detected (Wilcoxon signed rank test, $p = 0.9133$). However, surprisingly, the same is not true for the T2 interval ($p=0.0166$), in which the strength of spike coincidences is higher for inattentive trials.

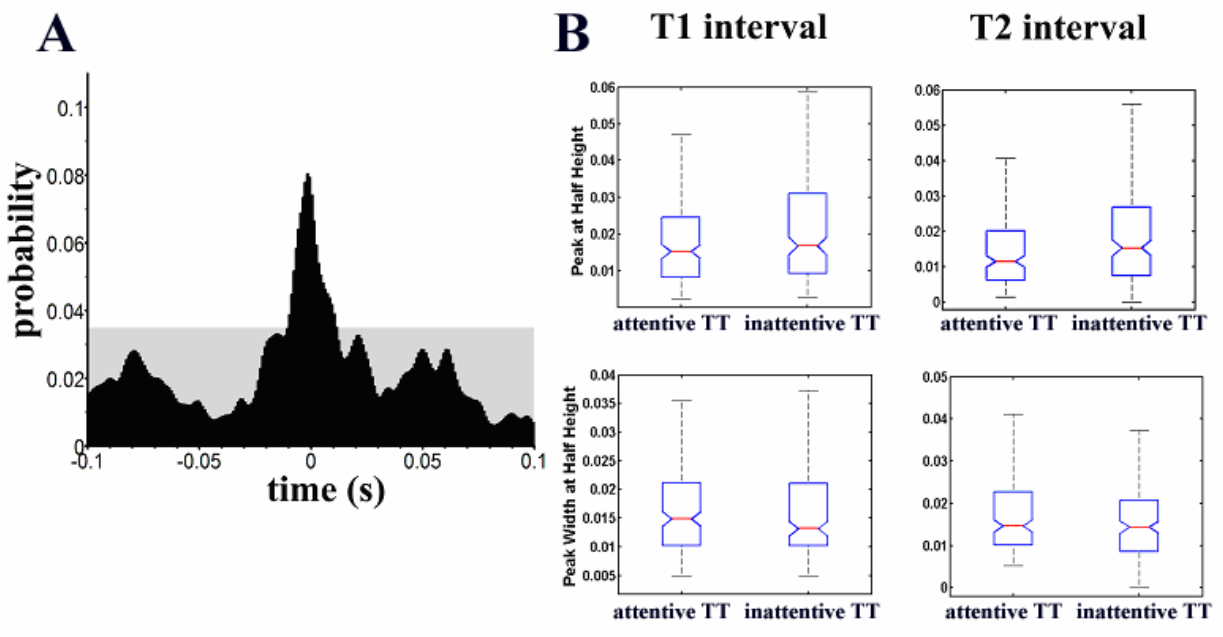

Figure 4.32. The strength of neuronal synchronization during T1 and T2 intervals is not significantly different in attentive and inattentive trials. Figure 4.32A shows an example of CCH where the Y axes is the probability of spike coincidences for various time shifts (abscissa: -100ms to +100ms). The shaded area indicates spike coincidences within 95% confidence intervals. Figure 4.32B shows a box plot for spike coincidences at half height peak of 434 combinations pairs (top graph) and the width at half height peak of those pars (bottom graph) during the T1 interval. Figure 4.32B also shows a box plot of the width (bottom) and half height peaks (top) for T2 intervals.

The synchronous precision of the neurons during attentive and inattentive trials was estimated by calculating the width at the half height peak which is a measure of the dispersion of the spike coincidences (Brosch et al, 1999). This analysis is shown in the bottom left (T1 interval) and bottom right (T2 interval) graph of Figure 4.32. The comparison of the width at the half height peak in attentive and inattentive trials during T1 intervals also did not reach significance ((Wilcoxon signed rank test, $p = 0.0546$). The same was also true for the T2 interval ($p = 0.1426$). In summary, there is an increase in the number of neurons that simultaneously fire action potentials during attentive trials as compared to inattentive trials. However, the strength of synchrony across the population is not significantly different between attentive and inattentive trials during the T1 interval. Moreover, the strength of the synchrony is higher for the inattentive trials during T2. Additionally, it appeared that the dispersion of the spike coincidences during the attentive trials was higher than the inattentive trials. However, the width at the half height peak did not reach statistical significance.

The synchrony of neurons in A1 was further measured by computing the coherence spectrogram (coherogram) and coherence during attentive and inattentive trials. This measurement offers the opportunity to study neuronal synchrony at different frequency ranges along the time axes. Figure 4.33 shows the coherogram during attentive (top right figure) and inattentive (top left figure) trials. This figure depicts the coherence (Z axes in color-coded scale) of the various frequencies (ordinate in Hz) that composes the spike train spectrum over time (abscissa in ms). The first and second tones occurred at time 0 ms and 200 ms. Figure 4.33 clearly shows that there is an increase in the coherence at tone onset and in during 100 ms thereafter. This increase in coherence

occurs whenever there is a tone. However, this increase in coherence is more pronounced for the first tone than the second tone. Moreover, this same trend is observed for attentive and inattentive TT trial types. The coherogram also shows that the increase in coherence occurs in frequencies below to 60 Hz for both attentive and inattentive trials. I further compared the coherence between spike trains in the attentive and inattentive trials by computing the coherence and its 95% confidence interval during T1 (0 to 200 ms) and T2 (200 to 400 ms) time intervals.

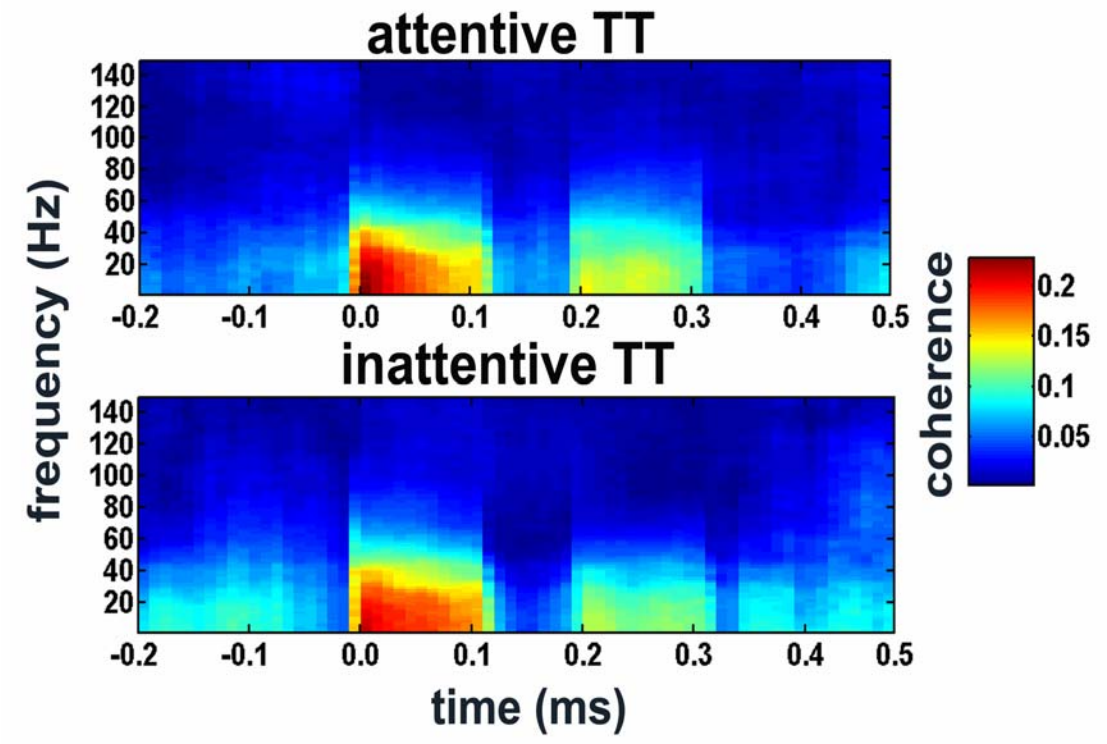

Figure 4.33. The coherence spectrogram of the spike train did not show striking differences between attentive and inattentive TT trial types .The top graphs show the coherence spectrogram during attentive trials (left graph) and inattentive trials (right graph). The Y axes show the frequency (Hz), the X axes show time (ms) and the Z axes show the coherence in a color-coded scale (red= high coherence and blue= low coherence).

Attention-related processes modulate spike train coherence during the T2 interval, however, it did not modulate the neuronal coherence during the T1 interval. Figure 4.34 shows the coherence along with its 95% confidence interval estimate during the time T1 (0 ms to 200 ms, top graph) and during time T2 (200 ms-400 ms, bottom graph). The top graph of Figure 4.34 demonstrates that there is no difference in the coherence for the attentive and inattentive trials during T1 interval across frequencies ranging from 1-150 Hz. However, the comparison between MUA-MUA coherence in the attentive and inattentive trials during the T2 interval showed a slightly different picture. There were significant differences at low frequency ranges (<30 Hz) between attentive and inattentive trials. There is more spike coherence for the inattentive trials than the attentive ones for this low frequency range, whereas for the high frequency ranges around 55-70 Hz the opposite was true (Jackknife U test, $p<0.01$).

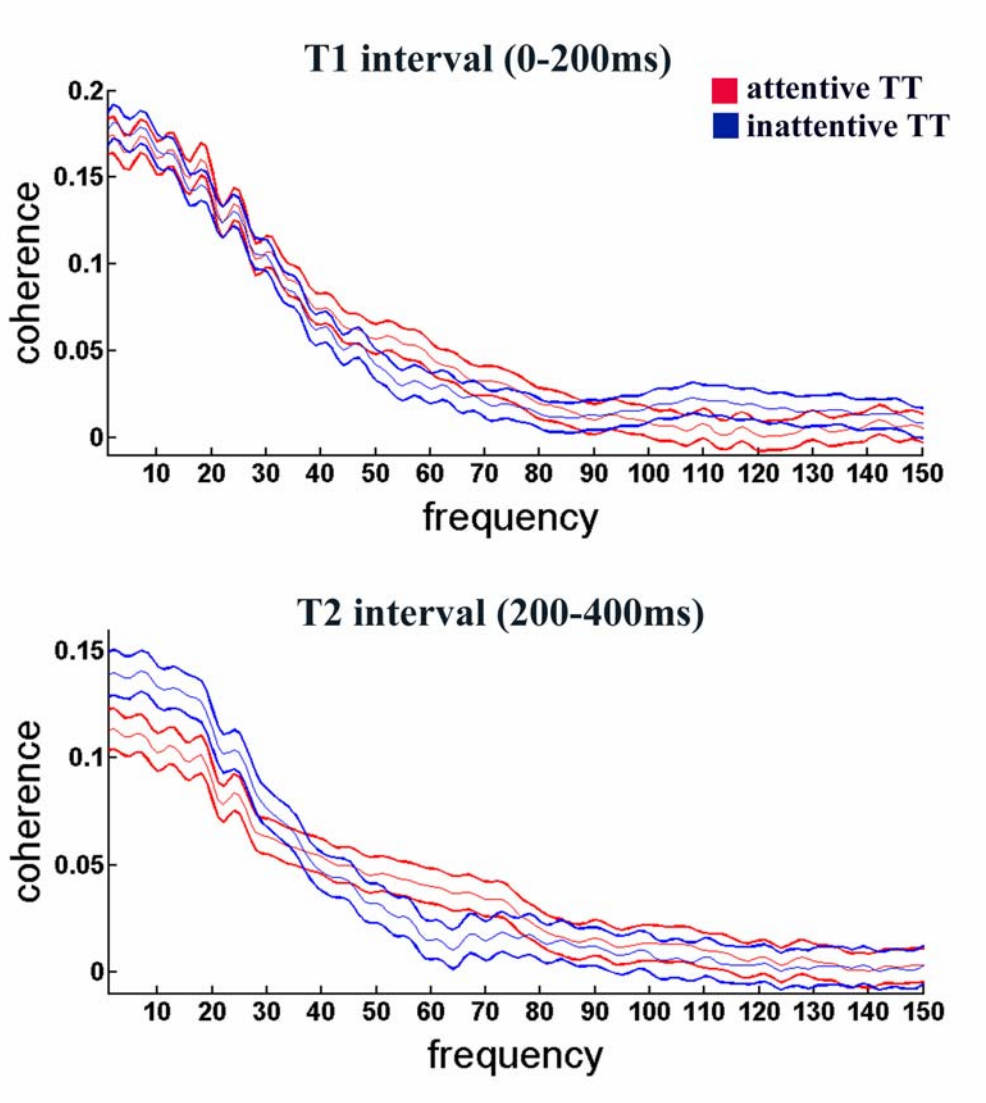

Figure 4.34. Attending to the second tone does not change the neuronal coherence during T1 but has a slightly effect at time T2. The top graph shows the MUA-MUA coherence during the T1 interval in the attentive trials (red line) and inattentive trials (blue line).The bottom graph shows the same analysis during the T2 interval.

4.4 Discussion

General Findings

I found that attention-related processes modulate the activity of A1 neurons in the inter-tone interval as well as after the second tone onset. This finding is consistent with previous reports (Hubel et al., 1959; Miller et al., 1972; Hocherman et al., 1976). I extended these previous studies by computing the analysis based on the signal detection theory which demonstrates that the activity of the neurons in A1 can reliably predict the behavioral outcome in the two-tone discrimination task. Furthermore, the prediction of the behavioral outcome based on the firing of the neurons in A1 occurs at two specific time periods: 1) during the inter-tone interval, and 2) after the second tone.

The tone onset response of neurons was not reliable to identify whether rats will lick or not lick the spout in order to receive a water reward in the two tone trial types. However, and somewhat surprisingly, the first tone onset response, the activity during the inter-tone interval, and the activity after second tone interval can be used to reliably categorize the attentive and the aroused trial types. Additionally, our time series (CCH) and spectral (SPK-SPK coherence) analysis of spike train synchrony suggested that that neurons in A1 do not use a temporal code to process temporal cues to correctly predict water rewards.

Behavior

Rats successfully discriminated two-tone versus one-tone trials. Rats licked to receive water in proximately 70% of the two-tone trials whereas they licked the spout in approximately 30% of the one-tone trials. Moreover, whenever they licked the spout, it was during the 800 ms reinforcement period. Additionally, the mean latency response

was around 450 ms regardless of the trial type. Thus, they quickly learned to make a prediction of when water would be available. Therefore, they must have used a temporal interval clock to anticipate a reward. Later on, they refined their interval clock by learning that two-tones are the acoustic cue necessary for predicting the reward. Thus, rats had to attend to the 200 ms interval between tones to maximize their chance to get water. The psychophysical results also reinforced the interpretation that the processing of the time between tones was relevant to rats to guide their decision to lick the spout anticipating a water reward. This test showed that they could discriminate between the one tone and two-tone trials with an interval of 10 ms or less between the first and second tone onsets. However, it suggests that they can discriminate between one and two-tone trials with inter-tone interval above 15 ms. A second possible interpretation is that rats are forming an acoustic object based on the temporal characteristics of the two-tone trial types. It is possible that they use a schema-drive mechanism to form the acoustic object, since it has gained significance in predicting a valuable resource. The two-tone discrimination behavior was also maintained during the recording sessions. Therefore, suggesting that the lack of response to the two-tone trials is not explained by a decrease in motivation to engage in the behavioral task. These combined results suggest that rats learned to use acoustic temporal cues, or are forming an acoustic object based on timing of acoustic elements, to guide goal-directed behaviors.

Studies measuring the temporal acuity of the auditory system have suggested that the auditory system has a temporal acuity of 1-3 ms in several mammalian species (Moore, 2004). Moreover, lesions in the temporal cortex disrupting temporal acuity strongly suggest that A1 is required for rapid temporal processing (Syke et al, 2002;

Bowen et al., 2003). These studies are based on the response of experimental animals to a silent gap in a continuous noise. Our results show that rats can not detect whether they heard a one or two-tones if the interval between the tone onsets is 10 ms apart. This value is lower than the behavioral measurements of temporal acuity using gap-detection paradigms (rats: Syke et al, 2002, Browen, et al, 2003; ferrets: Kelly et al, 1996). However, the neuronal coding for detection of a small change in a constant environment might not be the same in order to make temporal judgments. For instance, detecting a flash of light in a dark room or a silent gap in a constant noise is quite different from judging the duration of stimuli or to judge what is the minimum time interval between acoustic stimuli to detect whether they are distinct perceptual objects. In humans, accurate temporal order judgments require inter-click intervals of approximately 20 ms (Hirsh, 1959; Moore., 1997). Other studies show that a pure tone presented simultaneously has to have stimulus onset asynchronies of approximately 20 ms (Stevens & Weaver, 2005; Pastore et al., 1988). The results presented here are consistent with the data of Hirsch.

Representation of acoustic objects.

Because the acoustic environment consists typically of a mixture of sounds, the auditory cortex has to implement a set of algorithms in order to disentangle meaningful acoustic information from background noise. Acoustic Scene Analysis (ASA) is how psychologists name the algorithms implemented by the auditory system to group and follow acoustic events along time, thus, forming acoustic perceptual objects (also called auditory streaming) (Bregman, 1990). Frequency similarity, time onsets and time interval are physical attributes used by the auditory system to accomplish auditory streaming

(Dannenbring & Bregman, 1976; Bregman, 1990; Bregman et al., 2000). Moreover, subjective rhythm is a fundamental component for auditory grouping, music perception and language (Handel 1998; Larger & Jones, 1999). Some authors propose that auditory attention itself has evolved to predict time regularities of acoustic objects (Larger & Jones, 1999; Jones., 2004). Therefore these authors propose that temporal regularities of acoustic events would greatly capture auditory attention.

The two-tone discrimination test used in this study allowed us to infer if the neuronal activity of A1 can process temporal cues that are likely important for grouping acoustics events into perceptual acoustic streams. The results presented in this chapter show that the A1 neuronal activity is modulated in the attentive trials even during the inter-tone interval. During this interval, rats did not know if they would receive water or not. However, the internal state of the brain during this internal is fundamentally different between animals that lick the spout in response to the first tone only and animals that correctly pay attention to the second tone to lick the spout. In the second condition, the neuronal activity between tones could be indicative of temporal cue processing in A1. Therefore, by comparing the neuronal activity of A1 during attentive and inattentive two-tone trials and by subsequently comparing attentive two-tone and attentive one-tone trials, I was able to demonstrate that the activity of A1 is likely modulated by temporal cues. Additionally, in order to correctly perform the two-tone discrimination task, they likely grouped two separate acoustic events (two tones) into one single acoustic object. However, this experiment was not specifically designed to study the formation of acoustic objects solely based on acoustic temporal cues. Further experiments in awake behaving animals should be designed to specifically study the correlation of A1 activity

during auditory stream formation based on temporal processing acoustic cues. Regardless of the percept formed with these rats, the results showed in this chapter demonstrate that there is a higher percentage of neurons in which their activity is modulated by rats attending to the timing between tones. Note, however, that the results presented here about modulation of A1 activity by neuronal representation of temporal cues are quite different from the results of previous studies exploring neuronal representation of time-varying signals.

The majority of studies in the auditory system have focused on how its neurons respond to time-varying acoustic signals in anesthetized or passive listening animals. Studies using amplitude modulations, frequency modulations, tone or click repetitive sequences have shown that neurons in A1 (Creutzfelt et al., 1980; Eggermont, 1992, 1994; Lu & Wang, 2000; Liang et al., 2002) display synchronized action potentials to slow envelope variations of the acoustic stimulus in a range of 30-50 Hz. However, some authours reported that neurons can synchronize their action potentials to time-varying stimulus at rates of 100 Hz (DeRibaupierre et al., 1972) and 165 Hz (Anderson et al., 2006). Unlike brainstem structures which faithfully phase-lock to the carrier frequency as well as the envelope of the time -varying sounds (review in Altschler et al., 1991.; Langner, 1992.; Frisina, 2001.), the precision of a temporal based representation is greatly reduced in the auditory cortex (DeRibeaupierre et al., 1972; Creutzfeldt et al., 1980; Schreiner & Urbas, 1988; Liang & Wang, 1992). Some studies have found that a subclass of A1 neurons in awake marmosets can follow a very short inter-tone interval (2 to 10 ms), but with a non-synchronized firing rate-based code (Lu & Wang, 2002; Lu & Wang, 2004; Lu et al., 2001a, 2001b). Other studies, found that neurons in A1 are finely

synchronized to fast transitions in frequency and amplitude embedded in complex stimulus such as ripple noise or animal vocalizations (Elhilali et al, 2005; Schnupp et al, 2006; Walker et al., 2008). Therefore, it is unclear what neurons in A1 are precisely representing. Additionally, these studies implicitly assume that A1 behaves as a feature detection system that is tuned to acoustic features forming feature maps of the environment (DeCharms et al., 1998; Schreiner, 2000; Reid et al., 2004).

The results represented here indicate a different picture of the role of the primary auditory cortex in the processing of sounds. It suggests that A1 activity is modulated by task demands necessary to lead perception into goal-directed behaviors. Our results complement the findings of key experiments correlating A1 neuronal activity to available psychophysical data in humans (Nelken et al., 1999; Micheyl, et al., 2005; 2007; Petkov et al., 2007). These previous experiments have challenged the idea that A1 behaves as a passive devise that is segregating acoustic physical attributes into maps for further processing into high hierarchical areas. For instance, when tones are simultaneously played with modulated noise bands, the phase-locked firing rate to the envelope of the noise bands is greatly degraded (Nelken et al, 1999). This finding suggests that A1 activity underlies the co-modulation masking release (CMR) phenomenon in which the detection of tones is facilitated in a noisy environment (Schooneveldt & Moore, 1989; Nelken et al., 1999). Other studies have shown that neurons in A1 behave as if they were being activated by a continuous tone, when in fact the stimulus consisted of two tone sequences in which the gap between them was filled in by a brief noise (Petkov et al., 2007). This result demonstrates that neurons in A1 fill-in perceptual information. Psychophysical studies show that speech comprehension is greatly reduced when speech

segments are deleted from it. However, if these deleted segments are replaced by noise, the comprehension dramatically improves (Warren, 1970). Other studies found evidence that the activity in A1 correlates with the subjective perception of the build-up stream segregation phenomenon (Micheyl, et al., 2005; 2007). These results suggest that A1 is coding abstract auditory objects, and although it is activated by acoustic physical attributes of these auditory objects, the role of A1 activity might not be breaking down sounds in maps of basic physical attributes, but linking those physical attributes in auditory streams (Nelken, 1999).

The neuronal recordings of the studies described in the previous paragraph were performed in the auditory cortex of anesthetized or experimental awake animals passively listening to acoustic stimuli. These stimuli were cleverly designed to induce relevant, foreground, auditory signal segmentation from background noise. In order to fully explore the role of A1 in the formation of acoustic objects, it is important to perform studies in awake, behaving animals actively reporting that they perceived relevant auditory patterns. The experiments performed in this dissertation, in which the auditory stimulus can be maintained constant while the behavior of the animals varied, demonstrated that the primary auditory cortex is much more dynamic than a feature extraction filter. For instance, the results in this chapter suggested that attention to the elapsed time after the first tone activates neurons in A1. In this sense, the first tone acted as a warning signal that triggered a more sustained tonic response throughout the inter-tone interval. This sustained response occured in a subset of neurons (41.8 %) in A1 when the rat attended to the second tone. These results are consistent with data from the

literature showing that attention modulates the activity of neurons in A1 (Hubel et al., 1959; Miller et al., 1972; Hocherman et al., 1976; Fritz et al., 2003; 2005; 2007).

I explored if the activity of A1 can reliably predict behavioral performance by using a detection signal theory and computing the ROC curve. The results presented in this chapter demonstrate that an ideal observer is capable of correctly categorizing the rats' behavior by measuring the firing rate between tones (figures 4.28 and 4.30). Furthermore, the increase of this sustained activity between tones is not merely an indication of an overall increase in arousal to a tone. This is because an ideal observer can still correctly categorize whether the rat will correctly lick the spout in the two-tone trial types (see shaded gray squares in Figure 4.31B).

It is important to note, however, that the sustained activity after the first tone onset is not the only parameter that postsynaptic neurons in the secondary auditory cortex receive from A1 activity. The normalized tone onset response of these neurons is greatly reduced in the attentive OT condition. For instance, the signal-to-noise ratio (SNR) of the tone onset in the attentive TT trial types is much higher than the SNR to the attentive OT. This result provides experimental evidence supporting the hypothesis that attention modulates the effective gain of sensory stimuli (Reynolds et al., 2000; Reynolds & Chelazzi, 2004; Reynolds, 2004). This hypothesis proposes that top-down modulation by areas of the pre-frontal and the parietal cortex would enhance the processing of sensory features in relation to baseline activity in the primary cortices. Therefore, attention is a mechanism to bias the processing of relevant sensory attributes (Reynolds., 2004). The results of low SNR in the attentive OT trial types indicate a high level of activity during the baseline in a general arousal state. This high baseline activity in A1 likely decreases

the probability that a precise network of neurons receiving pre-synaptic potentials from A1 would convey reliable information to the pre-frontal and/or parietal cortex to implement correct goal-direct behavior. It is important to point it out that the high SNR signal from A1 is not the only parameter used by neurons receiving action potentials from A1. This is because in inattentive two-tone trials, there is a high SNR, but no goal directed behavior is implemented. For instance, during the first and second tone, the SNR is not different between the attentive and unattentive two-tone trial type conditions. Thus, the tonic activity of A1 neurons between tones combined with the correct SNR of the neurons responding to the tone onset would be necessary to convey the correct synaptic drive to downstream targets of A1. This result implies that a very abstract representation of the acoustic environment is present in A1.

The results presented in this chapter demonstrate that A1 activity is enhanced in the attentive trials that are important for goal-directed behavior. I also suggest that the neuronal activity of A1 is not a function of an enhanced vigilant or arousal state in these animals. This is because rats are in a vigilant state in the trials types in which they attended to the one tone. However, the neuronal activity in the inter-tone interval and after the second tone interval is still higher in the trial types in which rats correctly attended to the two tones. Moreover, the increased neuronal activity in the inter-tone interval cannot be explained by a reward expectation in the attentive two-tone trial types because rats only will acquire the information that there is a water reward after the second tone. Therefore, I interpret this result as that the A1 neuronal activity during the inter-tone interval is likely processing temporal information that is relevant to bind two otherwise separate acoustic elements into a single acoustic object. Moreover, I

hypothesize that the activity of A1 during this interval is likely modulated by the activity of neurons at higher hierarchical areas of the temporal, pre-frontal, or parietal cortex. Note, however, that while the higher activity of A1 during the correct performance of the the two-tone discrimination task suggest the formation of acoustic objects, further experiments are needed to establish that A1 activity correlates to acoustic streaming formation based on temporal cues.

Sensory memory

There is experimental evidence suggesting that A1 implements a primitive pre-attentive system to modulate the occurrence of new, and potentially relevant, sound. For instance, several studies have reported an EEG signature called mismatch negativity (MMN) in the auditory cortex (Näätänen et a., 1993; reviewed in Näätänen & Alho, 2004; Näätänen et al., 2007). The MMN is a specific increase in the amplitude of the auditory evoked EEG to an infrequent auditory stimulus embedded into a sequence of standard acoustic stimuli (reviewed in Fritz et al., 2007). It is thought that the MMN response is a correlate of a pre-attentive primitive sensory memory trace because it retains a sensory representation of the common stimuli and compares it to the novel stimuli (Fritz et al., 2007; Näätänen et al., 2007). The activity of A1 neurons have the same characteristics of the MMN which are not found in the MGB (Ulanovsky et al., 2003). Moreover, the MMN persists in anesthetized animals (Ulanovsky et al., 2003) and in comatose humans (reviewed in Frizt et al., 2007, Näätänen & Alho, 2004). These A1 neurons respond more strongly to the auditory stimulus when it occur rarely in a stream of more common stimuli. Thus, A1 neurons are strongly influenced by the context in which the auditory stimulus is occurring. Moreover they retain a pre-attentive sensory

memory which compares commonly occurring stimuli with rare and potentially relevant stimulus (Ulanovsky et al., 2003).

It is also important to note that during the inter-tone interval, attention is directed to an upcoming auditory event that signals a water reward. However, both tones have the same physical features. Thus, while an anticipation process is occurring in the inter-tone interval, a sensory memory process to discriminate two events based on their physical attributes is likely not driving the activity of A1 neurons in our paradigm. This is because the two-tone discrimination paradigm is different from experiments of delay match to sample experiments, or MMN experiments in which a sensory feature has to be maintained in working memory in order to compare with the new sensory event. I am proposing that the enhancement of A1 activity during the silent inter-tone interval period is related with abstract temporal processing cues that may be essential to grouping mechanisms. However, sensorial memory cannot be fully discarted as a possible explanation. Thus, further experiments where discrimination of physical attributes is required to get a reward could shed some light in the role of A1 in processing sensory memories.

This activity of A1 neurons during the inter-tone interval could indirectly activate auditory neurons in the dorsolateral and ventrolateral pre-frontal cortex (DLPFC and vPFC) (, Romansky et al., 1999; Romansky et al., 2002; Cohen et al., 2004; Cohen et al., 2007). It is described that A1 projects to secondary auditory areas that projects to the PFC (Romansky., 1999; Rauschecker & Tian., 2000). Thus, A1 is connected to the PFC through poly-synaptic connections in secondary auditory cortices (Romansky et al., 2002). These studies have shown that neurons in the PFC are activated by tones, clicks

and complex vocalizations with a latency of 80-200 ms (Romansky et al., 1999; Romansky et al., 2002; Cohen et al., 2007; Russ et al., 2008). Moreover, it has been proposed that those neurons are specially tuned to the meaning but not acoustic attributes of vocalizations (Cohen et al, 2006; Cohen et al., 2007; Russ et al., 2008a, 2008b). Studies in the PFC suggest that it is composed of several processing structures that are relevant for the processing of visual and auditory categories (Freedman et al.2001, Miller et al., 2003; Cohen et al., 2006) decision making processes and processing of values (Wallis et al., 2007a, 2007b), and representation of abstract rules to implement goal-directed behaviors (Wallis et al., 2001). Thus is possible that the activity of A1 in the tone onset could gate the activity of DLPFC and or/ vPFC which then would feedback to A1 greatly enhancing its activity throughout the trial session.

Areas of the parietal cortex could also be relevant in modulating A1 activity in the two-tone discrimination task as well. This is because areas of the posterior parietal cortex can be activated by auditory information (Cohen et al., 2004; Russ et al., 2006) and they are implicated in elapsed time processing (Leon et al., 2003; Janssen & Shadlen., 2005), decision making (Newsome & Shadlen, 1996), and auditory and visual spatial attention (reviewed in Romansky, 2004; 2007). Thus it is possible that A1 could signal an early processing of the elapsed time that could trigger more complex time processing centers located in the posterior parietal cortex.

It is not known if A1 receives a direct projection from the posterior parietal cortex or the PFC. However, A1 sends a feed-back projection to the TRN (Roger and Arnault, 1989) which is reciprocally connected to the MGB. Moreover, the TRN receives projections from the prefrontal cortex (Zikopoulos & Barbas., 2006). It is interesting to

note that the TRN areas that receive feedback projections from cortical sensory areas (caudal TRN: auditory sector; and TRN rostral: visual sector) showed extensive overlap with axon terminals from anterograde track-tracers injected into the PFC (Zikopoulos and Barbas, 2006). It is important to point it out the PFC have neurons that are activated by complex auditory stimuli (Cohen et al., 2007; Romansky et al., 1999, 2000; 2009). Thus, the auditory sector of the TRN receives an overlapping projection from A1 and PFC. Therefore, it is possible that an indirect projection from A1 via the secondary auditory cortical areas could reach the PFC which could then evaluate the significance of the sensory information. Once these areas process the auditory information, it could send a feedback projection to the auditory sector of the TRN. Therefore, the TRN neuronal network is in a unique position, perhaps as coincident detectors, to integrate high processed sensory information and to modulate incoming thalamic information. It is possible that reciprocal projections of the TRN and MGB, modulated by A1 and PFC inputs, could then modulate high frequency oscillations in the A1 allowing, perhaps, incoming sensory information to be grouped in an auditory stream.

Synchronization

There was a great variability of neuronal synchrony between attentive and inattentive TT trial types among experimental sessions during the T1 interval. In some experimental sessions there were larger differences between attentive and inattentive trial types, while in others I did not observed such differences. For example, the cross-correlogram results for the RAT-1A presented in Figure 4.31, suggested that there was a higher synchrony among neurons during attentive TT trials during the T1 interval. Moreover, the synchronous pattern is highly complex. The class of neurons showing the

highest levels of synchrony was present in both attentive and inattentive trial types. However, in the attentive trial types there were low levels of synchrony between neurons that were not synchronous during inattentive trial types. Thus there was an increase of neurons that become synchronous during this interval. Moreover, neuron pairs that were synchronous during the attentive TT trials are not necessarily the same pairs that were synchronous during inattentive TT trial types. Result from this experiment suggested that attention directed to the inter-tone intervals triggers low levels of synchrony in a larger neuronal population in A1. I further analyzed synchrony during T1 intervals in different experimental sessions of the same rat or across rats. I did not see any consistent pattern of synchrony among neurons in A1 that were correlated with attentive or inattentive TT trial types in these experiments. For instance, in some experimental sessions there was a higher number of synchronous neurons during attentive as compared to inattentive trial types. In other experiments the reverse was true (see Table 1a). Across the population, there were not significant statistical differences between attentive and inattentive TT trial types with respect to the number of synchronous neuronal pairs. Moreover, I also did not detect differences in synchrony strength (measured as half height peak of the CCH,) or temporal dispersion (measured as half height width of the CCH) between attentive or inattentive TT trial types across the population. Thus, I did not observe any consistent synchronous pattern of activity being modulated by paying attention to the inter-tone interval.

During the interval immediately after the second tone onset (T2 interval) I did not observe the same effects. During the T2 interval synchrony strength was lower during attentive versus inattentive TT trial types. The measurements of spike train coherence

across the population were also consistent with the measurements of CCH analysis. I did not detect significant differences in spike train coherence across a wide frequency range during attentive and unattentive trial types during the T1 interval, but, I did detect significant differences during the T2 interval. There was less synchrony in lower frequency ranges (<30 Hz) for the attentive compared to the unattentive trial types. However, for high frequency ranges (50-70 Hz) the opposite was true.

Several studies using CCH in the auditory cortex of anesthetized animals (mainly cats and monkeys) revealed that neurons with similar receptive fields and neurons that are close in space display high levels of neuronal synchrony (Decharms & Merzenich., 1996; Brosch et al., 1999; Eggermont., 2006a; 2006b). Thus neuronal synchrony could be a cellular mechanism in which coherence of neuronal features detectors would enable coherent perception (Eggermont, 2006). This view assumes that the primary auditory cortex handles perceptual information similarly to the primary visual cortex. It assumes that feature detector neurons process sensory information in parallel, and that, synchrony between these neurons would likely activate post-synaptic targets of A1, which would then enable the formation of coherent percepts.

Indeed, there are some parallels concerning the functional organization of primary sensory cortices. For instance, it is well established that V1 has a modular functional structure forming orientation tuning maps and ocular dominance columns (Hubel, 2000). Likewise, the functional organization of A1 displaying tonotopic frequency maps also displays iso-frequency columns (reviewed in Ehret, 1997; Schreiner et al., 2000; Read et al., 2002; Linden & Schreiner, 2003). However, this view posits several constrains in the dynamics of intrinsic temporal activity of A1 neurons. It is possible that top-down

cognitive processes are as important as receptive field properties in shaping the neuronal synchronous responses of A1 neurons.

In this chapter, I tested the hypothesis that perception of relevant sounds modulates synchrony of neuronal networks in the auditory cortex. The results presented in this chapter did not detect any consistent attentional modulation of the synchronous pattern between MUA clusters separated by approximately 250-300 μm during the T1 interval. Perhaps, other parameters like similarity of receptive field, spectral integration, FM, binaural response types could be also relevant in triggering synchronous activity of A1. However, I detected modulation in coherence among neurons during the T2 interval. The results of this chapter extends previous studies by showing that neurons synchrony is modulated by attentional demands to correctly anticipate rewards. Several recent results in the area V4 of the visual cortex also have shown that spatial and feature detection attention modulates the synchrony of neurons (Fries et al., 2001, 2008; Bichot et al., 2005; Wolmesdorf et al., 2006, 2008;). Moreover, these studies also demonstrate that synchrony at the gamma range frequencies shows the highest correlation with attentional demands. Attentional to an incoming acoustic event is likely important to effective performance in the two-tone trials. However, there were not consistent modulations of synchrony in the T1 interval. During the T2 interval other cognitive processes besides attention are likely relevant as well. For instance, decision making processes are clearly involved during this interval for animals that correctly lick the spout to receive water. Therefore, a combination of attention, anticipation to reward and decision making processes are dynamically modulating the synchronous activity of A1 to likely improve performance. Because I recorded MUA clusters with high impedance electrodes, it is

possible that I am mainly describing the properties of a particular class of large pyramidal neurons that displays large action potential currents. Therefore, it is possible that I am selecting a specific class of neurons that are not synchronous, but that other neurons could be synchronous. Because the local field potential (LFP) is believed to be the summed synaptic activity of hundreds of neurons around the electrode tip (Mizdorf, 1985; Logothesis., 2002), any increase in LFP amplitude is caused by a large synchronous neuronal population. Therefore, in the following chapter I will test the hypothesis that attention to temporal cues modulates the activity of small neuronal networks by recording local field potentials in the auditory cortex of rats performing the two-tone temporal discrimination task.

Chapter 5

Attending to the two-tone discrimination task modulates intrinsic temporal activity in the auditory cortex of rats.

5.1 Introduction

In previous chapters the hypothesis that active-listening changed the dynamics of temporal correlations was tested. Unlike passive listening, active listening necessarily involves the allocation of attention in order to process auditory stimuli. Chapter 3 demonstrates that active listening increases the power and coherence at the high frequency components of the LFP signal. However, those results are based on the comparison of two experimental groups belonging to two different rat populations. One of these rat populations underwent on extensive training protocol.

Training adds a confounding plasticity factor in our analysis. Likely, the auditory cortex of the trained group has its topography changed; expanding the population of neurons tuned to the 10 kHz tones. It could be that these high frequency oscillations are reflecting the fact that larger populations of neurons are tuned to 10 kHz tone. In this chapter, the same population of neurons in rats attending or not attending relevant sensory information will be compared. Active listening modulations of high frequency oscillations in this case could not be caused by a differentially modified topography of the auditory cortex.

There is a wealth of experimental data suggesting that the auditory system uses time regularities as invaluable information to group sounds in auditory perceptual streams (Handel 1989; Bregman, 1990; Moore, 1997). It is also known that individual acoustic events presented in a context of metrical regular sequences are easy to perceive and to

remember (Jones & Boltz, 1989; Large & Jones, 1999; Jones, 2004). Jones and collaborators propose that attention is highly affected by the degree of rhythm regularity of an event time structure (Jones, 2004). Moreover, they propose that intrinsic oscillations are the neuronal substrate to process sensory expectations based on expected acoustic temporal pattern shaped by experience (Large & Jones, 1999; Jones, 2004; Snyder & Large, 2005; Zanto et al., 2006). Other studies proposed that these oscillations would serve as a temporal binding mechanism of sensory stimuli, thus linking separate acoustic events in a unified percept (Llinas & Ribary, 1993; Joliot et al., 1994). Both theories implicitly assume that intrinsic oscillations would underlie acoustic streaming formation.

The results presented in chapter 4 suggested that based on sensory memory the A1 activity is processing temporal cues that could be important to anticipate acoustic regularities present in acoustic objects. In the prior chapter, I trained rats in a two-tone discrimination task to test if A1 neurons are modulated by attention-related processes, and to test if A1 activity can be a reliable parameter to classify a goal-directed behavior. I showed that the firing rate of A1 neurons can reliably predict behavior performance even before the occurrence of a second tone. Rats only received reward after correctly identifying the second tone. Moreover, it is important to point out that, in this two-tone discrimination paradigm, the interval between tones is regular. The second tone always occurs 200 ms after the first tone onset. So, I conjectured that, in the trials in which animals successfully licked to receive water, the activity of neurons in A1 during the interval between tones reliably indicated the presence of a future regular sensory event. Moreover, in the attentive two-tone trial types, A1 activity is likely integrating two

otherwise separate acoustic elements into an distinctive acoustic object that correctly signals reward. Thus, I postulated that if gamma oscillations are distinctly relevant for acoustic sensory processing, it should be highly modulated in the inter-tone interval of animals correctly performing the two-tone discrimination task. Therefore, a specific modulation of high frequency oscillations during the interval between tones could potentially indicate that these oscillations are a temporal binding mechanism, which will bind two otherwise separate acoustic events in a unified auditory object that acquired relevant specific meaning through experience.

The main goal of this chapter, was to investigate whether these high frequency oscillations are modulated by attention-related processes in the auditory cortex of awake rats performing a two-tone discrimination task; and moreover, if they are a good neuronal parameter to categorize goal-directed behaviors. Second, by comparing the interval immediately after the first tone onset across experimental trial types (see Chapter 4 for a complete description of the task), I will test the hypothesis that these high frequency oscillations are not merely modulated by attentional or motivational demands, but are modulated by predictions of regular auditory events as well.

5.2 Methods

Experimental conditions and hypothesis testing

In this chapter I will focus on the local field potential analysis collected in the same experimental sessions described in chapter 4. Therefore, the description of methods of animals training, behavioral apparatus, animal preparation, stimuli generation, and recording session are essentially the same as described in chapter 4.

I compared the spectrogram, power spectrum, and coherence spectrum of the LFP signal during the different behavioral conditions depicted in Figure 5.35. The two-tone discrimination task (see chapter 4) was designed to test : A) if high frequency oscillations are modulated by attention-related processes in A1 of awake behaving rats; B) and to test if high frequency oscillations are modulated by temporal cue processing in A1 of awake behaving rats.

The comparison between the attentive TT condition (A in Figure 5.35) and inattentive TT condition (B in the Figure 5.35) during the T2 interval (green arrows in Figure 5.35) might reveal if attention-related processes modulate the high frequency oscillations. To verify if modulation in the high frequency oscillations might be related to a specific increase in focused attention, I also compared the power spectrum and coherence during the T2 interval in the attentive TT condition (A in Figure 5.35) and in the attentive OT condition (C in Figure 5.35). Therefore, the comparison between conditions A and C during the T2 interval controls for the alternative explanation that increases in high frequency oscillations amplitude is correlated with an increase in general arousal.

The comparison between conditions A an B during the T1 interval (red arrows in the Figure 5.35) might reveal if processing sensory regularities modulates high frequency oscillations. This is because rats attending to the attentive TT trials processed the time interval between tones, while the processing of the time interval between tones did not occur in rats that did not attended to the two tones. Moreover, it is important to note that in the one-tone trials that rats licked to receive water they were not fully engaged in the two-tone discrimination task. In the attentive OT condition, rats are not processing the

time between the first tone and the second onset. On the other hand, it is important to note that they are wrongly anticipating a water reward because they licked the spout during the reinforcement period (see Chapter 4). However, this behavior is not contingent on the binding of two separate tones in an acoustic object. I defined the trials in which rats attended to one tone as a general increase in arousal, because the animals did not engage in the two-tone discrimination task to correctly receive water. They use a strategy of "whenever a tone occurs lick to receive water", and therefore, neither the interval between tones nor the second tone itself are processed as relevant information to guide the behavior. Thus the auditory system is not likely grouping two tones in a distinct acoustic object. It has been demonstrated that performance depends on the arousal level, such that too little or to much general arousal induces a decrease in behavioral performance (Yerkes & Dodson, 1908, Aston-Jones, 2007; reviewed in Diamond et al., 2007). This relationship is defined by an inverted U-shaped curve known as Yerkes-Dodson law (reviewed in Diamond et al., 2007). Therefore the attentive OT trial condition can be considered as a general increase in arousal. Moreover, it allowed to methodologically investigate possible processing of temporal regularities by A1.

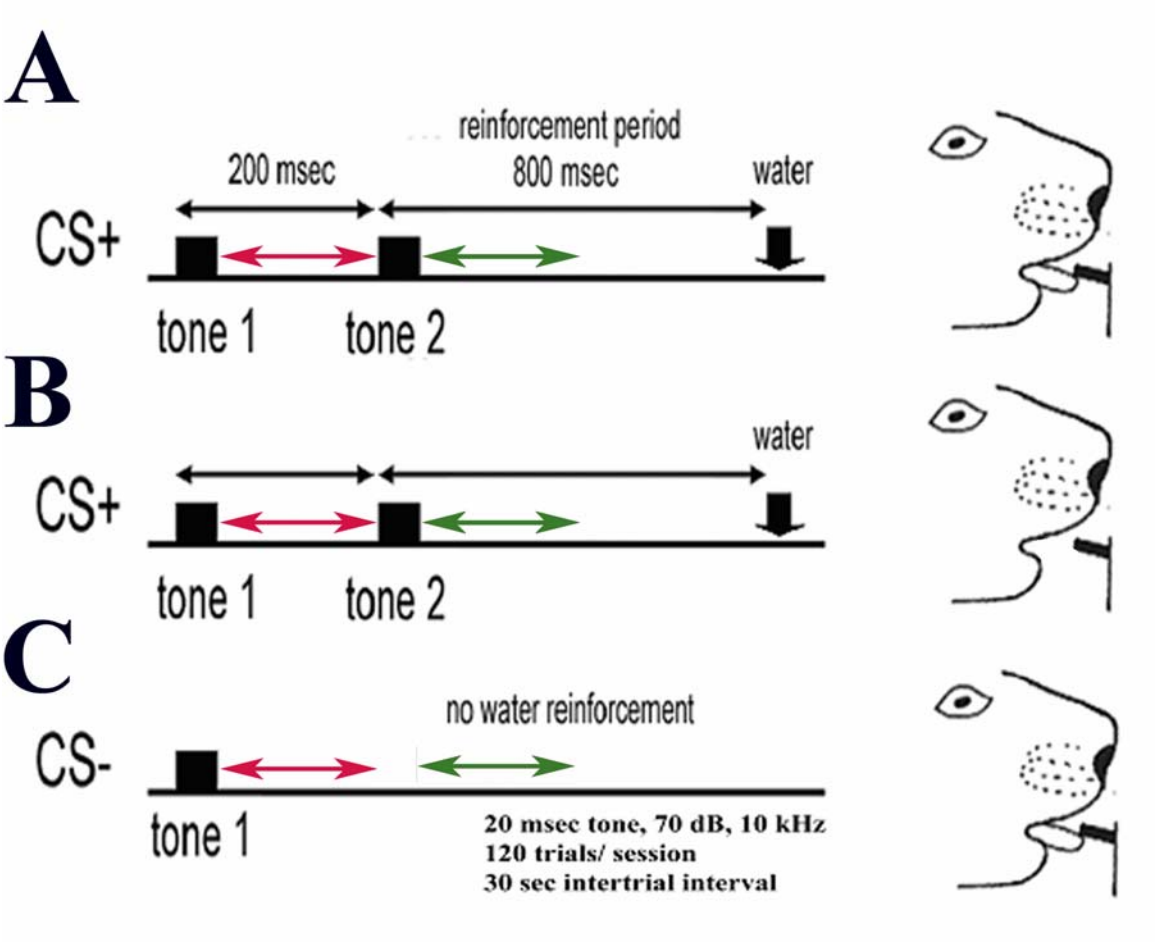

Figure 5.35. Description of the behavioral paradigm and experimental conditions. A) Top figure shows the positive conditional stimulus (CS+). In this condition, rats correctly pay attention to the second tone anticipating a water reward (**attentive TT condition**). B) The middle figure also shows the CS+. However, in this condition, rats ignore the second tone and did not lick the spout to receive water (**inattentive TT condition**). C) The bottom figure shows the negative conditional stimulus (CS-). However, in this condition rats incorrectly licked the spout, but they did not receive water (**inattentive OT condition**). The red (T1 interval, 30 to 200 ms) and green (T2 interval, 230 to 400 ms) arrows indicate the time periods in which spectrum analysis were performed.

Behavioral paradigm

Rats were trained in an instrumental operant paradigm in which they had to learn a two-tone discrimination task. This training paradigm is described in Figure 5.35, and it is also described in Chapter 4. Figure 5.35B shows the possible behavioral outcomes. The red arrows depicted in Figure 5.35A shows the time periods in which spectral analysis was performed. The CS+ consisted of two-tone trials, in which two 10 kHz tones with a 20 ms duration played at 75 dB sound pressure level separated by a 200 ms silence interval. Any time that the rat licked the spout during the reinforcement period (800 ms after second tone onset) it immediately received 40 µl water drop and the trials restarted. The middle figure shows the negative conditional stimulus (CS-), which consisted of a one tone trial, in which one 10 kHz tone with 20 ms duration was played. Any time that rats licked the spout within 1000 ms after the tone onset (the no water reinforcement period) the trial ended and a new trial restarted.

Recording session

Further description of the recording session and recording system can be found in chapter 4. Briefly, the LFP was recorded in parallel to the action potential signals. The LFP signal was filtered between 1-170 Hz, fed into an analog-digital card (PCI-6071E, National Intruments) in a host personal computer that sampled each analog channel at 1 kHz with 12 bit resolution. The LFP signal was further analyzed to detect movement and power-line noise artifacts. Only LFP sites that had evoked responses to the auditory stimulus with 3 SD from the background noise were selected for further analysis (see Figure 2.1 of chapter 2 for an example).

Preliminary analysis

The data set was pre-processed to select data segments without noise contamination caused by movements and power-line currents. I visualy inspected the LFP trace to detect movement noise. Then, I performed a power spectrum analysis to detect 60 Hz power-line contamination of the LFP. LFP traces that did have a distinct 60 Hz frequency in the power spectrum were not further analyzed. The data selection and off-line data analyses was performed with NEX and MATLAB (The MathWorks, Inc., Natick MA, USA). I used the on-line NEX spike train analysis software to compute peri-event histograms (PSTH) to select the LFP sites with the classical MAEP with short latency (15 ms) to the acoustic stimulias reported in literature to be generated in A1 (Talwar et al., 2001; Barth & Di, 1990, 1991; Franowicz & Barth, 1995). Then, the NEX programming language was used to select 20 trials of 1600 ms for each experimental condition. Each of these 1600 ms data segments had 500 ms of baseline and 1100 ms after the auditory stimulus onset.

Data set selection

Multiple single-units recordings (MUA) and LFP were recorded in awake and trained awake behaving rats performing the two-tone temporal discrimination task. The analysis was restricted to LFP sites showing the classic middle auditory evoked potential (MAEP) with short negative peak latencies referred as N1 (15 ms) to the 10 kHz tones and positive peak responses referred as P1 (≈50-60 ms). I selected 57 LFP sites from a pool of 6 experimental sessions in 3 rats. The LFP sites fom the 86 MUA recordings presented in chapter 4 had the MAEP signal typical of A1. However, noise artifacts prevented me to have the minimun of 20 trials for each experimental condition in two

experimental sessions of rats 1A and 2A. Therefore, the LFP sites of these experimental sessions were not further analyzed.

Spectral analysis

In order to study whether pure tones induce neuronal synchrony in the auditory cortex of the rat I also analyzed the spectrogram, the power spectrum, the coherence spectrogram, and the coherence spectrum of simultaneous recorded LFP sites. The spectral analysis was performed with the Chronux data analysis toolbox for Matlab (www.chronux.org) which uses multitaper methods to estimate the power spectrum of the spike train (point process) and derivate the spike spectrogram and coherence. The multitaper method has been extensively used in sensory-motor systems in several species (Prechtl et al., 1997; Mitra & Pesaran, 1999; Halliday & Rosenberg, 1999; Jarvis & Mitra, 2001; Pesaran et al., 2002; Mitra & Bokil, 2008) and it was discussed in chapters 2, 3 and 4.

In order to compute the coherence spectrograms and coherence of the MUA-LFP signal I used a time bandwidth product of 5 and 9 Slepian taper functions in 125 ms overlapping windows in 10 ms steps. For the LFP power spectrum density, the LFP-LFP coherence spectrogram, and LFP coherence, I used a bandwidth product of 3 and 5 tapers. The Chronux software provides measurements of 95% confidence interval of the spectrum and coherence estimation which can be used to test significant differences of coherence values across different experimental conditions. The jackknife method is a statistical resampling methodology that leaves one taper out for each coherence estimate across tapers and trials. This creates a set of coherence estimates in which the variance of the coherence can be computed and tested for difference in means by using a non

parametric t-test (Thomson & Chave, 1991; Efron & Tibshirani, 1993; Pesaran et al, 2002).

ROC analysis

The behavior paradigm employed here was designed to test if attention-related processes modulate the intrinsic temporal activity of A1 as indexed by the LFP signal. As described in Figure 5.35 there are four possible outcomes in this paradigm. As explained in Chapter 4, it is possible to use the *receiver operator characteristic (ROC)* analysis to quantify the reliability of classifying the attentive or inattentive TT trial types (or attentive OT trial types) based on a neuronal signal such as the spike train or, in this particular case, the spectrogram of the LFP signal. A given ROC value is the probability by which, based on each frequency derived from the LFP spectrogram, an ideal observer can reliably classify a trial as being attended (rat licked the spout in the two tone trial to receive water) or not attended (rat did not lick the spout in the two tone trial to receive water). I also employed the ROC analysis to study whether, based on each frequency from the LFP spectrogram, an ideal observer can reliably classify if the rats will correctly lick in the two-tone trial (attentive TT condition) or incorrectly lick in the one-tone trial (attentive OT condition). The detailed description of the ROC analysis is illustrated in Chapter 4.

To validate the results of obtained from the ROC analysis between the LFP spectrogram of the attentive TT and inattentive TT (or attentive OT), I computed a control ROC that has an averaged 0.5 AUC value. In order to compute this control ROC I randomly shuffle each LFP trial along the entire LFP recording. Moreover, I switched these random LFP traces between attentive TT and inattentive OT. Then I computed the

LFP spectrogram of these random LFP traials. Finaly, I performed the ROC analysis to obtain a matrix of random AUC values that do not have any correlation between the LFP and the behavior. Therefore, this random AUC value has in average a value of 0.5. The same procedure was performed to the attentive TT and attentive OT trial types. Then, I tested if each AUC value computed for the experimental trials were statistically different from the AUC computed from the random LFP traces. I used a Wilcoxon signed rank test (non parametric paired t test) for each data point of the AUC matrix along the time axes.

5.3 Results

In order to study if attention-related processing modulates high frequency oscillations in A1 a two-tone discrimination paradigm was designed. Rats were trained to respond to two 10 kHz brief tones (20 ms duration) separated by 200 ms silence interval and ignore a single 10 kHz tone (20 ms duration). The target behavior was a protrusion of the rat's tongue within an 800 ms time interval after the second tone onset. This paradigm is depicted in Figure 5.35. In this chapter we will focus in the LFP signals, because it allows to test if the synchronous activity of A1 is related to processing of attention-related processes in A1, and to investigate if the intrinsic oscillations present in the auditory cortex is related to processing of temporal regularities and/or acoustic object formation.

Rats learned to discriminate between one and two-tone trial types after approximately 3 weeks of training. However, the rats made mistakes in approximately 25 % to 30 % of the two-tone trial types in which they did not lick the spout and therefore did not receive water. The same level of mistakes was made for the one tone trials. Rats licked the spout after hearing one tone in approximately 20 to 30 % of the trials. It is

important to note that, regardless of the trial type, they licked the spout in the expected reinforcement period. Moreover, the average lick response latency is 450 ms whether or not rats made a mistake (see Figure 4.23 and 4.24 of Chapter 4). I used this response pattern in order to test if the high frequency oscillations in A1 is modulated by rats attending to tones irrespectively of their physical acoustic attributes.

The MAEP is modulated by attention-related processes

In order to study the effects of attention-related processes and temporal cue processing on high frequency oscillations I recorded 57 LFP sites in the primary auditory cortex of 3 rats engaged in the two-tone discrimination task. Figure 5.36 shows the average MAEP of these LFP sites. The first observation to be noted is the very short latency to tones. There is a negative peak (N1) at 15 ms after the tone onset. The response pattern is highly consistent across channels and it has been described before as coming from the primary auditory cortex (Barth and Di, 1990, 1991; Di and Barth, 1992; Eggermont and Ponton, 2001).

The second observation is that there is a clear attentional modulation of the P2 component of the MAEP. The P2 reflects a second positive peak that occurs 35 ms to 80 ms after the tone onset response (arrows). This P2 component of the MAEP had a polarity change in the attentive trial types (arrows). By visually inspecting and comparing the individual LFP traces between attentive and inattentive TT trial types, I found that 58% of the LFP have a second negative peak located at the P2 component of the MAEP. I am calling this peak the N2 component of the MAEP. Similar number was found by comparing the attentive OT with the inattentive TT trial types (60% of the LFP sites). This reversal of polarity was found after the first and second tone onsets. Figure 5.36

shows the grand average of all LFP sites which clearly demonstrates attentional modulation within the P2. This analysis demonstrates attentional-related modulation of the MAEP. However, I did not detect attentional modulation at the N1 component of the MAEP. Figure 5.37 shows the amplitude quantification of the N1 response by taking the root mean square (RMS) from 5 ms to 20 ms after tone onset of the mean of each LFP site and comparing attentive TT, inattentive TT, and attentive OT trial types. I did not detected statistical differences in the N1 component among the different behavioral conditions during the first tone onset (ANOVA, $F_{(2,152)=0.03}$, p=0.9703), and neither during the second tone onset of the attended and unattended trial types (wilcoxon paired test, p=0.4011).

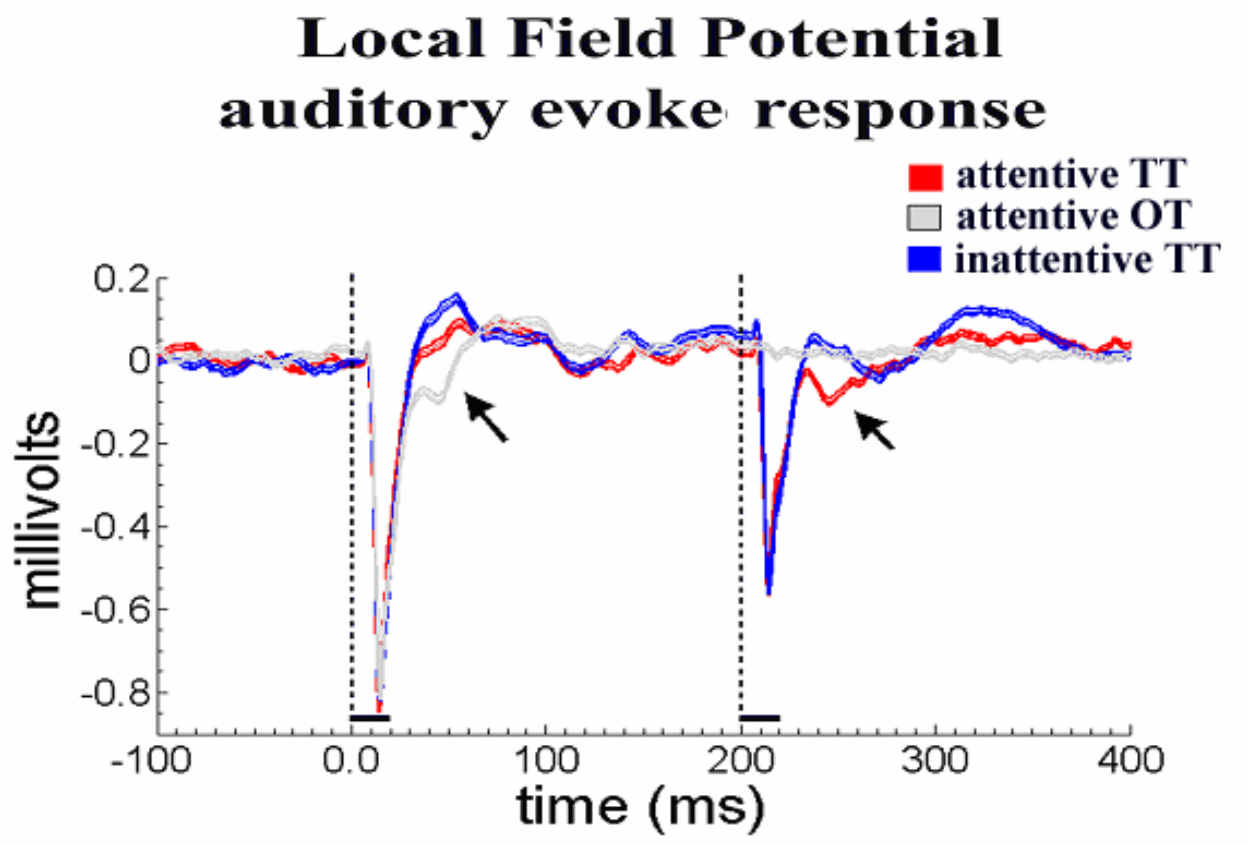

Figure 5.36. Attention-related processes modulate the N2 component of the MAEP. Averaged (thin line) ± SEM (thick line) of the LFP traces (57 LFP sites across 3 animals) of rats attending to two-tone trials (Attentive TT, red line), ignoring the second tone (Inattentive TT, blue line), or attending to one-tone trials (Attentive OT, gray line). Vertical dash lines are tone onset and thick horizontal bars are tone duration. Ordinate is in millivolts and abscissa is time in ms.

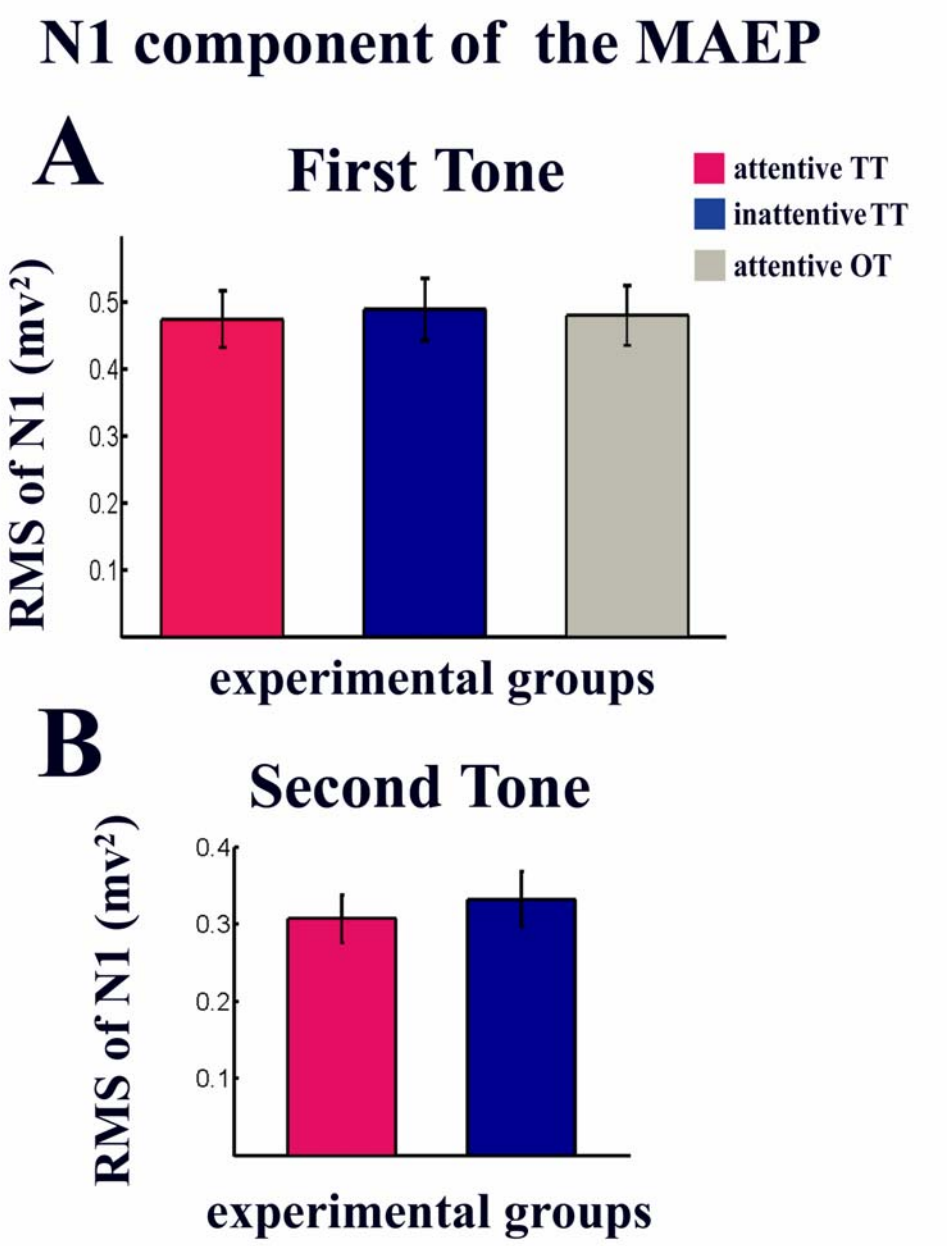

Figure 5.37. Attention-related processes do not the N1 component of the MAEP during first tone onset or the second tone onset. A) RMS of the N1 component during first tone onset. B) RMS of the N1 component during second tone onset (57 LFP sites across 3 animals, mean ± SEM).

There is no attention-related modulation of forward masking

Forward masking is defined as a attenuation of the neuronal response (spikes or LFP) to the second tone in relation to the neuronal response to the first tone in a two-tone sequence. Moreover, this response pattern is characteristic of A1 (Brosch & Schreiner, 1997, Wehr & Zador, 2005). One would think that this forward masking effect could be the main parameter that rats would use to attend to the second tone. Intuitively, one might think that a MAEP response to the second tone is a fundamental parameter used by the auditory cortex to indicate to high hierarchic areas that a goal-directed behavior should be implemented. After all, rats need to hear the second tone in order to accurately perform well in this two-tone discrimination task. Therefore, we should expect that in attentive TT trials there would be less forward masking than inattentive OT trial types. However, the averaged LFP traces shown in Figure 5.36 and 5.37 indicate that the outcome of the behavior is apparently independent of forward masking. These figures suggest that there are no differences in attentive and inattentive TT trials in relation to the forward masking. However, a visual inspection of the individual LFP traces showed that there is a great variability in the second tone responses. In some of the attentive TT and inattentive trials, there is a stronger MAEP response to the second tone than to the first one, while in other trials the opposite was true.

In order to further explorer if the forward masking effect was significantly different in attentive versus inattentive TT trials a ratio of the LFP N1 response of the second tone by the first tone was computed for each trial. This forward masking ratio (FMR) was averaged for each LFP site and statistical test was performed to compare attentive and inattentive trials. A higher forward masking ratio would indicate less

forward masking effect, and the prediction is that for the attentive TT trials there would be a higher ratio. Figure 5.38 shows an example of a LFP site in which this analysis was performed. Statistical differences in the forward masking ratio trials could not be detected in any of the LFP sites analyzed (Wilcoxon signed rank test, $p>0.01$) in a trial by trial basis between attentive and inattentive TT trials. Therefore, the null hypothesis that states that there are no differences in the FMR between these trial types could not be refuted. Thus, it appears that forward masking, based in the LFP measurements, is an intrinsic property of the primary auditory cortex that it is not different between attentive TT and inattentive TT trial types.

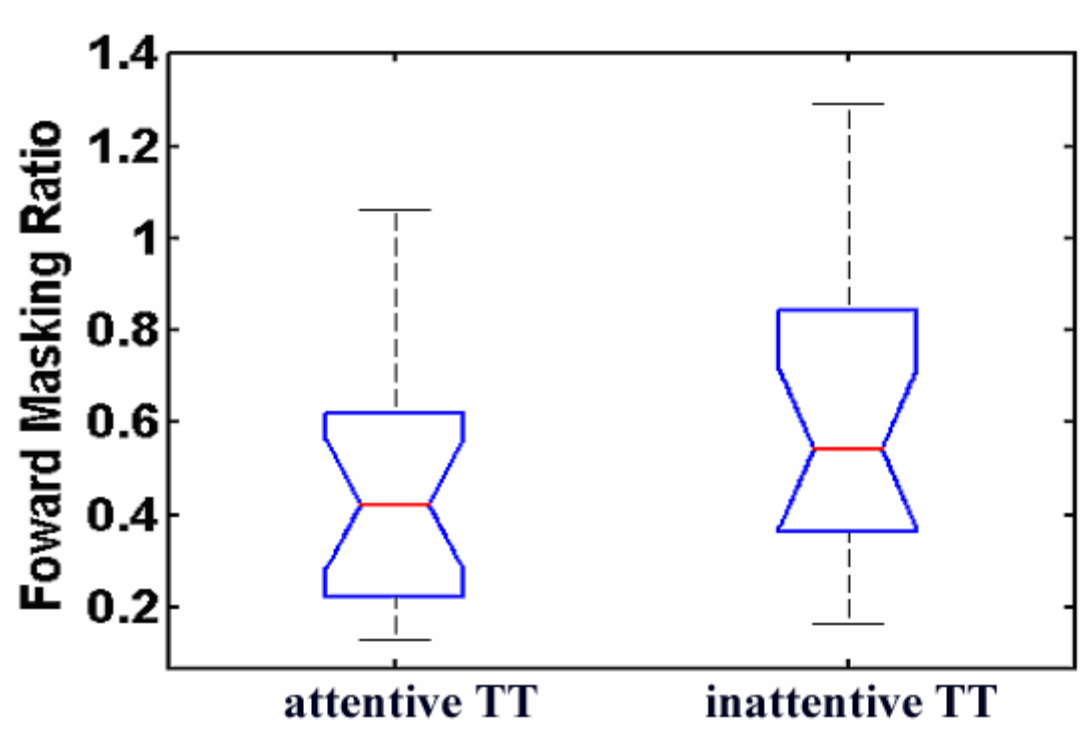

Figure 5.38. Forward masking is not modulated by attention-related processes . This figure shows a boxplot of a single LFP site example comparing the Forward Masking Ratio of the attentive and inattentive trials. Whiskers signalize the full data set extension, red line is the median, and the notch is the 95% confidence interval (paired t test, p = 0.1790).

The result showing that the MAEP is modulated by attention between 35-80 ms post tone onset was consistent to the results showed in Chapter 3. However, the presence of attention-related processes modulation at the N1 component of the MAEP is at odds with the results reported in this chapter. This suggests that the plasticity may play a role in the modulation of the N1 component by attention-related processes observed in Chapter 3. Moreover, in the Chapter 3, I showed that simple auditory stimuli induced high frequency oscillations, as measured by the normalized power spectrum of the LFP traces, and the increased power in these high frequency ranges are apparently modulated by active listening. Therefore, attention-related processes might play a strong role in the induction of high frequency oscillations as early as the primary auditory cortex. However, these results were obtained by comparing two groups (naïve versus trained rats) that had undergone two different experimental manipulations. As previously stated and now emphasized, the differential training schedules of these two experimental groups might be the main cause of increased high frequency oscillations in one of the groups. Perhaps, a larger neuronal population tuned to the 10 kHz tones might be the explanation of the increased power spectrum at high frequency ranges in rats of the active listening condition. The comparison between attentive and inattentive TT trials circumvents this problem because we are comparing the same neuronal population that underwent to the same training protocol.

Attending to the two-tone trials modulates high frequency oscillations

As a first analysis to determine if attention-related processes modulate the synchronous activity of A1, I used a band pass Butterworth filter at the LFP wide band. I selected the gamma range (40-70 Hz) and the high gamma range (90-150 Hz) of the wide

band LFP (1-170 Hz) for visual inspection. This analysis is displayed in Figure 5.39, which shows the wide band LFP signal from one channel in which the signal was filtered at gamma and high gamma frequencies in a single trial during attentive TT , inattentive TT and attentive OT conditions. This analysis shows that apparently there are no differences in the evoked response at gamma and high gamma frequency bands between these conditions. However, this was not the case for the induced gamma and high gamma frequency ranges. It appears that there were subtle differences in the inter-tone interval between attentive TT and inattentive TT trial types. For the high gamma frequencies, however, I detected induced bursts during the T1 interval and the T2 interval in the attentive TT, and somewhat surprisingly, in the attentive OT trial types as well.

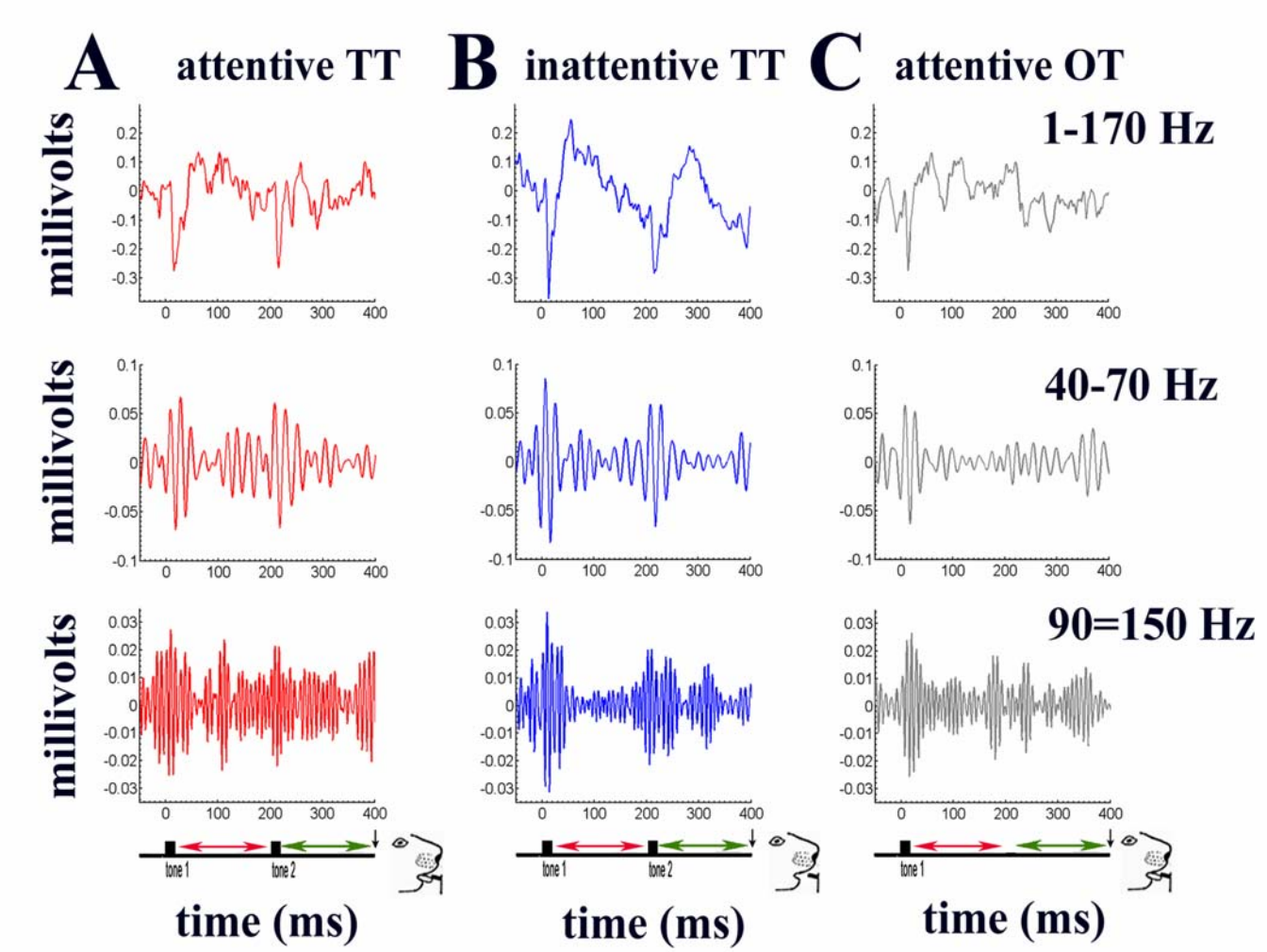

Figure 5.39. Correct performance at the two-tone discrimination task modulates high frequency oscillations in the auditory cortex. A) Column showing three LFP traces in single attended trial type. B) Column showing three LFP traces in a single unattended trial type. C) Column showing three LFP traces during the attended OT trial types. Top figure show the wide band LFP (1-170 Hz), the middle figure show the filtered LFP at gamma band (40-70 Hz), and the bottom figure show the filtered LFP at high gamma band (90-150 Hz). Below the LFP traces are shown a diagram of the attentive TT, inattentive TT and attentive OT conditions.

In order to further quantify if attention-related processes modulate high frequency oscillations in the auditory cortex the spectrogram of 57 LFP sites were computed during the three different trial type conditions. This analysis is shown in Figure 5.40. Apparently, there was not striking differences between attentive and inattentive trials. Overall, tones induced an increase in power mainly at low frequencies (<20 Hz) during 100-150 ms after the tone onset. Additionally,I noted an increase in power at high frequencies (>40 Hz, spectrogram on the right of the Figure 5.40) induced by the tones. However, this increase in power at low frequencies appears to be largely explained by the fast P1 and N1 components of the MAEP response. To further explore if any modulation of high frequency components of the LFP occurred in the trials in which rats attended to the two-tones, it was necessary to exclude this fast LFP component from subsequent analysis. The mean (SEM) normalized power spectrum density was computed for attentive TT , inattentive TT, and attentive OT trial types in order to further quantify any differences due to attention-related processes and/or temporal discrimination performed by the auditory cortex. Because, the spectrogram results suggested that the fast P1/N1 components of the MAEP might be skewing the power estimate. Therefore, I further explore whether high frequencies oscillations were differently modulated in the three experimental trials by computing the power spectrum at 30 ms to 200 ms after the tone onset for intervals between the two tones (T1 interval) and after the second tone (T2 interval). By choosing these intervals, the P1/N1 components of the LFP traces were excluded from the power spectrum density estimate. Thus, any differences in the spectrum among attentive TT, inattentive TT and attentive OT trials can not be attributed to P1/N1 components of the MAEP.

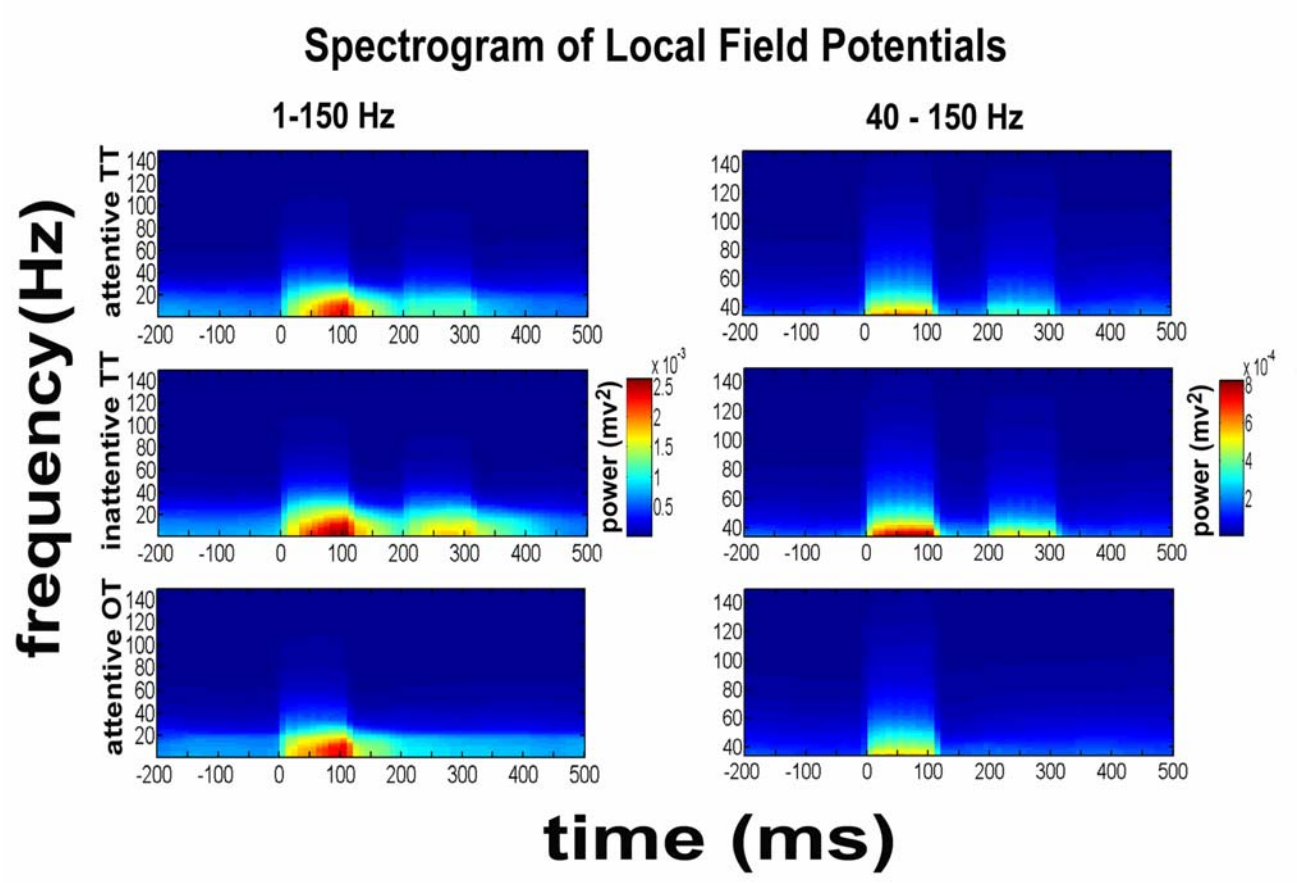

Figure 5.40. Spectrogram of the attentive TT, inattentive TT, and attentive OT trial types did not show striking differences among these conditions. The spectrogram on the left shows the full range (1-150 Hz) and the spectrogram on the right show frequencies ranging from 40-150 Hz. Ordinate is on frequency (Hz), abscissa is time (ms), and z-axes is coherence (color coded).

I compared the normalized power spectrum within the T2 interval in order to test the hypothesis that attention-related processes modulate the intrinsic synchronous activity of A1. During this interval rats already have the information, provided by the second tone, that a reward is coming. I controlled for general arousal and/or motor preparation to lick the spout as an explanation for the differences observed in the power spectrum, by comparing the T2 interval of the attentive TT and attentive OT. Figure 5.41 shows the result of these comparisons. The modulation of the frequency components of the LFP power spectrum has a similar pattern in the T2 interval whenever rats respond to tones. Figure 5.41 shows the normalized power spectrum analysis performed during 30 ms to 200 ms after the second tone onset for attentive TT (red), inattentive TT (blue) and attentive OT (gray) trial types. Statistical comparison among alpha/beta (1-30 Hz), gamma (40-70 Hz) and high gamma (90-150 Hz) frequency bands of the attentive TT trial types shows that the highest increase in normalized power was in the high frequency band (ANOVA, $F_{(2,146)=83.52}$, $p<0.001$; followed by a pot-hoc Scheffe test, $p<0.05$). For the attentive OT trial types there was a high increase in power between gamma and high gamma frequencies in comparison with low frequency ranges, but no differences between gamma and high gamma frequency bands (highest increase in normalized power was in the high gamma frequency band (ANOVA, $F_{(2,146)=77.54}$, $p<0.001$; followed by a post-hoc Scheffe test at 0.05). In the inattentive TT trial types there are no statistical differences among these frequency bands ((ANOVA, $F_{(2,146)=0.39}$, $p=0.6771$).

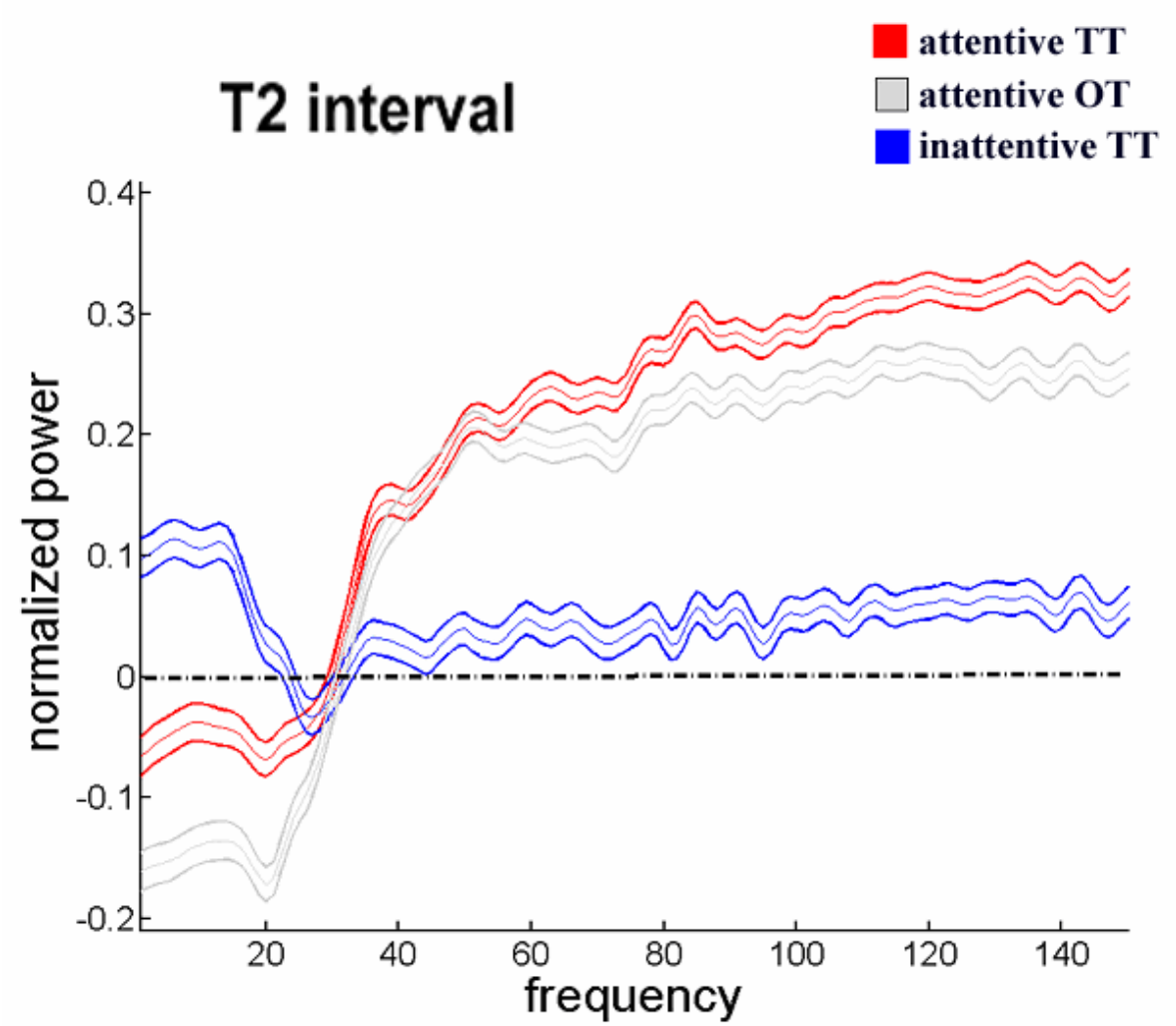

Figure 5.41. The normalized power spectrum reveals that the different frequency bands are modulated by attending one or two-tone trial types. This figure shows the normalized spectrum of attentive TT (red line), inattentive TT (blue line) and attentive OT(gray line) trials averaged across LFP sites (57 sites) during T2 interval. Ordinate is normalized power spectrum (mv^2), abscissa is frequency (Hz). The thin line is the mean and the thick line is SEM.

I compared frequency bands of the normalized power spectrum among the experimental trial types in order to explore whether correctly performing the discrimination task differently modulates alpha/beta, gamma, or high gamma frequencies. Figure 5.42 shows the statistical comparison among experimental trial types in the alpha/beta, gamma, and high gamma frequency bands. There was a decrease in amplitude of low frequency range (1-30 Hz) in the attentive TT and attentive OT as compared to the inattentive TT trial types. The highest increase in power at these frequencies was in inattentive TT followed by attentive TT and attentive OT trial types (ANOVA, $F_{(2,146)=15.82}$, $p<0.001$; followed by a pot-hoc Scheffe test, $p<0.05$). The statistical comparison at the gamma range revealed a different picture. There were significant differences among the attentive TT, inattentive TT, and attentive OT trial types in the gamma frequency range (ANOVA, $F_{(2,146)=28.8}$, $p<0.001$). However those differences were between attentive TT and inattentive TT, and also between attentive OT and inattentive TT, but not between attentive TT and attentive OT (ANOVA, $F_{(2,146)=28.8}$, $p<0.001$;, followed by Scheffe post hoc test, $p<0.05$) (see Figure 5.40). The comparison at high gamma range (90-150 Hz) showed that the highest increase in high gamma was in the attentive TT trials, followed by attentive OT trials and inattentive TT trial types (ANOVA, $F_{(2,146)=38.61}$, $p<0.001$; followed by Scheffe post hoc test, $p<0.05$). Thus there was a significant difference between attentive TT and attentive OT trial types in high gamma frequency bands and low frequency bands, but not at gamma frequency bands (see Figure 5.42).

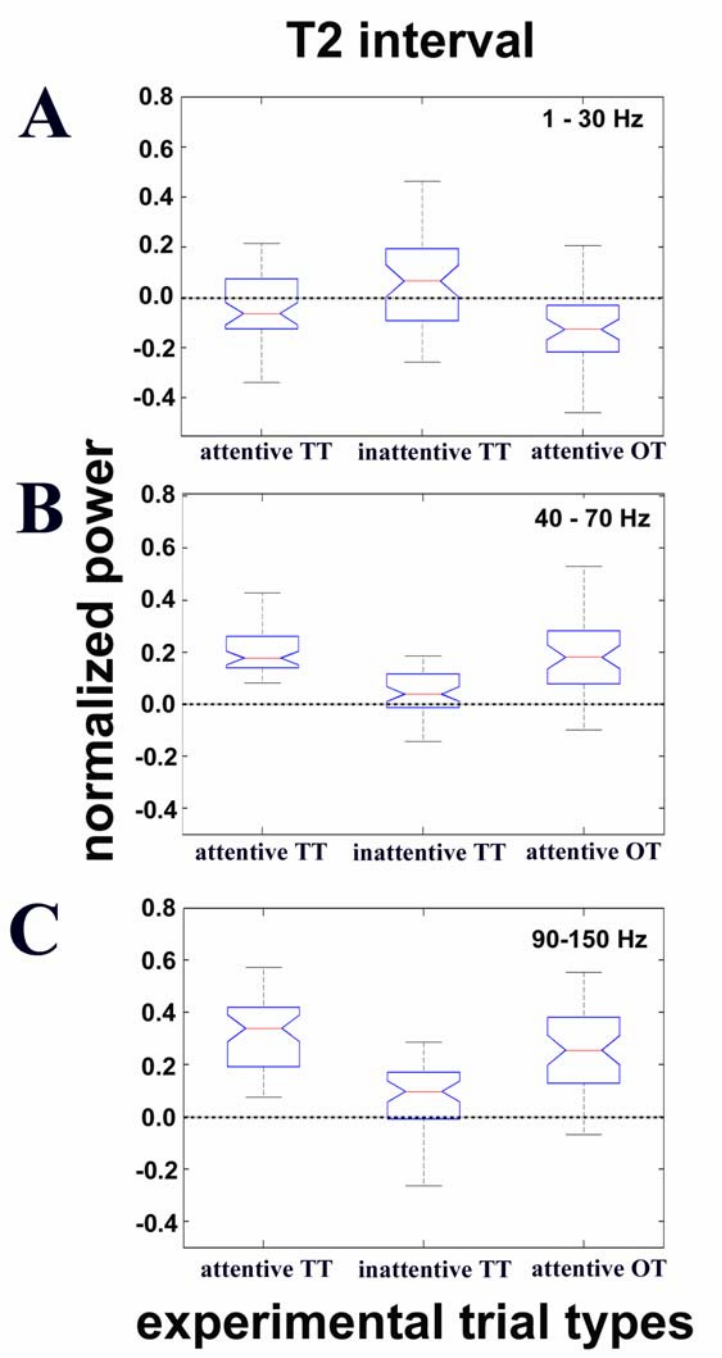

Figure 5.42. Attention-related processes differentaly modulate the different frequency bands in A1 during T2 interval. A) Box plot comparing the 1-30 Hz frequency range of attentive TT, inattentive TT, and attentive OT. B) Box plot comparing the 40-70 Hz frequency range of these experimental conditions. C) Box plot comparing the 90-150 Hz frequency range of these experimental conditions. Whiskers indicate the full data set extension, red line is the median, and the notch is the 95% confidence interval.

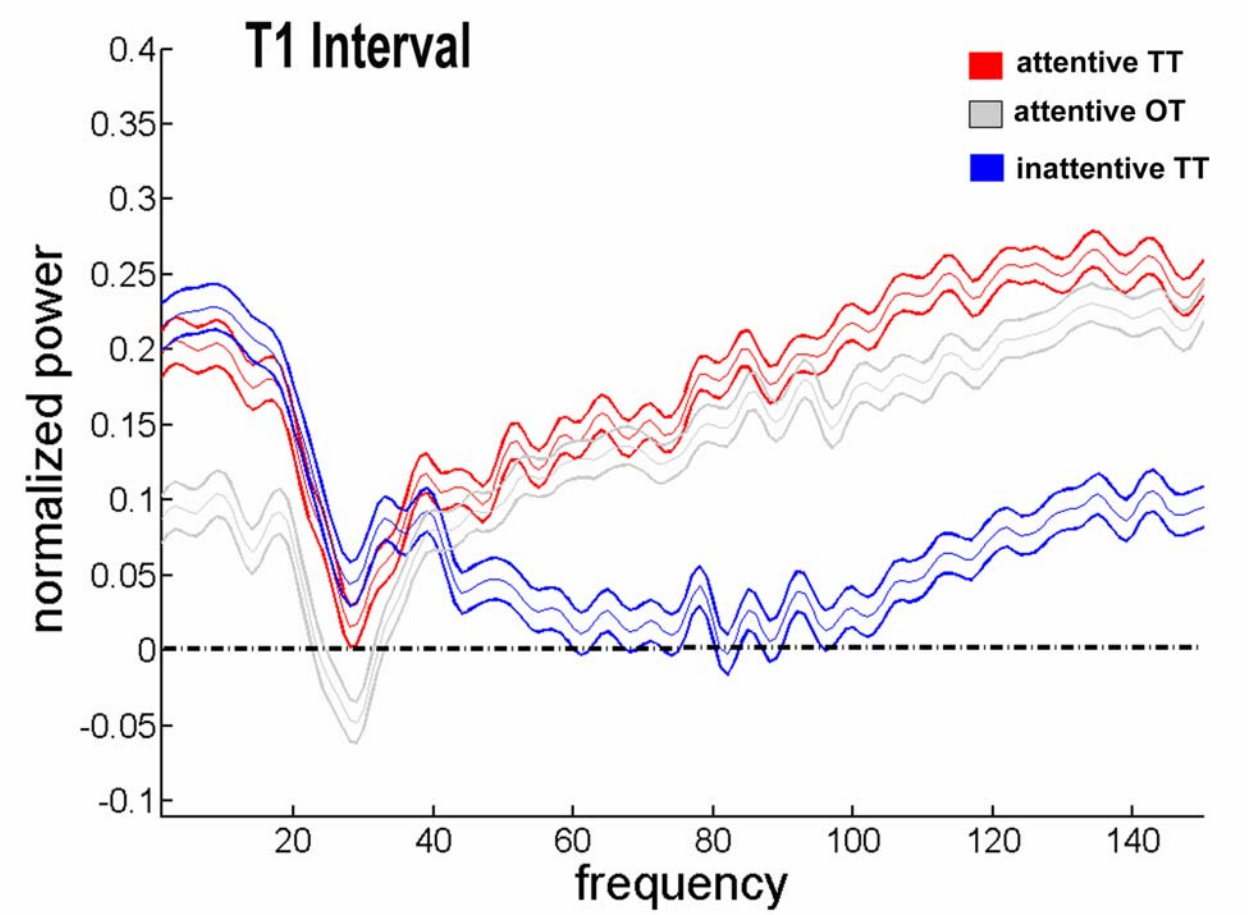

Figure 5.43. Attention-related processes modulate A1 synchronous activity during the inter-tone interval. This figure shows the normalized spectrum of attended (red line), unattended (blue line), and attended OT trial types averaged across LFP sites (57 sites) during T1 interval. Ordinate is normalized power spectrum (mv^2) and abscissa is frequency (Hz). Thin line is the PSD mean and thick line is SEM.

Figure 5.43 shows the results of the averaged (57 LFP sites) normalized spectrum for attentive and inattentive TT trials during 30 ms to 200 ms after the first tone onset. Within-comparison across frequencies in the attentive TT trials reveals that the highest increase in normalized power was at high frequencies (90 – 150 Hz), followed by alpha/beta and gamma range frequencies (ANOVA, $F_{(2,146)=14.43}$, $p<0.001$); followed by a pot-hoc Scheffe test, $p<0.05$) for the attentive TT trial types. The same pattern was also observed for the attentive OT trial types ((ANOVA, $F_{(2,146)=15.49}$, $p<0.001$; followed by a post-hoc Scheffe test, $p<0.05$). Within-comparison of the normalized frequency power during inattentie TT trial types shows that, differently from attentive TT or attentive OT trial types, the highest increase in power was in the low frequency ranges, followed by gamma and high gamma frequency ranges ((ANOVA, $F_{(2,146)=8.03}$, $p=0.0005$; followed by a post-hoc Scheffe test, $p<0.05$). Similar to the T2 interval, I also compared the three experimental trial types during alpha/beta, gamma, and high gamma frequency bands. This analysis is shown at Figure 5.44. Within the T1 interval the distribution of power at low frequency ranges was statistically different among the experimental groups. There were less power at the low frequency ranges for the attentive OT trials as compared to the attentive and inattentive TT trial types (ANOVA, $F_{(2,146)=7.37}$, $p=0.0009$; followed by a post-hoc Scheffe test, $p<0.05$).

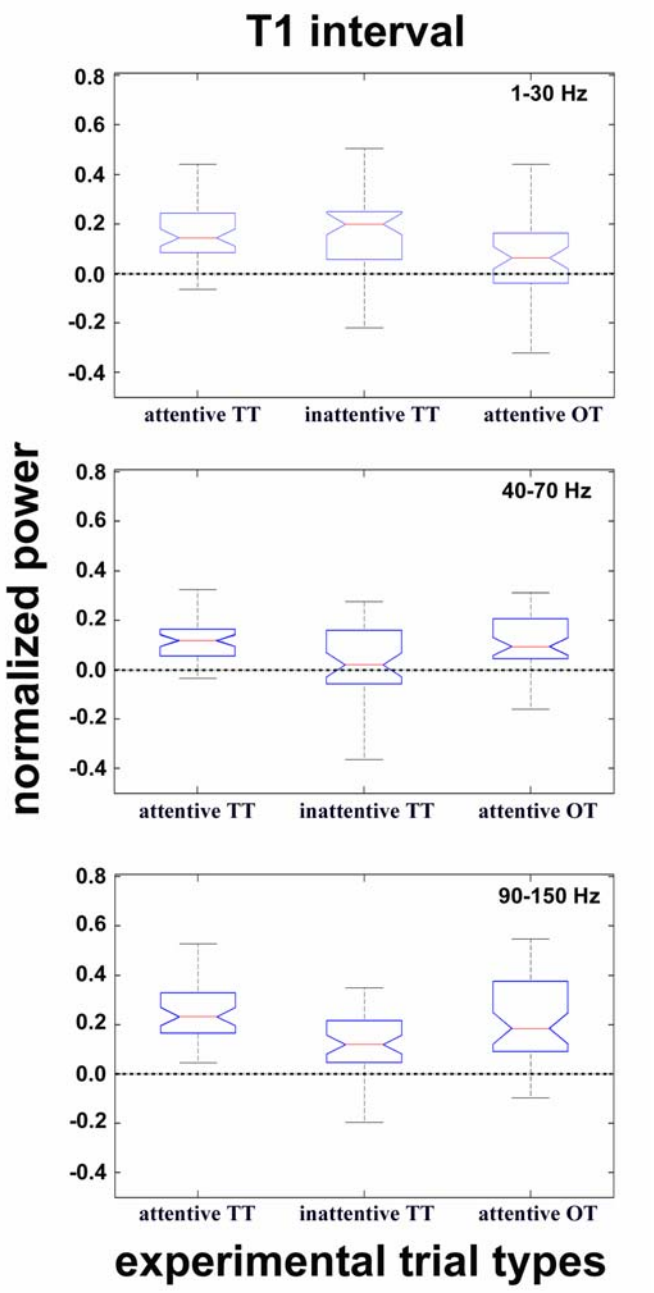

Figure 5.44. Different internal states differently modulate frequency bands in the primary auditory cortex during the T1 interval. A) Box plot comparing the 1-30 Hz frequency range of the attentive TT, inattentive TT, and attentive OT. B) Box plot comparing the 40-70 Hz frequency range among these experimental groups. C) Box plot comparing the 90-150 Hz frequency range of these experimental groups . Whiskers indicate the full data set extension, red line is the median, and the notch is the 95% confidence interval.

The results from the previous analysis show that paying attention to an upcoming relevant event modulates high and low frequency components of the LFP signal. Prior to the licking behavior, but after the second tone onset, there was a reduction in power at low frequency components and a concomitant increase in power at high frequency components. During the inter-tone interval, there was also an increase in power of the high frequency components of the LFP, however, unlike the T2 interval, there was also an increase in power of the low frequency components of the LFP signal. Thus, there is a differential distribution of normalized power during both the T1 and T2 interval. Although there is more power at high frequencies during trials in which rats are attentive to the second tone during both T1 and T2 time intervals, the same consistency does not occur for the power at low frequency ranges.

High-frequency bands are a reliable predictor to classify the behavior outcome.

The attentive and inattentive trials (or the attentive and attentive OT trials) can be thought of as two categories in a two-alternative forced task. As described in Chapter 4, it is possible to compute ROC curves in order to investigate whether an ideal observer can reliably classify a given behavioral outcome (to lick or not lick the two-tone trial; or, to lick to a one-tone trial or to lick to a two-tone trial) by using a neuronal signal as a parameter. If the power at different frequencies is a good parameter, then an ideal observer should be able to judge if rats will or will not lick the spout to receive water by measuring the LFP spectrogram. Thus, I calculated the LFP spectrogram (using 100 ms windows) of each trial for both attentive and inattentive trial types, which results in a time-frequency matrix showing the power of each frequency of the decomposed LFP along time. Then, for each element of these matrices the ROC analysis contrasting the

attentive and inattentive trials was computed. I utilized the area under each ROC curve (AUC) in order to quantify the reliability of different frequencies in classifying the attentive TT (correct trials category) and inattentive TT (incorrect trials category) categories. The AUC value is the probability with which, based on power of a given frequency, an ideal observer can reliably classify the trials as belonging to the attentive TT trials (correct trials) or inattentive TT trials (incorrect trials) category. A value of 0.5 indicates that the power of a given frequency at a particular time has an equal probability to be elicited in the attentive and inattentive trials. Values tending to 1.0 indicate that the high power at this frequency can be reliably utilized to classify the trials as being corrected trials, whereas the high power responses for the incorrect trials will have a value tending to 0.0. Additionally, I tested the hypothesis that experimental AUC matrix and the control AUC matrix are significantly different by computing the Wilcoxon signed rank test for each data point of the AUC matrix. There are 20 spectrogram matrixes for each attentive and inattentive trials along the time axes. These matrices were utilized to calculate the AUC. Figure 5.45, shows the results of these analyses.

The results of the ROC analysis confirmed the previous analysis depicted in figures 5.41 and 5.43. There was more power at high frequency ranges than low frequency ranges in trials where rats made a correct two-tone discrimination response. Moreover, there was a tight association between high frequency power and behavioral performance. Moreover, even before the two-tone task, the ROC revealed that there was more power at high frequencies that was associated with correct behavioral performance. This result is surprising, since the inter-tone interval presentation is randomly varied, thus, minimizing anticipation of trial types.

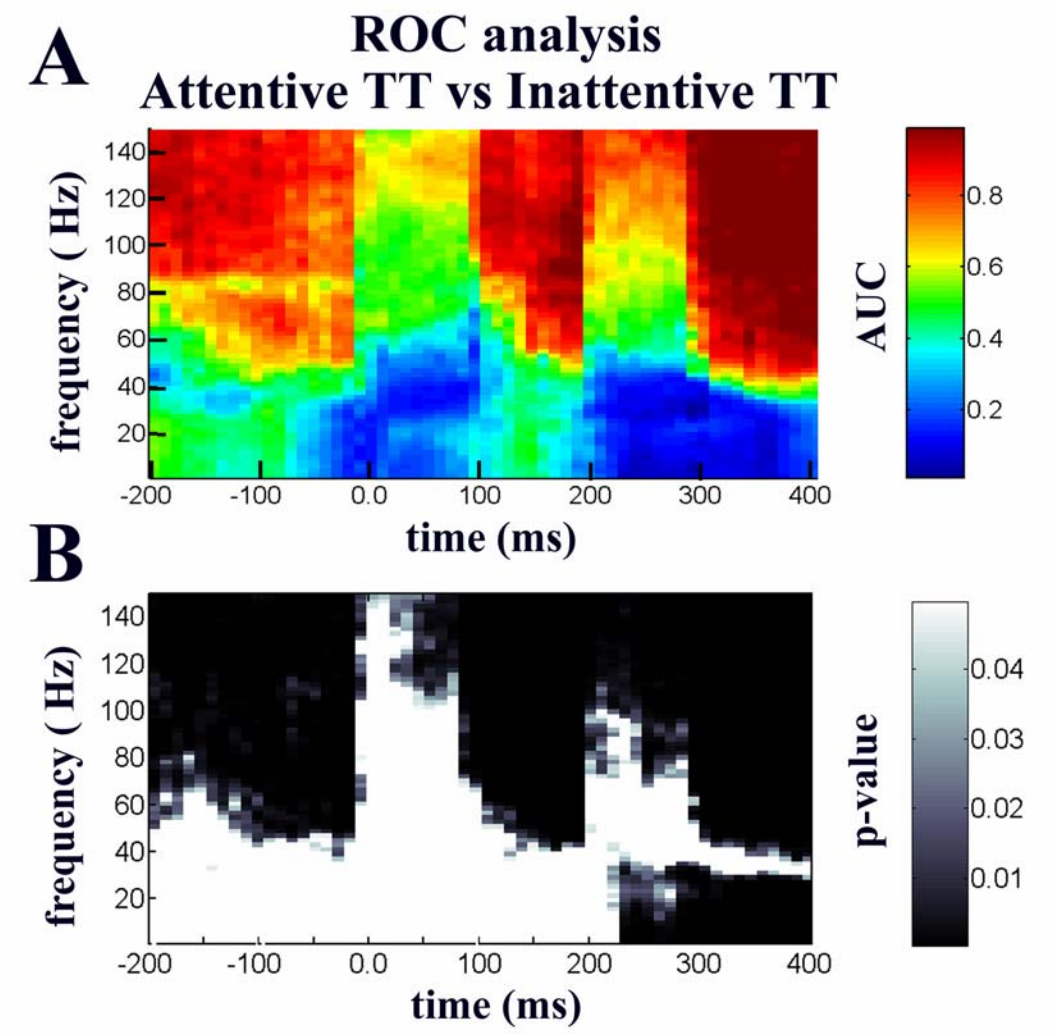

Figure 5.45. A ideal observed is able to categorize behavioral outcomes base on high frequency oscillations. A) This figure shows the AUC values obtained by comparing the power at various frequencies over time between attentive and inattentive TT trial types. Dark red indicates AUC values towards 1, which reflects a high probability that the increase in power is coming from attentive trials, conversely, dark blue indicates AUC values toward 0, which indicates the high probability that an increase in power is coming from inattentive trials. Green colors indicate a 0.5 value in which an increase in power has an equal probability to come from attentive or inattentive trial types. B) This figure shows the statistical comparison (only p-values<0.05; non-parametric t test) between the experimental AUC and the random AUC. The p-value is shown by a gray scale in the z-axes. A low p-value has a darker pixel than a high p-value.

In order to explore if the increase in power of high frequency ranges is also predictive of correctly engaging in the two-tone trials as opposed to being associated with a general increase in arousal, I contrasted the ROC measurements between attentive TT and attentive OT trial types. This analysis is displayed in Figure 5.46. This figure shows that the increase in power at high frequency ranges is also pronounced in attentive TT as opposed to attentive OT trials. However, this effect is restricted at gamma frequency ranges in the interval between tones and at high gamma frequency ranges after the second tone onset. Moreover, the increase in power at low frequency ranges was also predictive of a correct behavioral outcome. The increase in AUC values towards 1.0 during the second tone onset (200 ms) is an internal control which validates this method as very useful to classify the trial types using the spectrogram as a parameter.

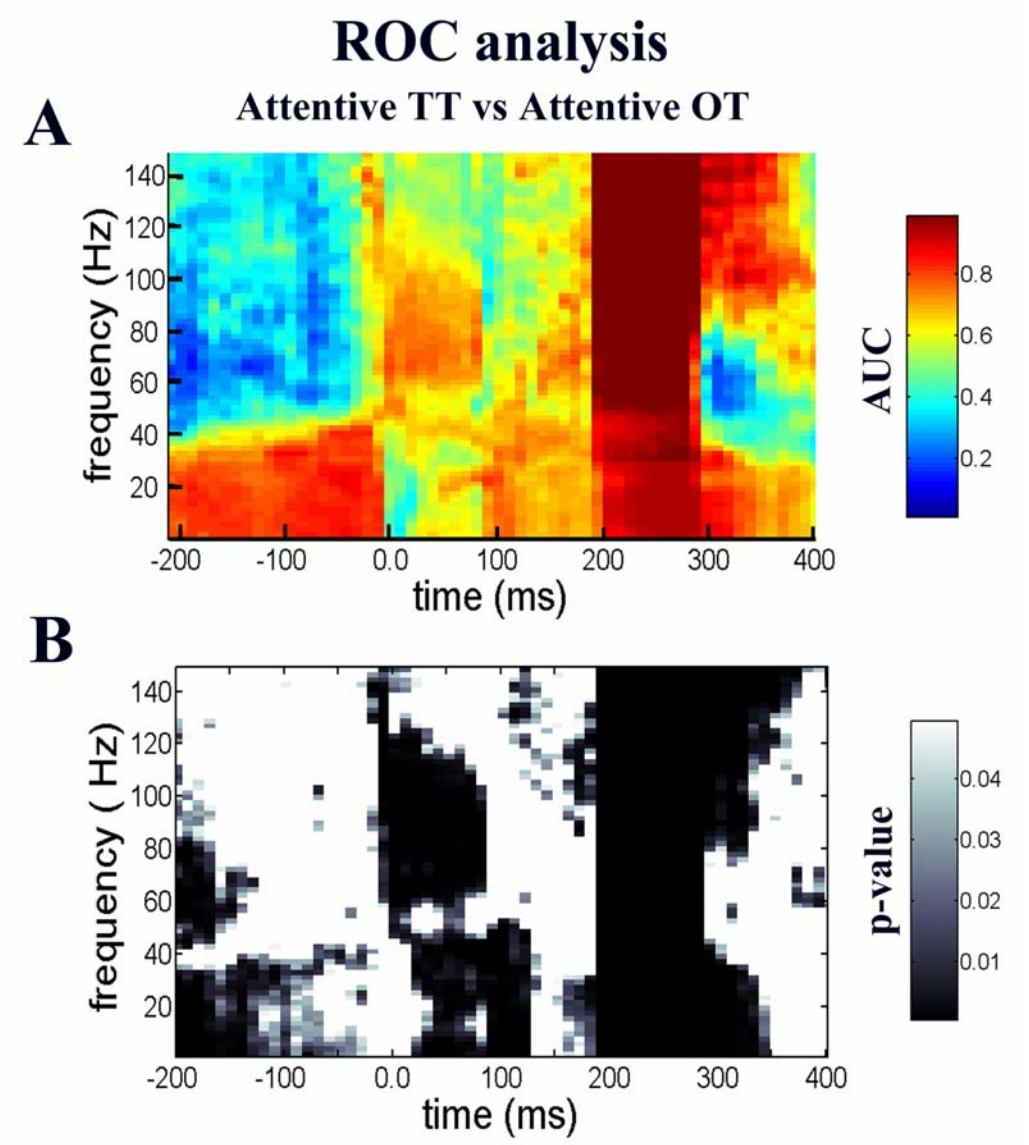

Figure 5.46 ROC analysis of the spectrogram of attentive TT vs attentive OT trial types shows that high frequency bands predict correct behavior. A) This figure shows the AUC values obtained by comparing the power at various frequencies over time between attentive TT and attentive OT trial types. Dark red indicates AUC values towards 1, which reflects a high probability that the increase in power is coming from attentive trials, conversely, dark blue indicates AUC values toward 0, which indicates the high probability that an increase in power is coming from attentive OT trials. Green colors indicate a 0.5 value in which an increase in power has an equal probability to come from attentive TT or attentive OT trial types. B) This figure shows the p-value (only p-values lower than 0.05) obtained by computing a non-parametric paired t test to compare the experimental AUC value from random AUC value . The p-value is shown by a gray scale in the z-axes. A low p-value has a darker pixel than a high p-value.

Attention-related processes modulate the global coherence of A1.

I test the hypothesis that attention-related processes modulate the synchrony among the LFP sites. I directly measured the coherence spectrum across the LFP sites in the attentive and inattentive TT trial types to test this hypothesis. While the power spectrum measures the synchrony of the synaptic activity around the electrode tip, the coherence spectrum measures the synchrony among the synaptic activity across several LFP sites.

The normalized power spectrum results demonstrated that attending to the second tone in the two-tone discriminated sequence enhances high frequency power. This result is consistent with the results from Chapter 3 which compared animals actively listening to tones to animals passively listening to tones. Moreover, the results in this chapter strongly suggested that the increase in power at high frequency components of the LFP cannot be explained only by-product of topographical changes caused by plasticity. Additionally, the results of chapter 3 suggested that the neuronal populations in A1 synchronize their activity across distances as large as 1,0 mm^2 during active listening. However, this result could also be explained by a tonotopic rearrangement in which there is a larger area of A1 representing the 10 kHz tones to which the conditioning occurred. In the following paragraphs I will focus on comparing the LFP coherence between attentive and inattentive TT trial types.

The Figure 5.47 shows that the discrimination of two tones changes the coherence among the LFP sites. The baseline coherence spectrogram among the LFP sites in the inattentive TT trial types was high at frequencies below 60 Hz. The baseline coherence spectrogram during the attentive TT trial types appears to be a little higher than the

coherence spectrogram at the inattentive TT trials (compare top and bottom Figure 5.47A). The difference between the baseline coherence spectrogram of the attentive and inattentive TT trials did not appear to be as big as the difference between the passive listening and active listening experimental groups of Chapter 3. This result suggests that plastic changes in A1 caused by training contingences have an effect in the synchronous activity of A1. However, a direct testing of this hypothesis will require chronic recordings throughout training schedules. Regardless of the effect of training and plasticity in A1, the comparison between attentive and inattentive trial types allowed us to test the hypothesis that attention-related processes dynamically change the synchrony of the neuronal population of A1.

The coherence spectrogram analysis showed in Figure 5.47A strongly suggests that attending to the second tone in the two-tone discrimination task modulates the LFP synchrony of A1. I further measured the coherence during the T1 (30 ms to 200 ms after the first tone onset) and T2 (30 ms to 200 ms post second tone onset) interval by computing the averaged LFP coherence along with its 95% interval confidence. Moreover, I used a non-parametric Arvesen's Jackknife U statistical t test to test the null hypothesis that the spectral coherence during T1 or T2 is not different between attentive and inattentive trial types. I found significant differences for frequencies between 25 to 50 Hz and between 80 to 100 Hz during T1 (Jackknife U statistical t test, $p<0.01$; see Figure 5.47B top). Additionally, I found significant differences during time T2 between attentive and inattentive trial types. There was high coherence at low frequency ranges for inattentive trials while the opposite was true for high frequency ranges (Jackknife U statistical t test, $p<0.01$).

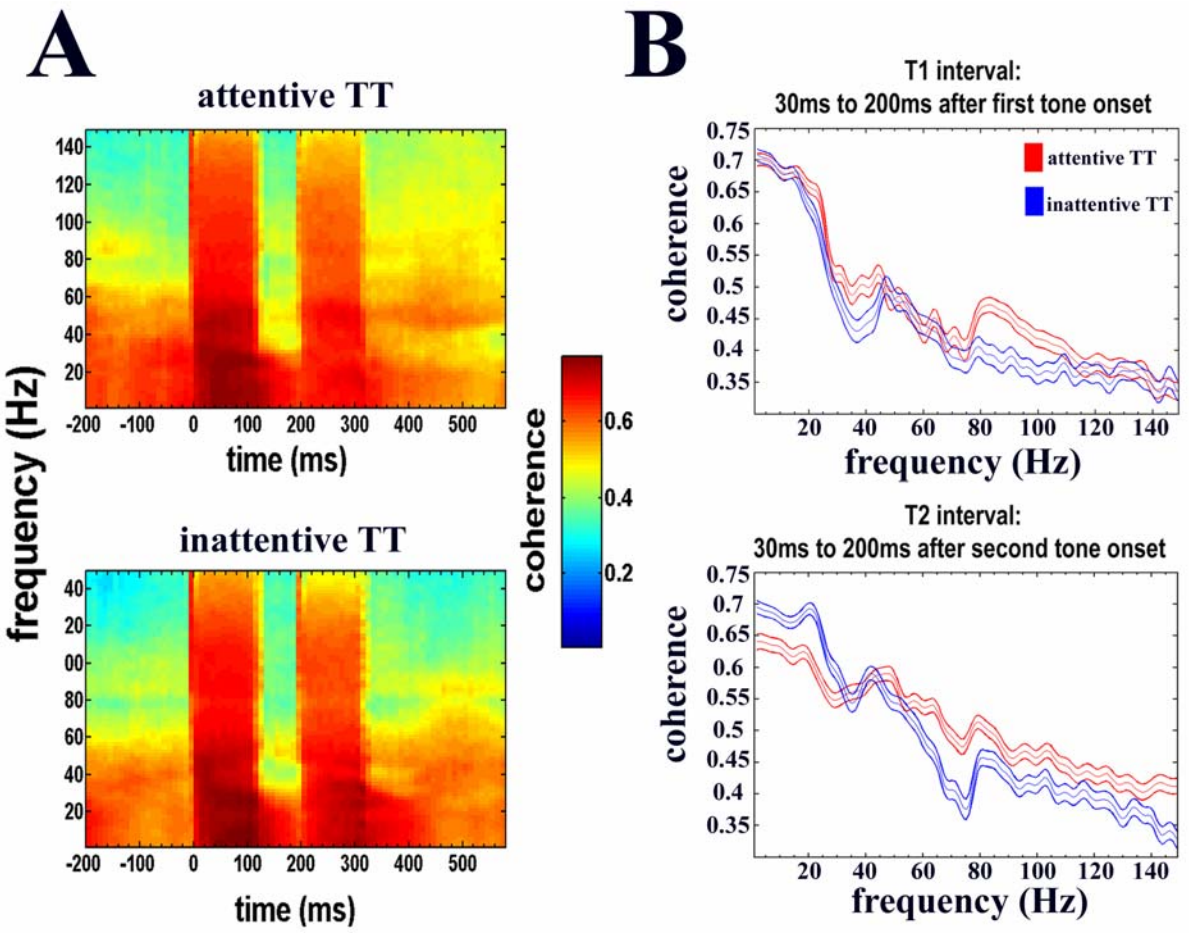

Figure 5.47. Attention-related processes modulate the coherence among LFP sites. A) Top graph shows the coherence spectrogram during attentive trial types. Bottom graph shows the coherence spectrogram during inattentive trial types (The ordinate is frequency (Hz), abscissa is time (ms) and the z-axes is color-coded coherence. B) Top graph shows the mean coherence plot (thin line) plus its 95% confidence interval (thick line) from a 30ms to 200 ms time period. Bottom graph shows the mean and the 95% confidence interval during the T2 interval (230 ms to 400 ms). Red line = attentive trial types; Blue line = inattentive trial types. The ordinate is coherence and the abscissa is frequency (Hz), (n=3 rats; 57 LFP sites; 200 pair combinations).

Attention-related processes modulate the local coherence of A1.

Similar to the comparison of the coherence among LFP sites between attentive and inattentive trial types, I also compared the MUA - LFP coherence between attentive and inattentive trial types. In Chapter 3, I described that there are different temporal dynamics among the neuronal population in the auditory cortex of animals actively perceiving tones compared to animals passively listening to tones. Moreover, this change in intrinsic temporal dynamics of the auditory cortex occurs not only at a global level, but also at a local level. This is because there was significant difference among LFP site coherence as well as between MUA-LFP coherence. Additionally, these significant differences occurred in particular frequencies, particularly at beta (20 Hz peak) and low gamma frequency ranges (40-70 Hz). However, these differences could be entirely explained by plastic changes imposed by training contingencies. This is because it is well documented that training modifies topographic representation of the relevant acoustic feature (Merzenich et al., 1990). Training also modifies receptive field properties of A1 neurons (Fritz et al., 2003; 2005; 2007). Therefore, I compared the MUA-LFP coherence to test the hypothesis that attention demands modulate local synchrony in the auditory cortex.

Local clusters of neuronal networks in the auditory cortex are modulated by attention-related processes that are necessary for correctly perform the two-tone discrimination task. Moreover, these attentional modulations of synchrony are more pronounced during the time periods (T2 interval) in which rats have to decide whether to lick the spout to receive water. However, I did not detected modulation of the local neuronal network coherence in A1 by attentional-related processes during the T1 interval. According to the

temporal binding hypothesis the synchronous activity of A1 in the gamma frequency bands would anticipate the second tone. Figure 5.58 show the results of the spike train and LFP coherence analysis. Figure 5.48A shows the MUA-LFP coherence spectrogram which plots the coherence in windows of 125 ms over 10 ms steps throughout the duration of the trial session. This analysis shows that the first tone evokes a high degree of synchronization as revealed by the increase in coherence between the spike train and the LFP signal. Importantly, attention does not modulate the MUA-LFP coherence during the tone onset. Moreover, there is a decrease in MUA-LFP coherence during the second tone onset for attentive and inattentive trial types as compared to the first tone onset. This effect is not surprising given that there is a forward masking effect in which the second tone evoked less activity in A1. The coherence spectrogram also suggests that there are attention modulations during the intervals between tones (T1 interval) and the interval after the second tone onset (T2 interval). I further quantify the MUA-LFP coherence by computing the 95% confidence interval during T1 and T2 intervals. Figure 5.48B shows that the MUA-LFP coherence at high frequency ranges is modulated by attention during the T2 interval, but not during the T1 interval. Differences between attentive and inattentive trial types were not detected in the MUA-LFP coherence during the T1 interval, except at low frequency ranges (< 20 Hz; Jackknife U statistical t test, $p<0.01$). During the T2 interval, the MUA-LFP coherence is statistically different between attentive and inattentive trials only at gamma frequency ranges (40-70 Hz; Jackknife U statistical t test, $p<0.01$), but not at high gamma or low frequency ranges (alpha/beta; 1-30 Hz).

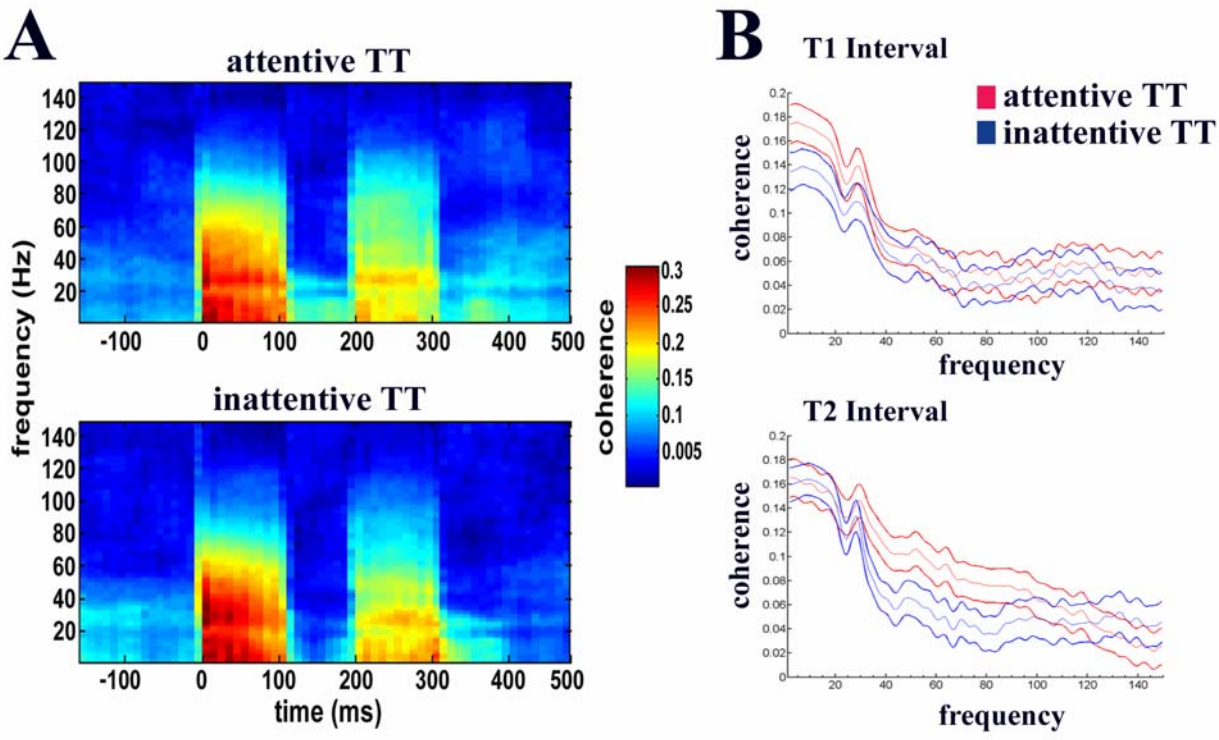

Figure 5.48. Attending to the two-tone discrimination task modulates local neuronal networks at gamma range. A) Top graph shows the MUA-LFP coherence spectrogram during attentive trial types. Bottom graph shows the MUA-LFP coherence spectrogram during inattentive trial types (The ordinate is frequency (Hz), abscissa is time (ms) and the z-axes is color-coded MUA-LFP coherence. B) Top graph shows the mean coherence plot (thin line) plus its 95% confidence intervals (thick line) from the T1 (20 ms to 200 ms) time period. Bottom graph shows the mean and the 95% confidence interval during the T2 interval (220 ms to 400 ms). Red line = attentive trial types; Blue line = inattentive trial types. The ordinate is coherence and the abscissa is frequency (Hz), (n=3 rats; 57 LFP sites; 200 pair combinations).

5.4 Discussion

General findings

The results presented in this chapter complemented and extended previous studies exploring the role of high frequency oscillations in the auditory cortex of experimental animals (Barth & MacDonald, 1996; Brosch et al., 2002; Steinschneider et al., 2008; Medvedev & Kenwal, 2008).This previous studies showed that sensory stimuli induced high frequency oscillation in the auditory cortex. Therefore, suggesting that these high frequencies might be a neuronal mechanism for sensory processing. I reasoned that if that was true, then high frequency oscillations would be modulated in the auditory cortex of rats reporting that they heard a sound.

In this chapter I tested the hypothesis that attention-related processes modulate neuronal synchrony of the auditory cortex. I was able to show that the normalized power spectrum of the LFP was differentialy modulated in trials that rats attended to relevant sensory events. Moreover, in the T2 time interval, an ideal observer can use the high gamma frequency band as a good parameter to reliably predict the correct performance of the rats. Because the LFP is caused by a synchronous synaptic activity of hundreds of neurons around the electrode tip (Nicholson & Llinas, 1974; Mizdorf, 1985; Logothetis, 2002; Katzner et al., 2009), the results presented in this chapter demonstrate that attention-related processes strongly modulate neuronal synchrony in the auditory cortex.

I compared the power spectrum in the inter-tone intervals during trials that rats either attended to or ignored two tones, and trials in which rats attended to a single tone. In the two-tone trials, the A1 activity during the inter-tone interval was modulated by the anticipation of a future acoustic event (see Chapter 4), which will signals reward.

Identification of two-tones was essential to correctly achieve good performance and receive water. There was a higher high frequency power during the two-tone trials in which rats attended to the second tone compared to trials in which rats ignored the task. This result suggested that oscillations at high frequency bands could underlie temporal binding of acoustic events into a coherent percept. In order to further explore this possibility, I compared the power spectrum of attentive TT trials with the attentive OT trial types in order to control for the alternative explanation that these high frequency oscillations were related with a vigilant state per se. This was because in these trials, rats are in a vigilant state, but were not engage in discriminating two tones from one tone.Thus, their auditory system were not processing the time between tones.

Attention-related modulation of MAEP components

The results presented in this chapter, demonstrate that the N1 component of the MAEP, is not modulated by attention-related processes. The N1 component is a consequence of a feedforward volley of activation coming from the activity of thalamic neurons that project to stellate cells within layers IV-II/III (Mizdorf, 1985; Steinschneider et al., 1992; Sukov & Barth, 1998, 2001). Therefore, it is reliably transferring sensory information from sub-cortical centers of auditory processing. However, while the N1 component of the MAEP is not modulated by attention, the P2 component is clearly modulated by attention-related processes.

Several studies of auditory and visual spatial selective attention have used EEG or MEG event-related potentials in human subjects to identify neural mechanisms of attention. These studies identified a early attention modulation of the N1 (N1m) and P1 (P1m) components of these macro-signals that are probably originated in extra-striate

areas(reviewed in Hermman & Knight, 2001; Alho-Vento et al., 2004). Others researchers have claimed that an even earlier component (20-50 ms) of these macro-signals (P20-P50) is modulated by auditory spatial attention (Woldorff et al., 1993) and by cross-modal attention (Poghosyan & Ioannides, 2008), thus suggesting that attention modulates neuronal activity at the primary cortices (Woldorff et al., 1993; Poghosyan & Ioannides, 2008). However, the poor spatial resolution of these macro-signals precluded firm conclusion that attention modulates early auditory processing.

In this chapter, I extended these previous observations by showing that attention modulates the P2 component (30-60 ms) of A1. However, since the vMGB projections also project to anterior and posterior auditory fields (Roullier, 1996; Winer, 1999), and that A1 is highly inter-connected to adjacent cortical secondary areas (Roger & Arnault 1989), it is possible that the P2 component could be modulated by adjacent auditory processing areas. Further multiple recordings in identified cortical auditory fields would be required for a better understanding of attention modulation of the P2 component of MAEP in A1.

The data presented in this chapter also indicates that the modulation of the N1 component of the MAEP observed in Chapter 3 was not caused by attention-related processes, but it is likely explained by plastic changes taking place in the auditory cortex of the trained rats. It is documented that associative learning modifies the receptive fields' sensitivity of A1 neurons (Weinberger, 2007). Moreover, frequency discrimination tasks modulate the frequency representation and tonotopic organization (Recanzone et al., 1993), and temporal discrimination tasks modulate temporal transfer functions of A1 neurons (Bao et al., 2004). Because the LFP signal is composed of the synaptic activity of

hundreds of neurons around the electrode tip (Mizdorf, 1985; Logothetis, 2002), it is likely that larger populations of neurons responding to the 10 kHz would increase the amplitude of the LFP signal. However, it is possible that these plastic changes are not intrinsic from the cortex, but driven by plastic changes taking place in sub-cortical structures. For instance, it has been shown that reorganization of topographic maps are not limited to the cortical neurons but also occur in sub-thalamic structures of the somatosensory system in rats (reviewed in Nicolelis, 2005; Krupta et al., 1995). Additionally, it is documented in rats exposed to an acoustic enriched environment there is a higher amplitude of the LFP evoked auditory response to auditory stimuli (Engineer, et al., 2004; Percaccio et al., 2005). However, these studies did not control for attention modulation of sounds associated with the enriched environment, and therefore, attention could modulate the amplitude of MAEP to tones or noise pulses. The combined results from Chapter 3 and this chapter, suggest the contrary, that structural changes taken place in the trained rats are the main factor in explaining higher MAEP N1 amplitude in animals exposed to the two-tone discrimination task. However, I did not measure receptive field properties or topographic representations. Therefore, further experiments using chronic LFP recording are required to test this hypothesis.

Forward masking

The activity of A1 is strongly modulated by the stimulus history in the sense that the first stimulus in a fast sequence (interval of usually ≤ 200 - 300 ms) strongly affects the activity of A1 to the subsequent upcoming stimulus (Calford & Semple, 1995; Brosch & Schreiner, 1997; Wehr & Zador, 2005; Ulanovsky et al., 2003). These studies defined forward masking (or paired pulse depression) as the suppression of firing rate in response

to a second auditory stimulus in a two tone (or two clicks) sequence. The degree of suppression is related to receptive field properties and/or intensity of the first tone. The more the receptive field of the neurons is alike, the more suppression there is (Brosch & Schreiner, 1997). Moreover, it is thought that the cellular mechanism explaining the forward masking phenomenon involves synaptic inhibition during the first 100 ms after the first tone onset, and synaptic depression thereafter (Wehr & Zador, 2005). In this chapter, I showed that the forward masking effect is not modulated by attention-related processes. There is an equal probability to find forward masking during attentive or inattentive trial types. To my knowledge, this is first time that forward masking is demonstrated to occur in awake behaving animals trained in a two-tone discrimination paradigm independent of the attention state of the animal. If forwarding masking is the cellular mechanism necessary for the formation of auditory streams (Micheyl et al., 2005, 2007), then the formation of auditory streams in the primary auditory cortex reflects a primitive bottom-up process which is independent of sensory expectation based on previous experiences of auditory acoustic patterns. On the other hand, auditory streams can be solely formed based on temporal cues. Thus it is possible that attention-related processes might be necessary in situations in which the acoustic grouping of acoustic elements required the processing of more complex spectral and temporal cues.

Attention-related modulation of high frequency bands

Prior results in anesthetized rats showed that high frequency oscillations in the auditory cortex are only induced in response to a series of repeated clicks at 40 Hz (Franowicz & Barth, 1995), but not to single clicks (MacDonald & Barth, 1995; Franowicz & Barth, 1995; Barth & MacDonald, 1996). The frequency of these

oscillations was restricted to the gamma range (40 Hz), with a similar location and spatial distribution (but not identical) to the N1 component of the MAEP at A1 as revealed by the isopotential maps (Franowicz & Barth, 1995). These earlier studies strongly suggested that the high frequency oscillations were not related to auditory processing of the physical features of the sound per se. Moreover, subsequent experimental evidence suggested that attention and/or arousal modulates high frequency oscillations in the auditory cortex. For instance, stimulation of the nucleus basalis in the anterior forebrain (NB) (Metherate et al., 1992), the thalamic reticular nucleus (TRN) (MacDonald et al, 1998) and posterior intralaminar nuclei (PIL) (Sukov & Barth., 1998, 2001; Barth & MacDonald., 1996; Bret & Barth, 1997) induces the occurrence of gamma oscillations in the auditory cortex immediately after the onset of the auditory stimulus (Metherate et al., 1992; Sukov & Barth., 1998, 2001; MacDonald et al., 1998; Barth & MacDonald., 1996; Bret & Barth, 1997). The activity of the NB, PIL, and TRN are related with arousal and/or focused attention since the stimulation of these structures activates cortical neurons (Steriade & Pare, 2007), and moreover, they receive cholinergic (and glutamatergic) projections from the pedunculopontine tegmentum nucleus (PPT) and the laterodorsal tegmental nucleus (LDT) located in the brainstem reticular formation (Sarter et al., 2005; reviewed in Steriade & Pare, 2007). Stimulation of the PPT/LDT induces a general state of alertness, while lesion of these structures disrupts arousal (Steriade & Pare, 2007). Moreover, stimulation of the NB and the brainstem reticular formation greatly induces gamma oscillations in the visual cortex (Munk et al., 1993; Herculano-Houzel et al., 1999; Rodriguez et al., 2004), as well as in the auditory cortex (Metherate et al.,1992).

Results from MUA and LFP recordings in awake monkeys have shown the induction of these frequencies in the primary auditory cortex during passive listening in studies conducted by Steinschneider (Steinschneider et al., 2008). Steinchneider and collaborators also demonstrated that these induced high frequency oscillations are tightly corrected with the tonopotic organization of A1. However, this increase in high gamma frequencies was not time-locked to the auditory stimuli (Steinschneider et al., 2008). Therefore, the role of these oscillations in auditory processing was not clear.

Taking the observations discussed in the previous paragraph in consideration, I tested the hypothesis that these high frequency oscillations are not necessary related to the physical attributes of processing the acoustic event, but are strongly modulated by attention demands to successfully implement goal-directed behaviors. I tested this hypothesis by maintaining constant the physical attributes of the sound and comparing animal behavior engaged in a two-tone discrimination task.

I showed in this chapter that the increase in high gamma oscillations is correlated to actively perceiving a relevant auditory stimulus. Rats that incorrectly licked the spout after hearing one tone also had a high increase in high gamma frequencies. However, there was an even higher increase of high frequency oscillations in rats that correctly anticipated a water reward after carefully discriminating between the one versus two-tone trials. Moreover, the increase in the amplitude of high frequencies occurred during the time T2 which is immediately before the rat licks the spout to receive water. Thus, this result demonstrates that high frequency oscillations are modulated in a time period in which animals are expecting a reward. Concomitant with this increase in high frequency power was a decrease in low frequency power. The results are consistent with

experiments performed in which stimulation of the reticular formation with concomitant recordings in the cortex and thalamus showed a decrease in power of low frequency accompanied with an increase in high frequency oscillations (Steriade et al., 1996a, 1996b; Buzsaki et al., 1988, 1992; reviewed in Steriade & Pare, 2007). However, in this study, the increased high frequency power and decreased low frequency power only occured after the second tone onset. One could argue that the increase in high frequency power is caused by a general increase in arousal. This explanation is plausible because it is well established that arousal levels modulate high frequency oscillations in the visual and somatosensory cortex (Steriade et al., 1996a, 1996b; Munk et al., 1993; Herculano-Houzel et al., 1999). To control for this possibility, I also computed the normalized power spectrum density of the T2 interval during the attentive OT condition since in the one-tone trial types in which the animal incorrectly licked to receive water, they were paying attention to the first tone, but were not carefully engaged in the two-tone discrimination task. Instead, they used the strategy: lick whenever hearing a sensory event. I detected that, although there was an increase in gamma and high gamma power during attentive TT and attentive OT trial types, there was still a statistical difference at high gamma ranges between these experimental groups. This result strongly suggested that focused attention related with the task at hand modulates the intrinsic synchronized activity of the primary auditory cortex. Furthermore, the modulation at high and low frequency ranges is not explained by an increase in general arousal to the tone itself, but instead, requires active engagement in the two-tone discrimination task. Thus, by performing a within-comparison of LFP sites in trials in which animals failed to accomplish the task with trials in which they successfully detected two sensory events that reliably predicted

reward, I show evidence that high gamma oscillations, but not gamma oscillations, correlate with task performance.

Are high frequency oscillations at gamma and high gamma bands necessary for abstract auditory object formation? In our experimental design, the auditory cortex could group two otherwise separate auditory events into a unified auditory object. The auditory object formation is strongly dependent on basic acoustic feature cues such as harmonicity of the spectral component of sound, co-variation of amplitude and frequency modulations over time, rhythmic structures of the sound, and location and loudness (Cusack & Carlyon., 2004). There are, however, groupings of sounds by more abstract cues. For instance, human subjects discriminate two synthetic vowels that have the same fundamental frequency and time onsets (Bergman., 1990). Presumably, listeners have an "internal template" of these vowels which enables them to discriminate between these very similar sounds (Bregman., 1990). This type of acoustic grouping is driven by top-down processing, which depends on previous experience of an acoustic element that has gained significance for the listener through experience. It is possible that rats are grouping the two-tones into one acoustic object since these two acoustic elements have gained a meaning in which they can correctly predict a water reward. Moreover, the results presented in this chapter demonstrate a correlation between gamma and high gamma frequency oscillations with attention-related processes that are likely involved in acoustic object formation. Additionally, the primary auditory cortex is a possible structure in which the processing of anticipated temporal regularities in acoustic patterns could take place. This is because its activity increases by the presence of novel or rare sounds in a sequence of common acoustic elements (Ulanovsky et al, 2003; 2004). This

property is not present in the MGB (Ulanovsky et al, 2003; 2004). This response pattern is called the mismatch negativity (MMN), and it is thought to be a correlate of a primitive and pre-attentive, sensory memory trace (Fritz et al., 2007; Alho et al., 2004). Thus, the activity of A1 could be related to monitoring any unexpected or irregular metric sequences. Moreover, it has been shown that a lesion in A1 impairs the discrimination of tone sequences (monkeys: Conwey & Weiskrantz, 1976; Colombo et al., 1996; ferrets: Kelly et al., humans: Griffiths et al., 1997; Liegeois-Chauvel et al., 1998; rats: Syke et al, 2002, Browen, et al, 2003), and that the activity of A1 is modulated in monkeys discriminating melodies (Yin et al., 2008).

The results presented in Chapter 4 could be interpreted that A1 activity during the inter-tone interval could be important in order to anticipate physical regularities of acoustic objects. It has been proposed that intrinsic oscillations at high frequency ranges could be a temporal binding mechanism of auditory sensory stimuli linking separate acoustic events in a unified auditory percept (Llinas & Ribary., 1993; Joliot et al., 1994).Other researchers have proposed that induced intrinsic oscillations could be the neuronal substrate to process sensory expectations based on expected temporal patterns (Snyder & Jones & Large., 1999; Jones ., 2004; Large, 2005; Zanto et al., 2006). Moreover, there is some evidence suggesting that acoustic streaming formation is taking place in A1 (Micheyl et al., 2005).

The temporal bind hypothesis proposes that gamma oscillations generate a time frame window in which acoustic elements are bound in a unfied acoustic object that will be followed over time (Llinas & Ribary, 1993; Joliot et al., 1994). It is not unreasonable to assume that in the attentive TT trial types rats are grouping the two tones into a

acoustic object based on ASA that requires attention and memory. This is because the two tones are played in a relative fast sucession. The inter-tone interval always has a 200 ms inter-tone interval across trials. Therefore, it can be perceived as a acoustic object in which its acoustic elements are regular and highly predictable. This temporal feature of the auditory stimulus employed in this dissertation may prevent rats to have time in judging the occorence of two completely independent percepts in order to guide the implementation of goal-directed behavior. Instead, they are likely matching this particular sound with a memory that associates an acoustic object having two tones with a water reward. Therefore, it is possible that rats are grouping the discriminated two-tones in a unified percept for the behavioral task utilized in this dissertation. If temporal binding has taken place in A1, then we should expect that high frequency oscillations would be enhanced during the inter-tone interval of the two-tone trials in which rats correctly lick the spout anticipating water. Indeed, there is an increase in frequencies above 40 Hz in the inter-tone interval of two-tones trials in which rats correctly anticipate water as compared to the two-tone trials in which they ignore the task. This result supports the idea that high frequency oscillations underlie temporal binding. However, the induced high frequency oscillations were not different during the inter-tone interval between the attentive TT and attentive OT trial types. In the one-tone trials there is no grouping occurring. Moreover, high frequency oscillations are not a reliably parameter to classify the behavior during the inter-tone interval. This result suggests that while high frequency oscillations correlate with temporal binding of sensory stimuli, it may no be a neuronal mechanism to bind acoustic elements in a coherent percept. Thus, the increase in the high frequency oscillations in inter-tone interval could be explained by a general increase in

arousal instead of a careful assessment by the auditory cortex of the presence of an acoustic object. On the other hand, it is possible that rats are relying on their decision to lick the spout by counting separate acoustic elements. Thus, they would not integrate two tones as a unified percept, but segregate them as separate perceptual events. Thus, the design of behavioral paradigms in which the formation of acoustic streams is carefully quantified could shed some light in the role of high frequency oscillations in the formation of acoustic streaming. Thus, in conclusion, further experiments are needed to explore the correlation between high frequency oscillations and acoustic streaming formation.

Attention-related modulation of low frequency bands

The results presented in this chapter suggest that low frequency oscillations are also modulated by internal cognitive states. During the time T2, I detected differences between attentive and unattentive trial types at low frequency ranges. Moreover, I also saw that there are differences between attentiveness to two-tones and attentiveness to one-tone trial types. There is more power at low frequencies in the inattentive TT trials, than in the attentive TT, and there is more power at low frequency ranges in the attentive TT trials than in the attentive OT. This result suggests that there is a range of modulation in low and high frequency ranges that is optimal for good performance and that the modulation of these low frequency ranges is also related with attention-related processes . It has been argued that increases in the alpha frequency range power often correlate with tasks demanding working memory, while decreases in power are found when subjects are focusing their attention to process sensory information (Palva & Palva, 2006). Working memory could be playing a role during the inter-tone inaterval of animals that attend to

the second tone. However, an increase in power was also found in inattentive rats. Thus, the significance of the modulations that I saw in low frequency ranges is not clear.

The differences seen among the experimental groups at low frequency ranges during the T1 and T2 interval also suggest that it is possible that there are differential attention modulations within low frequencies. For instance it could be possible that this attention modulation be restricted to beta (15 – 25 Hz), but not alpha (8-12 Hz) frequency ranges. However, the spectral analysis performed here combined with the fast time window of the spectral analysis (<200 ms) prevents us from differentiating theta, alpha, and beta frequencies. Instead, I lumped the frequencies of alpha/beta altogether. This procedure was necessary for the spectral analysis performed in this dissertation. This is because the resolution of high frequencies in such a fast time scale using spectral analysis is subjected to spectral leakage contamination by low frequencies. Using the multitaper method greatly minimizes this problem, since it concentrates frequencies at 20 Hz by using the combination of tapers and windows used here. However, this compromises the separation of alpha/beta frequencies. Thus, further experiments in which we could increase the interval between tones and the duration of the tones would be important to disentangle the affects attention modulations along the whole spectral continuum of the LFP signal.

Increased high frequency bands amplitude predicts performance

I also found that the increase in power of the high frequency bands in the auditory cortex is predictive of behavioral performance in this two-tone discrimination task. I used the ROC analysis to measure what is the probability to reliably categorize which behavior will occur based on the spectrogram of the LFP. Since the ROC analysis does not take

into account the posteriori statistical hypothesis, it is a powerful tool to reliably classify which of the behavioral categories will occur based upon a given neuronal signal used as a parameter. This analysis has been successfully used to correlate firing rates of the neurons in the temporal visual area (MT) and the PFC to behavioral performance of monkies discriminating visual motion (Britten & Newsome, 1992; Zaksas & Pasternak, 2005, 2006). Here, I've demonstrated that the neuronal intrinsic synchrony of the A1 predicts behavioral performance regardless of comparing the attentive versus inattentive trials or when comparing attentive TT versus attentive OT trial types. An ideal observer can still reliably classify two different categories by using the high frequency gamma band as a parameter in a ROC analysis. Therefore, the increase in high frequency gamma can not be explained entirely by somatosensory, pre-motor or motor processing.

It is interesting to note that the increase in power of high frequencies is observed even before the first tone occurs (see Figure 5.45). Although, the inter-stimulus interval presentation was randomly varied (± 5 seconds), it is possible that the animals are trying to predict when the inter-trial interval will occur. Moreover, it could be argued that the increased power at high frequencies during the baseline is due to an increased attention demand to correctly perform the task. It is possible that, given the relatively fast foreperiod (200 ms inter-tone interval) between the warning signal (the first tone) and the rewarding signal (the second tone), rats maximize their chance to get water by maintaining a high vigilant state during baseline periods in order to try to predict when the two-tones will occur. Longer two-tone intervals would likely require less attention effort during the baseline, thereby, reducing the burst of high frequency oscillations in the

baseline. Future experiments in which the foreperiod is manipulated should be helpful in testing this hypothesis.

It is interesting to observe that mammal's vocalizations, bird songs, and human words and phrases have a duration ranging between 50-500 ms. The duration of these sounds fall within the time range of the duration of high frequency oscillations induced by auditory stimuli. Particularly important is the finding that induced gamma oscillations are greatly reduced to time reversed complex specie-specific vocalizations in mustached bats (Medeved and Kenwall, 2008). Thus, it could be possible that high frequency oscillations are a neuronal mechanism to enhance auditory processing and to keep track of the formation of acoustic streams over time. Moreover, it has been proposed that the activity of the primary auditory cortex is strongly modulated by auditory stimulileading to acoustic object formation (Micheyl., et al., 2005; Nelken., 1999; Petkov et al., 2005). The results of this chapter also suggest a more complex role of the primary auditory cortex in processing acoustic information. Synchrony at high frequency is likely a neuronal mechanism to link neuronal networks that are processing non-acoustic information that is relevant for good performance of tasks involving auditory processing.

Attention-related modulation of global coherence

In the previous chapter I showed that perceiving a single tone also increases coherence among LPF sites. Therefore, suggesting that attention could enhance neuronal synchrony across 1,0 mm distances in the auditory cortex. Those results were based on the comparison between rats trained to perceive an acoustic event and naïve rats. Thus the increase in coherence could be a by-product of increased tonotopic representation of the physical attributes of the tone made relevant in the training procedure.

In this chapter I tested whether attending to the second tone in the two-tone discrimination task modulates the coherence among LFP sites. I showed in this chapter that there was an increase in coherence at 40 Hz and at 80 - 100 Hz in the attentive two-tone trials during the T1 interval. During the T2 interval the coherence of LFP sites at high frequency ranges was substantially higher for rats that will attend to the second tone. Concomitantly with an increase in coherence at high frequencies, there was also a decrease in coherence at low frequency ranges. Together these results rule out the effect that the expanded representation of the 10 kHz tones in trained rats might have in LFP coherence. Thus, the increased coherence of LFP sites is attributed to expectations directed to the upcoming second tone and/or temporal cue processing occurring during the inter-tone interval. During the T2 interval, other cognitive factors could also modulate the coherence among LFP sites, such as decision making processes and/or reward expectations.

As stated before, it could be argued that somatosensory processing and/or pre-motor processing is modulating the coherence at high frequency bands during the T2 interval. However, our normalized power spectrum density results and our ROC analysis results comparing attentive TT and attentive OT trial types suggest that this is not the case. First, there was an increase in power of high frequency bands between the inter-tone intervals. Rats did lick the spout during this interval. Second, despite that rats licked the spout during attentive TT and attentive OT trial types after the T2 internal (250-300 ms after the second tone onset), the AUC values of the high frequency range were still different between these two trial types. If the pre-motor and/or sensotosensory inputs in the auditory cortex were driving this increase in high frequency power, their value would

be the same whether animals licked to the two-tone or one-tone trials. This was not the case. However, I did not specifically measure the LFP-LFP coherence during the attentive OT trials. Further analysis would be necessary to completely rule-out the effects of pre-motor or somatosensory processing in the LFP-LFP coherence of the auditory cortex.

Attention-related modulation of local coherence

The measurements of MUA-LFP coherence are useful to detect whether the spike train and the local field potentials are time-locked at a particular frequency. The comparison of the MUA-LFP coherence between attentive and unattentive experimental groups tested the hypothesis that attention-related phenomenon modulated local neuronal networks. This is because the data from intracellular and high impedance microelectrode recordings in the hippocampus suggest that the maximum radius to detect spikes is estimated to be 150 μm (Henze et al., 2001) and the local field potentials are likely the sum of synaptic potentials in the radius of approximately 300 to 500 μm (Mizdorf, 1985; Logothetis, 2002; Katzner et al., 2009). The MUA-LFP coherence data presented here shows that there is a high coherence between spike trains and the LFP in the gamma frequency range when rats attended to the two-tone trials. However, this effect is only seen after the second tone onset. Therefore a combination of attention-related mechanisms, reward expectancies, or decision making processes drive synchrony at gamma frequency ranges of local neuronal networks in A1. The data are consistent with the normalized power analysis comparing attentive and inattentive TT trial types during the T2 interval. However, it is at odds with the LFP-LFP coherence analysis, which shows increased coherence at high gamma and gamma frequency ranges. It is important

to note that the LFP-LFP coherence indexes a complementary but different set of neuronal populations than the MUA-LFP coherence analysis. While the high impedance electrodes probably have a bias to collect action potentials from large pyramidal neurons, the LFP collects synaptic currents from inhibitory and excitatory inter-neurons as well. Thus it is possible that the MUA-LFP coherence data are missing fundamental temporal dynamics of small neurons with surrounding neuronal networks. Further experiments combining intracellular recordings and LFP recordings should clarify the LFP-LFP and MUA-LFP coherence data discrepancies seen in this chapter.

Potential cellular mechanisms

High gamma frequency oscillations (90-150 Hz) have been found in the temporal lobe in human subjects who have undergone surgery. It is reported that these oscillations are induced in human subjects listening to transient tones and phonemes (Edwards et al., 2005), discriminating pure tones and phonemes (Crones et al., 2001), word processing (Canolty et al., 2007), and in spatial auditory attention (Ray et al., 2008). High oscillations with some overlapping frequency range (100-200 Hz) have been described in the hippocampus (Buzsaki et al., 1992; Ylinen et al., 1995; Draguhn et al., 2000). They occur simultaneously with the depth negative phase of hippocampal sharp waves (Buzsaki et al., 1992; Ylinen, 1995). High gamma oscillations (90-200 Hz) have also been described in cortical neurons of the suprasylvian, ectosylvian, and marginal gyrus of cats (Grenier et al., 2001) as well as in the somatosensory of rats (Jones & Barth, 1999; Jones et al., 2000), in the somatosensory cortex of monkeys (Ray et al., 2008a, 2008b), in the auditory cortex of monkeys passively listening to tones (Steinheisser et al., 2008), and in the primary auditory cortex of anesthetized rats in responses to clicks (Jones & Barth,

1999). The study presented in this chapter extends these findings by showing that high frequency oscillations are induced by sensory processing and modulated by attention-related processes in the auditory cortex of the rodents. Moreover, the results of cross-correlation between LFP sites showing the coherence of sites greatly decreases with distance (Greiner et al., 2001). The direct measurements of LFP coherence and MUA-LFP coherence strongly suggest that the high frequency oscillations are generated by local networks (Chapter 2) and they are modulated by attention-related phenomenon (this chapter).

Results from simultaneous intracellular of fast spiking (FS) or fast rhythmic bursting (FRB) with LFP recoding in the suprasylvian gyrus of cats (Grenier et al., 2001) suggests that inhibitory neurons control the timing of the high frequency oscillations. This is because their firing rate is time-locked precisely to 2.5 ms before the depth-negative peak of the oscillations (Grenier et al., 2001). Vibrissa stimulation along with simultaneous epipial and intracellular recordings of FS and intrinsically bursting neurons (IB) in the barrel cortex of rats found similar results (Jones et al., 2000). However, the RS cells likely fire at the depth-negative peak, but not in every peak. In some trials they spike at the first depth-negative peak and skip the second one (Jones et al., 2000). Based on intracellular recordings combined with anatomical reconstruction, the FS neurons are classified as inhibitory interneuron (reviewed in Markran et al., 2004). It is also known that in the barrel cortex of mice and rats, inhibitory interneurons have electrical synapses and form inhibitory neuronal networks connected through gap junctions that are synchronized at the gamma frequency range (Gibson et al., 1999; Galarreta & Hestrin, 1999; Beierlein et al., 2000; Deans et al., 2001; Hormusdi et al., 2001). The anesthetic

halothane, which blocks gap junctions, greatly reduces these high frequency oscillations in cortical cells (Jones et al., 2000) and hippocampal cells (Ylinen et al., 1995). Therefore the high frequency oscillations that I detected are possibly intra-cortically generated by inhibitory interneuron networks connected through gap junctions in the auditory cortex of rats. The activity of these inhibitory networks could set the pace in which a sub-set of pyramidal cells could synchronize their firing during some trials but not others.

Potential thalamo-cortical mechanisms

Another possible mechanism by which internal states can drive oscillations in the auditory cortex is through cortico-thalamic loops. In particular, the auditory cortex – thalamic reticular nucleus (TRN) – vMGB- auditory cortex loop can be a possible candidate in driving neuronal oscillations in the auditory cortex. The TRN receives a projection from the primary auditory cortex in rats (Roger & Arnault, 1989; Crabtree., 1998). This nucleus is composed almost exclusively of GABAergic neurons that project their axons back to the all regions of the MBG (Jones, 2002). Importantly, activation of this nucleus by excitatory currents delivered by bipolar electrodes induced high frequency oscillations in simultaneous epipial recordings in the auditory cortex of the rat (Barth & MacDonald., 1996; MacDonal & Barth, 1998). Additionally, simultaneous recording in the TRN, vMGB and auditory cortex coupled with injections of the GABergic agonist muscimol shows that inactivation of the TRN abolishes spindle like oscillations (7- 15 Hz) in the auditory cortex (Cottilon-Williams & Edeline, 2000, 2004), while the opposite did not disrupt oscillations in the TRN or vMGB.

It has been shown that the TRN activity is strongly modulated in visual spatial attention. Recent simultaneous extracellular recordings in the TRN, parvocellular and

magnocellular neurons of the lateral geniculate nucleus (LGNp and LGNm) showed that the visual spatial attention differently modulates the activity of these areas (MacAlonan et al., 2008). For instance, attention directed to the receptive field as opposed to attention directed away from the receptive field of a given neuron inhibits the activity of the TRN at the same time that it enhances the activity of the LGNp and LGNm (MacAlonan et al., 2008). Moreover, the LGNm have an earlier latency followed by TRN and then LGNp (MacAlonan et al., 2008). Thus, visual spatial attention strongly modulates feedback loops between TRN and LGN. Furthermore, the TRN receives projections from the prefrontal cortex (areas 9, 10, 13 and 46) (Zikopoulos & Barbas, 2006). The TRN areas that receive feedback projections from cortical sensory areas showed extensive overlap with axon terminals from anterograde track-tracers injected into areas 46 and 13 of the PFC (Zikopoulos & Barbas, 2006). Thus, the auditory sector of the TRN receives overlapping projection from A1 and PFC. Additionally, it has been shown that the PFC has an auditory domain that is highly activated by complex specie-specific vocalization (Cohen et al., 2007; Romansky et al., 1999, 2000, 2004,2007). Therefore, it is possible that indirect projection from A1 via the secondary auditory cortical areas could reach the PFC which then could evaluate the significance of the sensory information. For instance, it has been shown that vocalizations with different acoustic properties that signal the same hyper-categories for food objects greatly trigger increases of the firing rate in the PFC (Cohen et al., 2007). Therefore, once these PFC areas process the auditory information, it could send a feedback projection to the auditory sector of the TRN. The TRN also receives a cortico-thalamic feedback projection from A1. Thus, the TRN could

act as coincident detector, to integrate high processed sensory information and to modulate incoming thalamic information.

In summary, the results presented in this chapter are consistent with previous studies showing high gamma oscillations induced by discrimination of pure tones and phonemes in humans (Crones et al., 2001), passively listening to transient tones and phonemes (Edwards et al., 2005), word processing (Canolty et al., 2007), and in selective attention (Ray et al., 2008) in the temporal cortex of human subjects undergoing surgery. These observations have suggested that the high gamma frequency in the auditory cortex is the frequency most related with high cognitive function. In this chapter, I extended these findings by showing that modulation of high gamma frequencies occurs in the primary auditory cortex and it is not related specifically with acoustic feature detection processing. This finding is important because it shows that a possible neuronal correlate of high cognitive function in a cortical area of a species is amenable to experimental manipulation.

Chapter 6

6.1 Discussion and conclusions

High frequency oscillations are a widespread cortical phenomenon correlated to sensory perception, motor and cognitive signal processing. It has been shown that these oscillations are induced by visual processing in the visual cortex in cats and monkeys (Engel et al., 1991a, 1991b, 1991c; Grey et al., 1989a, 1989b; Fries et al., 1997, 2002; reviewed in Singer, 1993, 1999), in pre-motor processing in the primary and frontal motor cortex during motor preparation (Sanes & Donoghue, 1993) in sensorimotor cortex during movements requiring focused attention (Murphy & Fetz, 1992, 1996a,1996b) in the somatosensory cortex of anesthetized cats (Steriade et al., 1996a, 1996b), and also in the olfactory system during stimulus processing (reviewed in Sannita, 2000; Wehr & Laurent, 1996; Laurent et al., 1996; Bressler & Freeman, 1980).

Based on the finding that synchronization at the gamma range is strongly modulated by a visual stimulus configuration (see Chapter 1), Wolf Singer and collaborators have proposed a binding by synchrony hypothesis (reviewed in Singer, 1999). This hypothesis proposes that neuronal synchrony at the gamma frequency range binds feature detector neurons in functional ensemble networks. These neuronal networks would jointly process several features of the visual scene. Ultimately these ensembles would activate postsynaptic neurons in extra-striate areas for further joint processing (Singer & Gray, 1995; Singer, 1999; Azouz & Gray, 2000; Engel et al., 2001). Thus, these oscillations would be the neuronal mechanism propitiating fast and flexible identification of neuronal ensembles that would ultimately allow coherent visual percept

formation (Singer & Gray, 1995; Singer, 1999; Engel et al., 1997; Engel et al., 2001; Munk & Neuenschwander, 2000).

The binding by synchrony hypothesis was brought about to explain how the visual system can integrate features of the visual scene in a coherent percept. This is because the visual system processes a visual scene in serial and parallel processing pathways that are specialized in particular features, such as color, form, or movement direction (reviewed in Livingstone & Hubel., 1988, Van Essen & Gallant, 1994; Hubel, 1995). For instance, the primary visual cortex is organized in micro-columns of visual processing, thereby, parceling the visual scene in simpler visual features (reviewed in Hubel, 1995). Moreover, it is well established that the visual system is organized in two parallel streams of visual processing: dorsal (where) and ventral (what) streams. The dorsal parietal stream processes spatial visual relations and the ventral infero-temporal stream processes pattern recognition (Van Essen & Gallant, 1994; Livingstone & Hubel, 1988). Therefore, it is necessary that the integration of the information processed in these areas form a coherent visual scene.

It is hypothesized that the auditory system, similar to the visual system, has serial and parallel streams of sensory processing (Rauschecker & Tian, 2000). Moreover, the primary auditory cortex also has a modular organization that is hypothesized to parcel the auditory scene in its basic feature components (Ehret, 1997; Schreiner et al., 2000; Read et al., 2002; Linden & Schreiner, 2003). This hypothesis is based on the fact that the auditory system has a cochleotopy organization as revealed by radial microelectrode penetration in A1 (Merzenich et al., 1974; Sally & Kelly, 1988) as well as in the AAF, PAF, and VPAF cortical fields (Roullier, 1992; Polley et al., 2007) Micro-columns of

characteristiciso-frequency bands (CF) running ventro-dorsally display low frequency preferences at the caudal, whereas high frequency show preferences at the rostral A1 (Rutkowski et al., 2003; Kalatski et al., 2005; Polley et al., 2007). Parallel to these CF maps is a directional selectivity map (down and up FM sweeps) (Zhang et al., 2003), and orthogonal to these CF maps are broad and narrow frequency integration maps, low and high intensity-threshold maps, long and short latency maps, and binaural integration maps (reviewed in Linden & Schreiner, 2003). Moreover, it has been hypothesized that, similar to the visual system, the auditory system is sub-divided into dorsal and ventral streams of processing (Rauschecker & Tian, 2000; Romanski et al., 1999; Tian et al., 2001). It is proposed that the dorsal stream processes where complex vocalizations are coming from, whereas, the ventral streams process the significance of the complex vocalizations (reviewed in Rauschecker & Tian, 2000). The binding by synchrony hypothesis predicts that neuronal areas that share similar morfo-functional principles of neuronal processing should display neuronal synchrony at high frequency oscillations (Singer & Gray, 1995; Singer, 1999;). In fact, this hypothesis was originally proposed to explain the cocktail-party problem (Von der Malsburg & Schreiner, 1986), which is foreground/background analysis carried out by the ASA in the auditory system (Bregman, 1990).

In the auditory cortex there are only a few studies exploring the correlation between high frequency oscillations and sensory processing in the auditory cortex of experimental animals. Moreover, they show conflicting experimental evidence that these high frequency oscillations are induced by sensory processing. In Chapter 2, I tested the hypothesis that oscillatory neuronal synchrony at high frequency ranges is induced by

auditory stimulus in the auditory cortex of awake rats. The results presented in that chapter demonstrate that auditory stimuli trigger evoked, time-locked and induced high frequency oscillations in awake naïve rats passively listening to the auditory stimulus. Different results were found in a prior study in awake rats (Cotillon-Williams & Edeline, 2003; Cottilon-Williams, 2004) and mustached bats (Horikawa et al., 1994). Differences in signal analysis techniques, in the analysis of different signals (LFP and single-units), and different experimental conditions might explain these discrepancies.

The results presented in Chapter 2 are consistent with the results previously found in anesthetized rats (Barth & MacDonald, 1996; MacDonald & Barth, 1998), anesthetized (Brosch et al., 2002) and awake monkeys (Steinschneider et al., 2008), awake mustached bats (Medvedev & Kanwall, 2008), and awake ferrets (Jeschke et al., 2009). Although there are discrepancies in some of the results in relation to latency and frequency ranges, all of the recent studies using LFP signals demonstrate that auditory stimuli induce these high frequency oscillations in the auditory cortex. I extended these previous results by showing that auditory stimuli induces oscillations above the traditional gamma frequency band (25-90 Hz) as well. Moreover, the spectral coherence analysis among spike trains and between the spike train and LFP signals suggests that the gamma frequency oscillations are a product of local neuronal synchrony (Chapter 2).

The results from Chapter 2 demonstrate that there is a correlation between acoustic processing and neuronal synchrony at gamma and high gamma frequency bands. But, what it is the significance of this finding for auditory stimulus processing? Some authors have proposed that gamma oscillations would be detrimental to processing acoustic features, since it would set a sluggish limit of how fast the auditory system could

process fast varying frequency and amplitude modulations (Cottilon-Williams & Edeline, 2003, 2004). However, The findings in Chapter 2 demonstrate that tones induce high gamma oscillations (up to 150 Hz). In principle, neurons that are time-locked to the troughs or peaks of such fast oscillations, could process acoustic features present at the syllabic level of specie-specific vocalizations. Experimental data shows that time-reversed vocalizations are not as optimal as forward vocalizations to induce gamma oscillations in the awake mustached bat (Medvedev & Kanwall, 2008). Thus, there is evidence that gamma oscillation amplitude is diminished when the fine temporal structure of vocalizations are experimentally disrupted. This data seems to be consistent with the role of gamma frequency oscillations in linking acoustic elements in acoustic objects.

On the other hand, by maintaining the auditory stimulus as simple as possible, I showed that the high frequency oscillations are induced by auditory stimuli with no need for these neurons to integrate complex acoustic features. This experimental finding is apparently inconsistent with the idea that high frequency oscillations reflect a mechanism for binding neurons extracting detail acoustic information from complex sounds in neuronal ensembles . Especially if one assumes that neurons in A1 act as feature detectors of the acoustic environment, that these neurons form narrow modular functional maps, and that the processing of pure tones would only require the activity of neurons in a labeled-line coding strategy provided by the anatomical lemniscal pathway. However, in our case, the auditory stimuli used were relatively loud (70 - 75 dB SPL), the recordings were relatively close in space (~ 1.0 mm^2), the neurons recorded responded to a wide frequency range, and the anatomical pattern of thalamo-cortical divergence is

spread over a wide range of CF (Huang, 2000; Lee et al., 2004). Moreover, a full characterization of the receptive field properties of the neurons was not performed in theserecording sessions. Thus, a detailed relationship between neuronal synchrony at high frequency ranges and receptive field configuration waits for further studies. Moreover, experiments correlating the occurrence of these oscillations with the acoustic stream segregation or acoustic stream fusion are not available. Such experiments would provide some insight into the role of high frequency oscillations in acoustic object formation. However, such experiments in experimental animals are not an easy task. Designing experimental paradigms of acoustic stream formation and training experimental animals to report them can be extremely time consuming. Additionally, recording from the auditory cortex while animals are performing such tasks is not an easy experiment. To undertake such a task, evidence that these high frequency oscillations are not merely correlated with sensory stimulation should be first collected. Demonstrating that these oscillations are related with sensory stimulation does not necessary show that they are a neuronal mechanism underling perceptual experience. For instance, they could be merely an epiphenomenon correlated with neuronal stimulation (Shadlen & Newsome, 1994). However, evidence showing that gamma oscillations are modulated in parallel to perception would greatly suggest that these high frequency oscillations are not an epiphenomenon.

It is clear that perception is inextricably related to attention-related processes (Allport, 1993; Itti & Koch, 2001; Connor et al., 2004; Fritz et al., 2007b, 2007c). For example, anyone walking in the streets of Rio de Janeiro or New York City would immediately realize that there is too much information for us to perceive at once.

Attention must be paid to some sensory objects while others are filtered out from further processing. Thus, attention-related systems must act in conjunction with the sensory system in order to bias processing of relevant sensory information to implement goal-directed behaviors (Allport, 1993; Desimone & Duncan, 1995; Reynolds & Chelazzi, 2004; Shipp, 2004; Maunshell & Treue, 2006). I reasoned that if these oscillations are indeed related with sensory perception, than they should be modulated by animals reporting a perception of simple acoustic stimuli. Additionally, the stimulation of areas related with arousal/attention, such as the NB, TRN and PIL induces the gamma oscillations at considerably short latencies in the auditory cortex (Metherate et al., 1992; Sukov & Barth, 1998, 2001; MacDonald et al., 1998; Barth & MacDonald, 1996). These results, combined with our findings showing that induced high frequency oscillations are highly variable across trials/LFP sites in the awake rats, prompted us to investigate if these high frequency oscillations could also be modulated by attention-related processes.

The results presented in Chapter 3 show that neuronal synchrony at gamma and high gamma frequency bands is indeed modulated by the perception of the tone. Thus, attention-related processes are modulating these high frequency oscillations. Rats actively listening to a tone to implement goal-directed behaviors have a higher normalized power spectrum across all frequency bands. However, the spectral coherence among LFP sites showed a slightly direct picture. In these rats, there is more coherence among LFP sites at gamma and high gamma frequency bands. Additionally, in rats actively listening to tones, the coherence analysis between spike trains and LFP showed a high coherence peaking at 25 Hz and at the gamma frequency range (40-70 Hz). Thus, attention-related processes seem to modulate neuronal synchrony at these frequencies. However, there was no spike-

LFP coherence at high gamma frequency bands. These results suggest that synaptic activity oscillating at high gamma frequency ranges (>90 Hz), as indexed by the LFP signal, does not translate to action potential at these high frequencies. Even though attention-related processes modulate synaptic synchrony at high frequencies, it seems that there are anatomical and/or physiological constrains preventing neurons from discharging synchronously at these high frequencies. However, other explanations are possible as well. Larger neurons have larger spike amplitudes that spread over larger distances than small neurons (Humphrey & Schmidt, 1990). Thus, extracellular recording techniques have an inherent sampling bias to bigger pyramidal cells that are highly spontaneous during the isolation process of the action potential (Humphrey & Schmidt, 1990). Therefore it is possible that I recorded from particular class of neurons that are not particularly synchronous at these high frequency ranges.

The results presented in Chapter 3 strongly suggest a complex relationship between attention-related processes and neuronal coherency in the primary auditory cortex of awake behaving animals. Additionally, these results also suggest that attention-related processes are synchronizing neuronal populations across different micro-columns of processing. However, it is possible that the increase of neuronal synchrony at high frequency ranges could be a by-product of neuronal plasticity of the tonotopic maps and/or receptive field properties that have taken place in the trained rats.

It is widely demonstrated that training modifies the topographic organization of A1 (Weinberger and Diamond, 1987; Recanzone et al 1993; Bao et al.,2004; Kilgard et al., 1999). Moreover, training also induces plasticity in the temporal response (Bao et al., 2004) as well as the spectral properties of receptive field properties of A1 neurons (Fritz

et al., 2003, 2005, 2007). However, the plasticity chances observed in A1 depends on the task at hand. For instance, training narrows the receptive field width in some tasks (Recanzone et al., 1993) while widening the receptive field width in others task (Wang et al., 1995; Recanzone et al., 1992). It has been proposed that receptive fields narrow in tasks requiring fine spatial discrimination while broadening in tasks requiring temporal judgments (Merzenich et al., 1990). Moreover, plastic changes in A1 depend on the physical attributes of the acoustic stimuli used in the training protocol that predicts reward (Polley et al., 2006) So far, the relationship between plasticity and neuronal synchrony is not well understood. Some results show that experimental manipulations that increase, receptive fields also increase synchronization. Others studies showed that experimental minipulations that decrase receptive fields also decrease synchrony. There other results showing that neuronal synchrony is independent of receptive field plasticity (reviewed in Kilgard et al., 2007). In subsequent chapters, because plastic chances could obscure some of the conclusions in Chapter 3, I aimed to measure neuronal synchrony in the same populations of neurons during trials in which rats attended to or did not attend a relevant auditory stimulus.

In Chapter 5, I described that high frequency oscillations are not likely explained by plastic changes taken place in the auditory cortex of trained rats. Because I am recording from the same LFP sites when rats attend to or do not attend to a trial during a temporal discrimination task, the neuronal synchrony that I detected is not due to structural plastic changes. In this chapter, I describe that the power spectrum of rats engaging in the discrimination task shows more power at gamma and high gamma frequency ranges. Moreover, I also described that coherence between the LFP sites is also

modulated by attention-related processes. For instance, there is more spectral coherence among the LFP sites in the gamma frequency and high frequency bands immediately after the first tone onset (interval T1; see Figure 5.13 B). This result is very similar to the results presented in Chapter 3. However, it is puzzling that I did not detect local network synchronization, as indexed by the MUA-LFP coherence in the same electrodes channel, during the T1 interval. However, after the second tone onset, during a period of time in which rats are expecting a reward and in which it is before they lick the spout, there was a particular modulation at high frequency ranges (in gamma: above 40 Hz, and high gamma: 90-150 Hz). Moreover, there was also particular modulation at the gamma frequency range in the local neuronal networks as index by MUA-LFP coherence. These results demonstrated that attention-related processes modulate the neuronal synchrony of the primary auditory cortex neurons. Moreover, they demonstrate that the modulation of these high frequencies is not due to plasticity of the tonotopic map of A1.

Chapter 3 tested the hypothesis that high frequency oscillations are modulated by rats perceiving a tone. Thus, suggesting that these oscillations are a relevant neuronal mechanism in integrating the processing of sensory inputs in a percept that signals a particular meaning. However, it could be possible that these high frequency oscillations are associated with a general arousal state, but not necessarily with a focused attention state in which a particular sensory event is carefully analyzed and identified. Indeed, in chapter 5, i found that some of the modulations in these high frequency ranges is explained by an increase in general arousal to the presence of a sensory event. This is because, gamma and high gamma frequency bands are increased in rats fully engaged in the two-tone trial discrimination and in rats wrongly responding to one-tone trial types

which do not signal a reward. However, there is a specific significant difference in high gamma frequency bands in rats engaged in the discrimination task as compared to rats reacting to tones. Moreover, this effect is only seen after the second tone. Therefore, after rats identify the sensory information that they need to implement a goal-directed behavior. Thus, there is a specific correlation between attention-related processes and high gamma frequencies in the auditory cortex. But, is there a correlation between high frequency oscillations and acoustic stream formation?

It is been proposed that attention is highly affected by the rhythmic regularity of an acoustic time structure (Jones, 2004). Sounds in a rhythmic sequence have an advantage in capturing our attention, thereby, inducing the formation of perceptual streams. It is been proposed that intrinsic oscillations are the neuronal mechanism underling sensory expectations based on expected temporal regularities that have been shaped by experience (Large & Jones, 1999; Jones, 2004; Snyder & Large, 2005; Zanto et al., 2006). Similar to this hypothesis is the proposed role of gamma oscillations in a temporal binding mechanism of sensory stimuli, thus linking separate acoustic events in a unified percept (Llinas & Ribary, 1993; Joliot et al., 1994).

The two-tone discrimination paradigm developed in this thesis allows us to begin to tackle some of the temporal bind predictions. I am arguing that there is a likely formation of acoustic streaming when rats identified the two tones and licked to receive water. Thus, the auditory system of the rats correctly identifying the two-tones as a single acoustic object in which two otherwise isolated acoustic events are bound together. There is no temporal binding in the one-tone trials in which rats responded to the tone. Therefore, the assumption that acoustic streaming is being formed during the two-tone

discrimination task is not unreasonable. Moreover, I reasoned that if intrinsic oscillations play a role in acoustic streaming, they would do so during the interval between tones. Thus, I measured the normalized power spectrum during the inter-tone interval, or in the interval immediately proceeding the first tone in the case of the one-tone trial type, to test if induced high frequency oscillations are modulated during the likely formation of acoustic streaming. If my interpretation of the acoustic streaming formation is correct, then intrinsic gamma oscillations are not likely the neural mechanism underling acoustic stream formation. This is because, although high gamma and gamma oscillations increased during the inter-tone interval of the attentive TT trials as compared to the inattentive TT trial, there are no significant differences between the power spectrum of the two-tone and one-tone attentive trial types. Therefore, my results suggest that the high frequency oscillations are related with attention-related processes associated with perception, but not with the binding of acoustic features in acoustic objects. For instance, it is possible that the high frequency oscillations are a mechanism to measure the time of an expected reward. Thus, although these oscillations might be triggered by acoustic sensory events, it would not be a mechanism to group sounds together. Clearly, further experiments in which temporal or spectral acoustic cues are manipulated to induce acoustic streaming could confirm the prediction that high frequency oscillations may not be related with acoustic object formation.

One could think that although, attention-related processes modulate these high frequencies, they would not necessary be correlated with behavioral outcomes. It could be possible that A1 is processing some particular sound parameter that would be relevant for the decision making process occurring in the posterior parietal or PFC cortex, but not

in the primary cortical areas. By keeping the auditory stimulus as simple as possible, and by correlating the pattern of neuronal response in A1 directly with the behavioral categories that are present in the two-tone discrimination task, I also found that synchronization at high frequency ranges, as indexed by local field potentials, and the firing rate of the neurons in A1, predicts behavioral outcomes. Moreover, although I detected that the firing rate to the tone onset is modulated by attention-related processes, the firing rates to onset were not sufficiently reliable to predict behavioral outcomes. Only the firing rate and synchronization after the second tone could strongly and reliably predict whether rats would or would not correctly lick to receive a water reward.

It has been long believed that A1 is the first stage of auditory cortical processing in which features of the sound would be analyzed (DeRibaupierre, 1996; Ehret, 1996). After this initial processing, subsequence cortical areas would then be engaged to elaborate on the significance of the acoustic input. Further processing would then take place in associative cortices in which attributes behavioral and predictive value of the acoustic signal to implement goal-directed behaviors (Romansky et al., 1999; Rauschecker & Tian, 2000). The results presented in this dissertaion challenge this hypothesis. The neuronal response to tone onsets was not sufficiently reliable to classify the behavioral outcome. However, the same neuron responses after the tone onset were tightly correlated with correct behavioral responses. Thus, the activity of A1 is processing high cognitive functions assumed to be processed by association cortices.

The idea that A1 processes the elementary physical attributes of sound relies on the observation that it has a modular organization. This observation, along with borrowed ideas from the functional organization of the visual cortex, has prompted researchers to

propose that A1 is essentially a feature detector area. However, some findings are not in line with this hypothesis. For instance, the findings of Petkov and collaborators show that A1 neurons behave as if they were being activated by a continuous tone, when in fact the stimulus consisted of two tone sequences in which the gap between them was filled by a brief noise (Petkov et al., 2007). In other words, they do not respond to the noise transitions and their responses were similar to the continuous tone, thus, they are not faithfully representing the physical attributes of sounds. Additionally, it was found that approximately 13 to 14% of A1 neurons display non-auditory responses that were correlated with features of the task being performed (Brosch et al., 2005; Yin et al., 2008). Their activity was related to the time of the reward or to non-acoustic cues that were relevant to correctly engage in the task (Brosch et al., 2005; Yin et al., 2008). Furthermore, it has been shown that in rats trained to associate a auditory stimulus with a particular reward, the activity of the medial, dorsal MGB, and PIL have a early phasic response to auditory stimulus, and a late tonic and sustained discharge (climbing response) to the time and value of a the reward (Komura et al., 2001). Additionally, the medial MGB is activated by light, somatosensory and vestibular stimuli (Komora, 2005; Blum & Gilman, 1979). Moreover, PIL and medial MGB have wide spread projections to A1 and adjacent auditory cortical areas (Linke, 1999; Huang & Winer, 2000). Additionally, it is reported that PIL stimulation induces gamma oscillations in A1 (Sukov & Barth, 1998, 2001; MacDonald et al.,1998; Barth & MacDonald, 1996). Thus, the results presented in this dissertation are consistent with a multi-sensory and cognitive processing role of the primary auditory cortex.

In summary, it has been reported that high frequency oscillations (90-150 Hz) are induced in the temporal lobe of humans during attention and auditory processing (Crones et al., 2001; Edwards et al., 2005 ; Canolty et al., 2007; Ray et al., 2008). In experimental animals these high frequency oscillations have been reported in the auditory cortex of anesthetized rats during click stimulation (Jones and Barth, 1999), and awake monkeys passively listening to tones (Steinheisser et al., 2008). Moreover, stationary visual stimulation induces high gamma frequency oscillations (60-120 Hz, called omega oscillations) in the retina and lateral geniculate nucleus (Neuenschwander & Singer, 1996; Munk & Neuenschwander, 2000). Oscillations at even higher frequency ranges (100-200 Hz) have been described in the hippocampus with the name of ripple oscillations (Buzsaki et al., 1992; Ylinen et al., 1995; Draguhn et al., 2000). They occur in the depth negative phase of hippocampal sharp waves (Buzsaki et al., 1992). High gamma oscillations (90-200 Hz) have been studied in cortical neurons of the suprasylvian, ectosylvian, and marginal gyrus in cats (Grenier et al., 2001) as well as in the somatosensory of rats (Jones & Barth, 1999; Jones et al., 2000) and monkeys (Ray et al., 2008a, 2008b). This thesis extended these previous findings by showing that high frequency oscillations are induced by perceptual processing in the auditory cortex of rodents. Moreover, the direct measurements of LFP coherence and MUA-LFP coherence suggest that the high frequency oscillations are generated by local networks (Chapter 2), and that this local coherence it define is modulated by attention-related phenomenon (Chapters 3 and 5). Additionally, I studied the correlation between these synchronization patterns and the internal states of rats performing a two-tone discrimination task while the acoustic physical attributes were maintained constant. I found that the neuronal activity

of the auditory cortex, as indexed as firing rate or oscillatory synchronization at high frequencies, predicts the behavioral performance of the rats. These results strongly support the hypothesis that the early stages of processing in the auditory cortex do not behave as a feature detection system, but process auditory objects and non-acoustic information that are relevant for goal-directed behavior. Moreover, it suggests that the local neuronal synchronization at the early auditory areas is a possible neuronal mechanism by which neurons ensemble, likely processing non-acoustic features that are related with acoustic tasks, and can have a distinctive advantage in driving postsynaptic neurons of the temporal cortex. These neurons could then drive the activity of the DLPFC and/or vPFC, which would modulate the auditory thalamic nuclei via the TRN through feedback projection to these nuclei.

Bibliography

Abeles, M. (1982), *Local Cortical Circuits: An Electrophysiological Study*, Springer-Verlag, Berlin.

Abeles, M. (1982), 'Quantification, smoothing, and confidence limits for single-units' histograms', *Journal of Neuroscience Methods* **5**(4), 317--325.

Adrian, E. D. (1950), 'The electrical activity of the mammalian olfactory bulb', *Electroencephalography and Clinical Neurophysiology* **2**(4), 377--388.

Ahissar, E.; Nagarajan, S.; Ahissar, M.; Protopapas, A.; Mahncke, H. & Merzenich, M. M. (2001), 'Speech comprehension is correlated with temporal response patterns recorded from auditory cortex', *Proceedings of the National Academy of Sciences of the United States of America* **98**(23), 13367--72.

Ahissar, M.; Ahissar, E.; Bergman, H. & Vaadia, E. (1992), 'Encoding of sound-source location and movement: activity of single neurons and interactions between adjacent neurons in the monkey auditory cortex', *Journal of Neurophysiology* **67**(1), 203--15.

Alain, C. & Arnott, S. R. (2000), 'Selectively attending to auditory objects', *Frontiers in Bioscience:* **5**, D202--12.

Alain, C.; Arnott, S. R. & Picton, T. W. (2001), 'Bottom-up and top-down influences on auditory scene analysis: evidence from event-related brain potentials', *Journal of Experimental Psychology. Human Perception and Performance* **27**(5), 1072--89.

Allport, A. (2003). Visual Attention. Chapter 16 *In Foundations of Cognitive Neuroscience* . Ed. Posner,M. Ed. The MIT Press.

Altschuler, R.P. *Neurobiology of Hearing:* volume 2, *The Central Auditory System*. Edited by R.A. Altschuler, R.P. Bobbin, B.M. Clopton, and D.W. Hoffman. New York: Raven Press, Ltd., 1991, 293-333.

Anderson, S. E.; Kilgard, M. P.; Sloan, A. M. & Rennaker, R. L. (2006), 'Response to broadband repetitive stimuli in auditory cortex of the unanesthetized rat', *Hearing Research* **213**(1-2), 107--117.

Anllo-Vento, L.; Schoenfeld M.A., Hillyard., S.A. (2004). " Cortical Mechanism of Visual Attention: Electrophysiological and Neuroimaging Studies ". In :. In Posner, M. I. (2004), *Cognitive Neuroscience of Attention*, Guilford Press.

Arnault, P. & Roger, M. (1990), 'Ventral temporal cortex in the rat: connections of secondary auditory areas Te2 and Te3', *The Journal of Comparative Neurology* **302**(1), 110--123.

Amitai, Y.; Gibson, J. R.; Beierlein, M.; Patrick, S. L.; Ho, A. M.; Connors, B. W. & Golomb, D. (2002), 'The spatial dimensions of electrically coupled networks of interneurons in the neocortex', *The Journal of Neuroscience: The Official Journal of the Society for Neuroscience* **22**(10), 4142--4152.

Aston-Jones, G. & Cohen, J. D. (2005), 'Adaptive gain and the role of the locus coeruleus-norepinephrine system in optimal performance', *The Journal of Comparative Neurology* **493**(1), 99--110.

Azouz, R. & Gray, C. M. (2003), 'Adaptive coincidence detection and dynamic gain control in visual cortical neurons in vivo', *Neuron* **37**(3), 513--523.

Azouz, R. & Gray, C. M. (2000), 'Dynamic spike threshold reveals a mechanism for synaptic coincidence detection in cortical neurons in vivo', *Proceedings of the National Academy of Sciences of the United States of America* **97**(14), 8110—8115

Bao, S.; Chang, E. F.; Woods, J. & Merzenich, M. M. (2004), 'Temporal plasticity in the primary auditory cortex induced by operant perceptual learning', *Nature Neuroscience* **7**(9), 974--981.

Barnes, R. & Jones, M. R. (2000), 'Expectancy, attention, and time', *Cognitive Psychology* **41**(3), 254--311.

Barrie, J. M.; Freeman, W. J. & Lenhart, M. D. (1996), 'Spatiotemporal analysis of prepyriform, visual, auditory, and somesthetic surface EEGs in trained rabbits', *Journal of Neurophysiology* **76**(1), 520--539.

Barth, D. S. & Di, S. (1991), 'The functional anatomy of middle latency auditory evoked potentials', *Brain Research* **565**(1), 109--15.

Barth, D. S. & Di, S. (1990), 'Three-dimensional analysis of auditory-evoked potentials in rat neocortex', *Journal of Neurophysiology* **64**(5), 1527--36.

Barth, D. S.; Goldberg, N.; Brett, B. & Di, S. (1995), 'The spatiotemporal organization of auditory, visual, and auditory-visual evoked potentials in rat cortex', *Brain Research* **678**(1-2), 177--90.

Barth, D. S. & MacDonald, K. D. (1996), 'Thalamic modulation of high-frequency oscillating potentials in auditory cortex', *Nature* **383**(6595), 78--81.

Bartlett, E. L. & Wang, X. (2007), 'Neural representations of temporally modulated signals in the auditory thalamus of awake primates', *Journal of Neurophysiology* **97**(2), 1005--1017.

Bee, M. A. & Klump, G. M. (2005), 'Auditory stream segregation in the songbird forebrain: effects of time intervals on responses to interleaved tone sequences', *Brain, Behavior and Evolution* **66**(3), 197--214.

Bee, M. A. & Klump, G. M. (2004), 'Primitive auditory stream segregation: a neurophysiological study in the songbird forebrain', *Journal of Neurophysiology* **92**(2), 1088--1104.

Bee, M. A. & Micheyl, C. (2008), 'The cocktail party problem: what is it? How can it be solved? And why should animal behaviorists study it?', *Journal of Comparative Psychology (Washington, D.C.: 1983)* **122**(3), 235--251.

Beierlein, M.; Gibson, J. R. & Connors, B. W. (2000), 'A network of electrically coupled interneurons drives synchronized inhibition in neocortex', *Nature Neuroscience* **3**(9), 904--910.

Bendor, D. & Wang, X. (2007), 'Differential neural coding of acoustic flutter within primate auditory cortex', *Nature Neuroscience* **10**(6), 763--771.

Bendor, D. & Wang, X. (2005), 'The neuronal representation of pitch in primate auditory cortex', *Nature* **436**(7054), 1161--1165.

Bichot, N. P. & Desimone, R. (2006), 'Finding a face in the crowd: parallel and serial neural mechanisms of visual selection', *Progress in Brain Research* **155**, 147--56.

Bichot, N. P.; Rossi, A. F. & Desimone, R. (2005), 'Parallel and serial neural mechanisms for visual search in macaque area V4', *Science (New York, N.Y.)* **308**(5721), 529--34.

Blum, P. S. & Gilman, S. (1979), 'Vestibular, somatosensory, and auditory input to the thalamus of the cat', *Experimental Neurology* **65**(2), 343--354.

Bordi, F. & LeDoux, J. E. (1994), 'Response properties of single units in areas of rat auditory thalamus that project to the amygdala. I. Acoustic discharge patterns and frequency receptive fields', *Experimental Brain Research. Experimentelle Hirnforschung. Expérimentation Cérébrale* **98**(2), 261--274.

Bordi, F. & LeDoux, J. E. (1994), 'Response properties of single units in areas of rat auditory thalamus that project to the amygdala. II. Cells receiving convergent auditory and somatosensory inputs and cells antidromically activated by amygdala stimulation', *Experimental Brain Research.* **98**(2), 275--286.

Bowen, G. P.; Lin, D.; Taylor, M. K. & Ison, J. R. (2003), 'Auditory cortex lesions in the rat impair both temporal acuity and noise increment thresholds, revealing a common neural substrate', *Cerebral Cortex (New York, N.Y.: 1991)* **13**(8), 815--822.

Bregman, A. S. (1994), *Auditory Scene Analysis: The Perceptual Organization of Sound*,

The MIT Press.

Bregman, A. S.; Ahad, P. A.; Crum, P. A. & O'Reilly, J. (2000), 'Effects of time intervals and tone durations on auditory stream segregation', *Perception & Psychophysics* **62**(3), 626--636.

Bressler, S. L. & Freeman, W. J. (1980), 'Frequency analysis of olfactory system EEG in cat, rabbit, and rat', *Electroencephalography and Clinical Neurophysiology* **50**(1-2), 19--24.

Bressler, S. L. (1984), 'Spatial organization of EEGs from olfactory bulb and cortex', *Electroencephalography and Clinical Neurophysiology* **57**(3), 270--276.

Bressler, S. L. (1987), 'Relation of olfactory bulb and cortex. I. Spatial variation of bulbocortical interdependence', *Brain Research* **409**(2), 285--293.

Brett, B.; Di, S.; Watkins, L. & Barth, D. S. (1994), 'A horseradish peroxidase study of parallel thalamocortical projections responsible for the generation of mid-latency auditory-evoked potentials', *Brain Research* **647**(1), 65--75.

Brett, B.; Krishnan, G. & Barth, D. S. (1996), 'The effects of subcortical lesions on evoked potentials and spontaneous high frequency (gamma-band) oscillating potentials in rat auditory cortex', *Brain Research* **721**(1-2), 155--66.

Brett, B. & Barth, D. S. (1997), 'Subcortical modulation of high-frequency (gamma band) oscillating potentials in auditory cortex', *Journal of Neurophysiology* **78**(2), 573--81.

Britten, K. H.; Shadlen, M. N.; Newsome, W. T. & Movshon, J. A. (1992), 'The analysis of visual motion: a comparison of neuronal and psychophysical performance', *The Journal of Neuroscience* **12**(12), 4745--4765.

Brosch, M. & Schreiner, C. E. (1997), 'Time course of forward masking tuning curves in cat primary auditory cortex', *Journal of Neurophysiology* **77**(2), 923--43.

Brosch, M. & Schreiner, C. E. (1999), 'Correlations between neural discharges are related to receptive field properties in cat primary auditory cortex', *The European Journal of Neuroscience* **11**(10), 3517--30.

Brosch, M.; Budinger, E. & Scheich, H. (2002), 'Stimulus-related gamma oscillations in primate auditory cortex', *Journal of Neurophysiology* **87**(6), 2715--25.

Brosch, M.; Selezneva, E. & Scheich, H. (2005), 'Nonauditory events of a behavioral procedure activate auditory cortex of highly trained monkeys', *The Journal of Neuroscience: The Official Journal of the Society for Neuroscience* **25**(29), 6797--6806.

Bullock, T.H; McClune. M.C. (1989). Lateral coherence of the electrocorticogram: a new measure of brain synchrony. *Electroencephalogr Clin Neurophysiol*. Dec;73(6):479-98

Bullock TH. (1997). Signals and signs in the nervous system: the dynamic anatomy of electrical activity is probably information-rich. Proc Natl Acad Sci U S A. Jan 7;94(1):1-6.

Buzsaki, G.; Bickford, R. G.; Ponomareff, G.; Thal, L. J.; Mandel, R. & Gage, F. H. (1988), 'Nucleus basalis and thalamic control of neocortical activity in the freely moving rat', *The Journal of Neuroscience* **8**(11), 4007--26.

Buzsáki, G.; Horváth, Z.; Urioste, R.; Hetke, J. & Wise, K. (1992), 'High-frequency network oscillation in the hippocampus', *Science (New York, N.Y.)* **256**(5059), 1025--1027.

Buzsáki, G. & Draguhn, A. (2004), 'Neuronal oscillations in cortical networks', *Science (New York, N.Y.)* **304**(5679), 1926--9.

Canolty, R. T.; Edwards, E.; Dalal, S. S.; Soltani, M.; Nagarajan, S. S.; Kirsch, H. E.; Berger, M. S.; Barbaro, N. M. & Knight, R. T. (2006), 'High gamma power is phase-locked to theta oscillations in human neocortex', *Science (New York, N.Y.)* **313**(5793), 1626--8.

Canolty, R. T.; Soltani, M.; Dalal, S. S.; Edwards, E.; Dronkers, N. F.; Nagarajan, S. S.; Kirsch, H. E.; Barbaro, N. M. & Knight, R. T. (2007), 'Spatiotemporal dynamics of word processing in the human brain', *Frontiers in Neuroscience* **1**(1), 185--96.

Cooke, J. E.; Zhang, H. & Kelly, J. B. (2007), 'Detection of sinusoidal amplitude modulated sounds: deficits after bilateral lesions of auditory cortex in the rat', *Hearing Research* **231**(1-2), 90--99.

Cohen, Y. E.; Russ, B. E.; Gifford, G. W.; Kiringoda, R. & MacLean, K. A. (2004), 'Selectivity for the spatial and nonspatial attributes of auditory stimuli in the ventrolateral prefrontal cortex', *The Journal of Neuroscience* **24**(50), 11307--11316.

Cohen, Y. E.; Cohen, I. S. & Gifford, G. W. (2004), 'Modulation of LIP activity by predictive auditory and visual cues', *Cerebral Cortex (New York, N.Y.: 1991)* **14**(12), 1287--1301.

Cohen, Y. E.; Theunissen, F.; Russ, B. E. & Gill, P. (2007), 'Acoustic features of rhesus vocalizations and their representation in the ventrolateral prefrontal cortex', *Journal of Neurophysiology* **97**(2), 1470--1484.

Cohen, Y. E.; Hauser, M. D. & Russ, B. E. (2006), 'Spontaneous processing of abstract categorical information in the ventrolateral prefrontal cortex', *Biology Letters* **2**(2), 261--265.

Connor, C. E.; Egeth, H. E. & Yantis, S. (2004), 'Visual attention: bottom-up versus top-down', *Current Biology: CB* **14**(19), R850--852.

Colombo, M.; Rodman, H. R. & Gross, C. G. (1996), 'The effects of superior temporal cortex lesions on the processing and retention of auditory information in monkeys (Cebus apella)', *The Journal of Neuroscience: The Official Journal of the Society for Neuroscience* **16**(14), 4501--4517.

Cotillon, N. & Edeline, J. M. (2000), 'Tone-evoked oscillations in the rat auditory cortex result from interactions between the thalamus and reticular nucleus', *The European Journal of Neuroscience* **12**(10), 3637--50.

Cotillon, N.; Nafati, M. & Edeline, J. M. (2000), 'Characteristics of reliable tone-evoked oscillations in the rat thalamo-cortical auditory system', *Hearing Research* **142**(1-2), 113--30.

Cotillon-Williams, N. & Edeline, J. (2003), 'Evoked oscillations in the thalamo-cortical auditory system are present in anesthetized but not in unanesthetized rats', *Journal of Neurophysiology* **89**(4), 1968--84.

Cotillon-Williams, N. & Edeline, J. (2004), 'Evoked oscillations in unit recordings from the thalamo-cortical auditory system: an aspect of temporal processing or the reflection of hyperpolarized brain states?', *Acta Neurobiologiae Experimentalis* **64**(2), 253--270.

Cowey, A. & Weiskrantz, L. (1976), 'Auditory sequence discrimination in Macaca mulatta: the role of the superior temporal cortex', *Neuropsychologia* **14**(1), 1--10.

Crabtree, J. W. (1998), 'Organization in the auditory sector of the cat's thalamic reticular nucleus', *The Journal of Comparative Neurology* **390**(2), 167--182.

Creutzfeldt, O.; Hellweg, F. C. & Schreiner, C. (1980), 'Thalamocortical transformation of responses to complex auditory stimuli', *Experimental Brain Research. Experimentelle Hirnforschung. Expérimentation Cérébrale* **39**(1), 87--104.

Crone, N. E.; Boatman, D.; Gordon, B. & Hao, L. (2001), 'Induced electrocorticographic gamma activity during auditory perception. Brazier Award-winning article, 2001', *Clinical Neurophysiology* (4), 565--82.

Crone, N. E.; Sinai, A. & Korzeniewska, A. (2006), 'High-frequency gamma oscillations and human brain mapping with electrocorticography', *Progress in Brain Research* **159**, 275--95.

Cusack, R. & Carlyon, R. (2004), “Auditory perceptual organization inside and outside the laboratory”. Chapter 2 in Neuhoff,, J. G. *Ecological psychoacoustics*.

Cunningham, M. O.; Whittington, M. A.; Bibbig, A.; Roopun, A.; LeBeau, F. E. N.; Vogt, A.; Monyer, H.; Buhl, E. H. & Traub, R. D. (2004), 'A role for fast rhythmic bursting neurons in cortical gamma oscillations in vitro', *Proceedings of the National Academy of Sciences of the United States of America* **101**(18), 7152--7.

Deans, M. R.; Gibson, J. R.; Sellitto, C.; Connors, B. W. & Paul, D. L. (2001), 'Synchronous activity of inhibitory networks in neocortex requires electrical synapses containing connexin36', *Neuron* **31**(3), 477--485.

Dannenbring, G. L. & Bregman, A. S. (1976), 'Effect of silence between tones on auditory stream segregation', *The Journal of the Acoustical Society of America* **59**(4), 987--989.

deCharms, R. C. & Merzenich, M. M. (1996), 'Primary cortical representation of sounds by the coordination of action-potential timing', *Nature* **381**(6583), 610--3.

deCharms, R. C.; Blake, D. T. & Merzenich, M. M. (1998), 'Optimizing sound features for cortical neurons', *Science (New York, N.Y.)* **280**(5368), 1439--43.

Desimone, R. & Duncan, J. (1995), 'Neural mechanisms of selective visual attention', *Annual Review of Neuroscience* **18**, 193--222.

Diamond, D. M.; Campbell, A. M.; Park, C. R.; Halonen, J. & Zoladz, P. R. (2007), 'The temporal dynamics model of emotional memory processing: a synthesis on the neurobiological basis of stress-induced amnesia, flashbulb and traumatic memories, and the Yerkes-Dodson law', *Neural Plasticity* **2007**, 60803.

Di, S. & Barth, D. S. (1992), 'The functional anatomy of middle-latency auditory evoked potentials: thalamocortical connections', *Journal of Neurophysiology* **68**(2), 425--31.

Dickson, J. W. & Gerstein, G. L. (1974), 'Interactions between neurons in auditory cortex of the cat', *Journal of Neurophysiology* **37**(6), 1239--61.

Donoghue, J. P.; Sanes, J. N.; Hatsopoulos, N. G. & Gaál, G. (1998), 'Neural discharge and local field potential oscillations in primate motor cortex during voluntary movements', *Journal of Neurophysiology* **79**(1), 159--73.

Doron, N. N. & Ledoux, J. E. (2000), 'Cells in the posterior thalamus project to both amygdala and temporal cortex: A quantitative retrograde double-labeling study in the rat', *The Journal of Comparative Neurology* **425**(2), 257--274.

Doron, N. N.; Ledoux, J. E. & Semple, M. N. (2002), 'Redefining the tonotopic core of rat auditory cortex: physiological evidence for a posterior field', *The Journal of Comparative Neurology* **453**(4), 345--360.

Draguhn, A.; Traub, R. D.; Bibbig, A. & Schmitz, D. (2000), 'Ripple (approximately 200-

Hz) oscillations in temporal structures', *Journal of Clinical Neurophysiology* (4), 361--376.

Edwards, E.; Soltani, M.; Deouell, L. Y.; Berger, M. S. & Knight, R. T. (2005), 'High Gamma Activity in Response to Deviant Auditory Stimuli Recorded Directly From Human Cortex', *J Neurophysiol* **94**(6), 4269--4280.

Efron, B. & Tibshirani, R. (1994), *An Introduction to the Bootstrap*, Chapman & Hall/CRC.

Eggermont, J. J. (1991), 'Rate and synchronization measures of periodicity coding in cat primary auditory cortex', *Hearing Research* **56**(1-2), 153--67.

Eggermont, J. J. (1994), 'Neural interaction in cat primary auditory cortex II. Effects of sound stimulation', *Journal of Neurophysiology* **71**(1), 246--70.

Eggermont, J. J. & Smith, G. M. (1995), 'Synchrony between single-unit activity and local field potentials in relation to periodicity coding in primary auditory cortex', *Journal of Neurophysiology* **73**(1), 227--45.

Eggermont, J. J. & Smith, G. M. (1996), 'Neural connectivity only accounts for a small part of neural correlation in auditory cortex', *Experimental Brain Research.* **110**(3), 379--91.

Eggermont, J. J. & Ponton, C. W. (2001), 'The neurophysiology of auditory perception: from single units to evoked potentials', *Audiology & Neuro-Otology* **7**(2), 71--99.

Eggermont, J. J. (2002), 'Temporal modulation transfer functions in cat primary auditory cortex: separating stimulus effects from neural mechanisms', *Journal of Neurophysiology* **87**(1), 305--21.

Eggermont, J. J. (2006), 'Properties of correlated neural activity clusters in cat auditory cortex resemble those of neural assemblies', *Journal of Neurophysiology* **96**(2), 746--64.

Ehret, G. (1997), 'The auditory cortex', *Journal of Comparative Physiology. A, Sensory, Neural, and Behavioral Physiology* **181**(6), 547--557.

Elhilali, M.; Fritz, J. B.; Klein, D. J.; Simon, J. Z. & Shamma, S. A. (2004), 'Dynamics of precise spike timing in primary auditory cortex', *The Journal of Neuroscience* **24**(5), 1159--1172.

Engel, A. K.; König, P.; Gray, C. M. & Singer, W. (1990), 'Stimulus-Dependent Neuronal Oscillations in Cat Visual Cortex: Inter-Columnar Interaction as Determined by Cross-Correlation Analysis', *The European Journal of Neuroscience* **2**(7), 588--606.

Engel, A.; Konig, P.; Kreiter, A. & Singer, W. (1991), 'Interhemispheric synchronization

of oscillatory neuronal responses in cat visual cortex', *Science (New York, N.Y.)* **252**(5009), 1177--1179.

Engel, A. K.; Kreiter, A. K.; König, P. & Singer, W. (1991), 'Synchronization of oscillatory neuronal responses between striate and extrastriate visual cortical areas of the cat', *Proceedings of the National Academy of Sciences of the United States of America* **88**(14), 6048--52.

Engel, A. K.; König, P.; Kreiter, A. K. & Singer, W. (1991), 'Interhemispheric synchronization of oscillatory neuronal responses in cat visual cortex', *Science (New York, N.Y.)* **252**(5010), 1177--9.

Engel, A. K.; König, P. & Singer, W. (1991), 'Direct physiological evidence for scene segmentation by temporal coding', *Proceedings of the National Academy of Sciences of the United States of America* **88**(20), 9136--40.

Engel, A. K.; Fries, P. & Singer, W. (2001), 'Dynamic predictions: oscillations and synchrony in top-down processing', *Nature Reviews. Neuroscience* **2**(10), 704--716.

Engineer, N. D.; Percaccio, C. R.; Pandya, P. K.; Moucha, R.; Rathbun, D. L. & Kilgard, M. P. (2004), 'Environmental enrichment improves response strength, threshold, selectivity, and latency of auditory cortex neurons', *Journal of Neurophysiology* **92**(1), 73--82.

Espinosa, I. E. & Gerstein, G. L. (1988), 'Cortical auditory neuron interactions during presentation of 3-tone sequences: effective connectivity', *Brain Research* **450**(1-2), 39--50.

Essen, D. C. V. & Gallant, J. L. (1994), 'Neural mechanisms of form and motion processing in the primate visual system', *Neuron* **13**(1), 1--10.

Faulkner, H. J.; Traub, R. D. & Whittington, M. A. (1998), 'Disruption of synchronous gamma oscillations in the rat hippocampal slice: A common mechanism of anaesthetic drug action', *British Journal of Pharmacology* **125**(3), 483_492.

Fawcett T., (2006). " A introduction of ROC analysis". *Pattern Recognition Letters* .**27:** 861-874.

Freedman, D. J.; Riesenhuber, M.; Poggio, T. & Miller, E. K. (2001), 'Categorical representation of visual stimuli in the primate prefrontal cortex', *Science (New York, N.Y.)* **291**(5502), 312--316.

Fell, J.; Fernández, G.; Klaver, P.; Elger, C. E. & Fries, P. (2003), 'Is synchronized neuronal gamma activity relevant for selective attention?', *Brain Research. Brain Research Reviews* **42**(3), 265--72.

Fettiplace, R. & Hackney, C. M. (2006), 'The sensory and motor roles of auditory hair cells', *Nature Reviews. Neuroscience* **7**(1), 19--29.

Fishman, Y. I.; Arezzo, J. C. & Steinschneider, M. (2004), 'Auditory stream segregation in monkey auditory cortex: effects of frequency separation, presentation rate, and tone duration', *The Journal of the Acoustical Society of America* **116**(3), 1656--1670.

Fishman, Y. I.; Reser, D. H.; Arezzo, J. C. & Steinschneider, M. (2001), 'Neural correlates of auditory stream segregation in primary auditory cortex of the awake monkey', *Hearing Research* **151**(1-2), 167--187.

Franowicz, M. N. & Barth, D. S. (1995), 'Comparison of evoked potentials and high-frequency (gamma-band) oscillating potentials in rat auditory cortex', *Journal of Neurophysiology* **74**(1), 96--112.

Freeman, W. J. (1978), 'Spatial properties of an EEG event in the olfactory bulb and cortex', *Electroencephalography and Clinical Neurophysiology* **44**(5), 586--605.

Frien, A. & Eckhorn, R. (2000), 'Functional coupling shows stronger stimulus dependency for fast oscillations than for low-frequency components in striate cortex of awake monkey', *The European Journal of Neuroscience* **12**(4), 1466--78.

Frien, A.; Eckhorn, R.; Bauer, R.; Woelbern, T. & Gabriel, A. (2000), 'Fast oscillations display sharper orientation tuning than slower components of the same recordings in striate cortex of the awake monkey', *The European Journal of Neuroscience* **12**(4), 1453--65.

Fries, P. (2005), 'A mechanism for cognitive dynamics: neuronal communication through neuronal coherence', *Trends in Cognitive Sciences* **9**(10), 474--80.

Fries, P.; Neuenschwander, S.; Engel, A. K.; Goebel, R. & Singer, W. (2001), 'Rapid feature selective neuronal synchronization through correlated latency shifting', *Nature Neuroscience* **4**(2), 194--200.

Fries, P.; Nikoli_, D. & Singer, W. (2007), 'The gamma cycle', *Trends in Neurosciences* **30**(7), 309--316.

Fries, P.; Reynolds, J. H.; Rorie, A. E. & Desimone, R. (2001), 'Modulation of oscillatory neuronal synchronization by selective visual attention', *Science (New York, N.Y.)* **291**(5508), 1560--3.

Fries, P.; Roelfsema, P. R.; Engel, A. K.; König, P. & Singer, W. (1997), 'Synchronization of oscillatory responses in visual cortex correlates with perception in interocular rivalry', *Proceedings of the National Academy of Sciences of the United States of America* **94**(23), 12699--12704.

Fries, P.; Schröder, J.; Roelfsema, P. R.; Singer, W. & Engel, A. K. (2002), 'Oscillatory neuronal synchronization in primary visual cortex as a correlate of stimulus selection', *The Journal of Neuroscience: The Official Journal of the Society for Neuroscience* **22**(9), 3739--3754.

Fries, P.; Womelsdorf, T.; Oostenveld, R. & Desimone, R. (2008), 'The effects of visual stimulation and selective visual attention on rhythmic neuronal synchronization in macaque area V4', *The Journal of Neuroscience: The Official Journal of the Society for Neuroscience* **28**(18), 4823--35.

Frisina, R. D. (2001), 'Subcortical neural coding mechanisms for auditory temporal processing', *Hearing Research* **158**(1-2), 1--27.

Fritz, J.; Shamma, S.; Elhilali, M. & Klein, D. (2003), 'Rapid task-related plasticity of spectrotemporal receptive fields in primary auditory cortex', *Nature Neuroscience* **6**(11), 1216--23.

Fritz, J.; Elhilali, M. & Shamma, S. (2005), 'Active listening: task-dependent plasticity of spectrotemporal receptive fields in primary auditory cortex', *Hearing Research* **206**(1-2), 159--176.

Fritz, J. B.; Elhilali, M. & Shamma, S. A. (2005), 'Differential Dynamic Plasticity of A1 Receptive Fields during Multiple Spectral Tasks', *J. Neurosci.* **25**(33), 7623--7635.

Fritz, J. B.; Elhilali, M.; David, S. V. & Shamma, S. A. (2007), 'Does attention play a role in dynamic receptive field adaptation to changing acoustic salience in A1?', *Hearing Research* **229**(1-2), 186--203.

Fritz, J. B.; Elhilali, M.; David, S. V. & Shamma, S. A. (2007), 'Auditory attention--focusing the searchlight on sound', *Current Opinion in Neurobiology* **17**(4), 437--55.

Fritz, J. B.; Elhilali, M. & Shamma, S. A. (2007), 'Adaptive changes in cortical receptive fields induced by attention to complex sounds', *Journal of Neurophysiology* **98**(4), 2337--46.

Frostig, R. D.; Gottlieb, Y.; Vaadia, E. & Abeles, M. (1983), 'The effects of stimuli on the activity and functional connectivity of local neuronal groups in the cat auditory cortex', *Brain Research* **272**(2), 211--21.

Fukuda, T.; Kosaka, T.; Singer, W. & Galuske, R. A. W. (2006), 'Gap junctions among dendrites of cortical GABAergic neurons establish a dense and widespread intercolumnar network', *The Journal of Neuroscience: The Official Journal of the Society for Neuroscience* **26**(13), 3434--3443.

Galambos, R.; Makeig, S. & Talmachoff, P. J. (1981), 'A 40-Hz auditory potential recorded from the human scalp', *Proceedings of the National Academy of Sciences of the*

United States of America **78**(4), 2643--7.

Galarreta, M. & Hestrin, S. (1999), 'A network of fast-spiking cells in the neocortex connected by electrical synapses', *Nature* **402**(6757), 72--75.

Galarreta, M. & Hestrin, S. (2001), 'Spike transmission and synchrony detection in networks of GABAergic interneurons', *Science (New York, N.Y.)* **292**(5525), 2295--2299.

Gibson, J. R.; Beierlein, M. & Connors, B. W. (1999), 'Two networks of electrically coupled inhibitory neurons in neocortex', *Nature* **402**(6757), 75--79.

Gifford, G. W. & Cohen, Y. E. (2005), 'Spatial and non-spatial auditory processing in the lateral intraparietal area', *Experimental Brain Research. Experimentelle Hirnforschung. Expérimentation Cérébrale* **162**(4), 509--512.

Gifford, G. W.; MacLean, K. A.; Hauser, M. D. & Cohen, Y. E. (2005), 'The neurophysiology of functionally meaningful categories: macaque ventrolateral prefrontal cortex plays a critical role in spontaneous categorization of species-specific vocalizations', *Journal of Cognitive Neuroscience* **17**(9), 1471--1482.

Grenier, F.; Timofeev, I. & Steriade, M. (2001), 'Focal synchronization of ripples (80-200 Hz) in neocortex and their neuronal correlates', *Journal of Neurophysiology* **86**(4), 1884--1898.

Gray, C. M.; König, P.; Engel, A. K. & Singer, W. (1989), 'Oscillatory responses in cat visual cortex exhibit inter-columnar synchronization which reflects global stimulus properties', *Nature* **338**(6213), 334--337.

Gray, C. M. & Singer, W. (1989), 'Stimulus-specific neuronal oscillations in orientation columns of cat visual cortex', *Proceedings of the National Academy of Sciences of the United States of America* **86**(5), 1698--702.

Gray, C. M.; Engel, A. K.; König, P. & Singer, W. (1990), 'Stimulus-Dependent Neuronal Oscillations in Cat Visual Cortex: Receptive Field Properties and Feature Dependence', *The European Journal of Neuroscience* **2**(7), 607--619.

Gray, C. M.; Engel, A. K.; König, P. & Singer, W. (1992), 'Synchronization of oscillatory neuronal responses in cat striate cortex: temporal properties', *Visual Neuroscience* **8**(4), 337--47.

Gray, C. M. & Prisco, G. V. D. (1997), 'Stimulus-dependent neuronal oscillations and local synchronization in striate cortex of the alert cat', *The Journal of Neuroscience: The Official Journal of the Society for Neuroscience* **17**(9), 3239--53.

Green, D.M and Swets, J.M. (1966). *Signal detection theory and psychophysics*. New York: John Wiley and Sons Inc..

Grimault, N.; Bacon, S. P. & Micheyl, C. (2002), 'Auditory stream segregation on the basis of amplitude-modulation rate', *The Journal of the Acoustical Society of America* **111**(3), 1340--1348

Griffiths, T. D.; Rees, A.; Witton, C.; Cross, P. M.; Shakir, R. A. & Green, G. G. (1997), 'Spatial and temporal auditory processing deficits following right hemisphere infarction. A psychophysical study', *Brain: A Journal of Neurology* **120 (Pt 5)**, 785--794.

Griffiths, T.D.; Warren, J.D.(2004) What is an auditory object?. Nat Rev Neurosci. Nov;5(11):887-92.

Gutschalk, A.; Oxenham, A. J.; Micheyl, C.; Wilson, E. C. & Melcher, J. R. (2007), 'Human Cortical Activity during Streaming without Spectral Cues Suggests a General Neural Substrate for Auditory Stream Segregation', *J. Neurosci.* **27**(48), 13074--13081

Hallanger, A. E.; Levey, A. I.; Lee, H. J.; Rye, D. B. & Wainer, B. H. (1987), 'The origins of cholinergic and other subcortical afferents to the thalamus in the rat', *The Journal of Comparative Neurology* **262**(1), 105--24.

Halliday, D.M. & Rosenberg, J.R. (1999). Time and frequency domain analysis of spike train and time series data. In: *Modern Techniques in Neuroscience Research*, (Eds. U. Windhorst & H. Johansson), Springer-Verlag, Ch 18, 503-543

Handel, S. (1989), *Listening: An Introduction to the Perception of Auditory Events (Bradford Books*, MIT Press.

Henze, D. A.; Borhegyi, Z.; Csicsvari, J.; Mamiya, A.; Harris, K. D. & Buzsaki, G. (2000), 'Intracellular Features Predicted by Extracellular Recordings in the Hippocampus In Vivo', *J Neurophysiol* **84**(1), 390--400.

Hesterberg. T; Moore., D.S.; Monaghan., S; Clipson, A.; Epstein, R. (2008). Bootstrap Methods and Permutation Tests . *In chaptern 14 of The Practice of Business Statistics: Using Data for Decisions.* Editors: Moore, D.S.; MacCabe, G.P., Duckworth, W.M.; Alwan, L., W. H. Freeman Company.

He, J. (2003), 'Corticofugal modulation of the auditory thalamus', *Experimental Brain Research.* **153**(4), 579--590.

Herculano-Houzel, S.; Munk, M. H.; Neuenschwander, S. & Singer, W. (1999), 'Precisely synchronized oscillatory firing patterns require electroencephalographic activation', *The Journal of Neuroscience* **19**(10), 3992--4010.

Herrmann, C. S. & Knight, R. T. (2001), 'Mechanisms of human attention: event-related potentials and oscillations', *Neuroscience and Biobehavioral Reviews* **25**(6), 465--76.

Hirch. I.J., Auditory perception of temporal order. *The Journal of the Acoustical Society of America* 31, 759-767.

Hocherman S, Benson DA, Goldstein MH Jr, Heffner HE, Hienz RD.”Evoked unit activity in auditory cortex of monkeys performing a selective attention task.” Brain Res. 1976 Nov 19;117(1):51-68

Horikawa, J.; Tanahashi, A. & Suga, N. (1994), 'After-discharges in the auditory cortex of the mustached bat: No oscillatory discharges for binding auditory information', *Hearing Research* **76**(1-2), 45--52.

Hormuzdi, S. G.; Pais, I.; LeBeau, F. E.; Towers, S. K.; Rozov, A.; Buhl, E. H.; Whittington, M. A. & Monyer, H. (2001), 'Impaired electrical signaling disrupts gamma frequency oscillations in connexin 36-deficient mice', *Neuron* **31**(3), 487--495.

Horton, J. C. & Adams, D. L. (2005), 'The cortical column: a structure without a function', *Philosophical Transactions of the Royal Society of London. Series B, Biological Sciences* **360**(1456), 837--862.

Hu, B. (2003), 'Functional organization of lemniscal and nonlemniscal auditory thalamus', *Experimental Brain Research. Experimentelle Hirnforschung. Expérimentation Cérébrale* **153**(4), 543--549.

Huang, C. L. & Winer, J. A. (2000), 'Auditory thalamocortical projections in the cat: laminar and areal patterns of input', *The Journal of Comparative Neurology* **427**(2), 302--331.

Hubel, D. H.; Henson, C. O.; Rupert, A. & Galambos, R. (1959), 'Attention units in the auditory cortex', *Science (New York, N.Y.)* **129**(3358), 1279--1280.

Hubel, D. H. & Wiesel, T. N. (1962), 'Receptive fields, binocular interaction and functional architecture in the cat's visual cortex', *The Journal of Physiology* **160**, 106--154.

Hubel, D. H. & Wiesel, T. N. (1963), 'Shape and arrangement of columns in cat's striate cortex', *The Journal of Physiology* **165**, 559--568.

Hubel, D. H. (1995), *Eye, Brain, and Vision*, W. H. Freeman.

Humphrey, D.R; Schmidt, E.M. (1990).” Extracellular Single-Unit Recording Methods”. In Neurophysiological Techniques: Applications to Neural Systems. Editors: Alan A. Boulton, A.A.; Baker, G.B.; Vanderwolf, G.H., Ed. Springer Protocols.

Ikegaya, Y.; Aaron, G.; Cossart, R.; Aronov, D.; Lampl, I.; Ferster, D. & Yuste, R. (2004), 'Synfire chains and cortical songs: temporal modules of cortical activity', *Science (New York, N.Y.)* **304**(5670), 559--564.

Itti, L. & Koch, C. (2001), 'Computational modelling of visual attention', *Nature Reviews. Neuroscience* **2**(3), 194--203.

Izumi, A. (2002), 'Auditory stream segregation in Japanese monkeys', *Cognition* **82**(3), B113--122.

Janssen, P. & Shadlen, M. N. (2005), 'A representation of the hazard rate of elapsed time in macaque area LIP', *Nature Neuroscience* **8**(2), 234--241.

Jarvis, M. R. & Mitra, P. P. (2001), 'Sampling properties of the spectrum and coherency of sequences of action potentials', *Neural Computation* **13**(4), 717--49.

Jeschke, M.; Lenz, D.; Budinger, E.; Herrmann, C. S. & Ohl, F. W. (2008), 'Gamma oscillations in gerbil auditory cortex during a target-discrimination task reflect matches with short-term memory', *Brain Research* **1220**, 70--80.

Johnson, J. L. & Welsh, J. P. (2003), 'Independently movable multielectrode array to record multiple fast-spiking neurons in the cerebral cortex during cognition', *Methods (San Diego, Calif.)* **30**(1), 64--78.

Joliot, M.; Ribary, U. & Llinás, R. (1994), 'Human oscillatory brain activity near 40 Hz coexists with cognitive temporal binding', *Proceedings of the National Academy of Sciences of the United States of America* **91**(24), 11748--51.

Jones, B. E. (2008), 'Modulation of cortical activation and behavioral arousal by cholinergic and orexinergic systems', *Annals of the New York Academy of Sciences* **1129**, 26--34.

Jones, E. G. (2002), 'Thalamic circuitry and thalamocortical synchrony', *Philosophical Transactions of the Royal Society of London. Series B, Biological Sciences* **357**(1428), 1659--1673.

Jones. M.R., . (2004), “Attention and Timing”. Chapter 3 in Neuhoff,, J. G. *Ecological psychoacoustics*.

Jones, M. R. & Boltz, M. (1989), 'Dynamic attending and responses to time', *Psychological Review* **96**(3), 459--491.

Jones, M. S. & Barth, D. S. (1999), 'Spatiotemporal organization of fast (200 Hz) electrical oscillations in rat Vibrissa/Barrel cortex', Journal of Neurophysiology **82**: 1599--1609

Jones, M. S.; MacDonald, K. D.; Choi, B.; Dudek, F. E. & Barth, D. S. (2000), 'Intracellular correlates of fast (200 Hz) electrical oscillations in rat somatosensory cortex', **84:** 1505--1518

Jones, M. S. & Barth, D. S. (1999), 'Spatiotemporal organization of fast (200 Hz) electrical oscillations in rat Vibrissa/Barrel cortex', Journal of Neurophysiology,

Kaiser, J. & Lutzenberger, W. (2005), 'Cortical oscillatory activity and the dynamics of auditory memory processing', *Reviews in the Neurosciences* **16**(3), 239--54.

Kalatsky, V. A.; Polley, D. B.; Merzenich, M. M.; Schreiner, C. E. & Stryker, M. P. (2005), 'Fine functional organization of auditory cortex revealed by Fourier optical imaging', *Proceedings of the National Academy of Sciences of the United States of America* **102**(37), 13325--13330.

Katzner, S.; Nauhaus, I.; Benucci, A.; Bonin, V.; Ringach, D. L. & Carandini, M. (2009), 'Local origin of field potentials in visual cortex', *Neuron* **61**(1), 35--41.

Kelly, J. B. (1973), 'The effects of insular and temporal lesions in cats on two types of auditory pattern discrimination', *Brain Research* **62**(1), 71--87.

Kelly, J. B.; Rooney, B. J. & Phillips, D. P. (1996), 'Effects of bilateral auditory cortical lesions on gap-detection thresholds in the ferret (Mustela putorius)', *Behavioral Neuroscience* **110**(3), 542--550.

Kilgard, M. P. & Merzenich, M. M. (1998), 'Plasticity of temporal information processing in the primary auditory cortex', *Nature Neuroscience* **1**(8), 727--31.

Kilgard, M. P. & Merzenich, M. M. (1999), 'Distributed representation of spectral and temporal information in rat primary auditory cortex', *Hearing Research* **134**(1-2), 16--28

Kilgard, M. P.; Pandya, P. K.; Vazquez, J.; Gehi, A.; Schreiner, C. E. & Merzenich, M. M. (2001), 'Sensory input directs spatial and temporal plasticity in primary auditory cortex', *Journal of Neurophysiology* **86**(1), 326--38.

Kilgard, M. P. & Merzenich, M. M. (2002), 'Order-sensitive plasticity in adult primary auditory cortex', *Proceedings of the National Academy of Sciences of the United States of America* **99**(5), 3205--9.

Kilgard, M. P.; Vazquez, J. L.; Engineer, N. D. & Pandya, P. K. (2007), 'Experience dependent plasticity alters cortical synchronization', *Hearing Research* **229**(1-2), 171--179.

Komura, Y.; Tamura, R.; Uwano, T.; Nishijo, H.; Kaga, K. & Ono, T. (2001), 'Retrospective and prospective coding for predicted reward in the sensory thalamus', *Nature* **412**(6846), 546--549.

Komura, Y.; Tamura, R.; Uwano, T.; Nishijo, H. & Ono, T. (2005), 'Auditory thalamus integrates visual inputs into behavioral gains', *Nature Neuroscience* **8**(9), 1203--1209.

Kruse, W. & Eckhorn, R. (1996), 'Inhibition of sustained gamma oscillations (35-80 Hz) by fast transient responses in cat visual cortex', *Proceedings of the National Academy of Sciences of the United States of America* **93**(12), 6112--7.

Kubovy, M. & Valkenburg, D. V. (2001), 'Auditory and visual objects', *Cognition* **80**(1-2), 97--126.

Lachaux, J. P.; Rudrauf, D. & Kahane, P. (2003), 'Intracranial EEG and human brain mapping', *Journal of Physiology, Paris* **97**(4-6), 613--628.

Lachaux, J.; Jerbi, K.; Bertrand, O.; Minotti, L.; Hoffmann, D.; Schoendorff, B. & Kahane, P. (2007), 'A Blueprint for Real-Time Functional Mapping via Human Intracranial Recordings', *PLoS ONE* **2**(10), e1094.

Lakatos, P.; Karmos, G.; Mehta, A. D.; Ulbert, I. & Schroeder, C. E. (2008), 'Entrainment of neuronal oscillations as a mechanism of attentional selection', *Science (New York, N.Y.)* **320**(5872), 110--3.

Lakatos, P.; Shah, A. S.; Knuth, K. H.; Ulbert, I.; Karmos, G. & Schroeder, C. E. (2005), 'An oscillatory hierarchy controlling neuronal excitability and stimulus processing in the auditory cortex', *Journal of Neurophysiology* **94**(3), 1904--11.

Langner, G. (1992), 'Periodicity coding in the auditory system', *Hearing Research* **60**(2), 115--142.

Langner, G. & Schreiner, C. E. (1988), 'Periodicity coding in the inferior colliculus of the cat. I. Neuronal mechanisms', *Journal of Neurophysiology* **60**(6), 1799--1822.

Large, E. W. & Jones, M. R. (1999). The dynamics of attending: How we track time varying events. *Psychological Review*, *106* (*1*), 119-159.

Laurent, G. (1996), 'Dynamical representation of odors by oscillating and evolving neural assemblies', *Trends in Neurosciences* **19**(11), 489--96.

Laurent, G.; Wehr, M. & Davidowitz, H. (1996), 'Temporal representations of odors in an olfactory network', *The Journal of Neuroscience: The Official Journal of the Society for Neuroscience* **16**(12), 3837--3847.

LeDoux, J. E. (2000), 'Emotion circuits in the brain', *Annual Review of Neuroscience* **23**, 155--184.

Lee, C. C.; Imaizumi, K.; Schreiner, C. E. & Winer, J. A. (2004), 'Concurrent tonotopic processing streams in auditory cortex', *Cerebral Cortex (New York, N.Y.: 1991)* **14**(4), 441--451.

Lee, C. C.; Schreiner, C. E.; Imaizumi, K. & Winer, J. A. (2004), 'Tonotopic and heterotopic projection systems in physiologically defined auditory cortex', *Neuroscience* **128**(4), 871--887.

Lee, C. C. & Winer, J. A. (2008), 'Connections of cat auditory cortex: I. Thalamocortical system', *The Journal of Comparative Neurology* **507**(6), 1879--1900.

Leon, M. I. & Shadlen, M. N. (2003), 'Representation of time by neurons in the posterior parietal cortex of the macaque', *Neuron* **38**(2), 317--327.

Liang, L.; Lu, T. & Wang, X. (2002), 'Neural representations of sinusoidal amplitude and frequency modulations in the primary auditory cortex of awake primates', *Journal of Neurophysiology* **87**(5), 2237--2261.

Liégeois-Chauvel, C.; Peretz, I.; Babaï, M.; Laguitton, V. & Chauvel, P. (1998), 'Contribution of different cortical areas in the temporal lobes to music processing', *Brain: A Journal of Neurology* **121 (Pt 10)**, 1853--1867.

Llinás R.R.; Ribary (1993). Coherence 40 Hz oscillation characterizes dream state in humans. *Proceedings of the National Academy of Sciences of the United States of America* 90(8):3593-7

Llinás RR, Steriade M. (2006). *Bursting of thalamic neurons and states of vigilance.*The Journal of Neurophysiology . *95(6):3297-308.*

Linden, J. F. & Schreiner, C. E. (2003), 'Columnar transformations in auditory cortex? A comparison to visual and somatosensory cortices', *Cerebral Cortex (New York, N.Y.: 1991)* **13**(1), 83--9.

Linke, R. (1999), 'Organization of projections to temporal cortex originating in the thalamic posterior intralaminar nucleus of the rat', *Experimental Brain Research. Experimentelle Hirnforschung. Expérimentation Cérébrale* **127**(3), 314--320.

Liu, J. & Newsome, W. T. (2006), 'Local field potential in cortical area MT: stimulus tuning and behavioral correlations', *The Journal of Neuroscience: The Official Journal of the Society for Neuroscience* **26**(30), 7779--90.

Liu, J. & Newsome, W. T. (2005), 'Correlation between speed perception and neural activity in the middle temporal visual area', *The Journal of Neuroscience: The Official Journal of the Society for Neuroscience* **25**(3), 711--22.

Liu, J. & Newsome, W. T. (2003), 'Functional organization of speed tuned neurons in visual area MT', *Journal of Neurophysiology* **89**(1), 246--56.

Livingstone, M. & Hubel, D. (1988), 'Segregation of form, color, movement, and depth: anatomy, physiology, and perception', *Science (New York, N.Y.)* **240**(4853), 740--749.

Logothetis, N. K. (2002), 'The neural basis of the blood-oxygen-level-dependent functional magnetic resonance imaging signal', *Philosophical Transactions of the Royal Society of London. Series B, Biological Sciences* **357**(1424), 1003--37.

Lu, T.; Liang, L. & Wang, X. (2001b), 'Neural representations of temporally asymmetric stimuli in the auditory cortex of awake primates', *Journal of Neurophysiology* **85**(6), 2364--2380.

Lu, T.; Liang, L. & Wang, X. (2001a), 'Temporal and rate representations of time-varying signals in the auditory cortex of awake primates', *Nature Neuroscience* **4**(11), 1131--1138.

Lu, T. & Wang, X. (2004), 'Information content of auditory cortical responses to time-varying acoustic stimuli', *Journal of Neurophysiology* **91**(1), 301--313.

MacDougall-Shackleton, S. A.; Hulse, S. H.; Gentner, T. Q. & White, W. (1998), 'Auditory scene analysis by European starlings (Sturnus vulgaris): perceptual segregation of tone sequences', *The Journal of the Acoustical Society of America* **103**(6), 3581--3587.

Macdonald, K. D.; Fifkova, E.; Jones, M. S. & Barth, D. S. (1998), 'Focal Stimulation of the Thalamic Reticular Nucleus Induces Focal Gamma Waves in Cortex', *J Neurophysiol* **79**(1), 474--477.

MacDonald, K. D.; Brett, B. & Barth, D. S. (1996), 'Inter- and intra-hemispheric spatiotemporal organization of spontaneous electrocortical oscillations', *Journal of Neurophysiology* **76**(1), 423--37.

Maldonado, P. E. & Gerstein, G. L. (1996), 'Reorganization in the auditory cortex of the rat induced by intracortical microstimulation: a multiple single-unit study', *Experimental Brain Research. Experimentelle Hirnforschung. Expérimentation Cérébrale* **112**(3), 420--430.

Mainen, Z. F. & Sejnowski, T. J. (1995), 'Reliability of spike timing in neocortical neurons', *Science (New York, N.Y.)* **268**(5216), 1503--1506.

von der Malsburg, C. & Schneider, W. (1986), 'A neural cocktail-party processor', *Biological Cybernetics* **54**(1), 29--40.

Markram, H; Toledo-Rodriguez, M; Wang, Y; Gupta, A; Silberberg,G; Wu, C. (2004). Interneurons of the neocortical inhibitory system. *Nature Reviews Neuroscience* . Oct;5(10):793-807.

Maunsell, J. H. R. & Cook, E. P. (2002), 'The role of attention in visual processing', *Philosophical Transactions of the Royal Society of London. Series B, Biological Sciences* **357**(1424), 1063--1072.

Maunsell, J. H. R. & Treue, S. (2006), 'Feature-based attention in visual cortex', *Trends in Neurosciences* **29**(6), 317--322.

McAlonan, K.; Cavanaugh, J. & Wurtz, R. H. (2008), 'Guarding the gateway to cortex with attention in visual thalamus', *Nature* **456**(7220), 391--4.

Medvedev, A. V. & Kanwal, J. S. (2008), 'Communication call-evoked gamma-band activity in the auditory cortex of awake bats is modified by complex acoustic features', *Brain Research* **1188**, 76--86.

Merzenich, M. M. & Reid, M. D. (1974), 'Representation of the cochlea within the inferior colliculus of the cat', *Brain Research* **77**(3), 397--415.

Merzenich, M. M.; Knight, P. L. & Roth, G. L. (1975), 'Representation of cochlea within primary auditory cortex in the cat', *Journal of Neurophysiology* **38**(2), 231--249.

Merzenich, M. M.; Recanzone, G. H.; Jenkins, W. M. & Grajski, K. A. (1990), 'Adaptive mechanisms in cortical networks underlying cortical contributions to learning and nondeclarative memory', *Cold Spring Harbor Symposia on Quantitative Biology* **55**, 873--887.

Metherate, R.; Cox, C. L. & Ashe, J. H. (1992), 'Cellular bases of neocortical activation: modulation of neural oscillations by the nucleus basalis and endogenous acetylcholine', *The Journal of Neuroscience***12**(12), 4701--11.

Metherate, R. & Cruikshank, S. J. (1999), 'Thalamocortical inputs trigger a propagating envelope of gamma-band activity in auditory cortex in vitro', *Experimental Brain Research.* **126**(2), 160--74.

Micheyl, C.; Carlyon, R. P.; Gutschalk, A.; Melcher, J. R.; Oxenham, A. J.; Rauschecker, J. P.; Tian, B. & Wilson, E. C. (2007), 'The role of auditory cortex in the formation of auditory streams', *Hearing research* **229**(1-2), 116_131.

Micheyl, C.; Tian, B.; Carlyon, R. P. & Rauschecker, J. P. (2005), 'Perceptual organization of tone sequences in the auditory cortex of awake macaques', *Neuron* **48**(1), 139--148.

Miller, E. K.; Nieder, A.; Freedman, D. J. & Wallis, J. D. (2003), 'Neural correlates of categories and concepts', *Current Opinion in Neurobiology* **13**(2), 198--203.

Miller JM, Sutton D, Pfingst B, Ryan A, Beaton R, Gourevitch G.”Single cell activity in the auditory cortex of Rhesus monkeys: behavioral dependency.” Science. 1972 Aug 4;177(47):449-51.

Mitra, P. & Bokil, H. (2007), *Observed Brain Dynamics*, Oxford University Press, USA.

Mitra, P. P. & Pesaran, B. (1999), 'Analysis of dynamic brain imaging data', *Biophysical Journal* **76**(2), 691--708.

Mitzdorf, U. (1985), 'Current source-density method and application in cat cerebral cortex: investigation of evoked potentials and EEG phenomena', *Physiological Reviews* **65**(1), 37--100.

Moore, B. C. (2003), *An Introduction to the Psychology of Hearing*, Academic Press.

Moruzzi, G. & Magoun, H. W. (1949), 'Brain stem reticular formation and activation of the EEG', *Electroencephalography and Clinical Neurophysiology* **1**(4), 455--73.

Mountcastle, V. B. (1997), 'The columnar organization of the neocortex', *Brain: A Journal of Neurology* **120 (Pt 4)**, 701--722.

Mountcastle, V. B. (1957), 'Modality and topographic properties of single neurons of cat's somatic sensory cortex', *Journal of Neurophysiology* **20**(4), 408--434.

Munk, M. H.; Roelfsema, P. R.; König, P.; Engel, A. K. & Singer, W. (1996), 'Role of reticular activation in the modulation of intracortical synchronization', *Science (New York, N.Y.)* **272**(5259), 271--274.

Munk, M. H. & Neuenschwander, S. (2000), 'High-frequency oscillations (20 to 120 Hz) and their role in visual processing', *Journal of Clinical Neurophysiology: Official Publication of the American Electroencephalographic Society* **17**(4), 341--60.

Murthy, V. N. & Fetz, E. E. (1992), 'Coherent 25- to 35-Hz oscillations in the sensorimotor cortex of awake behaving monkeys', *Proceedings of the National Academy of Sciences of the United States of America* **89**(12), 5670--5674.

Murthy, V. N. & Fetz, E. E. (1996a), 'Oscillatory activity in sensorimotor cortex of awake monkeys: synchronization of local field potentials and relation to behavior', *Journal of Neurophysiology* **76**(6), 3949--67.

Murthy, V. N. & Fetz, E. E. (1996b), 'Synchronization of neurons during local field potential oscillations in sensorimotor cortex of awake monkeys', *Journal of Neurophysiology* **76**(6), 3968--3982.

Näätänen, R.; Paavilainen, P.; Tiitinen, H.; Jiang, D. & Alho, K. (1993), 'Attention and mismatch negativity', *Psychophysiology* **30**(5), 436--50.

Naatanen.R, & Alho., K; (2004). " Mechanism of attention as revealed by the event-related potentials of the brain". In :. In Posner, M. I. (2004), *Cognitive Neuroscience of Attention*, Guilford Press.

Näätänen, R.; Paavilainen, P.; Rinne, T. & Alho, K. (2007), 'The mismatch negativity (MMN) in basic research of central auditory processing: a review', *Clinical Neurophysiology* **118**(12), 2544--2590.

Nelken, I.; Rotman, Y. & Yosef, O. B. (1999), 'Responses of auditory-cortex neurons to structural features of natural sounds', *Nature* **397**(6715), 154--7.

Nelken, I.; Fishbach, A.; Las, L.; Ulanovsky, N. & Farkas, D. (2003), 'Primary auditory cortex of cats: feature detection or something else?', *Biological Cybernetics* **89**(5), 397--406.

Nelken, I. (2004), 'Processing of complex stimuli and natural scenes in the auditory cortex', *Current Opinion in Neurobiology* **14**(4), 474--480.

Nelken, I. & Bar-Yosef, O. (2008), 'Neurons and Objects: The Case of Auditory Cortex', *Frontiers in Neuroscience* **2**(1), 107_113.

Neuenschwander, S.; Castelo-Branco, M.; Baron, J. & Singer, W. (2002), 'Feed-forward synchronization: propagation of temporal patterns along the retinothalamocortical pathway', *Philosophical Transactions of the Royal Society of London. Series B, Biological Sciences* **357**(1428), 1869--1876.

Nicolelis, M. A. L. (2005), 'Computing with thalamocortical ensembles during different behavioural states', *The Journal of Physiology* **566**(Pt 1), 37--47.

Ohl, F. W.; Scheich, H. & Freeman, W. J. (2001), 'Change in pattern of ongoing cortical activity with auditory category learning', *Nature* **412**(6848), 733--6.

Palva, S. & Palva, J. M. (2007), 'New vistas for alpha-frequency band oscillations', *Trends in Neurosciences* **30**(4), 150--158.

Pantev, C.; Makeig, S.; Hoke, M.; Galambos, R.; Hampson, S. & Gallen, C. (1991), 'Human auditory evoked gamma-band magnetic fields', *Proceedings of the National Academy of Sciences of the United States of America* **88**(20), 8996--9000.

Paré, D.; Smith, Y.; Parent, A. & Steriade, M. (1988), 'Projections of brainstem core cholinergic and non-cholinergic neurons of cat to intralaminar and reticular thalamic nuclei', *Neuroscience* **25**(1), 69--86.

Pastore, R. E.; Layer, J. K.; Morris, C. B. & Logan, R. J. (1988), 'Temporal order identification for tone/noise stimuli with onset transitions', *Perception & Psychophysics* **44**(3), 257--271.

Percaccio, C. R.; Engineer, N. D.; Pruette, A. L.; Pandya, P. K.; Moucha, R.; Rathbun, D. L. & Kilgard, M. P. (2005), 'Environmental enrichment increases paired-pulse depression in rat auditory cortex', *Journal of Neurophysiology* **94**(5), 3590--3600.

Percaccio, C. R.; Pruette, A. L.; Mistry, S. T.; Chen, Y. H. & Kilgard, M. P. (2007), 'Sensory experience determines enrichment-induced plasticity in rat auditory cortex', *Brain Research* **1174**, 76--91.

Perkel, D. H.; Gerstein, G. L. & Moore, G. P. (1967a), 'Neuronal spike trains and stochastic point processes. II. Simultaneous spike trains', *Biophysical Journal* **7**(4), 419--40.

Perkel, D. H.; Gerstein, G. L. & Moore, G. P. (1967b), 'Neuronal spike trains and stochastic point processes. I. The single spike train', *Biophysical Journal* **7**(4), 391--418.

Pesaran, B.; Pezaris, J. S.; Sahani, M.; Mitra, P. P. & Andersen, R. A. (2002), 'Temporal structure in neuronal activity during working memory in macaque parietal cortex', *Nature Neuroscience* **5**(8), 805--11.

Petkov, C. I.; O'Connor, K. N. & Sutter, M. L. (2007), 'Encoding of illusory continuity in primary auditory cortex', *Neuron* **54**(1), 153--165.

Petkov, C. I.; O'Connor, K. N. & Sutter, M. L. (2003), 'Illusory sound perception in macaque monkeys', *The Journal of Neuroscience: The Official Journal of the Society for Neuroscience* **23**(27), 9155--9161.

Phan, M. L. & Recanzone, G. H. (2007), 'Single-neuron responses to rapidly presented temporal sequences in the primary auditory cortex of the awake macaque monkey', *Journal of Neurophysiology* **97**(2), 1726--37.

Poghosyan, V. & Ioannides, A. A. (2008), 'Attention modulates earliest responses in the primary auditory and visual cortices', *Neuron* **58**(5), 802--813.

Polley, D. B.; Read, H. L.; Storace, D. A. & Merzenich, M. M. (2007), 'Multiparametric auditory receptive field organization across five cortical fields in the albino rat', *Journal of Neurophysiology* **97**(5), 3621--3638.

Polley, D. B.; Steinberg, E. E. & Merzenich, M. M. (2006), 'Perceptual learning directs auditory cortical map reorganization through top-down influences', *The Journal of Neuroscience: The Official Journal of the Society for Neuroscience* **26**(18), 4970--82.

Prechtl, J. C.; Cohen, L. B.; Pesaran, B.; Mitra, P. P. & Kleinfeld, D. (1997), 'Visual stimuli induce waves of electrical activity in turtle cortex', *Proceedings of the National Academy of Sciences of the United States of America* **94**(14), 7621--6.

Rademacher, J.; Morosan, P.; Schormann, T.; Schleicher, A.; Werner, C.; Freund, H. J. & Zilles, K. (2001), 'Probabilistic mapping and volume measurement of human primary auditory cortex', *NeuroImage* **13**(4), 669--83.

Raphael, Y. & Altschuler, R. A. (2003), 'Structure and innervation of the cochlea', *Brain Research Bulletin* **60**(5-6), 397--422.

Rauschecker, J. P. & Tian, B. (2000), 'Mechanisms and streams for processing of "what" and "where" in auditory cortex', *Proceedings of the National Academy of Sciences of the United States of America* **97**(22), 11800--11806.

Rauschecker, J. P.; Tian, B. & Hauser, M. (1995), 'Processing of complex sounds in the macaque nonprimary auditory cortex', *Science (New York, N.Y.)* **268**(5207), 111--114.

Ray, S.; Niebur, E.; Hsiao, S. S.; Sinai, A. & Crone, N. E. (2008a), 'High-frequency gamma activity (80-150Hz) is increased in human cortex during selective attention', *Clinical Neurophysiology: Official Journal of the International Federation of Clinical Neurophysiology* **119**(1), 116--33.

Ray, S.; Crone, N. E.; Niebur, E.; Franaszczuk, P. J. & Hsiao, S. S. (2008b), 'Neural correlates of high-gamma oscillations (60-200 Hz) in macaque local field potentials and their potential implications in electrocorticography', *The Journal of Neuroscience* **28**(45), 11526--11536.

Ray, S.; Hsiao, S. S.; Crone, N. E.; Franaszczuk, P. J. & Niebur, E. (2008c), 'Effect of stimulus intensity on the spike-local field potential relationship in the secondary somatosensory cortex', *The Journal of Neuroscience***28**(29), 7334--7343.

Read, H. L.; Winer, J. A. & Schreiner, C. E. (2002), 'Functional architecture of auditory cortex', *Current Opinion in Neurobiology* **12**(4), 433--440.

Recanzone, G.H.; Merzenich, M.M.; Jenkins, V.W.; Grajski, W.M.; Dinse, H.R. (1992). Topographic reorganization of the hand representation in cortical area 3b owl monkeys trained in a frequency-discrimination task. *The Journal of Neurophysiology*. 67, 1031—1056.

Recanzone, G. H.; Schreiner, C. E. & Merzenich, M. M. (1993), 'Plasticity in the frequency representation of primary auditory cortex following discrimination training in adult owl monkeys', *The Journal of Neuroscience: The Official Journal of the Society for Neuroscience* **13**(1), 87--103.

Reynolds, J. H.; Pasternak, T. & Desimone, R. (2000), 'Attention increases sensitivity of V4 neurons', *Neuron* **26**(3), 703--714.

Reynolds, J. H. & Desimone, R. (2003), 'Interacting roles of attention and visual salience in V4', *Neuron* **37**(5), 853--863.

Reynolds, J. H. & Chelazzi, L. (2004), 'Attentional modulation of visual processing', *Annual Review of Neuroscience* **27**, 611--647.

Reynolds, J.H. (2004). Attention and contrast gain control :. In Posner, M. I. (2004), *Cognitive Neuroscience of Attention*, Guilford Press.

Ribaupierre, F. D.; Goldstein, M. H. & Yeni-Komshian, G. (1972a), 'Cortical coding of repetitive acoustic pulses', *Brain Research* **48**, 205--225.

Ribaupierre, F. D.; Goldstein, M. H. & Yeni-Komshian, G. (1972b), 'Intracellular study of the cat's primary auditory cortex', *Brain Research* **48**, 185--204.

Ribaupierre, F.D., (1997). Acoustic Information Processing in the Auditory Thalamus and Cerebral Cortex . Chapter 5 In: The Central auditory system". Edited by Günter Ehret & Raymonf Romand

Roberts, B.; Glasberg, B. R. & Moore, B. C. J. (2002), 'Primitive stream segregation of tone sequences without differences in fundamental frequency or passband', *The Journal of the Acoustical Society of America* **112**(5 Pt 1), 2074--2085.

Rodriguez, R.; Kallenbach, U.; Singer, W. & Munk, M. H. J. (2004), 'Short- and long-term effects of cholinergic modulation on gamma oscillations and response synchronization in the visual cortex', *The Journal of Neuroscience* **24**(46), 10369--10378.

Roger, M. & Arnault, P. (1989), 'Anatomical study of the connections of the primary auditory area in the rat', *The Journal of Comparative Neurology* **287**(3), 339--356.

Romanski, L. M.; Tian, B.; Fritz, J.; Mishkin, M.; Goldman-Rakic, P. S. & Rauschecker, J. P. (1999), 'Dual streams of auditory afferents target multiple domains in the primate prefrontal cortex', *Nature Neuroscience* **2**(12), 1131--1136.

Romanski, L. M. & Goldman-Rakic, P. S. (2002), 'An auditory domain in primate prefrontal cortex', *Nature Neuroscience* **5**(1), 15--16.

Romanski, L. M. (2007), 'Representation and integration of auditory and visual stimuli in the primate ventral lateral prefrontal cortex', *Cerebral Cortex (New York, N.Y.: 1991)* **17 Suppl 1**, i61--69.

Ross, B.; Herdman, A. T. & Pantev, C. (2005), 'Stimulus induced desynchronization of human auditory 40-Hz steady-state responses', *Journal of Neurophysiology* **94**(6), 4082--93.

Rouiller, E. M., (1997). Functional organization of the auditory pathways. Chapter 1 In: The Central auditory system". Edited by Günter Ehret & Raymonf Romand,. Oxford University Press.

Roullier, E.M. . In: *Neurobiology of Hearing:* volume 2, *The Central Auditory System*. Edited by R.A. Altschuler, R.P. Bobbin, B.M. Clopton, and D.W. Hoffman. New York: Raven Press, Ltd., 1991, 293-333.

Russ, B. E.; Kim, A. M.; Abrahamsen, K. L.; Kiringoda, R. & Cohen, Y. E. (2006), 'Responses of neurons in the lateral intraparietal area to central visual cues', *Experimental Brain Research.* **174**(4), 712--727.

Russ, B. E.; Orr, L. E. & Cohen, Y. E. (2008), 'Prefrontal neurons predict choices during an auditory same-different task', *Current Biology: CB* **18**(19), 1483--1488.

Russ, B. E.; Ackelson, A. L.; Baker, A. E. & Cohen, Y. E. (2008), 'Coding of auditory-stimulus identity in the auditory non-spatial processing stream', *Journal of Neurophysiology* **99**(1), 87--95.

Rutkowski, R. G.; Miasnikov, A. A. & Weinberger, N. M. (2003), 'Characterisation of multiple physiological fields within the anatomical core of rat auditory cortex', *Hearing Research* **181**(1-2), 116--30.

Salazar, R. F.; Kayser, C. & König, P. (2004), 'Effects of training on neuronal activity and interactions in primary and higher visual cortices in the alert cat', *The Journal of Neuroscience* **24**(7), 1627--36.

Salinas, E. & Sejnowski, T. J. (2001), 'Correlated neuronal activity and the flow of neural information', *Nature Reviews. Neuroscience* **2**(8), 539--550.

Salinas, E. & Sejnowski, T. J. (2000), 'Impact of correlated synaptic input on output firing rate and variability in simple neuronal models', *The Journal of Neuroscience: The Official Journal of the Society for Neuroscience* **20**(16), 6193--6209.

Sarter, M.; Gehring, W. J. & Kozak, R. (2006), 'More attention must be paid: the neurobiology of attentional effort', *Brain Research Reviews* **51**(2), 145--160.

Sally, S. L. & Kelly, J. B. (1988), 'Organization of auditory cortex in the albino rat: sound frequency', *Journal of Neurophysiology* **59**(5), 1627--38.

Sanes, J. N. & Donoghue, J. P. (1993), 'Oscillations in local field potentials of the primate motor cortex during voluntary movement', *Proceedings of the National Academy of Sciences of the United States of America* **90**(10), 4470--4474.

Sannita, W. G. (2000), 'Stimulus-specific oscillatory responses of the brain: a time/frequency-related coding process', *Clinical Neurophysiology* **111**(4), 565--583.

Schnupp, J. W. H.; Hall, T. M.; Kokelaar, R. F. & Ahmed, B. (2006), 'Plasticity of temporal pattern codes for vocalization stimuli in primary auditory cortex', *The Journal of Neuroscience: The Official Journal of the Society for Neuroscience* **26**(18), 4785--4795.

Schooneveldt, G. P. & Moore, B. C. (1989), 'Comodulation masking release (CMR) as a function of masker bandwidth, modulator bandwidth, and signal duration', *The Journal of the Acoustical Society of America* **85**(1), 273--281.

Schreiner, C. E. & Langner, G. (1988), 'Periodicity coding in the inferior colliculus of the cat. II. Topographical organization', *Journal of Neurophysiology* **60**(6), 1823--1840.

Schreiner, C. E. & Urbas, J. V. (1988), 'Representation of amplitude modulation in the auditory cortex of the cat. II. Comparison between cortical fields', *Hearing Research* **32**(1), 49--63.

Schreiner, C. E. (1992), 'Functional organization of the auditory cortex: maps and mechanisms', *Current Opinion in Neurobiology* **2**(4), 516--521.

Schreiner, C. E.; Read, H. L. & Sutter, M. L. (2000), 'Modular organization of frequency integration in primary auditory cortex', *Annual Review of Neuroscience* **23**, 501--529.

Schwarz, C. & Welsh, J. P. (2001), 'Dynamic modulation of mossy fiber system throughput by inferior olive synchrony: a multielectrode study of cerebellar cortex activated by motor cortex', *Journal of Neurophysiology* **86**(5), 2489--504.
Shadlen, M. N. & Newsome, W. T. (1994), 'Noise, neural codes and cortical organization', *Current Opinion in Neurobiology* **4**(4), 569--579.

Shadlen, M. N. & Newsome, W. T. (1996), 'Motion perception: seeing and deciding', *Proceedings of the National Academy of Sciences of the United States of America* **93**(2), 628--633.

Shipp, S. (2004), 'The brain circuitry of attention', *Trends in Cognitive Sciences* **8**(5), 223--230.

Shinonaga, Y.; Takada, M. & Mizuno, N. (1994), 'Direct projections from the non-laminated divisions of the medial geniculate nucleus to the temporal polar cortex and amygdala in the cat', *The Journal of Comparative Neurology* **340**(3), 405--426.

Siegel, M.; Donner, T. H.; Oostenveld, R.; Fries, P. & Engel, A. K. (2008), 'Neuronal synchronization along the dorsal visual pathway reflects the focus of spatial attention', *Neuron* **60**(4), 709--19.

Simpson, G. V. & Knight, R. T. (1993), 'Multiple brain systems generating the rat auditory evoked potential. I. Characterization of the auditory cortex response', *Brain Research* **602**(2), 240--50.

Sinai, A.; Bowers, C. W.; Crainiceanu, C. M.; Boatman, D.; Gordon, B.; Lesser, R. P.; Lenz, F. A. & Crone, N. E. (2005), 'Electrocorticographic high gamma activity versus electrical cortical stimulation mapping of naming', *Brain* **128**(Pt 7), 1556--70.

Singer, W. (1993), 'Neuronal representations, assemblies and temporal coherence', *Progress in Brain Research* **95**, 461—74

Singer, W. (1999), 'Neuronal synchrony: a versatile code for the definition of relations?', *Neuron* **24**(1), 49--65, 111-25.

Singer, W. & Gray, C. M. (1995), 'Visual feature integration and the temporal correlation hypothesis', *Annual Review of Neuroscience* **18**, 555--586.

Singer, W.; Kreiter, A. K.; Engel, A. K.; Fries, P.; Roelfsema, P. R. & Volgushev, M. (1996), 'Precise timing of neuronal discharges within and across cortical areas: implications for synaptic transmission', *Journal of Physiology, Paris* **90**(3-4), 221--2.

Snyder, J. S. & Large, E. W. (2005), 'Gamma-band activity reflects the metric structure of rhythmic tone sequences', *Brain Research. Cognitive Brain Research* **24**(1), 117--26.

Snyder, J. S. & Alain, C. (2007), 'Toward a neurophysiological theory of auditory stream segregation', *Psychological Bulletin* **133**(5), 780--799.

Snyder, J. S.; Alain, C. & Picton, T. W. (2006), 'Effects of attention on neuroelectric correlates of auditory stream segregation', *Journal of Cognitive Neuroscience* **18**(1), 1--13.

Staba, R. J.; Bergmann, P. C. & Barth, D. S. (2004), 'Dissociation of slow waves and fast oscillations above 200 Hz during GABA application in rat somatosensory cortex', *The Journal of Physiology* **561**(Pt 1), 205--14.

Steinschneider, M.; Tenke, C. E.; Schroeder, C. E.; Javitt, D. C.; Simpson, G. V.; Arezzo, J. C. & Vaughan, H. G. (1992), 'Cellular generators of the cortical auditory evoked potential initial component', *Electroencephalography and Clinical Neurophysiology* **84**(2), 196--200.

Steinschneider, M.; Fishman, Y. I. & Arezzo, J. C. (2008), 'Spectrotemporal analysis of evoked and induced electroencephalographic responses in primary auditory cortex (A1) of the awake monkey', *Cerebral Cortex (New York, N.Y.: 1991)* **18**(3), 610--25.

Steriade, M.; Amzica, F. & Contreras, D. (1996), 'Synchronization of fast (30-40 Hz) spontaneous cortical rhythms during brain activation', *The Journal of Neuroscience* **16**(1), 392--417.

Steriade, M.; Contreras, D.; Amzica, F. & Timofeev, I. (1996), 'Synchronization of fast (30-40 Hz) spontaneous oscillations in intrathalamic and thalamocortical networks', *The Journal of Neuroscience* **16**(8), 2788--2808.

Steriade, M. & Amzica, F. (1996), 'Intracortical and corticothalamic coherency of fast spontaneous oscillations', *Proceedings of the National Academy of Sciences of the United States of America* **93**(6), 2533--8.

Steriade, M.; Paré, D.; Parent, A. & Smith, Y. (1988), 'Projections of cholinergic and non-cholinergic neurons of the brainstem core to relay and associational thalamic nuclei in the cat and macaque monkey', *Neuroscience* **25**(1), 47--67.

Steriade, M. & Pare, D. (2007), *Gating in Cerebral Networks*, Cambridge University Press.

Stevens, A. A. & Weaver, K. (2005), 'Auditory perceptual consolidation in early-onset blindness', *Neuropsychologia* **43**(13), 1901--1910.

Stopfer, M.; Bhagavan, S.; Smith, B. H. & Laurent, G. (1997), 'Impaired odour discrimination on desynchronization of odour-encoding neural assemblies', *Nature* **390**(6655), 70--74.

Sukov, W. & Barth, D. S. (2001), 'Cellular mechanisms of thalamically evoked gamma oscillations in auditory cortex', *Journal of Neurophysiology* **85**(3), 1235--45.

Sukov, W. & Barth, D. S. (1998), 'Three-dimensional analysis of spontaneous and thalamically evoked gamma oscillations in auditory cortex', *Journal of Neurophysiology* **79**(6), 2875--84.

Syka, J.; Suta, D. & Popelár, J. (2005), 'Responses to species-specific vocalizations in the auditory cortex of awake and anesthetized guinea pigs', *Hearing Research* **206**(1-2), 177--84.

Talwar, S. K.; Musial, P. G. & Gerstein, G. L. (2001), 'Role of mammalian auditory cortex in the perception of elementary sound properties', *Journal of Neurophysiology* **85**(6), 2350--8.

Tian, B.; Reser, D.; Durham, A.; Kustov, A. & Rauschecker, J. P. (2001), 'Functional specialization in rhesus monkey auditory cortex', *Science (New York, N.Y.)* **292**(5515), 290--293.

Tiitinen, H.; Sinkkonen, J.; Reinikainen, K.; Alho, K.; Lavikainen, J. & Näätänen, R. (1993), 'Selective attention enhances the auditory 40-Hz transient response in humans', *Nature* **364**(6432), 59--60.

Thomson, D. J., Chave and A. D. Jackknifed Error Estimates for Spectra, Coherences, and Transfer Functions, *Chapter 2 of ``Advances in Spectrum Estimation''*, S. Haykin (editor), Prentice, Hall, 1991, pp. 58-113.

Traub, R. D.; Bibbig, A.; LeBeau, F. E. N.; Cunningham, M. O. & Whittington, M. A. (2005), 'Persistent gamma oscillations in superficial layers of rat auditory neocortex: experiment and model', *The Journal of Physiology* **562**(Pt 1), 3--8.

Trautner, P.; Rosburg, T.; Dietl, T.; Fell, J.; Korzyukov, O. A.; Kurthen, M.; Schaller, C.; Elger, C. E. & Boutros, N. N. (2006), 'Sensory gating of auditory evoked and induced gamma band activity in intracranial recordings', *NeuroImage* **32**(2), 790--8.

Treue, S. & Maunsell, J. H. (1999), 'Effects of attention on the processing of motion in macaque middle temporal and medial superior temporal visual cortical areas', *The Journal of Neuroscience: The Official Journal of the Society for Neuroscience* **19**(17), 7591--602.

Tsuchitani, C. & Johnson, D.H., Binaural cues and signal processing in the superior olivary complex. In *Neurobiology of Hearing:* volume 2, *The Central Auditory System*. Edited by R.A. Altschuler, R.P. Bobbin, B.M. Clopton, and D.W. Hoffman. New York: Raven Press, Ltd., 1991, 163-193.

Uhlhaas, P. J. & Singer, W. (2006), 'Neural synchrony in brain disorders: relevance for cognitive dysfunctions and pathophysiology', *Neuron* **52**(1), 155--68.

Ulanovsky, N.; Las, L.; Farkas, D. & Nelken, I. (2004), 'Multiple Time Scales of Adaptation in Auditory Cortex Neurons', *J. Neurosci.* **24**(46), 10440--10453.

Ulanovsky, N.; Las, L. & Nelken, I. (2003), 'Processing of low-probability sounds by cortical neurons', *Nature Neuroscience* **6**(4), 391--8.

Wallis, J. D. (2007a), 'Neuronal mechanisms in prefrontal cortex underlying adaptive choice behavior', *Annals of the New York Academy of Sciences* **1121**, 447--460.

Wallis, J. D. (2007b), 'Orbitofrontal cortex and its contribution to decision-making', *Annual Review of Neuroscience* **30**, 31--56.

Wallis, J. D.; Anderson, K. C. & Miller, E. K. (2001), 'Single neurons in prefrontal cortex encode abstract rules', *Nature* **411**(6840), 953--956.

Walker, K. M. M.; Ahmed, B. & Schnupp, J. W. H. (2008), 'Linking cortical spike pattern codes to auditory perception', *Journal of Cognitive Neuroscience* **20**(1), 135--152.

Wang, D. & Chang, P. (2008), 'An oscillatory correlation model of auditory streaming', *Cognitive Neurodynamics* **2**(1), 7--19.

Wang, X.; Merzenich, M.M.; Sameshima, K.; Jenikins, W.M. (1995). Remodelling of hand representation in adult cortex determined by timing of tactile stimulation. Nature 378, 71-75.

Wang, X.; Lu, T.; Bendor, D. & Bartlett, E. (2008), 'Neural coding of temporal information in auditory thalamus and cortex', *Neuroscience* **157**(2), 484--494.

Wang, X.; Lu, T.; Snider, R. K. & Liang, L. (2005), 'Sustained firing in auditory cortex evoked by preferred stimuli', *Nature* **435**(7040), 341--346.

Wang, X.; Merzenich, M. M.; Beitel, R. & Schreiner, C. E. (1995), 'Representation of a species-specific vocalization in the primary auditory cortex of the common marmoset: temporal and spectral characteristics', *Journal of Neurophysiology* **74**(6), 2685--706.

Warren, R. M. (1970), 'Perceptual restoration of missing speech sounds', *Science (New York, N.Y.)* **167**(917), 392--393.

Weinberger, N. M. (2004), 'Specific long-term memory traces in primary auditory cortex', *Nature Reviews. Neuroscience* **5**(4), 279--290.

van Wassenhove, V. & Nagarajan, S. S. (2007), 'Auditory cortical plasticity in learning to discriminate modulation rate', *The Journal of Neuroscience: The Official Journal of the Society for Neuroscience* **27**(10), 2663--2672.

Wehr, M. & Laurent, G. (1996), 'Odour encoding by temporal sequences of firing in oscillating neural assemblies', *Nature* **384**(6605), 162--6.

Wehr, M. & Zador, A. M. (2003), 'Balanced inhibition underlies tuning and sharpens spike timing in auditory cortex', *Nature* **426**(6965), 442--6.

Wehr, M. & Zador, A. M. (2005), 'Synaptic mechanisms of forward suppression in rat auditory cortex', *Neuron* **47**(3), 437--45.

Weinberger, N. M. & Diamond, D. M. (1987), 'Physiological plasticity in auditory cortex: rapid induction by learning', *Progress in Neurobiology* **29**(1), 1--55.

Weisz, N.; Müller, S.; Schlee, W.; Dohrmann, K.; Hartmann, T. & Elbert, T. (2007), 'The neural code of auditory phantom perception', *The Journal of Neuroscience: The Official Journal of the Society for Neuroscience* **27**(6), 1479--84.

Welsh, J. P.; Ahn, E. S. & Placantonakis, D. G. (), 'Is autism due to brain desynchronization?', *International Journal of Developmental Neuroscience: The Official Journal of the International Society for Developmental Neuroscience* **23**(2-3), 253--63.

der Werf, Y. D. V.; Witter, M. P. & Groenewegen, H. J. (2002), 'The intralaminar and midline nuclei of the thalamus. Anatomical and functional evidence for participation in processes of arousal and awareness', *Brain Research. Brain Research Reviews* **39**(2-3), 107--40.

Wespatat, V.; Tennigkeit, F. & Singer, W. (2004), 'Phase sensitivity of synaptic modifications in oscillating cells of rat visual cortex', *The Journal of Neuroscience* **24**(41), 9067--9075.

Winer, J.A. The functional architecture of the medial geniculate body and the primary auditory cortex. In: *Springer Handbook of Auditory Research*, volume 1, *The Mammalian Auditory Pathways: Neuroanatomy*. Edited by D.B. Webster, A.N. Popper, and R.R. Fay. New York: Springer-Verlag, 1992, 222-409.

Winer, J.A. Anatomy of the medial geniculate body. In: *Neurobiology of Hearing:* volume 2, *The Central Auditory System*. Edited by R.A. Altschuler, R.P. Bobbin, B.M. Clopton, and D.W. Hoffman. New York: Raven Press, Ltd., 1991, 293-333.

Winer, J. A.; Sally, S. L.; Larue, D. T. & Kelly, J. B. (1999), 'Origins of medial geniculate body projections to physiologically defined zones of rat primary auditory cortex', *Hearing Research* **130**(1-2), 42--61.

Woldorff, M. G.; Gallen, C. C.; Hampson, S. A.; Hillyard, S. A.; Pantev, C.; Sobel, D. & Bloom, F. E. (1993), 'Modulation of early sensory processing in human auditory cortex during auditory selective attention', *Proceedings of the National Academy of Sciences of the United States of America* **90**(18), 8722--8726.

Womelsdorf, T.; Anton-Erxleben, K.; Pieper, F. & Treue, S. (2006), 'Dynamic shifts of visual receptive fields in cortical area MT by spatial attention', *Nature Neuroscience* **9**(9), 1156--60.

Womelsdorf, T. & Fries, P. (2006), 'Neuronal coherence during selective attentional processing and sensory-motor integration', *Journal of Physiology, Paris* **100**(4), 182--93.

Womelsdorf, T.; Fries, P.; Mitra, P. P. & Desimone, R. (2006), 'Gamma-band synchronization in visual cortex predicts speed of change detection', *Nature* **439**(7077), 733--6.

Womelsdorf, T. & Fries, P. (2007), 'The role of neuronal synchronization in selective attention', *Current Opinion in Neurobiology* **17**(2), 154--60.

Womelsdorf, T.; Schoffelen, J.; Oostenveld, R.; Singer, W.; Desimone, R.; Engel, A. K. & Fries, P. (2007), 'Modulation of neuronal interactions through neuronal synchronization', *Science (New York, N.Y.)* **316**(5831), 1609--12.

Yin, P.; Mishkin, M.; Sutter, M. & Fritz, J. B. (2008), 'Early stages of melody processing: stimulus-sequence and task-dependent neuronal activity in monkey auditory cortical fields A1 and R', *Journal of Neurophysiology* **100**(6), 3009--3029.

Ylinen, A.; Bragin, A.; Nádasdy, Z.; Jandó, G.; Szabó, I.; Sik, A. & Buzsáki, G. (1995), 'Sharp wave-associated high-frequency oscillation (200 Hz) in the intact hippocampus:

network and intracellular mechanisms', *The Journal of Neuroscience: The Official Journal of the Society for Neuroscience* **15**(1 Pt 1), 30--46.

Yuval-Greenberg, S.; Tomer, O.; Keren, A. S.; Nelken, I. & Deouell, L. Y. (2008), 'Transient induced gamma-band response in EEG as a manifestation of miniature saccades', *Neuron* **58**(3), 429--41.

Zaksas, D. & Pasternak, T. (2006), 'Directional signals in the prefrontal cortex and in area MT during a working memory for visual motion task', *The Journal of Neuroscience***26**(45), 11726--11742.

Zaksas D & Pasternak T. (2005) Area MT neurons respond to visual motion distant from their receptive fields. J Neurophysiol. 94(6):4156-67.

Zanto, T. P., Snyder, J. S., Large, E. W. (2006). Neural correlates of rhythmic expectancy. *Advances in Cognitive Psychology*, *2 (2–3*), 221-231.

Zeitler, M.; Fries, P. & Gielen, S. (2006), 'Assessing neuronal coherence with single-unit, multi-unit, and local field potentials', *Neural Computation* **18**(9), 2256--81.

Zhang, L. I.; Tan, A. Y. Y.; Schreiner, C. E. & Merzenich, M. M. (2003), 'Topography and synaptic shaping of direction selectivity in primary auditory cortex', *Nature* **424**(6945), 201--5.

Zikopoulos, B. & Barbas, H. (2006), 'Prefrontal projections to the thalamic reticular nucleus form a unique circuit for attentional mechanisms', *The Journal of Neuroscience: The Official Journal of the Society for Neuroscience* **26**(28), 7348--7361.

Zurita, P.; Villa, A. E.; de Ribaupierre, Y.; de Ribaupierre, F. & Rouiller, E. M. (1994), 'Changes of single unit activity in the cat's auditory thalamus and cortex associated to different anesthetic conditions', *Neuroscience Research* **19**(3), 303--16.